MATHEUS CASARINI SIQUEIRA

Respostas de tolerância de espécies da Mata Atlântica a metais pesados e ozônio troposférico

Tese apresentada ao Instituto de Pesquisas Ambientais, da Secretaria de Meio Ambiente, Infraestrutura e Logística, como parte dos requisitos exigidos para a obtenção do título de DOUTOR em BIODIVERSIDADE VEGETAL E MEIO AMBIENTE, na Área de Concentração de Plantas Vasculares em Análises Ambientais.

SÃO PAULO

2026

MATHEUS CASARINI SIQUEIRA

Respostas de tolerância de espécies da Mata Atlântica a metais pesados e ozônio troposférico

Tese apresentada ao Instituto de Pesquisas Ambientais, da Secretaria de Meio Ambiente, Infraestrutura e Logística, como parte dos requisitos exigidos para a obtenção do título de DOUTOR em BIODIVERSIDADE VEGETAL E MEIO AMBIENTE, na Área de Concentração de Plantas Vasculares em Análises Ambientais.

SÃO PAULO

2026

MATHEUS CASARINI SIQUEIRA

Respostas de tolerância de espécies da Mata Atlântica a metais pesados e ozônio troposférico

Tese apresentada ao Instituto de Pesquisas Ambientais, da Secretaria de Meio Ambiente, Infraestrutura e Logística, como parte dos requisitos exigidos para a obtenção do título de DOUTOR em BIODIVERSIDADE VEGETAL E MEIO AMBIENTE, na Área de Concentração de Plantas Vasculares em Análises Ambientais.

ORIENTADOR: DRA. MARISA DOMINGOS

CO-ORIENTADOR: DR. ARMANDO REIS TAVARES

Ficha Catalográfica elaborada pelo NÚCLEO DE BIBLIOTECA E MAPOTECAS

Siqueira, Matheus Casarini

C268d Respostas de tolerância de espécies da Mata Atlântica à metais pesados e ozônio troposférico / Matheus Casarini Siqueira -- São Paulo, 2026. 165 p. il.

Tese (Doutorado) -- Instituto de Pesquisas Ambientais, Secretaria de Meio Ambiente, Infraestrutura e Logística, São Paulo, 2026

Bibliografia.

1 Poluição. 2 Cobre. 3 Zinco. 4 Níquel. 5 Ozônio. 6 plantas nativas da Mata Atlântica. 7 Hábito de vida. 8. Efeito hormético I. Título

BANCA EXAMINADORA

Dra. Marisa Domingos (Orientadora)
Instituto de Pesquisas Ambientais (IPA)

Dra. Catarina Carvalho Nievola
Instituto de Pesquisas Ambientais (IPA)

Dra. Silvia Ribeiro de Souza
Instituto de Pesquisas Ambientais (IPA)

Dra. Fernanda Anselmo Moreira
Instituto de Pesquisas Ambientais e Universidade de São Paulo (IPA-USP)

Dr. Evandro Alves Vieira
Instituto Tecnológico Vale (ITV)

À minha família,

à minha esposa,

aos meus amigos e colegas de dentro e fora do instituto,

e a todos aqueles que me auxiliaram nessa trajetória acadêmica,

Dedico

"A natureza não é um recurso, é a nossa matriz.
A natureza não é um cenário, é a essência.
Eu não percebo que algo exista que não seja natureza.
Tudo é natureza, é onde jorra a vida"

Ailton Krenak

Agradecimentos

Ao Programa de Pós-Graduação em Biodiversidade Vegetal e Meio Ambiente, e ao Instituto de Pesquisas Ambientais pela realização do presente estudo.

À FAPESP (Processos 2021/09686-9; 2017/50341-0, 2023/16524-0 e 2025/15561-5) pela concessão da bolsa de doutorado, BEPE e suporte financeiro ao desenvolvimento do projeto de pesquisa.

À minha orientadora Dra. Marisa Domingos, pela dedicação em me orientar, auxiliar e por me ajudar onde quer que eu (até na Itália) ou ela (em campo, coleta e reuniões) esteja e por tirar todas as minhas dúvidas (por mais simples que fossem). E principalmente, por sempre ter confiado em mim, apoiado minhas deciões, acreditado no meu potencial e me inspirado a seguir mais longe.

Ao meu Co-orientador Dr. Armando Reis Tavares, que mesmo de outro instituto, me ajudou e auxiliou em tudo que precisei, além de ter sido a base que me impulsionou do mestrado ao doutorado.

Aos pesquisadores do Instituto de Pesquisas Ambientais que me passaram valiosos conhecimentos, incentivos e ideias.

Aos pesquisadores e alunos do CNR-IRET, Barbara, Yasutomo, Elena, Giulia, Luigi, Sabatini, Yacopo, Cesare, Leo, Martina, Giulia, Agostina, Raffaela, Isabela, Giacomo, Giorgia, Ryoji, Emiliano, Andrea e tantos outros que me acolheram e me fizeram sentir parte da equipe desde o primeiro dia em Firenze. Me ajudaram a aprender o italiano, entrar no ritmo de trabalho, me ensinaram tanto e me proporcionaram experiências profissionais e pessoais inesquecíveis.

Aos membros da banca de qualificação e defesa pelas contribuições e sugestões para a melhoria do trabalho.

Aos alunos, ex-alunos e amigos que fiz nos diferentes núcleos do Instituto de Pesquisas Ambientais: Os ecólogos Ruan, Leo Tristão, Leo Ganz, Letícia Sapucaia, Gabriela, Carol, Darah, Renata, Alex, Geane, Regina, João, Guilherme, Fernanda, Cíntia, Tarcísio, Cássia, Augusto, Letícia Candido; Os fisiologistas Lucas, Allan, Edson, Barbara e Maria Fernanda; Os técnicos Kauê e Kátia. Vocês não só aliviavam o estresse e me faziam rir diariamente, como me mantinham no eixo, me davam forças e sempre me colocavam pra cima. O apoio e companheirismo diário de vocês foram mais que essenciais.

À Júlia, minha inicialmente namorada, então noiva e agora esposa, tudo isso durante o período do doutorado. Por todo amor, carinho, compreensão, apoio, convivência e motivação durante esse tempo. Por ter ficado ao meu lado em cada decisão e momento difícil. Te amo!

Aos meus amigos que sempre estiveram comigo e nunca me deixaram desistir dos meus sonhos.

À toda minha família e parentes que sempre me incentivaram e apoiaram em qualquer caminho que eu decidi trilhar, em especial: Minha mãe Valnise, meu pai Tadeu, meu irmão Guilherme, meus avós Bruno e Cleonice e tio Douglas.

À Deus, pelas oportunidades e acontecimentos que me foram permitidos ao longo da vida.

Muito obrigado!

SUMÁRIO

RESUMO

Cobre (Cu), zinco (Zn) e níquel (Ni) são metais pesados (MPs) e micronutrientes essenciais para o crescimento e desenvolvimento vegetal. No entanto, devido ao aumento das ações antrópicas, há a entrada crescente desses elementos nos ambientes naturais, principalmente em locais próximos às fontes emissoras como fragmentos florestais urbanos, impondo riscos ao meio ambiente e à biota. Além de aumento nos níveis de metais pesados, atividades poluidoras atmosféricas também vêm causando elevação na concentração de gases potencialmente tóxicos, como o ozônio (O_3). A fim de garantir sua sobrevivência, as plantas desenvolveram diversos mecanismos fisiológicos e bioquímicos de proteção a estes agentes estressores, como antioxidantes, ácidos orgânicos radiculares, fitoquelatinas e regulação de aminoácidos. Contudo, a capacidade de síntese destes compostos orgânicos, bem como respostas fisiológicas à combinação de estressores abióticos, ainda são desconhecidas em diversas espécies vegetais, em especial as espécies da Mata Atlântica. Espécies de diferentes hábitos de vida e taxas de crescimento devem apresentar estratégias de tolerância distintas frente à estressores ambientais. O projeto teve os objetivos de 1) Sistematizar método de cultivo hidropônico para espécies nativas da Mata Atlântica; 2) Avaliar a tolerância e produção de compostos bioquímicos de defesa em mudas de espécies de diferentes hábitos de vida, nativas da Mata Atlântica, cultivadas em solução hidropônica enriquecida com MPs (Cu + Zn + Ni); 3) Investigar os efeitos do O_3 em uma espécie tolerante à MPs; 4) Verificar se a combinação de estressores (MPs + O_3) influencia na capacidade de manutenção da tolerância da espécie nativa tolerante aos MPs. A tese consistiu em etapas experimentais, divididas em capítulos. Na primeira etapa foi realizada a determinação do método hidropônico e das concentrações de MPs em uma espécie modelo (*Schinus terebinthifolia*). Na segunda etapa, foi realizada a determinação da capacidade de tolerância de 5 espécies de diferentes hábtios de vida (*Schinus terebinthifolia* - arbórea - crescimento rápido; *Cariniana legalis* - arbórea - crescimento lento; *Seemania sylvatica* - herbácea – crescimento rápido, *Passiflora edulis* - liana – cresciemnto rápido; *Aechmea fasciata* – epífita – crescimento lento) através da análise de parâmetros fisiológicos e bioquímicos de tolerância. Na terceira etapa foi realizado experimento com a espécie tolerante à MPs (*S. terebinthifolia*) identificada na etapa anterior. Nesta etaá, foi realizada a exposição ao ozônio isoladamente, e também em combinação de estressores (MPs + O_3). Na primeira etapa identificamos que o método hidropônio “Dutch Bucket” é viável para o cultivo de *S. terebinthifolia* sob perlita ou espuma fenólica. Nesta etapa, estabelecemos as concentrações máximas de MPs capazes de induzir estresse sem comprometer a sobrevivência das plantas (50 µM de cobre, zinco e níquel). Na segunda etapa identificamos que *Schinus terebinthifolia* e *Aechmea fasciata* são espécies tolerântes à MPs, *Cariniana legalis* é

moderadamente tolerante, enquanto *Passiflora edulis* e *Seemania sylvatica* são espécies sensíveis, sugerindo que o hábito de vida das plantas aparenta ter relação com a capacidade de tolerância à HMs, enquanto que a taxa de crescimento (cresciemnto rápido x crescimento lento) não se mostra um preditor confiável como ferramenta de análise de tolerância. Na terceira etapa, identificamos que a espécie tolerante a MPs (*Schinus terebinthifolia*) é também tolerante ao O_3 isoladamente, exibindo alta atividade estomática e resposta hormética na biomassa. Identificamos que a combinação de estressores (HMs + O_3) não interferiu na capacidade de tolerância desta espécie aos MPs, evidenciando a alta capacidade de tolerância desta espécie à estressores ambientais.

Palavras-chave: Poluição, cobre, zinco, níquel, ozônio, hábito de vida, efeito hormético.

ABSTRACT

Copper (Cu), zinc (Zn), and nickel (Ni) are heavy metals (HMs) and micronutrients essential for plant growth and development. However, due to increased anthropogenic activities, there is a growing influx of these elements into natural environments, mainly in locations near emission sources such as urban forest fragments, posing risks to the environment and biota. In addition to increased levels of heavy metals, atmospheric pollution activities are also causing an increase in the concentration of potentially toxic gases, such as ozone (O_3). In order to ensure their survival, plants have developed various physiological and biochemical mechanisms to protect against these stressors, such as antioxidants, root organic acids, phytochelatins, and amino acid regulation. However, the capacity for synthesis of these organic compounds, as well as physiological responses to the combination of abiotic stressors, are still unknown in several plant species, especially those of the Atlantic Forest. Species with different life habits and growth rates should exhibit distinct tolerance strategies in the face of environmental stressors. The project had the following objectives: 1) To systematize a hydroponic cultivation method for native species of the Atlantic Forest; 2) To evaluate the tolerance and production of biochemical defence compounds in seedlings of species with different life habits, native to the Atlantic Forest, cultivated in a hydroponic solution enriched with MPs (Cu + Zn + Ni); 3) To investigate the effects of O3 on a species tolerant to MPs; 4) To verify if the combination of stressors (HMs + O_3) influences the ability to maintain tolerance in the native species tolerant to HMs. The thesis consisted of experimental stages, divided into chapters. In the first stage, the hydroponic method and the concentrations of HMs in a model species (*Schinus terebinthifolia*) were determined. In the second stage, the tolerance capacity of 5 species with different life habits was determined (*Schinus terebinthifolia* - tree - fast growth; *Cariniana legalis* - tree - slow growth; *Seemania sylvatica* - herbaceous - fast growth; *Passiflora edulis* - liana - fast growth; *Aechmea fasciata* - epiphyte - slow growth) through the analysis of physiological and biochemical tolerance parameters. In the third stage, an experiment was conducted with the HMs-tolerant species (*S. terebinthifolia*) identified in the previous stage. In this stage, exposure to ozone was carried out both alone and in combination with stressors (HMs + O3). In the first stage, we identified that the "Dutch Bucket" hydroponic method is viable for cultivating S. terebinthifolia under perlite or phenolic foam. In this stage, we established the maximum concentrations of HMs capable of inducing stress without compromising plant survival (50 µM of copper, zinc, and nickel). In the second stage, we identified that *S. terebinthifolia* and *A.fasciata* are HM-tolerant species, *C.legalis* is moderately tolerant, while *P.edulis* and *S. sylvatica* are sensitive species, suggesting that the life habit of the plants appears to be related to their tolerance capacity to HMs, while the growth rate (fast

growth vs. slow growth) does not prove to be a reliable predictor as a tool for tolerance analysis. In the third stage, we identified that the HM-tolerant species (*S. terebinthifolia*) is also tolerant to O_3 in isolation, exhibiting high stomatal activity and a hormetic response in biomass. We identified that the combination of stressors (HMs + O_3) did not interfere with this species' tolerance capacity to HMs, demonstrating this species' high tolerance capacity to environmental stressors.

Key words: Pollution, copper, zinc, nickel, life-habit, hormetic effect

LISTA DE ABREVIATURAS

μ: Velocidade do vento (Wind speed)

A: Assimilação líquida de CO_2 (Net CO_2 assimilion)

AA: Ar ambiente (Ambient air)

AAr: Ácido ascórbico reduzido (Reduced scorbic acid)

AAt: Ácido ascórbico total (Total ascorbic acid)

AIC: Critério de informação de Akaike (Akaike Information Criteria)

ANOVA: Análise de variância (Analysis of variance)

AOT40: exposição acumulada de ozônio acima do limite de 40 ppb (Accumulated Ozone exposure over a Threshold of 40 ppb)

B_{final}: Biomassa final (Final biomass)

B_{ref}: Biomassa de referência (Reference biomass)

Chl: Clorofila (Chlorophyll)

CL: Níveis críticos (Critical levels)

Cu: Cobre (Copper)

DAD: Detector de matriz de diodos (Diode array detector)

DOY: Dia do ano (Day of year)

DW: Massa seca (Dry weight)

EC: Condutividade elétrica (Electrical conductivity)

FACE: Exposição controlada ao ar aberto (Free-Air Controlled Exposure)

f_{min}: Fração da mínima condutância estomática (Minimal stomatal conductance in fraction)

f_{phen}: Fenologia (Phenology)

F_v/F_m: Rendimento máximo do fotossistema II (Maximum efficiency of photosystem II)

FW: Massa fresca (Fresh weight)

g_{max}: Condutância estomática máxima (Maximum stomatal conductance)

GSH: Glutationa (Glutahione)

gsw: Condutância estomática ao vapor de água (Stomatal conductance to water vapor)

H_3PO_4: Ácido ortofosfórico (Ortophosphoric acid)

HA: Solução nutritiva de Hoagland e Arnon (Hoagland and Arnon nutrient solution)

HMs: Metais pesados (Heavy metals)

HPLC: Cromatografia líquida de alta pressão (High pressure liquid chromatography)

HPO_3: Ácido Metafosfórico (metaphosphoric acid)

IRGA: Analisador de gases por infravermelho (Infra-red gaz analyzer)

KH_2PO_4: Fosfato de potássio monobásico (Potassium phosphate monobasic)

L_d: Dimensão da folha transversal ao vento (Cross-wind leaf dimension)

Ni: Níquel (Nickel)

O_3: Ozônio (Ozone)

PAR: Radiação Fotossinteticamente Ativa (Photosynthetically active radiation)

PCA: Análise de componentes principais (Principal component analysis)

PCs: Fitoquelatinas

POD_y: Dose fitotóxica de ozônio acima do limite ‘y’(Phytotoxic Ozone Dose above a threshold 'y')

PPFD: Densidade de fluxo de fótons fotossintéticos (Photosynthetic Photon Flux Density)

R^2: Coeficiente de determinação (Coefficient of determination)

r_b: Resistência da camada limítrofe da folha (Leaf boundary layer resistance)

r_c: Resistência da superfície da folha (Leaf surface resistance)

RH: Umidade relativa (Relative humidity)

ROAs: Ácidos orgânicos radiculares (Root organic acids)

SD: Desvio padrão (Standard deviation)

SR: Radiação solar (Solar radiation)

T: Temperatura (Temperature)

T_0: Tempo inicial do experimento (Begginning of experiment)

VPD: Déficit de pressão de vapor (Vapor pressure deficit)

Zn: Zinco (Zinc)

LISTA DE FIGURAS

Capítulo I

and C) or roots (B and D) of pioneer tree, non-pioneer tree, herbaceous, liana and epiphyte cultivated in balanced nutrient solution (C = Control) or balanced nutrient solution with excess Cu, Zn and Ni (T = CuZnNi).

Fig. II 5. Mean concentration of root organic acids (µg ml-1) exuded pioneer tree (A), non-pioneer tree (B), herbaceous (C), liana (D) and epiphyte (E) seedlings cultivated in balanced nutrient solution (Control) or balanced nutrient solution with excess Cu, Zn and Ni (CuZnNi). Different letters indicate a significant difference between treatments, according to the t-test ($p \leq 0.05$). "x" indicates undetected acid.

Fig. II 6. Heatmap of the standardized data of all biomarkers analyzed in the pioneer tree, non-pioneer tree, herbaceous, liana and epiphyte species under CuZnNi stress. HM: Heavy metal accumulation. As: Antioxidants. PCs: Phytochelatins. ROA: Root organic acids. L: Leaf. R: Root. r: reduced. t: total. Cells with X indicate undetected compounds.

--

Fig. II S 1. Mean phytochelatins concentrations (PC2 to PC6; ng mg-1 fresh mass) in leaves or roots of pioneer tree (A), non-pioneer tree (B), herbaceous (C), liana (D) and epiphyte (E) cultivated in balanced nutrient solution (Control) or balanced nutrient solution with excess Cu, Zn and Ni (CuZnNi). Different letters indicate significant difference between treatments within same organ, while * indicates a significant difference between organs within same treatment, according to two-way ANOVA followed by the Šídák test ($p \leq 0.05$). "x" indicates undetected phytochelatin.

Fig. II S 2. Mean pH and conductivity values (µS cm-1) of hydroponic solutions during 5 weeks of cultivation of pioneer tree (A), non-pioneer tree (B), herbaceous (C), liana (D) and epiphyte (E) grown in balanced nutrient solution (Control) or balanced nutrient solution with excess of Cu, Zn and Ni (CuZnNi). Different letters indicate a significant difference between weeks in the same treatment (lowercase letters compare in Control treatment; while uppercase letters compare in CuZnNi treatment), and * indicates a significant difference between treatments within the same week, according to two-way ANOVA followed by Šídák test ($p \leq 0.05$).

Capítulo III

Fig. III 1. A. Daily means of solar radiation (SR), relative humidity (RH) and air temperature during the experiment. B. Daily means of tropospheric O3 exposure in ambient (AA), 1.5 times ambient (1.5×), and 2.0 times ambient (2.0×). The dashed vertical line represents the

midterm of the experiment and when part of the plants exposed to AA were switched to 2.0× (AA → 2.0×) and vice-versa (2.0× → AA).

Fig. III 2. Total (A) and leaf (B) dry weight (DW) of S. *terebinthifolia plants* after 90 days of O3 exposure in ambient air (AA), 1.5 times ambient air (1.5×), 2.0 times ambient air (2.0×), ambient to 2.0× after 45 days (AA→2.0×) and 2.0× to ambient after 45 days (2.0×→AA) conditions. Distinct letters indicate significant differences according to one-way ANOVA followed by Tukey's test ($p \leq 0.05$). Bars denote standard error (n = 9).

Fig. III 3. Linear regressions of total (A) and leaf (B) biomass of *S. terebinthifolia* plants exposed to distinct O3 treatments and calculated reference biomass. Bars denote standard errors (n = 9). The red shaded areas represent the confidence intervals (95%). The regression equations and coefficient of determinations (R2) are indicated in the upper right corner.

Fig. III 4. Modeling of stomatal conductance (gsw - mol H2O m-2 s-1) of *S. terebinthifolia* as a function of temperature (°C), radiation (PPFD - µmol m-2 s-1), vapor pressure deficit (VPD - kPa), and phenological activity (DOY - day of year). Black dots represent the measured stomatal conductance of *S. terebinthifolia*, and the solid red line represents the calculated parametrization model for each environmental parameter.

Fig. III 5. Nonlinear Bragg.4 model applied as a predictor of *S. terebinthifolia* relative total biomass as a function of POD16 (A), and relative leaf biomass as a function of POD15. The black dashed line represents the hypothetical relative biomass in the pre-industrial era (Brel = 1.00). The blue dots and blue dashed line represent the O3 critical levels to achieve 0.96 of relative biomass (4% biomass loss from the pre-industrial era). The black symbols represent *S. terebinthifolia* relative biomass (± SD) under each O3 treatment, and the solid red line represents the calculated nonlinear model.

--

Fig. III S 1 Schematic representation of experimental design and ozone treatments.

Fig. III S 2. Linear regression of measured and estimated stomatal conductance (gsw) in *Schinus terebinthifolia* leaves. RMSE = Root mean square error.

Fig. III S 3. Nonlinear UCRS.5a applied as a predictor of *S. terebinthifolia* relative total biomass of as a function of POD16 (A), and nonlinear UCRS.4a applied as a predictor of *S. terebinthifolia* relative total biomass of as a function of POD19. Black dashed line represents the hypothetical relative biomass in pre-industrial era (Brel = 1.00). The Blue dashed line

regions of main stem of *S. terebinthifolia* submitted to different ozone levels (AA, 1.5×, 2.0×) and nutrient solutions (Control and HM). Lowercase letters compare ozone treatments, while * indicates significant difference between nutrient solution treatments in the same ozone level, according to two-way ANOVA followed by post-hoc Šídák's test (bar graphs) or Scheirer-Ray-Hare followed by post-hoc Dunn's test (box-plot graphs) ($p \leq 0.05$).

Fig. IV 17. Amino acids in roots of *S. terebinthifolia* submitted to different ozone levels (AA, 1.5×, 2.0×) and nutrient solutions (Control and HM). Lowercase letters compare ozone treatments, while * indicates significant difference between nutrient solution treatments in the same ozone level, according to two-way ANOVA followed by post-hoc Šídák's test (bar graphs) or Scheirer-Ray-Hare followed by post-hoc Dunn's test (box-plot graphs) ($p \leq 0.05$).

LISTA DE TABELAS

Capítulo I

Capítulo II

mass) and dry biomass, with standard deviation (±) in leaves, stem and roots of pioneer tree, non-pioneer tree, herbaceous, liana and epiphyte species cultivated in nutrient solution (C - Control) or nutrient solution with excess of Cu, Zn and Ni (T - CuZnNi).

Capítulo III

Tab. III 1. Stomatal conductance parameterization of *S. terebinthifolia*, measured under natural conditions along the entire experimental period. gmax is maximum conductance; fmin is the minimum stomatal conductance (fraction); ftemp, flight, fVPD and fphen are the variation in gmax with temperature (T, °C), photosynthetic photon flux density (PPFD, μmol m2 s-1), vapor pressure deficit (VPD, kPa) and phenology (day of the year), respectively. Tmax, Topt and Tmin, are the maximum, optimal, and minimum air temperature for stomatal opening. The constant a determines the shape of the exponential relationship for flight function. VPDmax and VPDmin are the vapor pressure deficit for attaining maximum and minimum stomatal aperture. Start and End are the days of start and end of the experiment. $fphen_{a}$ and $fphen_{b}$ are the number of days for fphen to reach its maximum and minimum, respectively.

--

Tab. III S 1. AOT40 and PODy values (0 – 22) of *S. terebinthifolia* cultivated in ambient (AA), 1.5 times ambient (1.5×), 2.0 times ambient (2.0×), ambient to 2.0× after 45 days (AA → 2.0×) and 2.0× to ambient after 45 days (2.0× → AA) conditions.

Tab. III S 2. Akaike indication criteria (AIC), coefficient of determination (R2) and ranking of linear and the tree best non-linear models as function of AOT40 or POD0-22 to predict relative *leaf biomass* in S. terebinthifolia. The line in bold font denotes the best predictor model.

Tab. III S 3 Akaike indication criteria (AIC), coefficient of determination (R2) and ranking of linear and the three best non-linear models as function of AOT40 or POD0-22 to predict relative *total biomass* in S. terebinthifolia. The line in bold font denotes the best predictor model.

Introdução Geral

Nas últimas décadas, o aumento das atividades antropogênicas poluidoras tem se tornado uma questão ambiental crítica. Emissões provenientes de indústrias e frota automotiva, mineração e refinarias, descarte incorreto de resíduos e esgoto, uso excessivo de fertilizantes e outras atividades, têm promovido o acréscimo nos níveis de alguns elementos potencialmente tóxicos como metais pesados no solo (DalCorso et al., 2019), e/ou precursores de ozônio troposférico (O_3) no ar (Donzelli e Suarez-Varela, 2024).

Cobre (Cu), zinco (Zn) e níquel (Ni) são micronutrientes essenciais para o crescimento e desenvolvimento vegetal, usualmente encontrados em baixas concentrações em ambientes não perturbados e fazem parte da composição mineral natural dos solos (Panagos et al., 2018). Estes elementos atuam em processos fisiológicos e bioquímicos e estão relacionados com atividades metabólicas primárias (crescimento e reprodução) e secundárias (proteção e defesa), sendo vitais para o adequado desenvolvimento das espécies vegetais (Kabata-Pendias, 2011; Barker e Pealbem, 2015). Cu está envolvido na biossíntese de pigmentos fotossintéticos, lignificação de tecidos, cadeia transportadora de elétrons, regulação da permeabilidade da parede celular, na sinalização hormonal e proteção contra o estresse oxidativo através de enzimas antioxidantes (Shabbir et al., 2020). Ni é componente integral de metaloenzimas envolvidas no metabolismo de carbono e nitrogênio como urease, Ni-Fe hidrogenase, monóxido de carbono desidrogenase, sendo vital em diversas fases do desenvolvimento vegetal (Ahmad e Ashraf, 2012). Zn é componente integral de lipídios e proteínas, atua na catálise de enzimas, na produção e regulação de hormônios de crescimento, no metabolismo de carbono, e na proteção contra patógenos e estresses ambientais (Tsonev e Lindon, 2011).

Apesar de essenciais, altas concentrações de Cu, Ni e Zn podem causar fitotoxidez, estresse oxidativo e impactar negativamente as funções fisiológicas e metabólicas das plantas (Nagajyoti et al., 2010). Cu, Zn e Ni estão entre os metais pesados mais contaminantes e difundidos nos diferentes compartimentos ecossistêmicos de solos florestais urbanos (Argyraki et al., 2018; Nakazato et al., 2021). A fitotoxidez por metais pesados pode ocasionar a redução da absorção de água e nutrientes, e acúmulo de carboidratos (Li et al., 2019), além de mudanças morfológicas nas raízes e folhas (Martins et al., 2020). Essas alterações morfofisiológicas podem resultar em desbalanços nutricionais por interação entre nutrientes, inibição do crescimento, redução na biomassa, redução da concentração de pigmentos, acarretando risco à sobrevivência das plantas (Saleem et al., 2019). A formação descontrolada de espécies reativas de oxigênio (EROs) é também um dos efeitos mais evidentes da entrada excessiva de metais pesados nas células vegetais, ocasionando oxidação de biomoléculas, membranas lipídicas e organelas vitais, levando ao estresse oxidativo com danos irreversíveis à componentes

celulares, resultando em desordens no metabolismo vegetal e eventual morte (Mahmud et al., 2019).

A fim de tolerar os potenciais efeitos tóxicos, as espécies vegetais desenvolveram sistemas fisiológicos e bioquímicos de proteção e defesa contra o estresse abiótico induzido pelo excesso de metais pesados (Sarma et al., 2018). Uma das primeiras estratégias de proteção das plantas contra o excesso de metais pesados é a limitação/restrição na absorção destes elementos, através da excreção radicular de ácidos orgânicos e demais exsudatos (Jones, 1998). Os ácidos orgânicos atuam contra o estresse por metais pesados principalmente por duas formas: através da quelação de metais pesados no meio extracelular, dificultando a entrada nas células (exclusão); e pelo controle do pH da rizosfera (Girkin et al., 2018). Por se tratar de ácidos, a excreção destes compostos orgânicos diminui o pH do solo/solução, o que torna os nutrientes mais biodisponíveis para serem absorvidos (Taiz et al., 2017). A adequada absorção dos demais nutrientes atua na manutenção da homeostase vegetal e diminui os efeitos adversos causados pelo excesso de metais pesados (Kobayashi et al., 2019). Os principais ácidos orgânicos da rizosfera em exsudatos de plantas são os ácidos acético, málico, cítrico, oxálico, succínico e fumárico (Mimmo et al., 2014). A detecção de ácidos orgânicos exsudatos pelas raízes pode atuar na sinalização de mecanismos de tolerância e adaptação.

Outra estratégia de proteção das plantas contra o excesso de metais pesados ocorre pela produção de moléculas que atuam na quelação (aprisionamento) e compartimentalização de metais pesados em organelas celulares, como fitoquelatinas e metalotioneinas. Fitoquelatinas (PCs) são polipeptídios não proteicos ricos em cisteínas (grupos tióis), sintetizadas através da enzima fitoquelatina sintase (Phytochelatin synthase, EC 2.3.2.15), utilizando a glutationa (γ-Glu-Cys-Gly) como substrato precursor (Ogawa et al., 2010). PCs consistem em apenas três aminoácidos: glutamato (Glu), cisteína (Cys) e glicina (Gly), organizados em uma estrutura básica [$(\gamma\text{-Glu-Cys})_n$-Gly, onde n = 2-11], e são classificadas de acordo com número de repetições do grupo glutamato-cisteína (PC_n) (Cobbett e Goldsbrough, 2002). As PCs são conhecidas pela capacidade de desintoxicação e compartimentalização de metais pesados, por meio da formação de complexos com os íons metálicos livres no citosol, que são posteriormente transportados ao vacúolo e outros compartimentos subcelulares (Yadav, 2010). Estudos verificaram que existe correlação positiva entre o aumento da concentração de metais nos tecidos e o aumento na produção de fitoquelatinas (Beladi et al., 2011; Cao et al., 2019; Navarrete et al., 2019). Ainda, as PCs possuem alta capacidade de translocação entre raízes e folhas, e quando ligadas aos metais pesados, podem contribuir na homeostase e transporte de metais nas plantas (Chen et al., 2006). Por utilizarem a glutationa reduzida (GSH) como substrato, a indução da biossíntese de PCs pode resultar em depleção de GSH (Zhang et al.,

2005; Rabêlo et al., 2018). Dessa forma, alterações nas concentrações de GSH e PC podem ser úteis indicadores para detecção de respostas bioquímicas de proteção contra a toxicidade por metais pesados em plantas.

Além de contaminação do solo por metais pesados, o aumento de substâncias potencialmente tóxicas na atmosférica, como dióxido de carbono (CO_2), ozônio troposférico (O_3), óxido nitroso (N_2O) e outros compostos voláteis, impõem novos desafios e estresses abióticos às espécies vegetais, principalmente em áreas urbanas (Matyssek et al., 2014). A combinação de estressores ambientais (no solo e no ar) pode ser ainda mais desafiadora para a sobrevivência de espécies vegetais, em comparação com apenas estressores isolados. Por exemplo, *Lolium perenne* e *L. multiflorum* elevam a síntese de fitoquelatinas quando cultivadas em solo contaminado com Cd, porém quando cultivadas em solo contaminado, mas submetidas à elevação na concentração de CO_2 atmosférico, há redução na concentração de fitoquelatinas e menor capacidade de tolerância ao Cd (Jia et al., 2010).

O O_3, além de impulsionador de mudanças climáticas, é um poluente altamente oxidativo, sendo considerado uma ameaça aos ecossistemas terrestres e à biodiversidade, causando efeitos adversos em plantas e microbiota do solo, entre outros organismos presentes nos ecossistemas. Ao interferir na composição das comunidades microbianas do solo, esse poluente pode alterar exsudatos das raízes, atividades enzimáticas no solo e a ciclagem de nutrientes (Agathokleous et al., 2020). O O_3 causa inúmeros efeitos fisiológicos adversos nas espécies vegetais, como a redução da condutância do mesofilo da folha e na capacidade de carboxilação com consequente limitação do processo fotossintético (Xu et al., 2019), redução na taxa fotossintética saturada de luz, eficiência fotoquímica do fotossistema II (PSII), conteúdo de clorofila, massa foliar por área e biomassa radicular (Shang et al., 2017), além de senescência foliar acelerada devido ao aumento da peroxidação lipídica, juntamente com alterações na atividade de enzimas antioxidantes (Dai et al., 2017). Além dos efeitos isolados do O_3, a disponibilidade de nutrientes (ou metais pesados) pode afetar a tolerância das plantas à exposição a este poluente atmosférico, bem como a intensidade das alterações em parâmetros fisiológicos como biomassa total (Zhang et al., 2018). Enquanto alguns estudos mostram que a combinação de metais pesados e ozônio podem causar efeitos mais acentuados do que a exposição a um estressor isolado (Ormrod, 1977; Castagna et al., 2015), revelando que o efeito combinado da toxicidade por MPs e O_3 afetam negativamente crescimento vegetal, processo fotossintético e regulação do sistema de defesa antioxidante (Dawud et al., 2026), outros encontraram ausência de interação entre esses estressores (Xu et al., 2020). Portanto, verificar se o aumento da disponibilidade de Cu, Zn e Ni pode amplificar os efeitos negativos do O_3 é de extrema importância levando em consideração o aumento conjunto destes estressores abióticos

no ambiente (Calfapietra et al., 2015).

Espécies pertencentes a diferentes grupos funcionais e hábitos de vida apresentam respostas fisiológicas, metabólicas e moleculares distintas (Krämer, 2010), e é esperado que essa diversidade de respostas ocorra na Mata Atlântica, que é *megadiversa* em espécies vegetais com diversos hábitos de vida e distribuídas em estratos (Marques et al., 2021). Devido à variedade de hábitos de vida e estratégias de sobrevivência, espécies nativas da Mata Atlântica apresentam potencial de estudo sobre mecanismos de tolerância contra estressores abióticos conjuntos. Estudo experimental de Brandão (2020), revelou que o conteúdo absoluto de Ni e Zn em espécies arbóreas refletiu diretamente o nível desses metais nas formas disponíveis no solo, sendo mais alto em espécies pioneiras (crescimento rápido) do que nas espécies não pioneiras (crescimento lento), com distintas estratégias de defesa antioxidante das espécies ao estresse imposto pelos metais. Outro estudo experimental evidenciou que espécies arbóreas da Mata Atlântica apresentam alta capacidade de tolerância ao Cu, devido à presença de mecanismos fisiológicos como acúmulo radicular e restrição na translocação (Siqueira et al., 2021).

Contudo, a capacidade de tolerância através da produção de exsudatos (ácidos orgânicos radiculares), síntese de moléculas quelantes de metais pesados (fitoquelatinas) e antioxidantes (ácido ascórbico e glutationa) são ainda desconhecidas em diversas espécies nativas da Mata Atlântica, em especial em espécies com diferentes hábitos de vida. Adicionalmente, o conhecimento sobre a tolerância de espécies vegetais submetidas à combinação de estressores ambientais (metais pesados + ozônio), que são eventos interconectados em áreas antropizadas, ainda é incipiente e necessita de maior atenção. Nesse contexto, o presente estudo foi desenvolvido com o objetivo de ampliar o entendimento sobre essa temática.

As hipóteses gerais testadas foram:

1) Espécies nativas da Mata Atlântica, quando cultivadas em solução com concentrações elevadas de metais pesados, elevam a produção de compostos bioquímicos de tolerância como forma de mitigar danos fisiológicos;

2) Espécies vegetais de diferentes hábitos de vida e taxa de crescimento apresentam níveis distintos de tolerância frente à exposição à metais pesados;

3) A espécie tolerante a metais pesados também pode ser tolerante à exposição a outro estressor abiótico (O_3);

4) A exposição combinada a metais pesados e ozônio causará efeitos deletérios mais expressivos do que quando aplicados isoladamente, reduzindo sua capacidade de tolerância aos metais pesados.

Os objetivos gerais foram:

1) Estabelecer sistema hidropônico, substrato e concentração de metais pesados para estudo com diferentes espécies da Mata Atlântica;

2) Avaliar se a capacidade de tolerância de espécies vegetais nativas da Mata Atlântica possui relação com o hábito de vida e/ou taxa de crescimento, e desvendar seus mecanismos bioquímicos de tolerância;

3) Verificar os efeitos de concentrações crescentes de ozônio troposférico na biomassa de uma espécie nativa da Mata Atlântica;

4) Investigar se a presença do ozônio troposférico afeta a capacidade de tolerância à metais pesados de uma espécie tolerante, e se a combinação de estressores abióticos (Metais pesados + ozônio) causa efetivos negativos acentuados.

Para investigar esses efeitos e explorar melhor a capacidade de tolerância de espécies vegetais nativas da Mata Atlântica frente a esses estressores, esta tese foi organizada em quatro capítulos, os quais foram concebidos de forma sequencial e integrada, com os resultados de cada etapa fundamentando as perguntas, metodologia e aplicação da seguinte etapa.

No Capítulo 1, foram apresentados resultados de 2 experimentos para estabelecer e otimizar as bases metodológicas do estudo, definindo o sistema de cultivo hidropônico, o substrato mais adequado e as concentrações de metais pesados (Cu, Zn e Ni) a serem utilizadas nos experimentos subsequentes.

No Capítulo 2, utilizando o sistema hidropônico otimizado no capítulo anterior, foram apresentadas as variações na capacidade de tolerância, acúmulo de metais e respostas fisiológicas e bioquímicas frente a uma concentração elevada de Cu, Zn e Ni de 5 espécies de diferentes formas de vida e taxas de crescimento.

Com base no resultado do Capítulo 2, após identificar a espécie mais tolerante aos metais pesado, foi realizado experimento visando a elucidar as respostas desta espécie ao ozônio troposférico de forma isolada, focando na biomassa e níveis críticos de O_3 (Capítulo 3) e na investigação dos mecanismos de tolerância frente à combinação de estressores (HMs + O_3) (Capítulo 4).

Vale destacar que os Capítulos 2 e 3 são constituídos por manuscritos publicados ou aceitos para publicação nos periódicos *Science of the Total Environment* e *Journal of Forestry Research*, respectivamente. Esses manuscritos foram incluídos nesta tese na forma em que serão publicados, em conformidade com as políticas de direitos autorais das respectivas editoras (*Elsevier* e *Springer Nature*).

Revista pré-definida para submissão: Hoehnea

Capítulo I

Growth and Physiological Responses of *Schinus terebinthifolia* to Increasing Heavy Metal Concentrations in an Optimized Hydroponic System

Matheus Casarini Siqueira[a*], João Vítor Casimiro[a], Alex do Nascimento[b], Mirian Cilene Spasiani Rinaldi[a], Armando Reis Tavares[c], Marisa Domingos[a]

[a] *Instituto de Pesquisas Ambientais, São Paulo, São Paulo, Brasil. Av. Miguel Estefno, 3687 - CEP 04301-012*

[b] *Universidade Federal do ABC, Santo André, São Paulo, Brasil. Av. dos Estados, 5001 - CEP 09280-560*

[c] *Instituto Agronômico, Jundiaí, São Paulo, Brasil. Av. Barão de Itapura, 1481 - CEP 13020-902*

*Corresponding author: matheus.casarini1@gmail.com

ABSTRACT

Contamination by multiple heavy metals (HMs) poses a growing global environmental threat, and the assessment of plant HM tolerance is vital especially for important forest species such as *Schinus terebinthifolia*, a native tree of the Atlantic Forest, a threatened biodiversity hotspot. Hydroponic studies offer some experimental advantages to unravel plant responses under heavy metal stress, but defining efficient growing system and appropriate substrate is crucial. To address these points, two studies were conducted with *S. terebinthifolia* under circular hydroponics using the "Dutch Bucket" method. In the first study, the species was grown in expanded perlite or phenolic foam, then growth and biomass characteristics were accessed to determine the best inert substrate. In the second study, *S. terebinthifolia* was subjected to increasing concentrations (0, 25, 50, or 100 μmol) of a combination of copper (Cu), zinc (Zn), and nickel (Ni) for 4 weeks, and its morphological, physiological and survival rate parameters were analyzed to assess the species' tolerance to multiple heavy metals. Our results demonstrated that expanded perlite or phenolic foam are equally suitable for *S. terebinthifolia* cultivation. When exposed to combined heavy metals, the species displayed toxicity symptoms but maintained survival rate up to 50 μmol. Tolerance was conferred through root metal accumulation and restriction without compromising root biomass. Our findings demonstrate the *S. terebinthifolia* tolerance and phytoremediation potential for multi-heavy metal contaminated sites.

Key-words: expanded perlite, phenolic foam, copper, zinc, nickel

INTRODUCTION

Environmental contamination with heavy metals (HMs) is among the main worldwide problems and concerns of current time, due to their bioaccumulation in living organisms and ecotoxicity (Zwolak et al., 2019). Combined exposure to multiple HMs presents a greater risk to organisms and ecosystems than single-metal exposure (Timothy and Willians, 2019). Multiple HMs such as Copper (Cu), Zinc (Zn) and Nickel (Ni) have been detected at concerning levels in urban soils (Swain et al., 2024), and in forest fragments such as in the Atlantic Forest, a biodiversity hotspot in Brazil (Nakazato et a. 2021). The excess of HMs in plants result in reduced biomass, yield, photosynthetic capacity, and metabolic disturbances (Nagajyoti et al., 2010). However, plants have different HM-tolerance levels and capacities, and therefore, understanding the effects of HMs on plant species, as well as the search for tolerant species, has become an increasingly relevant research topic.

The effects of HMs on plants can be studied using several experimental approaches, including cultivation of plants in mining-impacted soils (Zabergja-Ferati et al., 2021), in natural forest soils with controlled HM additions (Siqueira et al., 2021), and in hydroponic systems

(Sumalan et al., 2023). A significant number of studies have already been conducted on plants cultivated under excess HMs in soils. However, soil-based studies present some challenges in understanding the interaction between HMs and plants, as soils exhibit substantial physicochemical variability that influences the complexation of HMs (Caporale and Violante, 2016). This is due to interactions between metals and negatively charged clay particles, as well as the presence of organic matter, affecting the available concentrations for plant absorption (Fan et al., 2015). This also complicates the determination of the total metal concentrations to which the plant is effectively exposed. Furthermore, the presence of microorganisms (e.g. algae, fungi, and bacteria) in soils can alter the dynamics of nutrient availability and competition (Hassani et al., 2018). Therefore, hydroponic techniques offer important methodological advantages by enabling establishing precise control of nutrient concentrations supplied to plants. Hydroponic methods are based on growing plants directly in a nutrient solution. Compared to soil-based systems, hydroponic systems allow precise control over the concentration of added nutrients (including HMs) and optimization of their bioavailability, providing appropriate conditions to studies aimed at understanding plant responses to abiotic nutritional stresses (Mattos et al., 2023). Hydroponic systems ensure maximum nutrient absorption through pH control, absence of complexation with soil particles, and constant water supply, thereby facilitating and isolating the effect of HMs on plant physiology (Sathyanarayan et al., 2023).

Additionally, inert substrates can be added to hydroponic system, to further provide some realistic advantages, as seedlings are subjected to conditions of mechanical resistance and porosity structure similar to those of soil, thus simulating a more natural physiological root growth (Rani et al., 2021). The choice of substrate in hydroponic systems can influence plant growth, development, and productivity, while also affecting the observability of specific traits such as root anatomy and compound exudation (Patil et al., 2020). Therefore, evaluating the viability of hydroponic cultivation with different inert substrates is essential for optimizing both experimental conditions and phenotypic observations, particularly for elucidating plant responses to HM toxicity.

This study aimed to optimizing the hydroponic system model “Dutch Bucket” to investigating the effect of multiple heavy metals (Cu, Zn, and Ni) on the growth, physiology and consequently to determining HM-tolerance level of a key pioneer tree from the Atlantic forest. *Schinus terebinthifolia* Raddi, popularly known as “Brazilian pepper tree” was chosen as a model species due to its ornamental, economic and ecological importances (Lorenzi 2016) and to its fast growth and high biomass production (Meyer, 2011), which facilitates the detection of changes in seedling growth and physiology. The optimization of a system to

cultivate and study *S. terebinthifolia* and unravel its tolerance capacity to multiple HMs could be essential for conservation and restoration programs.

MATERIAL AND METHODS

Two experiments were conducted with *S. terebinthifolia* seedlings, as described below. The first aimed to optimize the hydroponic system and select the most suitable inert substrate. The second experiment investigated its uptake capacity, as well as growth and physiological responses to increasing concentrations of HMs (Cu, Ni, and Zn), using the optimized hydroponic method, thereby enabling the discussion of its tolerance levels.

Experiment 1 – Setting up the hydroponic system and substrate test

Two hydroponic systems were set up in a greenhouse under semi-controlled conditions of temperature, relative humidity, and light (on average, 25 ºC, 80%, and 640 µmol m^{-2} s^{-1}). The hydroponic system adopted was based on the Dutch Bucket System method described in Ghorbel et al. (2021). In this continuous circulation system, the plants were placed in black pots with holes at the bottom for drainage and were continuously supplied with a balanced nutrient solution through automatic water pumps, as shown in the representation below (Fig. I1).

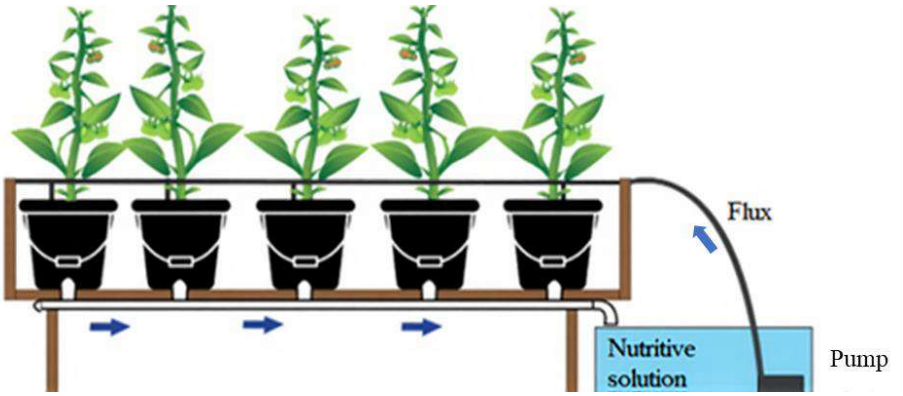

Fig. I 1. Representation of a "Dutch Bucket" hydroponic system. Source: Adapted from NoSoilSolution.com, 2025.

In system A, the saplings were grown in expanded perlite (Fig. I2A), and in system B the seedlings were grown in phenolic foam (Fig. I2B), both acquired from commercial hydroponic grade producers and placed inside the pots. The loss of both substrates through the holes was prevented by means of a nylon mesh inserted inside the pot. In each system, fifteen 6 month-old *Schinus terebinthifolia* saplings were grown for 2 weeks under 10% strength balanced HA nutrient solution (Hoagland and Arnon, 1950), followed for 4 weeks under 25% strength balanced HA, which was renewed weekly. Prior to cultivation in hydroponic systems, the roots were washed in distilled water to completely remove the original substrate (composted soil).

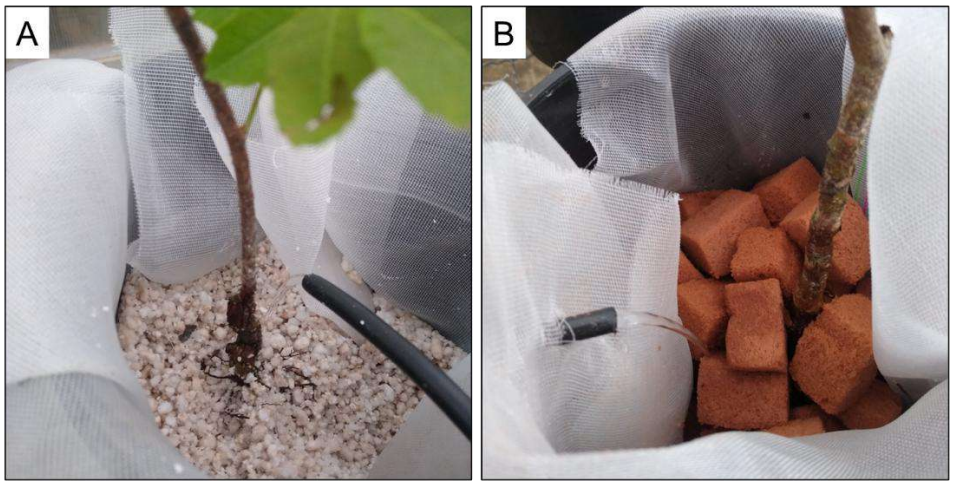

Fig. I 2. *Schinus terebinthifolia* hydroponically cultivated under expanded perlite (A) or phenolic foam (B).

At the end of experiment (4 weeks), the individuals were removed from the system, and the height, stem diameter, number of leaves, relative chlorophyll content (SPAD index) and pigment concentration (Minocha et al., 2009) were measured. The plants were then separated into leaves, stems and roots dried at 60 ºC until constant weight, and the dry biomass was measured in analytical scale.

Experiment 2 – Increasing heavy metal concentrations study

The results of the first experiment (as shown in detail below) indicated that perlite is an adequate inert substrate and confirmed the successful establishment of *S. terebinthifolia* under the hydroponic system, allowing to conduct this second experiment.

S. terebinthifolia saplings were cultivated in perlite under a control solution (25% strength HA nutrient solution) or to three increasing concentrations of combined heavy metals (Cu, Ni, and Zn) added to the nutrient solution (T1 to T3), as bellow:

Control: 25% strength of HA nutrient solution (Hoagland & Arnon, 1950).

T1: 25% HA + 25, 25, 25 µM Cu, Ni and Zn, respectively.

T2: 25% HA + 50, 50, 50 µM Cu, Ni and Zn, respectively.

T3: 25% HA + 100, 100, 100 µM Cu, Ni and Zn, respectively.

Heavy metal concentrations were defined based on studies with different species cultivated in hydroponics enriched with metals (Soares et al., 2000; Vassilev et al., 2007; Pietrini et al., 2015). Solutions were ionically balanced to avoid increase of nutrients other than Cu, Zn and Ni (Table I1). All solutions were adjusted to 5.6 pH and weekly renewed.

Tab. I 1. Hoagland and Arnon (1950) balanced nutrient solution (25% strength - Control), or enriched with 25 (T1), 50 (T2) or 100 (T3) µM of Cu, Zn, and Ni.

Nutrient Source	Control	T1	T2	T3
--		µM		
KNO_3	1500	1500	1500	1500

$Ca(NO_3)_2$ $4H_2O$	1000	1000	1000	1000
$NH_4H_2PO_4$	500	500	500	500
$MgSO_4$ $7H_2O$	250	250	250	250
KCl	50	50	50	50
H_3BO_3	25	25	25	25
$MnSO_4$ H_2O	0.6	0.6	1	1
H_2MoO_4 (85%)	0.5	0.5	1	1
Fe - EDTA	19	19	19	19
$CuSO_4$ $5H_2O$	**0.100**	**25**	**50**	**100**
$ZnSO_4$ $7H_2O$	**0.500**	**25**	**50**	**100**
$NiSO_4$ $6H_2O$	**0.001**	**25**	**50**	**100**
$(NH_4)_2SO_4$	299	225	150	0
NH_4NO_3	0	74	149	299

The experimental design adopted was completely randomized, with 4 treatments and 15 plants per treatment, totaling 60 plants The experiment lasted 45 days, with 14 days for adaptation to the hydroponic system (all plants received 10% HA in the first 7 days, then 25% HA up to 14 days), and 31 days of exposure to control or HMs treatments. The acclimatation phase (increasing nutrient solution strength for 14 days) was based in established hydroponic protocols (Jones, 2014), while the experiment phase (30 days of constant exposure) was based on the species biomass accumulation and growth rate (Meyer, 2011). At the end of experiment, the visible, morphological and physiological measurements were performed to assess plant tolerance and responses to increasing HM concentrations.

Analytical methods

Survival rate and biometrics

Survival rate (%) was performed by counting the number of living plants. The biometric parameters analyzed at the end of experiment were plant height (cm), stem diameter (m) and number of leaves.

Solution pH and electrical conductivity

Weekly, at the day of nutrient solution replacement, 50 mL of the solution was collected and the solution pH (ranging from 0-14) and electrical conductivity (µS cm^{-1}) was analyzed using a portable multiparameter sensor (Combo-5, AKSO).

Physiological parameters

The physiological parameters of gas exchange, chlorophyll fluorescence, relative chlorophyll content (SPAD index) and pigment concentration were determined in the 1st physiologically mature leaf of each plan

Net CO_2 assimilation (*A*, µmol CO_2 m^{-2} s^{-1}), stomatal conductance (*gsw*, mol H_2O m^{-2}

s^{-1}) and the maximum efficiency of photosystem II in the dark-adapted state (F_v/F_m) were measured with a portable infrared gas analyzer (IRGA) (LI6800 – Li-Cor). Measurements were carried out between 8 am and 12 pm at 400 ppm CO_2, 50% relative humidity and 25ºC temperature as established conditions. The ideal value of photosynthetically active radiation (PAR, µmol photons m^{-2} s^{-1}) was obtained t. through assimilation curve in response to the decrease in PAR flux (from 2,000 to 0 µmol m^{-2} s^{-1}) carried out in healthy individuals (plants from control treatment, n = 3). F_v/F_m measurements were performed in dark-adapted leaves (20 minutes covered in aluminum foil), by applying a 660 nm saturating rectangular flash (3,000 µmol photons m^{-2} s^{-1}) for 3 milliseconds.

The SPAD index was determined using a SPAD-502 manual chlorophyll meter (Konica Minolta), averaging 5 leaf sections from each plant. Total chlorophyll (*a* + *b*) and carotenoid concentrations (µg g^{-1} leaf fresh weight) were determined in three discs (Ø = 0.5 cm) removed from the central region of the leaf, avoiding the veins. Leaf samples disks were immersed in 96% ethanol kept in the dark for 24 hours, periodically vibrated to ensure extraction homogeneity. The extract was spectrophotometrically analyzed at λ = 471 nm, 649 nm, 664 nm and 750 nm, and then chlorophyll *a* (*Chl a*), chlorophyll *b* (*Chl b*) and total carotenoids were determined by the formulas derived from Minocha et al. (2009):

$$Chl\ a = (13.36 \times A664) - (5.19 \times A649)$$

$$Chl\ b = (27.43 \times A649) - (8.12 \times A664)$$

$$Carotenoids = [(1000 \times A470) - (2.13 \times Chl\ a) - (97.64 \times Chl\ b)] \div 209$$

Biomass and heavy metal content in tissues

The plant was separated into roots, stem and roots, and oven-dried at 60 ºC until constant weight for dry mass determination (g). The dry plant samples (leaf, stem and roots) were crushed in a knife mill until became a homogeneous powder, and later sent to Fertility Laboratory, Agronomic Institute, Campinas, Sãoo Paulo State, Brazil, to determine copper (Cu), zinc (Zn) and nickel (Ni) concentrations (mg g^{-1} tissue), performed by Flame Absorption Spectrometry (Raij et al., 2001).

Image processing

The images of the plants (Fig. I3 and I7) have been optimized for improved visual clarity through contrast adjustments, brightness enhancement, background removal and scale insertion using the GNU Image Manipulation Program (GIMP, version 3.0.4). The original, unprocessed images are available from the corresponding author upon request.

Statistical analysis

Statistical analyses were performed using GraphPad Prism (v 9.0). Data from both experiments were assessed for normality (Shapiro-Wilk test) and homoscedasticity (Brown-Forsythe test). When assumptions were met, differences between treatments were analyzed by one-way ANOVA followed by Tukey's post hoc test ($p \leq 0.05$). If assumptions were violated, data were log-transformed and re-analyzed. If transformed data still violated assumptions, the non-parametric Kruskal-Wallis's test was applied, followed by Dunn's post hoc test for multiple comparisons. For HM concentration in tissues, a two-way ANOVA (factors: plant tissues (leaf, stem and roots) and HM treatments) was performed, with significant interactions explored using Tukey's post hoc test.

RESULTS

Experiment 1

The *S. terebinthifolia* saplings were able to grow and accumulate biomass compared to the beginning of the experiment conducted under hydroponic conditions (Fig. I3). There were no significant visual differences in *S. terebinthifolia* between cultivation under expanded perlite (Fig. I3B) or phenolic foam (Fig. I3C).

Fig. I 3. *Schinus terebinthifolia* at the beginning of the experiment (A), and after 30 days cultivated in "Durch bucket" hydroponic system under perlite (B) or phenolic foam (C). Red line scale= 10 cm.

There was no difference in the height, stem diameter, number of leaves and total biomass of *S. terebinthifolia* grown in expanded perlite or phenolic foam (Fig. I4).

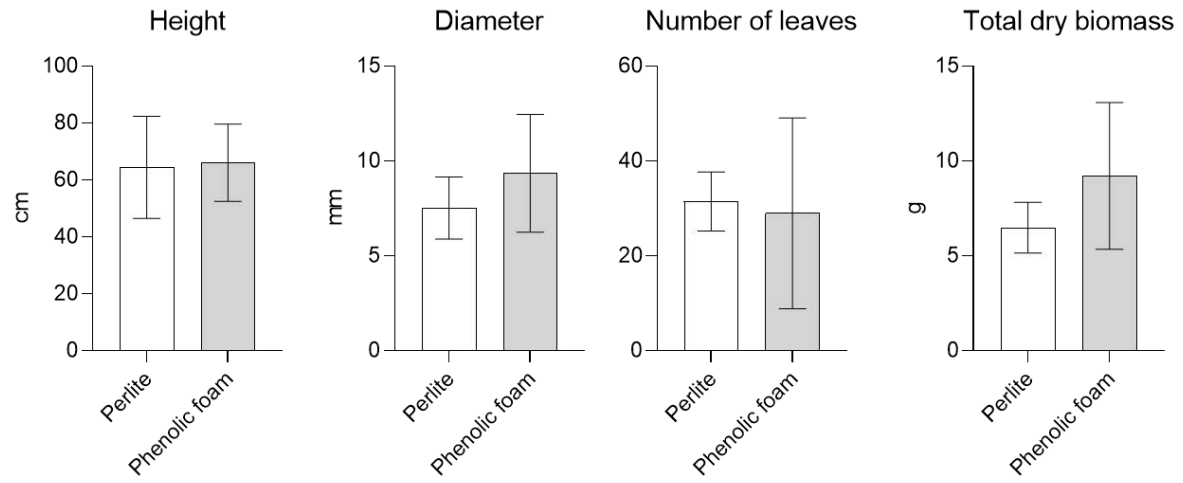

Fig. I 4. Height, stem diameter, number of leaves and total dry biomass of *S. terebinthifolia* cultivated under expanded perlite, or phenolic foam.

There was no difference in the relative chlorophyll content (SPAD index), nor in the concentration of chlorophylls and carotenoids in the leaves of *S. terebinthifolia* grown under expanded perlite or phenolic foam (Fig. I5).

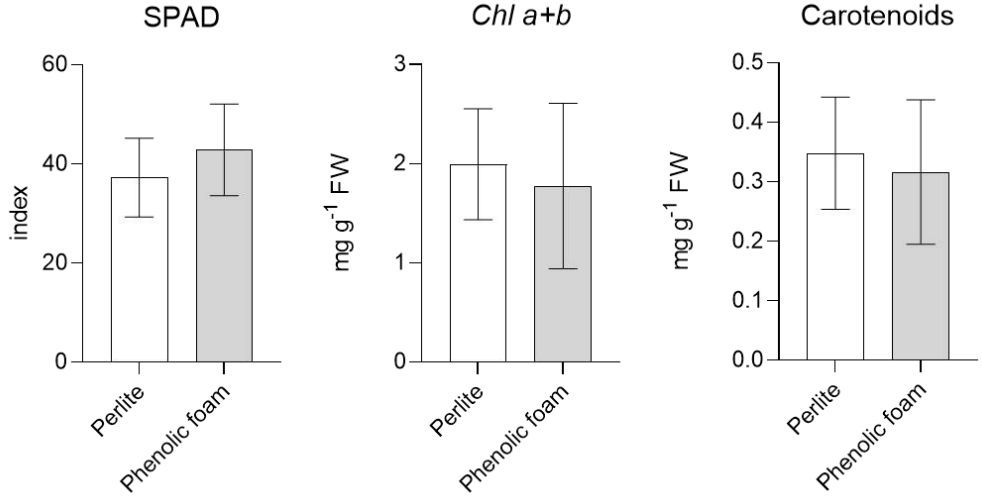

Fig. I 5. Relative chlorophyll content (SPAD index), total chlorophyll (*Chl a+b*) and carotenoids concentration in leaves of *S. terebinthifolia* cultivated under expanded perlite or phenolic foam.

Experiment 2

Biometrics, biomass and survival rate

There was a reduction in *S. terebinthifolia* height in treatments T1, T2, and T3, compared to the control (Fig. I6). There was no change in stem diameter between treatments. There was a progressive reduction in the number of leaves in *S. terebinthifolia* cultivated under increasing heavy metals

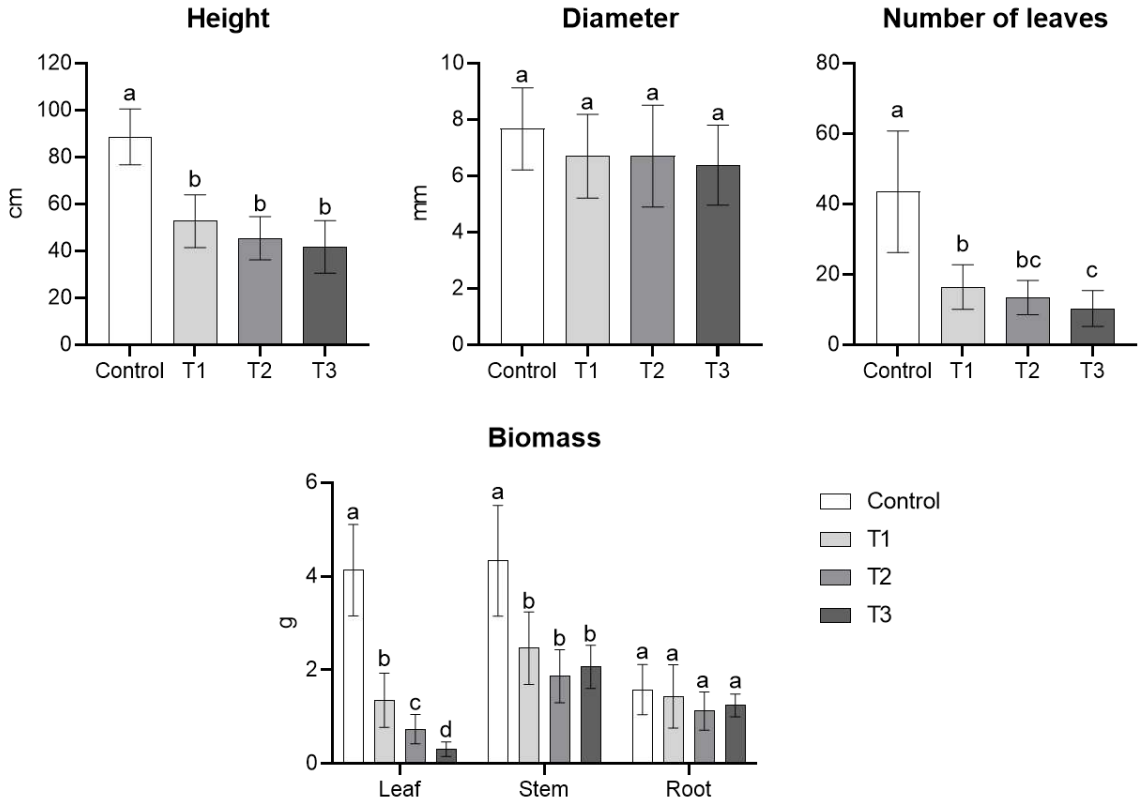

Fig. I 6. Height, stem diameter, number of leaves, and leaf, stem and root dry biomass of *S. terebinthifolia* cultivated under Control (balanced nutrient solution), T1 (25 µM Cu, Zn and Ni), T2 (50 µM Cu, Zn and Ni) or T3 (100 µM Cu, Zn and Ni). Different letters indicate significant difference between treatments, according to Tuckey test ($p \leq 0.05$).

There was a progressive decrease in *S. terebinthifolia* leaf dry mass under T1, T2 and T3, respectively, compared to control. The dry biomass of stems was significantly reduced in treatments T1, T2, and T3, compared to the control. There was no change in root dry biomass between treatments (Fig. I6).

In treatment T3, 60% of *S. terebinthifolia* plants survived, contrasting with the survival rate observed in control, T1 and T2 (94% survival each). Under control, T1 and T2, one individual did not survive, while in T3 six individuals did not survive at the end of experiment. The visual aspects of the plants reflected the heavy metal stress and survival rate (Fig. I7).

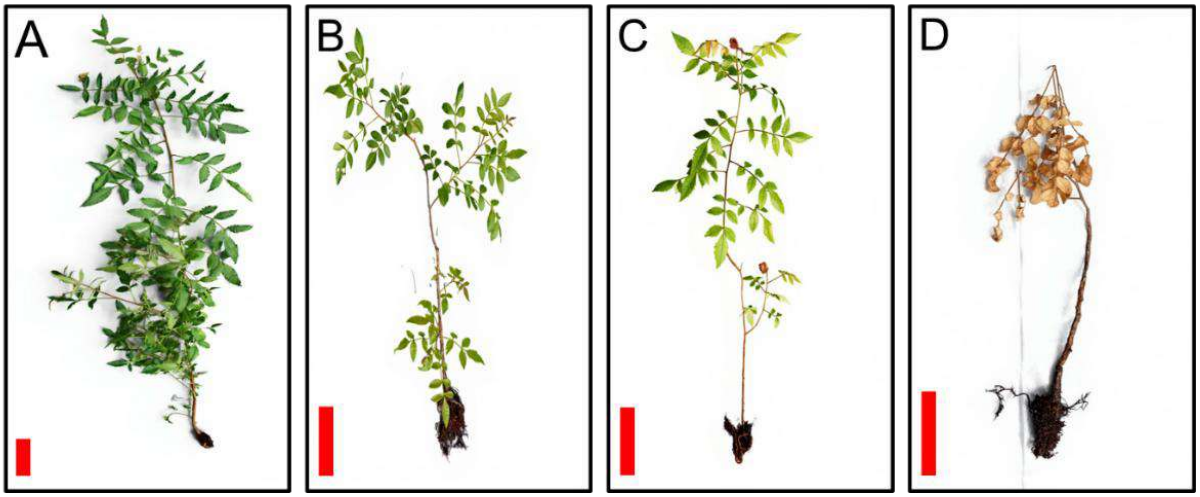

Fig. I 7. *Schinus terebinthifolia* grown in hydroponic solution under control (balanced nutrient solution - A), T1 (25 µM Cu, Zn and Ni - B), T2 (50 µM Cu, Zn and Ni - C), T3 (100 µM Cu, Zn and Ni - D). (In Figure D, the photo of a dead individual was chosen to emphasize the high mortality rate in this treatment. Red scale bar = 10 cm.

Heavy metal content in tissues

In *S. terebinthifolia* leaves, there was an increase in Cu concentration in treatment T3 compared to the others, while the opposite was observed for Zn, with a reduction in treatment T3 (Fig. I8). There was no difference in Cu or Zn between the control, T1, and T2 treatments. For Ni in the leaves, there was an increase in treatment T3 compared to the control, with a greater increase in treatments T1 and T2, with no difference between them (T1 = T2).

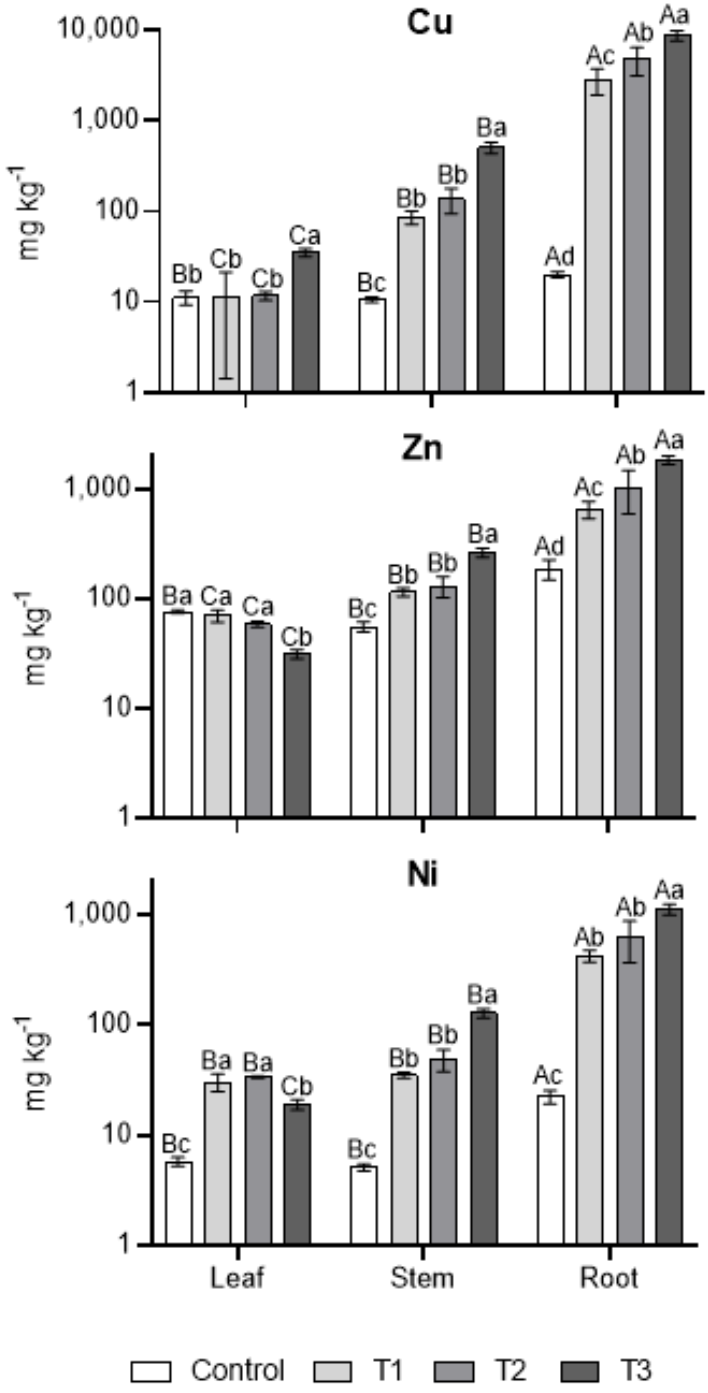

Fig. I 8. Mean concentrations of copper (Cu), zinc (Zn) and nickel (Ni) (mg kg^{-1} dry mass), in leaves, stem and roots of *S. terebinthifolia* cultivated under Control (balanced nutrient solution), T1 (25 µM Cu, Zn and Ni - B), T2 (50 µM Cu, Zn and Ni - C) or T3 (100 µM Cu, Zn and Ni - D). Distinct lowercase letters indicate significant differences between HM treatments in the same tissue, while uppercase letters indicate differences between tissues in the same HM treatment, according to Tuckey test ($p \leq 0.05$).

In the stem, the three added heavy metals, Cu, Zn, and Ni, show the same accumulation pattern: the lowest values were found in the control treatment, with an increase in treatments T1 and T2, which did not differ from each other (T1 = T2), and the greatest increase in treatment T3.

In the roots, there was a continuous increase in the concentration of Cu, Zn, and Ni,

corresponding to the increase in the concentration of these metals in the nutrient solution. Only for Ni was there no difference in the concentration of this element in the roots between treatments T1 and T2.

In the control treatment, there was no difference in the concentration of Cu, Zn, or Ni between leaves and stem, while the root showed the highest concentrations. In the treatments with added metals, there was a progressive increase in their concentration following this order: Leaf (lowest accumulation), stem (intermediate accumulation), and root (highest accumulation).

Physiological parameters

There was a reduction in net carbon assimilation (*A*) and stomatal conductance of *S. terebinthifolia* in treatments T1, T2, and T3 compared to the control, with no difference in *A* between treatments T2 and T3, and no difference in gsw for all treatments with added HMs (T1 = T2 = T3) (Fig. I9). There was a progressive reduction in the maximum efficiency of photosystem II (Fv/Fm) of *S. terebinthifolia* leaves in treatments T1, T3, and T2, respectively.

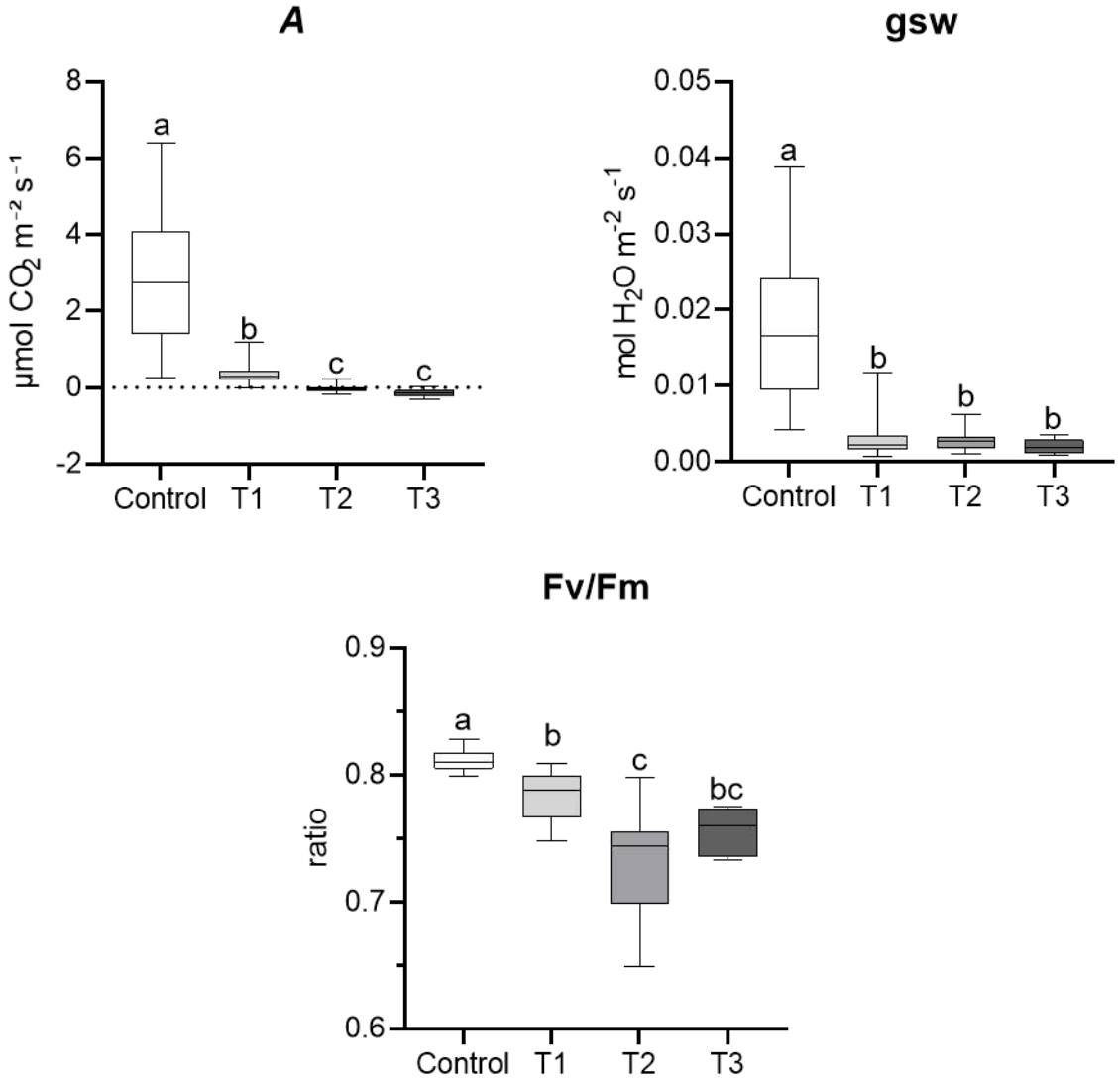

Fig. I 9. Net carbon assimilation (*A*), stomatal conductance (*gsw*), and maximum efficiency of the photosystem II of dark-adapted leaves (Fv/Fm) of *S. terebinthifolia* cultivated under Control (balanced nutrient solution), T1 (25 µM Cu, Zn and Ni - B), T2 (50 µM Cu, Zn and Ni - C) or T3 (100 µM Cu, Zn and Ni - D). Distinct letters indicate significant differences between treatments, according to Dunn's test ($p \leq 0.05$).

There was a reduction in the total chlorophyll and carotenoids concentration, and in the relative chlorophyll content (SPAD index) of *S. terebinthifolia* leaves cultivated under T1, T2 and T3, equally, compared to control (Fig. I10).

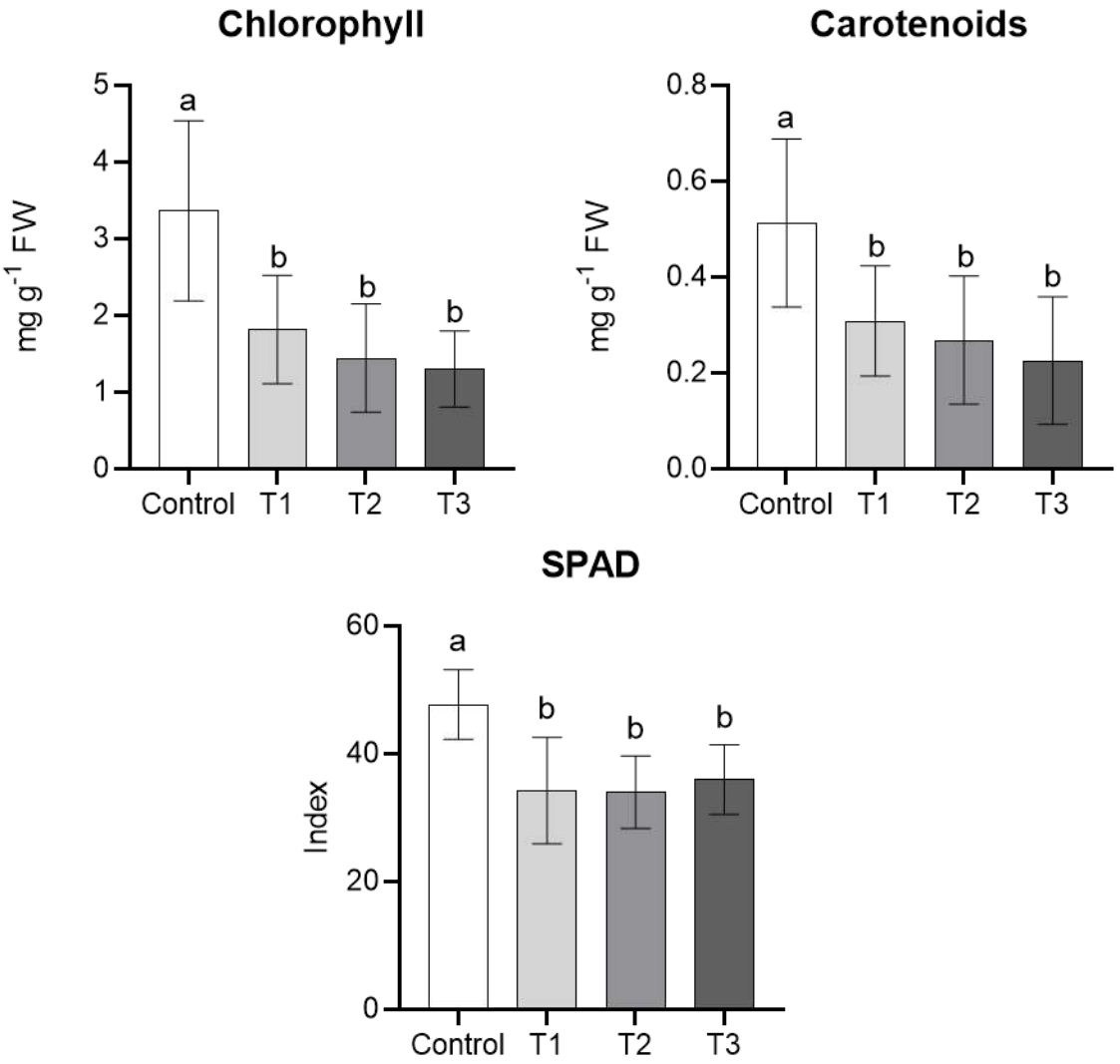

Fig. I 10. Total chlorophyll, carotenoids, and relative chlorophyll content (SPAD index) of *S. terebinthifolia* cultivated under Control (balanced nutrient solution), T1 (25 µM Cu, Zn and Ni - B), T2 (50 µM Cu, Zn and Ni - C) or T3 (100 µM Cu, Zn and Ni - D).

pH and conductivity

There was an increase in the pH of the solutions with heavy metals, ranging from 4.5 (control) to 5.6 (T2 and T3) at the end of experiment (Fig. I11). There was no difference for electrical conductivity (EC) between treatments.

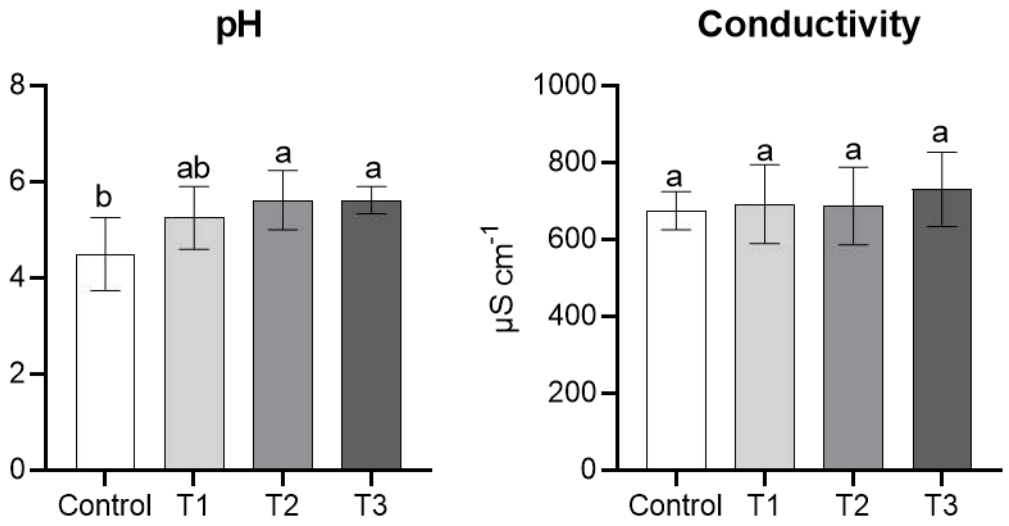

Fig. I 11. pH and electrical conductivity of the control nutrient solution, T1, T2 and T3.

DISCUSSION

Experiment 1

The continuous circulation "Dutch Bucket" hydroponic system proved to be efficient for the cultivation of *S. terebinthifolia*. Most hydroponics studies are conducted with vegetables and herbaceous species of agricultural interest, while studies involving forest species are still scarce (Erere et al., 2021), especially Atlantic Forest species. Although some hydroponic studies with *S. terebinthifolia* exist (Dobbss et al., 2018; Silva et al., 2021; Mattos et al., 2023), to our knowledge, this is the first study testing the effectiveness and viability of different substrates media in growth outcome of *S. terebinthifolia* cultivated under the circular hydroponic "Dutch Bucket" system.

Both perlite and phenolic foam proved to be equally viable and effectively inert substrate media for *S. terebinthifolia* hydroponic cultivation. Despite the similarity in the outcomes, some details should be considered when choosing a substrate, as price, accessibility, and the physical characteristics (Rani et al., 2021). Perlite offers high aeration and porosity that facilitate root growth, along with low cost and reusability; however, it has low water retention capacity. In contrast, phenolic foam provides high water retention but at a higher cost (Han et al., 2014). This factor is particularly important in active hydroponic systems, as power outages that interrupt nutrient solution circulation for extended periods may lead to plant loss due to water deficiency; in this context, phenolic foam offers a clear advantage. The cultivation objective is also highly relevant in the choice of substrate, which was decisive in our study. Perlite proved to be much easier to remove from the roots, causing little or no interference to the roots after removal, while phenolic foam required greater effort for complete root removal, resulting in greater mechanical wear (data not shown). Therefore, for studies aimed at analyzing

root morphology, anatomy, and functionality (such as exudation and biochemical analysis of compounds), expanded perlite is preferable. Given the need for a substrate that is low-cost, easy to handle and remove, and does not require strict control of plant hydration, perlite was selected for use in the subsequent experiment.

Experiment 2

When cultivated under increasing concentrations of HM, there was a negative effect on virtually all growth and physiological parameters measured in *S. terebinthifolia*. These effects are the result of metabolic, nutritional, and biochemical disruptions caused by HM toxicity (Dubey et. al., 2018). One of the precursors of physiological impairments in plant physiology is the excessive production of reactive oxygen species (ROS), which affects normal cell function and results in negative impacts on plant growth and development (Shahid et. al., 2014). The effects of these possible disruptions were manifested in *S. terebinthifolia* by reduced height growth, shoot biomass, photosynthetic pigments and activity (gas exchange and chlorophyll fluorescence). These are clear symptoms of HM-toxicity (Huihui et al., 2020). Treatments T2 and T3 proved to be aggressive to the photosynthesis of *S. terebinthifolia* seedlings, highlighted by negative carbon assimilation (photorespiration) and severe disruption of photosystem efficiency.

In addition to the physiological parameters affected, the negative impact of excess HM became visible. The leaves showed special sensitivity to HM-toxicity by reduced number and biomass production, while the stem and roots showed lesser impacts revealed by constant diameter size and root biomass. In the treatment with the highest concentration of heavy metals (T3), in addition to alive plants with high toxicity symptoms, a high mortality rate (40%) was observed, demonstrating that the concentration of 100 µmol of the combination of Cu, Zn and Ni was toxic to *S. terebinthifolia* in only 4 weeks of exposure. Further studies aiming to understand biochemical, molecular, and more detailed responses of *S. terebinthifolia* under HM-stress, should preferably be conducted using concentrations lower than 50 µmol of Cu, Zn, and Ni, in order to obtain measurable tolerance responses while avoiding high mortality.

The pH of the nutrient solution gradually increased with higher heavy metal concentrations. Under stress, plants can release root exudates to increase pH and limit further HM the uptake (Javed et al. 2013). This is a tolerance strategy to promote phytostabilization of toxic elements, avoiding their absorption while maintaining water absorption capacity (Siyar et al., 2020). This could be a tolerance strategy adopted by *S. terebinthifolia*. Further studies investigating the root exudation capacity and compounds profile will elucidate this tolerance mechanism.

A progressive increase in Cu, Ni, and Zi levels were observed in all tissues of *S. terebinthifolia* cultivated under excess HM. However, the accumulation differed among plant tissues. Regardless of the HM (Cu, Zn, or Ni), the main organ of accumulation was the roots, followed by the stem and leaves. This suggests that *S. terebinthifolia* possibly possesses active mechanisms to restrict the translocation of metals to the aerial parts, in order to preserve the photosynthetic organ. These mechanisms of HM restriction in roots may involve transporter remodeling and accumulation in the cell wall (Wei et al., 2023), morphological and anatomical changes of roots (Ambrosini et al. 2018), or through chelation and storage of metals in the vacuole by the action of biochemical compounds such as phytochelatins (Xu et al., 2017). Restriction by active mechanisms is plausible in *S. terebinthifolia*, given the large-scale increase in root accumulation of HM, but no significant reduction in root biomass. This indicates that the greater accumulation in the roots was not the result of a "concentration" effect that can occur due to decreased biomass, but rather a real increase in the absorption and accumulation of the metal by the tissue. The accumulation of HMs in the roots, along with the maintenance of root biomass, is a confirmed manifestation of tolerance in HM-tolerant species (Clemens, 2006).

The high absorption of HMs in the different organs is a clear evidence that hydroponics is a technique that allows for high availability of nutrients (and/or heavy metals) through pH control, absence of chelating agents, and complexation with substrate particles (Gillespie et al., 2020). Therefore, our results prove that the hydroponic technique facilitates nutritional and physiological studies of tree species subjected to varying concentrations of nutrients and/or heavy metals.

Overall, the most accumulated HM was Cu, mainly in roots. This corroborates a previous study that showed that *S. terebinthifolia* is tolerant to excess copper and is recommended as a phytostabilizer of this metal, due to its high absorption and retention in the roots (Siqueira et al., 2021). In the leaves, zinc was the most accumulated metal, while nickel was the least absorbed metal overall in all tissues. This is possibly related to the general nutritional requirements of plants for each element. It is known that zinc is one of the micronutrients required in the largest quantities, while nickel is required in minimal concentrations (Lilay et al., 2024). In our study, this was evident in the *S. terebinthifolia* seedlings grown in the treatment without the addition of HMs (control), where the plant leaves contained naturally high levels of zinc and minimal amounts of nickel in this organ.

Despite exhibiting negative impacts on physiology and growth, *S. terebinthifolia* demonstrated tolerance to HM exposure up to 50 μM of the Cu, Zn, and Ni, as there was no alteration in the seedling survival rate. Treatment with 100 μM of HMs induced higher mortality but still 60% of seedling survival. Additionally, it is important to note that *S. terebinthifolia*

was exposed to a combination of metals. Given that the combined effects of multiple HMs can cause severe damage due to synergistic interactions among elements (Redha et al., 2021), the survival of *S. terebinthifolia* under elevated HM exposure further supports its classification as a HM–tolerant species. Evidence of tolerance was characterized by the maintenance of root biomass and stem diameter, the ability to restrict heavy metals in the roots, and indications of absorption restriction through pH modulation of the solution.

CONCLUSIONS

The Dutch Bucket continuous circulation hydroponic system is efficient for cultivating *S. terebinthifolia*. Expanded perlite or phenolic foam are equally viable substrates for cultivating *S. terebinthifolia*. However, perlite is more suitable for studies aimed at anatomical and physiological roots analyses, as it allows for easier removal with less mechanical damage. This methodological approach increases the range of possibilities for further studies in hydroponics with this key species.

Under severe HM stress, *S. terebinthifolia* shows signs of toxicity by decreased shoot biomass production and imbalanced physiological traits. However, the species may exhibit tolerance mechanisms evidenced by the maintenance of root biomass and stem diameter, accumulation of metals in the roots with restricted translocation to the leaves. *S. terebinthifolia* can tolerate the combination of Cu, Zn, and Ni at concentrations up to 50 μM, as survival rate is not affected. The species proves to be an excellent candidate for phytoremediation of Cu, Zn and Ni, in addition to its attributes as a model species for studies of plant HM-stress.

Acknowledgements

We would like to thank to Fundação de Amparo à Pesquisa do Estado de São Paulo (FAPESP) for financial support (Processes 201750341-0 and /2021/09686-9) and to Instituto de Pesquisas Ambientais for infrastructure support.

Author contributions:

Matheus Casarini Siqueira: Conceptualization; Data Curation; Formal Analysis; Investigation; Methodology; Validation; Visualization; Writing – Original draft; Writing – Review and editing

João Vítor Casimiro: Investigation; Methodology

Alex do Nascimento: Formal Analysis; Investigation; Methodology

Mirian Cilene Spasiani Rinaldi: Conceptualization; Validation; Visualization

Armando Reis Tavares: Conceptualization; Funding acquisition; Project administration; Resources; Supervision; Validation

Marisa Domingos: Conceptualization; Data curation; Formal analysis; Funding acquisition; Project administration; Resources; Supervision; Validation; Visualization; Writing – original draft; Writing – review and editing

Funding sources

This work was supported by Fundação de Amparo à Pesquisa do Estado de São Paulo (FAPESP) (Processo FAPESP 2021/09686-9 and 2017/50341)

REFERENCES

Ambrosini, V. G., Rosa, D. J., de Melo, G. W. B., Zalamena, J., Cella, C., Simão, D. G., ... & Brunetto, G. (2018). High copper content in vineyard soils promotes modifications in photosynthetic parameters and morphological changes in the root system of 'Red Niagara'plantlets. *Plant Physiology and Biochemistry*, *128*, 89-98.

Caporale, A. G., & Violante, A. (2016). Chemical processes affecting the mobility of heavy metals and metalloids in soil environments. *Current Pollution Reports*, *2*(1), 15-27.

Clemens, S. (2006). Toxic metal accumulation, responses to exposure and mechanisms of tolerance in plants. *Biochimie*, *88*(11), 1707-1719.

Dobbss, L. B., Dos Santos, T. C., Pittarello, M., de Souza, S. B., Ramos, A. C., & Busato, J. G. (2018). Alleviation of iron toxicity in Schinus terebinthifolius Raddi (Anacardiaceae) by humic substances. *Environmental Science and Pollution Research*, *25*(10), 9416-9425

Dubey, S., Shri, M., Gupta, A., Rani, V., & Chakrabarty, D. (2018). Toxicity and detoxification of heavy metals during plant growth and metabolism. *Environmental Chemistry Letters*, *16*(4), 1169-1192.

Erere, A., Adeniyi, V. A., Adekiya, A. O., Abiodun, J., Abolusoro, S. A., Aremu, C. O., ... & Ifeoluwa, A. (2021). Hydroponics Research Trends: A Review and Bibliometric Analysis (2008-2018). *Nat. Volatiles & Essent. Oils*.

Fan, T. T., Wang, Y. J., Li, C. B., Zhou, D. M., & Friedman, S. P. (2015). Effects of soil organic matter on sorption of metal ions on soil clay particles. *Soil Science Society of America Journal*, *79*(3), 794-802.

Ghorbel, R., Chakchak, J., Malayoğlu, H. B., & Çetin, N. S. (2021). Hydroponics "Soilless Farming": The Future of Food and Agriculture–A. In *5th International Students Science Congress Proceedings Book* (p. 45).

Gillespie, D. P., Kubota, C., & Miller, S. A. (2020). Effects of low pH of hydroponic nutrient solution on plant growth, nutrient uptake, and root rot disease incidence of basil (Ocimum basilicum L.). *HortScience*, *55*(8), 1251-1258.

Han, J. J., Lee, S. B., Park, Y. G., & Jeong, B. R. (2014). Flower yield and quality of two rose

cultivars grown in phenolic foam LC slab and phenolic foam RC slab in comparison to perlite and rockwool slab. *Horticulture, Environment, and Biotechnology*, *55*(2), 70-78.

Hassani, M. A., Durán, P., & Hacquard, S. (2018). Microbial interactions within the plant holobiont. *Microbiome*, *6*(1), 58.

Huihui, Z., Xin, L., Zisong, X., Yue, W., Zhiyuan, T., Meijun, A., ... & Guangyu, S. (2020). Toxic effects of heavy metals Pb and Cd on mulberry (Morus alba L.) seedling leaves: Photosynthetic function and reactive oxygen species (ROS) metabolism responses. *Ecotoxicology and environmental safety*, *195*, 110469.

Javed, M. T., Stoltz, E., Lindberg, S., & Greger, M. (2013). Changes in pH and organic acids in mucilage of Eriophorum angustifolium roots after exposure to elevated concentrations of toxic elements. *Environmental Science and Pollution Research*, *20*(3), 1876-1880.

Lilay, G. H., Thiébaut, N., du Mee, D., Assunção, A. G., Schjoerring, J. K., Husted, S., & Persson, D. P. (2024). Linking the key physiological functions of essential micronutrients to their deficiency symptoms in plants. *New Phytologist*, *242*(3), 881-902.

Lorenzi H (2016) Árvores brasileiras: manual de identificação e cultivo de plantas arbóreas nativas do Brasil. 7 ed. Plantarum, Nova Odessa

Mattos, J. P. O., Aguilar, M. V. M., Alves, J. D. S., Birck, T. P., Kuinchtner, C. C., Tarouco, C. P., ... & Tabaldi, L. A. (2023). Selenium does not ease growth inhibition caused by aluminum in Schinus terebinthifolius seedlings. *Journal of Plant Nutrition*, *46*(14), 3469-3486.

Meyer, R. (2011). *Schinus terebinthifolius*. US Department of Agriculture, Forest Service, Rocky Mountain Research Station, Fire Sciences Laboratory.

Minocha, R., Martinez, G., Lyons, B., Long, S., 2009. Development of a standardized methodology for quantifying total chlorophyll and carotenoids from foliage of hardwood and conifer tree species. Can. J. For. Res. 39(4), 849–861.

Nagajyoti, P. C., Lee, K. D., & Sreekanth, T. V. M. (2010). Heavy metals, occurrence and toxicity for plants: a review. *Environmental chemistry letters*, *8*(3), 199-216.

Nakazato, R.K., Lourenço, I.S., Esposito, M.P., Lima, M.E., Ferreira, M.L., O.A. Campos, R., Rinaldi, M.C.S., Domingos, M., 2021. Trace metals at the tree-litter-soil-interface in Brazilian Atlantic Forest plots surrounded by sources of air pollution. Environ. Pollut. 268, 115797.

No Soil Solution. 2025. Dutch Bucket (Bato Bucket) Hydroponic System – Beginner-Friendly Guide. Available at: https://nosoilsolutions.com/dutch-bucket-hydroponic-system/ (accessed at 10-08-2025).

Patil, S. T., Kadam, U. S., Mane, M. S., Mahale, D. M., & Dhekale, J. S. (2020). Hydroponic growth media (substrate): a review. *International Research Journal of Pure and Applied Chemistry*, *21*(23), 106-113.

Rani, R. S., Kumar, H. H., Mani, A., Reddy, B. S., & Rao, C. S. (2022). Soilless cultivation technique, hydroponics—A review. *Current Journal of Applied Science and Technology*, *41*(13), 22-30.

Redha, A., Al-Hasan, R., & Afzal, M. (2021). Synergistic and concentration-dependent toxicity of multiple heavy metals compared with single heavy metals in Conocarpus lancifolius. *Environmental Science and Pollution Research*, *28*(18), 23258-23272.

Sathyanarayan, S. R., Warke, V. G., Mahajan, G. B., & Annapure, U. S. (2023). Soil free nutrient availability to plants. *Journal of Plant Nutrition*, *46*(5), 801-814.

Shahid, M., Pourrut, B., Dumat, C., Nadeem, M., Aslam, M., & Pinelli, E. (2014). Heavy-metal-induced reactive oxygen species: phytotoxicity and physicochemical changes in plants. *Reviews of Environmental Contamination and Toxicology Volume 232*, 1-44.

Silva, R. C., Rondina, A. B. L., Zangaro, W., & Oliveira, H. C. (2021). Inorganic nitrogen sources alter the root morphology of neotropical tree seedlings from different successional groups. *Trees*, *35*(3), 875-887

Siqueira, M. C., Kanashiro, S., Domingos, M., Rinaldi, M. C. S., & Tavares, A. R. (2021). Physiological and biochemical changes in tree seedlings growing in urban forest soil contaminated with copper in São Paulo, Brazil. *Plant and Soil*, *464*(1), 149-163.

Siyar, S., Sami, S., & Majeed, A. (2020). Heavy metal stress in plants: effects on nutrients and water uptake. In *Cellular and Molecular Phytotoxicity of Heavy Metals* (pp. 89-98). Cham: Springer International Publishing.

Sumalan, R. L., Nescu, V., Berbecea, A., Sumalan, R. M., Crisan, M., Negrea, P., & Ciulca, S. (2023). The impact of heavy metal accumulation on some physiological parameters in Silphium perfoliatum L. plants grown in hydroponic systems. *Plants*, *12*(8), 1718.

Swain, C. K. (2024). Environmental pollution indices: a review on concentration of heavy metals in air, water, and soil near industrialization and urbanisation. *Discover Environment*, *2*(1), 5

Timothy, N. A., & Williams, E. T. (2019). Environmental pollution by heavy metal: an overview. *International Journal of Environmental Chemistry*, *3*(2), 72-82.

Wei, H. Y., Li, Y., Yan, J., Peng, S. Y., Wei, S. J., Yin, Y., ... & Cheng, X. (2023). Root cell wall remodeling: a way for exopolysaccharides to mitigate cadmium toxicity in rice seedling. *Journal of hazardous materials*, *443*, 130186.

Xu, Q., Wang, C., Li, S., Li, B., Li, Q., Chen, G., ... & Wang, F. (2017). Cadmium adsorption, chelation and compartmentalization limit root-to-shoot translocation of cadmium in rice (Oryza sativa L.). *Environmental Science and Pollution Research*, *24*(12), 11319-11330.

No Soil Solution. 2025. Dutch Bucket (Bato Bucket) Hydroponic System – Beginner-Friendly

Guide. Available at: https://nosoilsolutions.com/dutch-bucket-hydroponic-system/ (accessed at 10-08-2025)

Zabergja-Ferati, F., Mustafa, M. K., & Abazaj, F. (2021). Heavy metal contamination and accumulation in soil and plant from mining area of Mitrovica, Kosovo. *Bulletin of Environmental Contamination and Toxicology*, *107*(3), 537-543.

Zwolak, A., Sarzyńska, M., Szpyrka, E., & Stawarczyk, K. (2019). Sources of soil pollution by heavy metals and their accumulation in vegetables: A review. *Water, air, & soil pollution*, *230*(7), 164.

Jones Jr, J. B. (2014). Complete guide for growing plants hydroponically. CRC press.

Capítulo II

--

Manuscrito publicado na revista "Science of the Total Environment", incluído com permissão de acordo com a política de direitos de autor da Elsevier para teses e dissertações. [*Reproduced with permission from Elsevier* – This article is originally published in: Science of the Total Environment, Vol 1024, Issue 181368, 1 February 2026, https://doi.org/10.1016/j.scitotenv.2026.181368].

--

Heavy Metal Tolerance in Atlantic Forest Species: Antioxidants, Phytochelatins, or Root Exudates?

Matheus Casarini Siqueira[a*], João Vítor Casimiro[a], Alex do Nascimento[b], Mirian Cilene Spasiani Rinaldi[a], Armando Reis Tavares[c], Marisa Domingos[a]

[a] *Instituto de Pesquisas Ambientais, São Paulo, São Paulo, Brasil. Av. Miguel Estefno, 3687 - CEP 04301-012*

[b] *Universidade Federal do ABC, Santo André, São Paulo, Brasil. Av. dos Estados, 5001 - CEP 09280-560*

[c] *Instituto Agronômico, Jundiaí, São Paulo, Brasil. Av. Barão de Itapura, 1481 - CEP 13020-902*

*Corresponding author: matheus.casarini1@gmail.com

ABSTRACT

Environmental contamination by heavy metals (HM) threatens plant physiology; however, some species tolerate it via strategies like root exudation of organic acids (ROAs), phytochelatin (PC) synthesis, and antioxidants (ascorbic acid - AA, glutathione - GSH). We hypothesized that plant life-form and growth-rate may influence HM-tolerance. We experimentally studied five Atlantic Forest (a hotspot for biodiversity conservation) species: fast-growth pioneer tree (*Schinus terebinthifolia*), slow-growth non-pioneer tree (*Cariniana legalis*), fast-growth herbaceous (*Seemannia sylvatica*), fast-growth liana (*Passiflora edulis*), and slow-growth epiphyte (*Aechmea fasciata*). Plants were hydroponically exposed to Cu, Ni, and Zn (CuZnNi) for 45 days, and their physiological responses (gas exchange, chlorophyll fluorescence, pigments, biomass) and HM-tolerance strategies (PCs, ROAs, AA, GSH) were measured. Distinct HM-tolerance levels and mechanisms were found. The pioneer tree and epiphyte were the most tolerant species, showing mild physiological disturbances. The pioneer tree combined avoidance (phytic acid exudation), immobilization (leaf PC3), and mitigation (AA) mechanisms. The epiphyte relied on avoidance (diverse ROAs) and immobilization (leaf PC2). The non-pioneer tree was moderately tolerant, using immobilization (leaf PC6) and mitigation (AA) strategies, but still exhibited significant physiological imbalances. Despite their respective defense mechanisms, the herbaceous (avoidance: oxalic acid; immobilization: leaf PC4) and liana (mitigation: GSH) were highly sensitive, showing severe toxicity. Our results suggest that plant life-form influences heavy-metal accumulation and tolerance, whereas growth rate was not a reliable predictor. Broader investigations, including additional species, metals, and environmental conditions, are needed to determine whether these patterns reflect life-form effects or taxon-specific responses.

Keywords: Tree, Herbaceous, Liana, Epiphyte, Pollution

INTRODUCTION

Tropical plant species are increasingly challenged to survive amidst climate change, urbanization, forest fragmentation, and environmental pollution. One of the main global concerns regarding anthropic pollution is the environmental contamination by heavy metals (HMs). These elements can be harmful to plants through their accumulation in the plant-soil system, leading to toxicity (Vardhan et al., 2019; Zwolak et al., 2019). In the Atlantic Forest, an important biodiversity hotspot in Brazil, contamination by multiple HMs such as copper (Cu), zinc (Zn), and nickel (Ni) has been documented (Marques et al., 2021; Nakazato et al., 2021). Anthropogenic activities such as vehicle emissions and industrial processes have raised Cu, Zn, and Ni levels to concerning concentrations in the Atlantic Forest, especially in urban fragments or areas close to large urban/industrial centers (Dafré-Martinelli, 2020; Vasconcellos et al., 2021). Cu, Zn, and Ni are essential for plant growth and development, but at high concentrations can disrupt plant physiology, reducing net carbon assimilation, light use efficiency, pigment levels, while increasing oxidative damage and altering biomass allocation (Ghori et al., 2019; Gong et al., 2019). Although understanding the effects of Cu, Zn and Ni individually is important, the combined toxicity of multiple HMs in polluted soils poses a higher risk to organisms and ecosystems compared to single HM exposure, and therefore deserves greater attention (Chen et al., 2020).

It is well-established that plants have developed several physiological and biochemical protective strategies to avoid, tolerate, or mitigate HM toxicity. One of the primary strategies for protecting plants against excess HMs is the exudation of root organic acids (ROAs) (Osmolovskaya et al., 2018). ROAs act as metal chelators, binding to free metals in soil to form insoluble HM-ROA complexes, which in turn limit HMs uptake by plant roots (Kar et al., 2021), thereby functioning as an avoidance mechanism. Another key biochemical strategy involves the synthesis of non-protein polypeptides rich in cysteine (thiol groups), known as phytochelatins (PCs) (Cobbett and Goldsbrough, 2002). PCs function after HM uptake by chelating and subsequently compartmentalizing the PC-HMs complexes into cell vacuoles (Pandey et al., 2019), serving as an intracellular accumulation mechanism. Studies have shown that many species increase PC synthesis in response to HM stress (Beladi et al., 2011; Navarrete et al., 2019; Talukder, 2020).

While mechanisms such as uptake restriction and chelation can effectively mitigate adverse effects of HMs, oxidative damage may still occur due to increased production of reactive oxygen species (ROS) (Mahmud et al., 2019). To counteract oxidative damage, plants can synthesize enzymatic antioxidants, such as catalase (CAT), superoxide dismutase (SOD), ascorbate peroxidase (APX), glutathione peroxidase (GPX), as well as non-enzymatic

antioxidants like ascorbic acid (AA) and glutathione (GSH). AA and GSH work synergistically, playing a crucial role in reducing toxicity by scavenging excess ROS. Moreover, GSH is as a precursor for PCs synthesis (Liu et al., 2015).

In a megadiverse biome like the Atlantic Forest, plant species exhibit distinct life-forms and occupy different ecological niches (Marques et al., 2021). These different life-forms may result in distinct strategies to avoid, accumulate and tolerate HMs stress (Singh et al., 2020). Research has shown that fast-growing pioneer tree species from the Atlantic Forest of Brazil possess effective antioxidant systems and exhibit higher tolerance to oxidative stress (Brandão et al., 2017; Esposito et al., 2018), accumulate more HMs and show less biomass imbalances than slow-growing non-pioneer tree species (Brandão et al., 2022; Barbosa et al., 2024). However, the specific defense strategies employed by native species from Atlantic Forest against combined HM stress, -such as production of ROAs, PCs, AA or GSH-remain largely unknown. Exposing plants experimentally to multiple HMs can provide valuable insights into their tolerance mechanisms (Xie et al., 2018). Furthermore, no studies have yet investigated potential differences in tolerance strategies and HMs accumulation capacities among plant species with distinct life-forms coexisting in forest environments.

To address this gap, we propose two hypotheses. I: Plant species with different life-forms are naturally adapted to varying environmental conditions and therefore exhibit different HMs accumulation levels and tolerance strategies; II: Fast-growing species (including herbaceous, climbing and pioneer trees) are more tolerant than slow-growing species (such as epiphytes and non-pioneer trees). To test these hypotheses, we studied five species from the Atlantic Forest with different life forms and growth rates. The species were hydroponically cultivated under normal or high HM-concentrations, and their metal accumulation capacity, key physiological aspects (carbon assimilation, chlorophyll fluorescence, pigments content, and biomass production) and biochemical defense mechanisms (ROAs, PCs, and non-enzymatic antioxidants) were evaluated.

MATERIAL AND METHODS

Experimental design and sampling procedures

The experiments were carried out in a greenhouse with semi-controlled conditions (mean temperature: 25ºC, mean humidity: 50%; mean photosynthetic photon flux density (PPDF) from natural sunlight: 1,200 μmol m^{-2} s^{-1}) located in the Instituto de Pesquisas Ambientais (Environmental Research Institute), São Paulo, São Paulo State, Brazil (23º30'S and 46º40'W; 770 m altitude).

Seedlings of the five Atlantic Forest species that are characterized by distinct life-forms were obtained from commercial nurseries: 1) pioneer tree (*Schinus terebinthifolia* Raddi, Anacardiaceae); 2) non-pioneer tree (*Cariniana legalis* (Mart.) Kuntze, Lecythidaceae); 3) herbaceous (*Seemannia sylvatica* (Kunth) Hanst., Gesneriaceae); 4) liana (*Passiflora edulis* Sims, Passifloraceae); 5) epiphyte (*Aechmea fasciata* (Lindl.) Baker, Bromeliaceae). The seedlings purchased from local producers originated from naturally germinated seeds (i.e. non-genetically manipulated), collected from a wide broad variety of mother trees to ensure natural genetic variability. To standardize physiological age and developmental stage across species and ensure comparable responses, we use only young pre-flowering plants. The species were selected by the criteria: 1) good representativeness of the life-form group; 2) native to the Atlantic Forest and 3) possibility of obtaining standardized seedlings in local plant nurseries. The non-pioneer tree *C. legalis* and the epiphyte *A. fasciata* are endangered Brazilian species, and studies aiming the understanding of their tolerance mechanisms to environmental pollution are highly necessary.

The experiments with each plant species were conducted in a recirculation "Dutch Bucket" hydroponic system (Ghorbel et al., 2021; Bhat et al., 2023), which consisted of growing the plants in 5 L reservoirs filled with perlite, through the nutrient solutions were continuously circulated. The experimental design was composed of 2 treatments (Control or CuZnNi), with 2 replicates each containing 15 plants, totaling 30 plants per treatment (n = 30). The plants were continuously supplied with nutrient solutions stored in 20 L gallons and prepared as follows:

Control: 25% strength Hoagland and Arnon balanced nutrient solution (Hoagland & Arnon, 1950).

CuZnNi: 25% strength of Hoagland and Arnon balanced nutrient solution + 25 μM Cu, Ni and Zn.

The concentrations of Cu, Zn and Ni added were based on several studies with different species grown in hydroponic systems and exposed to solutions enriched with Cu, Zn or Ni

(Soares et al., 2000; Vassilev et al., 2007; Sagardoy et al., 2009; Bouazizi et al., 2010; Pietrini et al., 2015; Rizwan et al., 2017). The solutions were ionically balanced to avoid the increase of other nutrients (mainly nitrogen and sulfur) than Cu, Zn and Ni (Table IIS1). Solutions were adjusted to pH 5.6 and renewed weekly.

The experiment with each species lasted 45 days (15 days of adaptation to hydroponic system and 30 days of experimentation). All physiological and biochemical analyses were carried out at the end of the experiment.

Net CO_2 assimilation and chlorophyll fluorescence (n = 30) were determined in the 1st physiologically mature leaf of each plant. In sequence, the plants were removed from the hydroponic system, their roots washed with distilled water to remove all perlite particles and then placed in bottles filled with 100 ml of deionized water for 2 hours. After that, 15 ml of solutions from every 3 plants randomly chosen from the same treatment were joined to obtain 10 composite samples with 45 ml for analyses of organic acid exudation (n = 10).

Composite samples of leaves were immediately crushed into liquid nitrogen and stored at -80ºC for biochemical analyses. Each sample of leaves was obtained by assembling leaves of 3 plants per treatment chosen for analyses of organic acid exudation. Ascorbic acid/pigments, glutathione and phytochelatin were analyzed in composite samples of the 1st, 2nd and 3rd physiologically mature leaves, respectively. We have defined the physiologically mature leaves according to the particularity of each species. For pioneer tree, non-pioneer tree and climbing species, we considered the first mature leaf as the third leaf counting from the apex downward. For the herbaceous species we considered the third leaf of the youngest shoot while for the epiphyte species we considered the third leaf counting from tank center to edge. Composite samples of root tips were also similarly prepared and stored for phytochelatin analyses.

Finally, the plants were separated into leaves, stems, and roots, oven-dried at 60 ºC until constant weight to determine dry mass and Cu, Zn and Cu concentrations in each organ.

Analytical technics

pH and electrical conductivity of nutrient solutions

Solution pH and electrical conductivity (µS cm^{-1}) were weekly measured directly in nutrient solutions with a portable multiparameter sensor (Combo-5, AKSO) one day before the solution renewal.

Biomass and heavy metal accumulation

After drying at 60 °C in a circulating-air oven until constant mass, the roots, stems, and leaves were weighed (g). The values of leaf and stem biomasses were summed to compose the

shoot biomass and calculate root/shoot ratios. The dried samples were crushed in a knife mill until become a homogeneous powder, then 100 mg of each sample was sent to Fertility Laboratory at Instituto Agronômico (Agronomical Institute), Campinas, São Paulo State, Brazil for Cu, Zn and Ni analysis (mg g^{-1} dry mass). Plant tissues were digested using nitric and perchloric acids and HM concentration was determined by flame atomic absorption spectrophotometry (Raij et al., 2001).

Physiological indicators of stress and visible alterations

Net CO_2 assimilation (*A*, μmol CO_2 m^{-2} s^{-1}) of each species was measured with a portable infrared gas analyzer (IRGA) (LCpro, ADC-Bioscience, UK). Measurements were carried out between 8 am and 12 pm at 400 ppm CO_2, 50% relative humidity and 25ºC temperature as established conditions. The ideal value of photosynthetically active radiation (PAR, μmol photons m^{-2} s^{-1}) for each species was obtained through assimilation curve in response to the decrease in PAR flux (from 2,000 to 0 μmol m^{-2} s^{-1}) carried out in healthy individuals (plants from control treatment, n = 3). Gas exchange was not only analyzed in the epiphyte species due to its CAM metabolism (stomata opens at night).

The maximum efficiency of photosystem II in the dark-adapted state (F_v/F_m) was determined in the same leaves used for measuring net CO_2 assimilation, previously dark-adapted for 30 minutes, with a portable modulated pulse fluorometer OS5p (Opti-Sciences, Hudson, USA). The light Fluorescence measurement was performed with a 660 nm saturating rectangular flash of 3,000 μmol photons m^{-2} s^{-1} for 3 milliseconds.

Total chlorophyll (*a* + *b*) and carotenoid concentrations (μg g^{-1} leaf fresh weight) were determined in frozen composite leaf samples immersed in 96% ethanol kept in the dark for 24 hours. The extract was spectrophotometrically analyzed at λ = 471 nm, 649 nm, 664 nm and 750 nm, and then chlorophyll *a* (*Chl a*), chlorophyll *b* (*Chl b*) and total carotenoids were determined by the formulas derived from Minocha et al. (2009):

$$Chl\ a = (13.36 \times A664) - (5.19 \times A649)$$

$$Chl\ b = (27.43 \times A649) - (8.12 \times A664)$$

$$Carotenoids = [(1000 \times A470) - (2.13 \times Chl\ a) - (97.64 \times Chl\ b)] \div 209$$

Visible alterations were evaluated by noticeable differences in plant height, number of leaves, leaf chlorosis or necrosis, root volume and color between plants under Control or CuZnNi treatments.

Antioxidants

Ascorbic acid (AA) concentration in reduced (AA_r) and total (AA_t) forms (mg g^{-1} leaf fresh weight) was determined in frozen composed samples, after extraction with

metaphosphoric acid (HPO_3), followed by centrifugation at 11,393.4 × g (10,000 rpm) for 15 minutes at 2 ºC. The supernatant was collected, filtered in hydrophilic nylon syringe filters (0.22 µm), and AA concentrations were determined in RP-HPLC on a C-18 column, flow rate set to 1 ml min^{-1}, 25 ºC and detection under diode array detector (DAD) at λ = 245 nm, using isocratic elution of water acidified at pH 2.3 with H_3PO_4 (López et al., 2005).

Glutathione (GSH) concentration in reduced (GSHr) and total (GSHt) forms (mg g^{-1} leaf fresh weight) was determined in frozen composite samples, after extraction with sulfosalicylic acid, followed by centrifugation at 11,393.4 × g (10,000 rpm) for 15 minutes at 2 ºC. The supernatant was collected and GSH concentrations were determined in spectrophotometer at λ = 412 nm (Anderson, 1985).

Quantification and detection of ascorbic acid and glutathione were determined after calibration curve (Table IIS2) with analytical grade commercial standards (Supelco, Merck Sigma-Aldrich) as reference.

The reduced/total ratio of ascorbic acid and glutathione was calculated to evaluate their redox state. Values < 0.5 indicate the predominance of oxidized state and values ≥ 0.5 the predominance of reduced state of both antioxidants (Burkey et al., 2006).

Phytochelatins (PC)

Phytochelatin (PC2 to PC6) concentrations (µg g^{-1} leaf or root fresh weight) were determined in frozen composite samples, after extraction with 60% perchloric acid, vortexing for 1 minute, followed by centrifugation at 11,393.4 × g (10,000 rpm) for 15 minutes at 2 ºC. The supernatant was collected, filtered in hydrophilic nylon syringe filters (0.22 µm) and PC detection were determined in RP-HPLC (reverse phase high performance liquid chromatographic) on a C-18 column, flow rate set to 1 ml min^{-1}, 25 ºC and detection under DAD at λ = 214, using (A) 99.9% deionized water + 0.1% trifluoroacetic acid (v/v) and (B) acetonitrile for 25 minutes under linear elution gradient (1% decrease in A and 1% increase in B per minute) (Hunaiti et al., 2003). Quantification and detection were determined after calibration curve (Table IIS2) with commercially laboratory synthesized phytochelatins (Anaspec, USA) as standard reference.

Root organic acids (ROA)

The composite solutions (15 mL) were filtered through qualitative cellulose membranes (grade 42) with 0.22 µm porosity, freeze-dried and resuspended in 500 µl distilled water acidified at pH 4.0 with H_3PO_4. Identification and quantification of ROAs were carried out in a RP-HPLC system, using a C-18 column and an isocratic elution of (A - 93%) 25 mM KH_2PO_4 in water and (B - 7%) methanol, with flow rate set to 1 ml min^{-1}, 25 ºC and detection under

DAD at λ = 210 nm. Commercial organic acids (Acetic, Adipic, Ascorbic, Benzoic, Butyric, Citric, Formic, Fumaric, Isobutyric, Isocitric, Lactic, Maleic, Malic, Malonic, Oxalic, Phytic, Propionic, Quinic, Shikimic, Succinic and Tartaric - organic acids kit, Supelco, Merck Sigma-Aldrich) were used as a standard reference, and the identification of organic acids in the samples (μg ml^{-1}) was performed by first adding the standard to a blank sample (deionized water) and comparing the retention times of the sample with the standard reference, and second by adding the standard to a random sample and observing the increase in the corresponding organic acid peak. Quantification and detection were determined after calibration curve (Table IIS2) with analytical grade commercial reference standard (Cawthray, 2003).

Statistical analyses

Data was analyzed in the statistical software GraphPad Prism v 9.0. Differences between Control and CuZnNi treatments regarding biomass ratio, leaf gas exchange, chlorophyll fluorescence, pigment content, ascorbic acid, glutathione and root organic acids were identified through t-test ($p \leq 0.05$). Heavy metal and phytochelatin concentrations in each organ were analyzed using Two-Way ANOVA (factors: treatment × organ), while pH and conductivity of the nutrient solution weekly renewed were assessed with Two-Way ANOVA (factors: treatment × time), followed by Šídák's multiple comparison test ($p \leq 0.05$) to identify differences between variables and their interactions. The residual data were subjected to Shapiro-Wilk normality (normal distribution) and Brown-Forsythe homoscedasticity (equality of variances) tests. Non-normal or heteroscedastic data were transformed (log or sqrt) to meet ANOVA assumptions. Synthesis of Two-way ANOVA results can be found at Supplementary material (Table IIS3 and IIS4).

Phytochelatins were also analyzed through Principal Component Analysis (PCA), to identify species-specific phytochelatins (PC2 – PC6) and detect if heavy metal excess influences PC concentration and preference.

A graphical construction of Heatmap was performed to represent the overall HM accumulation, biochemical defenses and physiological responses of the 5 species studied. To ensure comparability, the data were variance-scaled (standardized) to be incorporated into the heatmap.

RESULTS

Heavy metal accumulation

The metal accumulation capacity varied among species, according to the following order of magnitude (Fig. II1, Table IIS5): Herbaceous > liana > pioneer tree > epiphyte = non-pioneer tree.

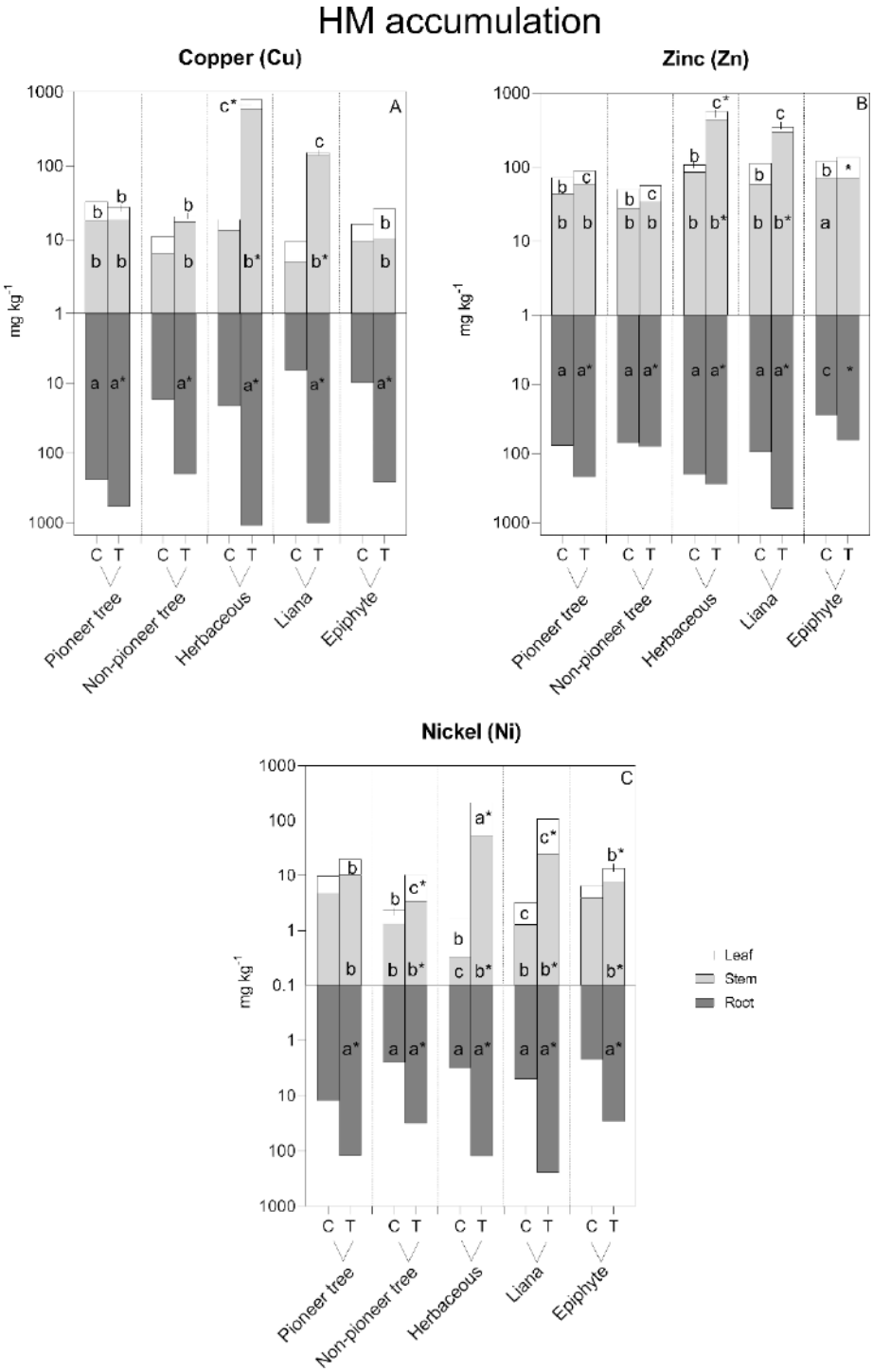

Fig. II 1. Mean concentrations of copper (Cu - A), zinc (Zn - B) and nickel (Ni - C) (mg kg^{-1} dry mass), in leaves, stem and roots of pioneer tree, non-pioneer tree, herbaceous, liana and epiphyte species cultivated in nutrient solution (C - Control) or nutrient solution with excess of Cu, Zn and Ni (T - CuZnNi). Distinct letters indicate significant difference between organs in the same treatment, while * indicates significant difference between Control and CuZnNi in the same organ, according to two-way

ANOVA followed by the Šídák test ($p \leq 0.05$).

There was no difference in Cu concentration between organs of plants grown in Control, except for the pioneer tree, which accumulated significantly more Cu in its roots. Ni concentrations in non-pioneer tree, herbaceous and liana were higher in roots than in stem or leaves in the Control. However, for the pioneer tree and epiphyte, no significant difference in Ni concentration between organs was observed in the Control. Plants of all species cultivated in CuZnNi accumulated higher levels of Cu, Zn and Ni in their roots than in the stem or leaves, except for the epiphyte, which showed similar Zn concentrations in all organs under the same treatment.

All plant species exposed to CuZnNi exhibited elevated heavy metal concentrations in their tissues relative to the Control group; however, the patterns of accumulation varied among the different species. Cu, Zn and Ni concentrations increased only in roots of the pioneer tree roots, with no changes in leaves or stems. Cu concentration increased only in roots of the non-pioneer tree, while Ni concentration increased in all organs, but no difference of Zn concentration for all organs. Cu, Zn and Ni concentrations increased in all organs of the herbaceous species. Cu and Zn increased in roots and stems of the Liana species, while Ni concentration increased in all organs. Cu concentrations increased only in the roots of the epiphyte species, while Ni concentration increased in all organs, and Zn concentration increased in roots and leaves.

Physiological indicators of stress and visible alterations

All species showed physiological adjustments under HM stress (Table II1). Net carbon assimilation (*A*) was reduced for all species under CuZnNi; the herbaceous and liana species reached negative assimilation values (e.g., photorespiration). Except for the pioneer-tree, maximum efficiency of photosystem II in the dark-adapted state (F_v/F_m) decreased in all species under CuZnNi. Chlorophyll and carotenoid concentrations decreased for the herbaceous and lianas species under CuZnNi. Root/Shoot biomass ratio was altered for the non-pioneer tree, herbaceous and liana under CuZnNi.

Tab. II 1. Mean values ± standard deviation of net carbon assimilation (*A*, μmol CO_2 m^{-2} s^{-1}), maximum efficiency of photosystem II in the dark-adapted state (F_v/F_m, ratio), chlorophyll and carotenoid concentrations (mg g^{-1} fresh mass), and biomass root/shoot (ratio) of pioneer tree, non-pioneer tree, herbaceous, liana and epiphyte seedlings cultivated in balanced nutrient solution (Control) or balanced nutrient solution with excess Cu, Zn and Ni (CuZnNi). Means in bold indicate a significant difference between treatments, according to t-test ($p < 0.05$). Net carbon assimilation not performed in Epiphyte due to CAM-type metabolism.

Species	Treatment	*A*	F_v/F_m	Chlorophyll	Carotenoids	Root/Shoot
--	--	μmol CO_2 m^{-2} s^{-1}	ratio	mg g^{-1}		ratio
Pioneer tree	Control	**5.88 ± 3.18**	0.68 ± 0.11	1.50 ± 1.00	0.5 ± 0.15	0.18 ± 0.04

	CuZnNi	1.61 ± 1.33	0.66 ± 0.09	1.41 ± 0.49	0.25 ± 0.09	0.24 ± 0.16
Non-pioneer tree	Control	**4.93 ± 1.04**	**0.64 ± 0.02**	1.91 ± 0.42	0.32 ± 0.08	0.22 ± 0.04
	CuZnNi	0.51 ± 0.59	0.52 ± 0.04	2.28 ± 1.23	0.42 ± 0.22	**0.29 ± 0.05**
Herbaceous	Control	**10.88 ± 5.96**	**0.71 ± 0.02**	**1.14 ± 0.14**	**0.18 ± 0.03**	0.20 ± 0.15
	CuZnNi	-0.04 ± 4.27	0.50 ± 0.11	0.51 ± 0.17	0.09 ± 0.03	**0.33 ± 0.61**
Liana	Control	**3.68 ± 1.96**	**0.70 ± 0.03**	**2.78 ± 0.59**	**0.51 ± 0.09**	**0.43 ± 0.12**
	CuZnNi	-0.28 ± 0.68	0.55 ± 0.10	0.78 ± 0.13	0.23 ±0.03	0.27 ± 0.07
Epiphyte	Control	--	**0.60 ± 0.07**	0.12 ± 0.03	0.04 ± 0.01	0.16 ± 0.04
	CuZnNi	--	0.52 ± 0.07	0.12 ± 0.04	0.03 ±0.01	0.15 ± 0.08

All species showed visible alterations when cultivated under HM stress (Figure II2). The pioneer tree showed fewer visible injuries after cultivation under CuZnNi stress than the other species, with a reduction in height and root volume. In all other species, darkening and expressive root volume reduction were observed under CuZnNi. In the shoots of plants under CuZnNi, wilted leaves were noticeable in the non-pioneer tree; leaf chlorosis and leaves size reduction, and smaller plants were observed in the liana; and leaf necrosis, chlorosis and size reduction were evident in the herbaceous species. The epiphyte showed leaf opacity and reduced root development under CuZnNi.

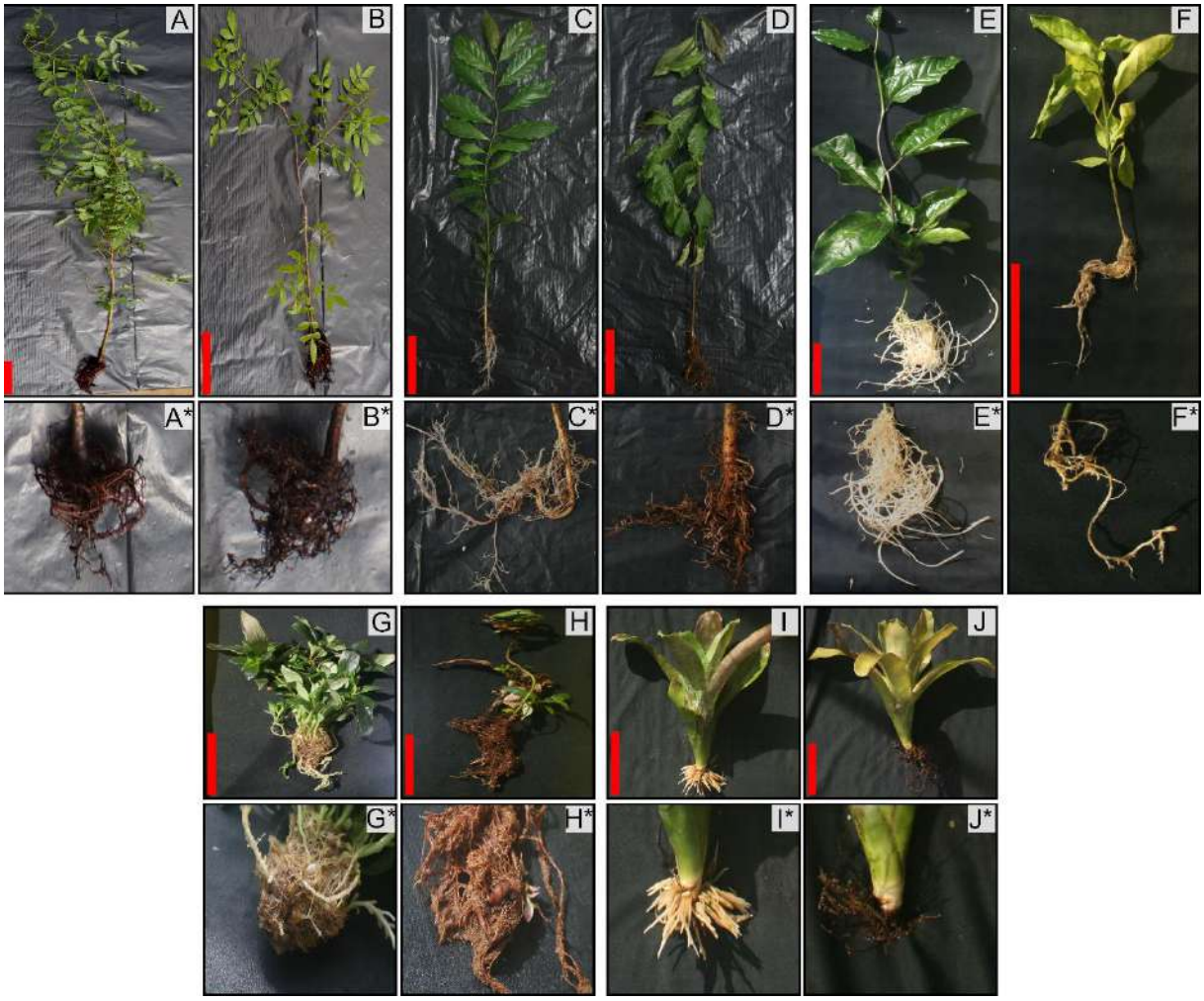

Fig. II 2. Visual aspects of pioneer tree (A-B), non-pioneer tree (C-D), liana (E-F), herbaceous (G-H)

and epiphyte (I-J) seedlings cultivated under control nutrient solution (figures A, C, E, G and I) or balanced nutrient solution with excess of Cu, Zn and Ni (figures B, D, F, H and J). Letters with * highlights plant roots. Red bar scale = 10 cm.

Antioxidants

Leaf concentrations of total ascorbic acid (AA_t) and total glutathione (GSH_t) varied among species according to following order of magnitude (Fig. II3):

AA_t: Liana > pioneer tree = non-pioneer tree > epiphyte > herbaceous

GSH_t: Liana > pioneer tree = epiphyte = herbaceous > non-pioneer tree

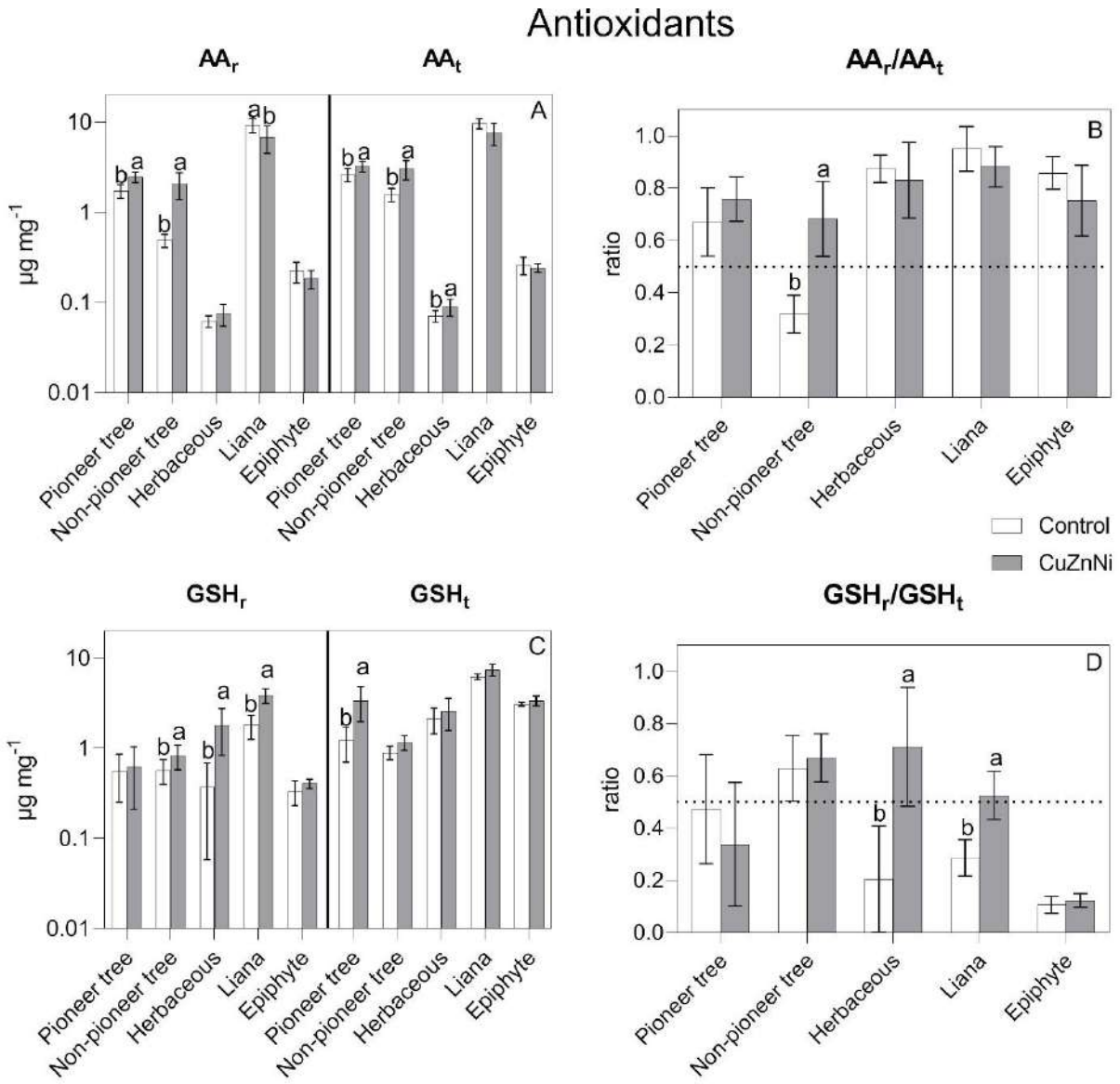

Fig. II 3. Mean concentrations (µg mg^{-1} fresh mass) of reduced and total ascorbic acid (AA_r and AA_t - A) and glutathione (GSH_r and GSH_t - B), and respective redox status (AA_r/AA_t, GSH_r/GSH_t) in leaves of pioneer tree, non-pioneer tree, herbaceous, liana and epiphyte seedlings cultivated in balanced nutrient solution (Control) or balanced nutrient solution with excess Cu, Zn and Ni (CuZnNi). Distinct letters indicate significant difference between treatments, according to t-test ($p \leq 0.05$).

Reduced ascorbic acid levels (AA_r) and total ascorbic acid levels (AA_t) increased in the

pioneer and non-pioneer tree under CuZnNi, while only AA_t increased in the herbaceous plant, but AA_r decreased in the liana species. Leaf AA_r or AA_t concentrations of the epiphyte species did not differ between treatments. Ascorbic acid redox state (AA_r/AA_t) increased in the non-pioneer tree under CuZnNi, switching from oxidized state (< 0.5) to reduced state (> 0.5). For the other species, there was no variation in AA_r/AA_t between treatments and were characterized by the predominance of the reduced state (> 0.5).

Reduced glutathione (GSH_r) increased in the non-pioneer tree, herbaceous and liana species under CuZnNi, while total glutathione (GSH_t) increased in the pioneer tree. Glutathione redox state (GSH_r/GSH_t) increased in the herbaceous and liana species under CuZnNi, switching from oxidized (< 0.5) to reduced state (> 0.5). For the other species, there was no change in GSH_r/GSH_t between treatments. Both with or without CuZnNi stress, the pioneer tree and epiphyte species were characterized by predominating oxidized state of glutathione, while the non-pioneer tree was characterized by the reduced state of glutathione.

Phytochelatins

PCA explained 56.80% of the total variability in leaf phytochelatins of the five species studied (Fig. II4). Axis 1 explained 29.76% ($p = 0.02$) of the variance and was mainly composed of PC2, PC3 and PC5. Axis 2 explained 27.06% ($p < 0.01$) of the variance and was mainly composed of PC3 and PC4. In roots, PCA explained 62.30% of the total variability in root phytochelatins. Axis 1 explained 37.32% ($p < 0.01$) of the variance and was mainly composed of PC2, PC3 and PC5. Axis 2 explained 24.98% ($p = 0.01$) of the variance and was mainly composed of PC4 and PC6 (Fig. II4).

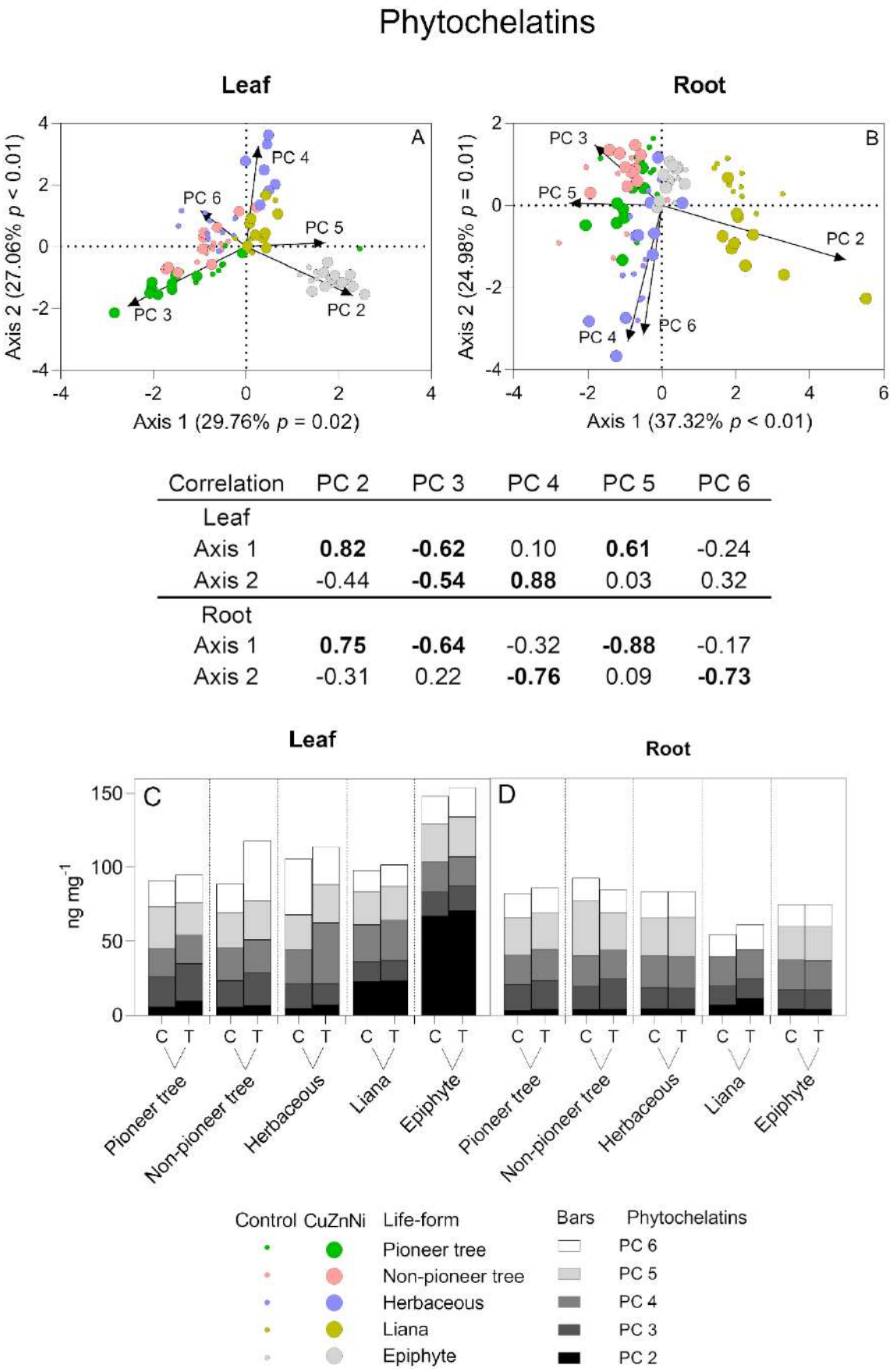

Correlation	PC 2	PC 3	PC 4	PC 5	PC 6
Leaf					
Axis 1	**0.82**	**-0.62**	0.10	**0.61**	-0.24
Axis 2	-0.44	**-0.54**	**0.88**	0.03	0.32
Root					
Axis 1	**0.75**	**-0.64**	-0.32	**-0.88**	-0.17
Axis 2	-0.31	0.22	**-0.76**	0.09	**-0.73**

Fig. II 4. Graphical representation of principal component analysis (PCA) and mean concentrations (ng mg^{-1}; bar graph) of phytochelatins (PC2 to PC6) detected in leaves (A and C) or roots (B and D) of pioneer tree, non-pioneer tree, herbaceous, liana and epiphyte cultivated in balanced nutrient solution (C = Control) or balanced nutrient solution with excess Cu, Zn and Ni (T = CuZnNi).

In general, phytochelatin concentrations were higher in leaves than roots; except PC5 in non-pioneer tree under Control, and PC6 in liana under CuZnNi. The PCAs also revealed that the species produced higher levels of specific phytochelatins, as summarized below (Fig. II4).

High leaf concentration of PC3 was detected in pioneer tree species, with an increase observed in trees grown under CuZnNi, whereas a similar tendency was not evident in their roots. Non-pioneer tree species were characterized by high concentrations of PC3 and PC6 in leaves, showing an increase under CuZnNi and by elevated levels of PC3 in the roots, also increasing under CuZnNi.

Herbaceous species exhibited a high concentration of PC6 in leaves under the Control. However, under the CuZnNi, PC6 decreased while PC4 increased in their leaves. High concentrations of both PC4, PC5 and PC6 were detected in the roots; with no differences observed between treatments.

Liana species did not exhibit a high production of any specific leaf phytochelatin. However, a high concentration of PC2 was detected in their roots in both treatments, compared to the other species.

High concentration of PC2 was detected in leaves of the epiphyte, with no distinction between treatments. All phytochelatins were measured at low levels in their roots, with no differences observed between treatments.

In general, the two-way ANOVA and multiple comparison tests confirmed that each species adjusted its leaf and root concentrations of specific phytochelatins in response to increased metal levels in the hydroponic solution (Table IIS3).

Root organic acids and hydroponic solution

A total of thirteen root organic acids (ROA) were identified: phytic, oxalic, tartaric, malonic, lactic, maleic, acetic, citric, succinic, fumaric, propionic, isobutyric and shikimic (Fig. II5). Oxalic acid was the only ROA detected in all plant species. The diversity of exuded ROA varied among species, as follows:

Epiphyte (10) > liana (9) > herbaceous (8) > pioneer tree (2) = non-pioneer tree (2)

The species also exuded distinct levels of total ROA, as follows:

Pioneer tree > liana > epiphyte = non-pioneer tree > herbaceous

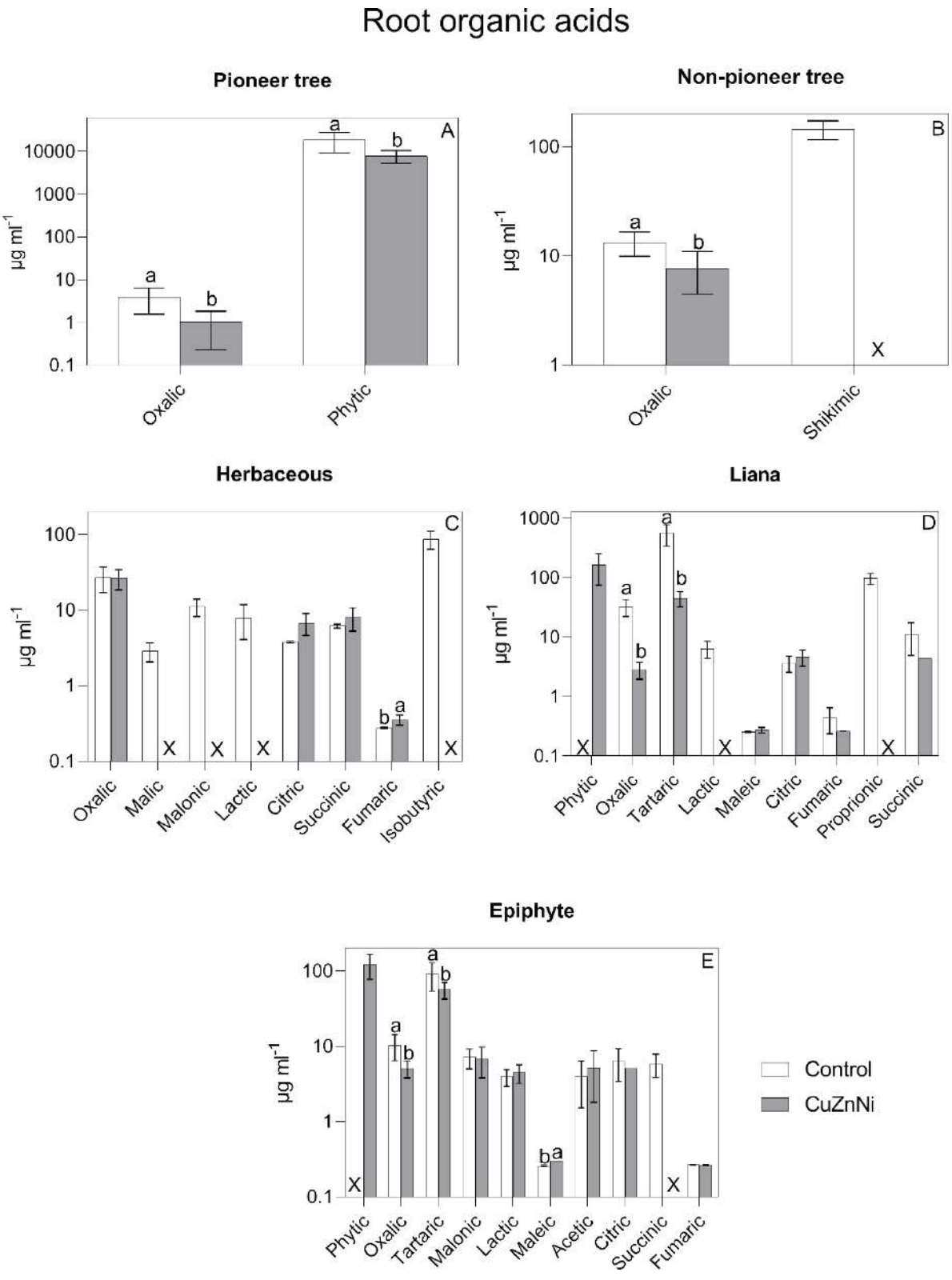

Fig. II 5. Mean concentration of root organic acids (µg ml^{-1}) exuded pioneer tree (A), non-pioneer tree (B), herbaceous (C), liana (D) and epiphyte (E) seedlings cultivated in balanced nutrient solution (Control) or balanced nutrient solution with excess Cu, Zn and Ni (CuZnNi). Different letters indicate a significant difference between treatments, according to the t-test ($p \leq 0.05$). "x" indicates undetected acid.

Overall, ROA exudation by all species decreased after cultivation under the CuZnNi. Oxalic acid was exuded by all species, and decreased under CuZnNi in all species, except in

herbaceous species; phytic acid by pioneer tree; tartaric acid by liana; fumaric by herbaceous and tartaric and maleic acids by epiphyte. The production of shikimic (by non-pioneer tree), malic, malonic, lactic, isobutyric (by herbaceous), lactic, propionic (by lianas) and succinic (by epiphytes) acids occurred only in the Control. In contrast, phytic acid was exudated by liana and epiphyte only in the CuZnNi (Fig. II5).

The pH values of the hydroponic solutions used in the experiments ranged between 3.75 and 5.78. Solutions with excess of Cu, Zn and Ni used to cultivate all species decreased in pH over time. Similar pH decreases were observed in the Control solution used to cultivate species of pioneer tree and epiphyte species. Significant differences in pH values between the two treatments were observed during the experiments conducted with non-pioneer tree, herbaceous, and pioneer tree species, although without following a pattern (Fig. IIS2).

The conductivity values of hydroponic solutions ranged between 580 and 670 μS cm^{-1} during experiments with pioneer tree and non-pioneer tree species, between 300 and 500 μS cm^{-1} during experiment with herbaceous, between 30 and 170 μS cm^{-1} during experiment with liana, and between 30 and 50 μS cm^{-1} during experiment with epiphyte species. The conductivity values of both Control and CuZnNi solutions used to cultivate all species fluctuated significantly over time and differences between the conductivity of Control and CuZnNi solutions were observed, albeit without following a pattern (Fig. IIS2).

DISCUSSION

Heavy metal accumulation

All species accumulated the excess heavy metals (HM) mainly in roots, reducing translocation to aboveground tissues as a protective mechanism, consistent with several other studies (Galal et al., 2015; Wang et al., 2015; Zang et al., 2020). HM accumulation in roots occurs passively in the cell walls, which act as a selective barrier preventing entry into the cytoplasm and avoiding cellular damage (Parrotta et al., 2015). Between 70-90% of all absorbed HM can accumulate in the cell walls of roots (Jia et al., 2019). However, significant differences in HM accumulation patterns were observed among the species studied. Notably, the herbaceous and liana species accumulated more HM in their organs than the other species, and as a result, presented more severe physiological imbalances. The extreme high contents of heavy metal in tissues in herbaceous and liana, especially Cu in roots (> 1000 mg kg^{-1}, table S5), highlights their HM sensitivity, resulting from excessive metal uptake (weak avoidance) and reduced root biomass. More evidently, the herbaceous species showed the higher heavy metal concentrations in leaves of all species, indicating its low translocation retention capacity, which was followed by the most evident visual damage and physiological disruption.

Conversely, the pioneer tree, non-pioneer tree and epiphyte, which showed lower HM accumulation, displayed fewer physiological imbalances. This highlights that avoidance (reducing HM uptake), together with immobilization (limiting HM translocation to shoots), are key mechanisms to prevent HM stress. Although HM was mainly accumulated in roots, no increase in root phytochelatin synthesis was observed for most species, indicating that this active method of chelation and subsequent entrapment in vacuoles may not be their main strategy for HM accumulation. It is possible that, regardless of the plant life-form, root cell wall storage should be the main strategy for HM accumulation in the studied species. The differences in metal concentrations found between species in our study can be attributed to inherent biological variations, such as metabolism and nutrient uptake rates, receptor types and amounts, presence of lignified roots, and metal selectivity of each species (Filipović-Trajković et al., 2012; Pasricha et al., 2021).

Physiological indicators of stress

All five species showed some degree of physiological imbalance when cultivated under CuZnNi, indicating that 25 µM of combined Cu, Zn and Ni supplied hydroponically for 45 days was phytotoxic. The decrease in net carbon assimilation rate observed in the species cultivated under HM stress was expected, as excessive HM affects negatively plant physiology and homeostasis (Ghori et al., 2019). Chlorophyll fluorescence stability verified in the pioneer tree indicates that light absorption and photosynthetic efficiency were not affected (Kalaji et al., 2016), highlighting its higher tolerance to HM compared to other species. Maintaining light absorption efficiency is essential for pioneer species, which must tolerate high light intensities in open, sunny environments, such as degraded areas (Favaretto et al., 2011). Therefore, this pioneer tree can be recommended for forest restoration of HM-contaminated open areas. The non-pioneer tree species was able to survive and maintain its photosynthetic pigment concentrations after exposure to CuZnNi, despite reductions in both net carbon assimilation rate and chlorophyll fluorescence. Therefore, this species could also be considered for restoration programs, particularly in areas with lower contamination of Cu, Zn and Ni, and preferably after plantation of pioneer trees.

The epiphyte species was tolerant to HM stress, as evidenced by the absence of alterations in pigment concentration or biomass allocation. It is noted that epiphyte exhibited the lowest levels of photosynthetic pigments of all species, regardless of the presence of the CuZnNi treatment. Low pigment values are common in this epiphyte species, and it's related to their adaptation to partial shade under the forest canopy (Holcman and Sentelhas, 2013). Since our experiment was conducted under natural sunlight, the species reduces the chlorophyll

content and exhibits opaque leaves coloration (Figure 2), but that did not influence the species ability to tolerate HM. Because epiphytes live in such a unique environment (attached to other plants and under the canopy), the species naturally possesses several morphophysiological adaptations that enable it to thrive in stressful environments, including leaf tank formation, CAM photosynthesis and absorptive leaf trichomes (Silvestro et al., 2014). A recent study further emphasized the epiphyte's responsiveness and high tolerance to environmental pollution, attributed to the effective maintenance of its antioxidant defense system (Giampaoli et al., 2021). Interestingly, the experiment with this epiphyte species revealed the greatest diversity of root ROA, the lowest conductivity values of hydroponic solutions and the highest total levels of PCs. This suggests that, among the studied species, epiphyte has the greatest capacity to regulate nutrient bioavailability through high ROA exudation (Panchal et al., 2021). This finding is important for an epiphyte bromeliad, highlighting additional functionalities of epiphyte roots beyond substrate (host tree) fixation (Young et al., 2022). Furthermore, our study revealed that the epiphyte species efficiently inactivates free HMs within cells by forming complexes with PCs, mainly PC2 in leaves, thus reducing HM toxicity (Asgher et al., 2017).

Herbaceous and liana species were the only ones to show a reduction in pigment concentration, accompanied by negative photosynthetic rates. Decreased photosynthetic pigments levels are a clear indicator of toxicity and represent a severe loss in overall photosynthetic capacity (Zaouali et al., 2020). These species also exhibited changes in biomass allocation between plant organs, resulting in alterations in the root/shoot ratio. This indicates their heightened vulnerability to HM contamination. From an ecological perspective, the biomass reduction and allocation shifts observed in herbaceous and liana species under HM stress can have detrimental effects on their competitiveness and hinder their establishment, particularly in contaminated areas (Michalet et al., 2023).

Antioxidants

The increase in antioxidant levels, such as ascorbic acid and glutathione, are clear indicators of tolerance against oxidative damage caused by ROS generated by excess HM in cells (Maleki et al., 2017; Singh et al., 2019). In our study, only the pioneer and non-pioneer trees species increased both AAr and AAt concentration under excess HM, indicating a high biochemical adaptability and protection against oxidative stress (Gill and Tuteja, 2010). Conversely, herbaceous and liana species exhibited higher capacity to elevate GSH_r under HM stress, prioritizing the regeneration of GSH to its reduced state rather than utilizing it in other metabolic pathways. GSH_r is an exceptionally efficient antioxidant molecule that combats ROS, preventing oxidative damage, and protects cellular structures (Noctor et al., 2012). Additionally,

GSH_r acts as the primary defense mechanism against metal toxicity before PCs synthesis reaches effective levels of metal complexation (Boojar, 2010).

The predominance of AA in the reduced redox state ($AA_r/AA_t > 0.5$) across species in our study suggests a high capacity for AA renewal and an antioxidant system prepared to combat oxidative agents (Brandão et al., 2017). However, GSH, which serves as both an essential antioxidant (Kunert and Foyer, 2023) and precursor of PC (Asgher et al., 2017), was predominantly in the reduced redox state ($GSH_r/GSH_t > 0.5$) only in the non-pioneer tree and herbaceous species cultivated under excess HMs. The predominance of oxidized GSH observed in the pioneer tree species under both HM stress and Control indicates a high utilization of this compound in other metabolic pathways (Noctor et al., 2012). Additionally, the non-pioneer species exhibited the lowest basal levels of total glutathione (GSHt) but responded to excess HM with a significant increase in long-chain phytochelatins (PC6). Similarly, the epiphyte exhibited the highest total levels of phytochelatins, supposedly prioritizing the utilization of GSH for PCs synthesis. Conversely liana species showed the highest level of GSHt in leaves but exhibited lower overall levels of PCs (especially in roots), indicating a prioritization of antioxidant defence over HM-chelating mechanism.

Phytochelatins

The PCA graph highlighted that each species produces higher levels of specific PCs with defined chain-length in response to HM stress. This finding suggests that these PCs could serve as target molecules to indicate HM tolerance level of plant species (Liu et al., 2015). The primary leaf PC-indicators for each species were: PC3 for the pioneer tree, PC6 for the non-pioneer tree and PC4 for the herbaceous species. In contrast, no specific leaf phytochelatin emerged as a consistent indicator of HM stress in the liana and epiphyte species studied. It is well established that the longer chain length of a phytochelatin molecule, the greater its HM-binding capacity and the higher the stability of the PC-HM complex (Chekmeneva et al., 2011). The decrease in PC6 levels but increase in PC4 levels in herbaceous leaves under HM stress may indicate that the species loses the ability to synthesize long-chain phytochelatins, resulting in higher sensitivity to HM stress, consistent with the observed with the physiological damage in these species.

Despite the significant accumulation of HM in roots, all species prioritized PC synthesis in leaves, a trend observed in previous studies (Zhang et al., 2010; Mohamed et al., 2012; Bankaji et al., 2015; Cao et al., 2019). After HM uptake by roots, PCs are among the most effective components of a plant's biochemical defense system for immobilizing absorbed HMs (Boojar, 2010; Singh et al., 2019) and preventing ROS production and consequent oxidative

damage (Cobbett, 2000; Yadav, 2010). The epiphyte species studied exhibited the highest PC2 production among the species studied. Furthermore, its elevated basal PC content likely contributed to its high tolerance to HMs, as evidenced by low physiological damage.

Root organic acids and hydroponic solution parameters

Each species exhibited distinct capacities for ROA exudation, both in terms of diversity and concentration levels. The exudation of ROA depends on several factors, including species, developmental stage, root architecture and the presence or absence of stress (Sandnes et al., 2005; Badri and Vivanco, 2009). In our study, ROA diversity was greater in species with shorter life cycles (epiphyte, liana and herbaceous) compared to those with long life cycles (trees). This supports our hypothesis that HM tolerance mechanisms vary between species with different life-forms.

The diversity of ROA among different life-form species is critical fact to consider in phytoremediation projects targeting HM-contaminated areas, as ROAs play essential roles in regulating nutrient bioavailability and plant-microbiota interactions (Weisskopf et al., 2008). Each ROA also serves specific functions in nutrient availability and plant-soil relationships (Bais et al., 2006). Therefore, herbaceous, liana, and epiphyte species could be valuable for urban greening projects in cities within Atlantic Forest domain. Their higher capacity for ROA exudation can help regulate soil pH and nutrient bioavailability, thereby enhancing beneficial plant-soil interactions. These species are well suited for late-stage ecological restoration of HM-contaminated areas. On the other hand, tree species included in this study may be recommended for the initial phases of ecological restoration programs.

The complete inhibition of exudation of certain ROAs observed in the studied species (except for pioneer tree) under HM stress highlights the significant impact that HM contamination may have on the regulation of natural processes in plants (Badri and Vivanco, 2009). The reduction or inhibition of exuded ROAs contradicts our hypothesis that there would be an increase in ROAs under HM stress, which was based on the results of previous studies (Zhu et al., 2011; Montiel-Rozas et al., 2016). The ROA reduction found in our study may result from decreased carbon availability due to reduced assimilation via photosynthesis and/or metabolism imbalance due to high stress. ROAs are carbon molecules; approximately 11% of the total fixed carbon and 27% of the carbon allocated to roots are exuded into the rhizosphere (Vives-Peris et al., 2020). This percentage can vary depending on plant species, nutritional status, and plant age. Young plants, such as those in our study, can allocate around 30-40% of the total fixed carbon in root exudates (Whipps, 1990). In our study, all species showed a reduction in net carbon assimilation under HM stress, which may lead to lower allocation to

roots and consequently reduced ROA exudation. Additionally, the species may actively reduce ROAs exudation as a strategy to maintain essential acids involved in the tricarboxylic acid (TCA) cycle (such as oxalic, malic, fumaric, citric and succinic), since these are exuded by roots in lesser amounts than non-TCA cycle acids. These compounds play key roles in the energy metabolism of plants and are crucial for maintaining minimal physiological and photosynthetic activities of plants, especially under stress (Zhang and Fernie, 2023).

The pioneer tree exuded extremely high quantities of phytic acid and exhibited the lowest physiological alterations of all species. Phytic acid has a high affinity for various metallic ions, such as Zn^{2+}, Cu^{2+}, Cd^{2+}, Ni^{2+} and Pb^{2+} (Kim et al., 2017) and forms stable complexes that reduce their bioavailability for plant uptake (Crea et al., 2008). Therefore, it is plausible that the high exudation of phytic acid represents one of the primary strategies this species employs to tolerate HM stress. In contrast, the liana and epiphyte species only exuded phytic acid when subjected to stress, indicating that increased phytic acid exudation may serve as an active protective mechanism against excess HMs in these species. This response has been observed in other studies as well; for example, species from the genus *Pteris* increase phytic acid exudation when grown in soil contaminated with arsenic (Liu et al., 2016).

The reduction in pH of hydroponic solutions containing excess HMs over time indicates that progressive acidification occurred. This acidification cannot be explained by increased exudation of root ROAs, as exudation decreased under HM stress, in some cases, was completely inhibited. Instead, it may have resulted from the increased exudation of other compounds, such as phenols, amino acids, proteins, and mucilage, which also lower solution pH and may be released under HM stress (Bali et al., 2020). The varying conductivity levels of nutrient solutions suggest that the uptake rates of nutrients (including the HMs targeted in this research) differ among species. Electrical conductivity (EC) is a measurement that indirectly indicates the quantity of free ions in a solution, thus estimating the availability of nutrients (Velazquez-Gonzalez, 2022). In our study, the conductivity values appear to be related to the diversity of ROAs exuded by each species. The lowest conductivity values (indicating lower available nutrients) were observed in epiphyte, liana and herbaceous species, which also exhibited the highest diversity of ROAs. This supports the idea that ROAs can act as nutrient regulators by complexing free ions in the solution, thereby reducing nutrient availability (Ma et al., 2020).

Overall tolerance strategies and study limitations

Overall, the plant species studied focused more on strategies that immobilize HMs within the cells (such as phytochelatins synthesis) or mitigate oxidative stress under Cu, Zn and

Ni stress (via non-enzymatic antioxidant synthesis) than on avoidance mechanisms like ROAs exudation. The species exhibited distinct abilities to exude high concentrations and/or a high diversity of ROAs, which may reduce HM bioavailability and confer benefits, even although ROAs synthesis was not triggered by excess HM levels. Additionally, root cell wall storage emerged as another important strategy for restricting the deleterious effects of Cu, Zn and Ni in the studied species, particularly in the liana and pioneer tree species (Figure II6).

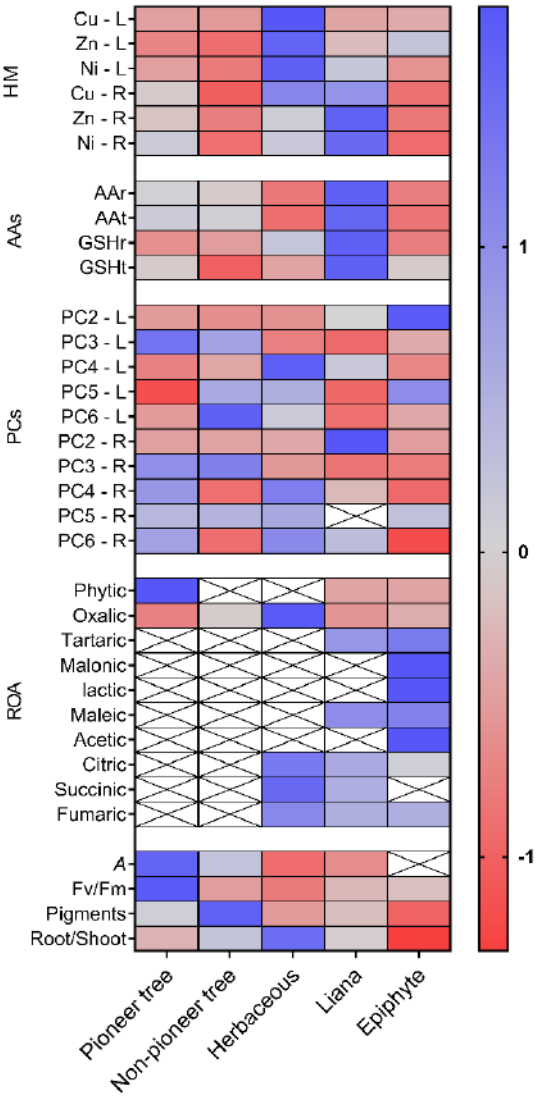

Fig. II 6. Heatmap of the standardized data of all biomarkers analyzed in the pioneer tree, non-pioneer tree, herbaceous, liana and epiphyte species under CuZnNi stress. HM: Heavy metal accumulation. As: Antioxidants. PCs: Phytochelatins. ROA: Root organic acids. L: Leaf. R: Root. r: reduced. t: total. Cells with X indicate undetected compounds.

Based on the overall evaluation and metal accumulation and physiological damage, we were able to rank the studied species according to their tolerance strategies and level of stress responses to Cu, Zn and Ni, as follows:

Pioneer tree (*S. terebinthifolia*) = epiphyte (*A. fasciata*) > non-pioneer tree (*C. legalis*) > liana (*P. edulis*) = herbaceous (*S. sylvatica*).

The tolerant pioneer tree species was characterized by effective avoidance (high exudation of phytic acid), immobilization (increased synthesis of PC3 on leaves), and mitigation (enhanced production of AA) strategies. As a result, this species accumulated intermediate amounts of metals in its leaves and exhibited minimal physiological damage. Similarly, the tolerant epiphyte species demonstrated both avoidance (the greatest diversity of exuded ROAs) and immobilization (high synthesis of phytochelatin PC2 in leaves) mechanisms, which coincided with proportionally lower levels of HM accumulation in both leaves and roots. The non-pioneer tree could not be clearly categorized as tolerant, as it exhibited significant physiological imbalances despite maintaining overall growth and showing some tolerance responses through immobilization (increased synthesis of phytochelatin PC6 in leaves) and mitigation (enhanced production of AAs). This was observed in response to low heavy metal accumulation in its leaves. The herbaceous and liana species were the most sensitive species studied, exhibiting severe physiological damage and alterations in biomass allocation. The tolerance strategies observed in both herbaceous (increased leaf contents of phytochelatin PC4 and high oxalic acid exudation) and the liana species (high antioxidant activity and increased synthesis of phytochelatin PC2 in roots) were not sufficient to fully mitigate the stress induced by the equivalently high HMs contents in their leaves and/or roots, as indicated by the heatmap.

Although we could identify the main tolerance strategies and accumulation capacity of the studied species, we understand that our study has intrinsic limitations, highlighting: 1) We adopted only one species as the representative model for each plant life-form. To obtain a broader understanding, studies with more species are needed to verify if the response patterns found here are consistent within each life-form group. 2) The individuals in our study were young pre-flowering plants. The responses dynamics of adult plants and/or in reproductive phase to multiple HM-stress may be different. New studies with mature plants and under different physiological phases are needed to better elucidate the strategies and tolerance levels of each life-form. 3) Our study focused on the combined effect of three heavy metals (Cu + Zn + Ni) at an equal concentration (25 μM) since the objective was not to differentiate the stress intensity caused by each individual element. Future studies investigating these elements individually and across a range of concentrations may provide more detailed and element-specific insights. 4) Our study employed simple salts and hydroponic cultivation to ensure high metal absorption and to emphasize biochemical responses. However, studies conducted in soil systems and involving metals complexed with chelators can reveal a more comprehensive understanding of these species' behavior in natural environments.

CONCLUSIONS

The native Atlantic Forest species with different life-forms studied in the present study (pioneer tree, non-pioneer tree, herbaceous, liana and epiphyte) exhibited distinct tolerance strategies and HM accumulation, confirming our hypothesis I. *S. terebinthifolia* (pioneer tree – fast growth) is a HM-tolerant species, employing a combination of avoidance, immobilization, and mitigation mechanisms. *A. fasciata* (epiphyte – slow growth) is also a HM-tolerant species, relying on avoidance and immobilization mechanisms. *C. legalis* (non-pioneer tree – slow growth) is a HM-moderately tolerant species employing relevant immobilization and mitigation mechanisms but presents significant physiological imbalances under HM-stress. *S. sylvatica* (herbaceous – fast growth) and *P. edulis* (liana – fast growth) are HM-sensitive species exhibiting severe physiological damage under HM-stress due to less effective HM-tolerance mechanisms. Growth rate (fast growth x slow growth) was not a reliable predictor of HM-tolerance across the studied plant species, refuting our hypothesis II.

Our results expand the scientific knowledge about plants HM-tolerance by demonstrating that the plant life-form not only defines its ecological role but also may influence HM-tolerance and HM-accumulation capacity. Our findings can contribute to the identification of HM-tolerant plant species using life-form traits and support their selection for conservation and restoration of HM-contaminated areas. The trees *Schinus terebinthifolia* and *Cariniana legalis* are recommended for the initial phases of ecological restoration programs of HM-contaminated areas, while herbaceous *Seemannia sylvatica*, liana *Passiflora edulis* and epiphyte *Aechmea fasciata* could be suited for late-stage phases to promote soil-microbiological dynamics improvement interactions due to higher ROAs diversity exudation.

The detection and evaluation of biochemical tolerance compounds such ascorbic acid, glutathione, root organic acids and phytochelatins are effective biochemical indicators of HM-tolerance, since the more evident these mechanisms are, less physiological damage are observed. Future studies with more species, different HMs diversity and concentrations, and environmentally realistic conditions are essential to better understand the HM-tolerance mechanisms and plant-stress dynamics, and to confirm whether distinct biochemical strategies are more related to plant life form than taxonomic aspects.

Acknowledgements

We would like to thank to Fundação de Amparo à Pesquisa do Estado de São Paulo (FAPESP) for financial support (Processes 201750341-0 and /2021/09686-9) and to Instituto de Pesquisas Ambientais for infrastructure support.

Author contributions:

Matheus Casarini Siqueira: Conceptualization; Data Curation; Formal Analysis; Investigation; Methodology; Validation; Visualization; Writing – Original draft; Writing – Review and editing

João Vítor Casimiro: Data curation; Investigation; Methodology

Alex do Nascimento: Data curation; Formal Analysis; Investigation; Methodology

Mirian Cilene Spasiani Rinaldi: Conceptualization; Validation; Visualization; Writing – review and editing

Armando Reis Tavares: Conceptualization; Funding acquisition; Project administration; Resources; Supervision; Validation; Writing – review and editing

Marisa Domingos: Conceptualization; Data curation; Formal analysis; Funding acquisition; Project administration; Resources; Supervision; Validation; Visualization; Writing – original draft; Writing – review and editing

Funding sources

This work was supported by Fundação de Amparo à Pesquisa do Estado de São Paulo (FAPESP) (Processo FAPESP 2021/09686-9 and 2017/50341-0).

REFERENCES

Anderson, M.E., 1985. Determination of glutathione and glutathione disulfide in biological samples. Method. Enzymol. 113, 548–554. https://doi.org/10.1016/S0076-6879(85)13073-9

Asgher, M., Per, T.S., Anjum, S., Khan, M.I.R., Masood, A., Verma, S., Khan, N.A., 2017. Contribution of glutathione in heavy metal stress tolerance in plants. In: M. Iqbal R. Khan, Nafees A. Khan (Eds.), Reactive oxygen species and antioxidant systems in plants: role and regulation under abiotic stress, Springer, Singapore, pp297-313. https://doi.org/10.1007/978-981-10-5254-5_12

Badri, D.V., Vivanco, J.M., 2009. Regulation and function of root exudates. Plant Cell Environ. 32(6), 666–681. https://doi.org/10.1111/j.1365-3040.2009.01926.x

Bais, H.P., Weir, T.L., Perry, L.G., Gilroy, S., Vivanco, J.M., 2006. The role of root exudates in rhizosphere interactions with plants and other organisms. Annu. Rev. Plant Biol. 57, 233–266. https://doi.org/10.1146/annurev.arplant.57.032905.105159

Bali, A.S., Sidhu, G.P.S., Kumar, V., 2020. Root exudates ameliorate cadmium tolerance in plants: a review. Environ. Chem. Lett. 18(4), 1243–1275. https://doi.org/10.1007/s10311-020-01012-x

Bankaji, I., Caçador, I., Sleimi, N., 2015. Physiological and biochemical responses of *Suaeda fruticosa* to cadmium and copper stresses: growth, nutrient uptake, antioxidant enzymes, phytochelatin, and glutathione levels. Environ. Sci. Pollut. Res. 22, 13058–13069. https://doi.org/10.1007/s11356-015-4414-x

Barbosa, G.M., Calixto, R., Nakazato, R.K., Tavares, A.R., Domingos, M., Rinaldi, M.C.S., 2024. Effects of heavy metals and high temperature on Atlantic Forest species: analysis of their tolerance capacity. Chemosphere, 142449. https://doi.org/10.1016/j.chemosphere.2024.142449

Beladi, M., Kashani, A., Habibi, D., Paknejad, F., Golshan, M., 2011. Uptake and effects of lead and copper on three plant species in contaminated soils: role of phytochelatin. Afr. J. Agric. Res. 6(15), 3483–3492.

Bhat, A.G., Mukherjee, S., Hasan, M., Pardarkar, V., 2023. Growing beyond ground: unravelling the potential of dutch bucket hydroponics. Sci. World J. 3(10), 2689–2692. https://doi.org/10.5281/zenodo.10051606

Boojar, M., 2010. Role of antioxidant enzyme responses and phytochelatins in tolerance strategies of *Alhagi camelorum* Fisch growing on copper mine. Acta Bot. Croat. 69(1), 107–121.

Bouazizi, H., Jouili, H., Geitmann, A., El Ferjani, E., 2010. Copper toxicity in expanding leaves of *Phaseolus vulgaris* L.: antioxidant enzyme response and nutrient element uptake. Ecotoxic.

Environ. Saf. 73(6), 1304–1308. https://doi.org/10.1016/j.ecoenv.2010.05.014

Brandão, S.E., Barbosa, G.M., Siqueira, M.C., de O.A. Campos, R., Dalsin, A.C., Rinaldi, M.C., Domingos, M., 2022. Nickel and zinc absorption and growth of Atlantic Forest trees cultivated in polluted soil. Plant Soil, 1–13. https://doi.org/10.1007/s11104-021-05228-w

Brandão, S.E., Bulbovas, P., Lima, M.E., Domingos, M., 2017. Biochemical leaf traits as indicators of tolerance potential in tree species from the Brazilian Atlantic Forest against oxidative environmental stressors. Sci. Total Environ. 575, 406–417. https://doi.org/10.1016/j.scitotenv.2016.10.006

Burkey, K.O., Neufeld, H.S., Souza, L., Chappelka, A.H., Davison, A.W., 2006. Seasonal profiles of leaf ascorbic acid content and redox state in ozone-sensitive wildflowers. Environ. Pollut. 143(3), 427–434. https://doi.org/10.1016/j.envpol.2005.12.009

Cao, Y.Y., Qi, C.D., Li, S., Wang, Z., Wang, X., Wang, J., Ren, S., Li, X., Zhang, N., Guo, Y.D., 2019. Melatonin alleviates copper toxicity via improving copper sequestration and ROS scavenging in cucumber. Plant Cell Physiol. 60(3), 562–574. https://doi.org/10.1093/pcp/pcy226

Cawthray, G.R., 2003. An improved reversed-phase liquid chromatographic method for the analysis of low-molecular mass organic acids in plant root exudates. J. Chromatogr. 1011(1-2), 233–240. https://doi.org/10.1016/S0021-9673(03)01129-4

Chekmeneva, E., Gusmão, R., Díaz-Cruz, J.M., Ariño, C., Esteban, M., 2011. From cysteine to longer chain thiols: thermodynamic analysis of cadmium binding by phytochelatins and their fragments. Metallomics, 3(8), 838–846. https://doi.org/10.1039/c1mt00028d

Chen, S., Lin, R., Lu, H., Wang, Q., Yang, J., Liu, J., Yan, C., 2020. Effects of phenolic acids on free radical scavenging and heavy metal bioavailability in *Kandelia obovata* under cadmium and zinc stress. Chemosphere, 249, 126341. https://doi.org/10.1016/j.chemosphere.2020.126341

Cobbett, C., Goldsbrough, P., 2002. Phytochelatins and metallothioneins: roles in heavy metal detoxification and homeostasis. Ann. Rev. Plant Biol. 53(1), 159–182. https://doi.org/10.1146/annurev.arplant.53.100301.135154

Cobbett, C.S., 2000. Phytochelatins and their roles in heavy metal detoxification. Plant Physiol. 123(3), 825–832. https://doi.org/10.1104/pp.123.3.825

Crea, F., De Stefano, C., Milea, D., Sammartano, S., 2008. Formation and stability of phytate complexes in solution. Coord. Chem. Rev. 252(10–11), 1108–1120. https://doi.org/10.1016/j.ccr.2007.09.008

Dafré-Martinelli, M., Figueiredo, A.M.G., Domingos, M., 2020. Trace element leaf accumulation in native trees from the remaining Semideciduous Atlantic Forest in Brazil.

Atmospheric Pollution Research, 11(5), 871-879. https://doi.org/10.1016/j.apr.2020.01.015

Esposito, M.P., Nakazato, R.K., Pedroso, A.N.V., Lima, M.E.L., Figueiredo, M.A., Diniz, A.P., Kozovits, A.R., Domingos, M., 2018. Oxidant-antioxidant balance and tolerance against oxidative stress in pioneer and non-pioneer tree species from the remaining Atlantic Forest. Sci. Total Environ. 625, 382–393. https://doi.org/10.1016/j.scitotenv.2017.12.255

Favaretto, V.F., Martinez, C.A., Soriani, H.H., Furriel, R.P., 2011. Differential responses of antioxidant enzymes in pioneer and late-successional tropical tree species grown under sun and shade conditions. Environ. Exp. Bot. 70(1), 20–28. https://doi.org/10.1016/j.envexpbot.2010.06.003

Filipović-Trajković, R., Ilić, Z.S., Šunić, L., Andjelković, S., 2012. The potential of different plant species for heavy metals accumulation and distribution. J. Food Agric. Environ. 10(1), 959–964.

Galal, T.M., Shehata, H.S., 2015. Bioaccumulation and translocation of heavy metals by *Plantago major* L. grown in contaminated soils under the effect of traffic pollution. Ecol. Indic. 48, 244–251. https://doi.org/10.1016/j.ecolind.2014.08.013

Ghorbel, R., Chakchak, J., Malayoğlu, H.B., Çetin, N.S., 2021. Hydroponics "soilless farming": the future of food and agriculture–A. International Students Science Congress Proceedings Book, Ege.

Ghori, N.H., Ghori, T., Hayat, M.Q., Imadi, S.R., Gul, A., Altay, V., Ozturk, M., 2019. Heavy metal stress and responses in plants. Int. J. Environ. Sci. Technol. 16(3), 1807–1828. https://doi.org/10.1007/s13762-019-02215-8

Giampaoli, P., Tavares, A.R., Domingos, M., 2021. Physiological responses of two different epiphytic bromeliads exposed in a polluted subtropical region in southeast Brazil characterized by seasonal climate. Ecol. Indic. 120, 106945. https://doi.org/10.1016/j.ecolind.2020.106945

Gill, S.S., Tuteja, N., 2010. Reactive oxygen species and antioxidant machinery in abiotic stress tolerance in crop plants. Plant Physiol. Biochem. 48(12), 909–930. https://doi.org/10.1016/j.plaphy.2010.08.016

Gong, Q., Wang, L., Dai, T., Zhou, J., Kang, Q., Chen, H., Li, K., Li, Z., 2019. Effects of copper on the growth, antioxidant enzymes and photosynthesis of spinach seedlings. Ecotoxicol. Environ. Saf. 171, 771–780. https://doi.org/10.1016/j.ecoenv.2019.01.016

Hoagland, D.R., Arnon, D.I., 1950. The water-culture method for growing plants without soil. Circular. California agricultural experiment station, 347(2nd edit), Berkeley.

Holcman, E., & Sentelhas, P. C. (2013). Bromeliads production in greenhouses associated to different shading screens. Hortic. Bras. 31 (3), 386-391. https://doi.org/10.1590/S0102-05362013000300008

Hunaiti, A.A., Abukhalaf, I.K., Silvestrov, N., Bayorh, M., 2003. Rapid HPLC procedure for the quantitation of phytochelatins in plant tissue extracts. J. Liq. Chromatogr. 26(20), 3463–3473. https://doi.org/10.1081/JLC-120025602

Jia, H., Wang, X., Wei, T., Zhou, R., Muhammad, H., Hua, L., Ren, X., Guo, J., Ding, Y., 2019. Accumulation and fixation of Cd by tomato cell wall pectin under Cd stress. Environ. Exp. Bot. 167, 103829. https://doi.org/10.1016/j.envexpbot.2019.103829

Kalaji, H.M., Jajoo, A., Oukarroum, A., Brestic, M., Zivcak, M., Samborska, I.A., Kusaka, M., Łukasik, I., Goltsev, V., Ladle, R.J., 2016. Chlorophyll a fluorescence as a tool to monitor physiological status of plants under abiotic stress conditions. Acta Physiol. Plant. 38, 1–11. https://doi.org/10.1007/s11738-016-2113-y

Kar, S., Agrahari, R.K., Panda, S.K., 2021. Metal ion toxicity and tolerance mechanisms in plants growing in acidic soil. J. Soil Sci. Agroclim. 18(1), 107–114. https://doi.org/10.20961/stjssa.v18i1.51254

Kim, H.J., Im, S., Kim, J.C., Hong, W.G., Shin, K., Jeong, H.Y., Hong, Y.J., 2017. Phytic acid doped polyaniline nanofibers for enhanced aqueous copper (II) adsorption capability. ACS Sustain. Chem. Eng. 5(8), 6654–6664. https://doi.org/10.1021/acssuschemeng.7b00898

Kunert, K.J., Foyer, C.H., 2023. The ascorbate/glutathione cycle. In: Advances in botanical research (Vol. 105, pp. 77-112). Academic Press, Cambridge. https://doi.org/10.1016/bs.abr.2022.11.004

Liu, W., Zhang, X., Liang, L., Chen, C., Wei, S., Zhou, Q., 2015. Phytochelatin and oxidative stress under heavy metal stress tolerance in plants. In: Gupta, D., Palma, J., Corpas, F. (eds) Reactive oxygen species and oxidative damage in plants under stress. Springer, Cham., pp191-217. https://doi.org/10.1007/978-3-319-20421-5_8

Liu, X., Fu, J.W., Guan, D.X., Cao, Y., Luo, J., Rathinasabapathi, B., Chen, Y., Ma, L.Q., 2016. Arsenic induced phytate exudation and promoted FeAsO4 dissolution and plant growth in As-hyperaccumulator *Pteris vittata*. Environ. Sci. Technol. 50(17), 9070–9077. https://doi.org/10.1021/acs.est.6b00668

López, A., Montaño, A., Garcia, P., Garrido, A., 2005. Note: Quantification of ascorbic acid and dehydroascorbic acid in fresh olives and in commercial presentations of table olives. Food Sci. Techn. Intern. 11(3), 199–204. https://doi.org/10.1177/1082013205054421

Ma, H., Li, X., Wei, M., Zeng, G., Hou, S., Li, D., Xu, H., 2020. Elucidation of the mechanisms into effects of organic acids on soil fertility, cadmium speciation and ecotoxicity in contaminated soil. Chemosphere, 239, 124706. https://doi.org/10.1016/j.chemosphere.2019.124706

Mahmud, J., Bhuyan, M.B., Anee, T.I., Nahar, K., Fujita, M., Hasanuzzaman, M., 2019.

Reactive oxygen species metabolism and antioxidant defense in plants under metal/metalloid stress. Plant Abiotic Stress Tolerance: Agronomic, Molecular and Biotechnological Approaches, 221-257. https://doi.org/10.1007/978-3-030-06118-0_10

Maleki, M., Ghorbanpour, M., Kariman, K., 2017. Physiological and antioxidative responses of medicinal plants exposed to heavy metals stress. Plant Gene, 11, 247–254. https://doi.org/10.1016/j.plgene.2017.04.006

Marques, M.C.M., Trindade, W., Bohn, A., Grelle, C.E.V., 2021. The Atlantic Forest: an introduction to the megadiverse Forest of South America. In: Marques, M.C.M., Grelle, C.E.V. (eds) The Atlantic Forest. Springer, Cham.https://doi.org/10.1007/978-3-030-55322-7_1

Michalet, R., Delerue, F., Liancourt, P., 2023. Disentangling the effects of biomass and productivity in plant competition. Ecol. 104(1), e3851. https://doi.org/10.1002/ecy.3851

Minocha, R., Martinez, G., Lyons, B., Long, S., 2009. Development of a standardized methodology for quantifying total chlorophyll and carotenoids from foliage of hardwood and conifer tree species. Can. J. For. Res. 39(4), 849–861. https://doi.org/10.1139/X09-015

Mohamed, A.A., Castagna, A., Ranieri, A., di Toppi, L.S., 2012. Cadmium tolerance in *Brassica juncea* roots and shoots is affected by antioxidant status and phytochelatin biosynthesis. Plant Physiol. Biochem. 57, 15–22. https://doi.org/10.1016/j.plaphy.2012.05.002

Montiel-Rozas, M.M., Madejón, E., Madejón, P., 2016. Effect of heavy metals and organic matter on root exudates (low molecular weight organic acids) of herbaceous species: An assessment of sand and soil conditions under different levels of contamination. Environ. Pollut. 216, 273–281. https://doi.org/10.1016/j.envpol.2016.05.080

Nakazato, R.K., Lourenço, I.S., Esposito, M.P., Lima, M.E., Ferreira, M.L., O.A. Campos, R., Rinaldi, M.C.S., Domingos, M., 2021. Trace metals at the tree-litter-soil-interface in Brazilian Atlantic Forest plots surrounded by sources of air pollution. Environ. Pollut. 268, 115797. https://doi.org/10.1016/j.envpol.2020.115797

Navarrete, A., González, A., Gómez, M., Contreras, R.A., Díaz, P., Lobos, G., Brown, M.T., Sáez, C.A., Moenne, A., 2019. Copper excess detoxification is mediated by a coordinated and complementary induction of glutathione, phytochelatins and metallothioneins in the green seaweed *Ulva compressa*. Plant Physiol. Biochem. 135, 423–431. https://doi.org/10.1016/j.plaphy.2018.11.019

Noctor, G., Mhamdi, A., Chaouch, S., Han, Y.I., Neukermans, J., Marquez-Garcia, B., Queval, G., Foyer, C.H., 2012. Glutathione in plants: an integrated overview. Plant Cell Environ. 35(2), 454–484. https://doi.org/10.1111/j.1365-3040.2011.02400.x

Osmolovskaya, N., Dung, V.V., Kuchaeva, L., 2018. The role of organic acids in heavy metal tolerance in plants. Biol. Comm. 63(1), 9–16. https://doi.org/10.21638/spbu03.2018.103

Panchal, P., Miller, A.J., Giri, J., 2021. Organic acids: versatile stress-response roles in plants. J. Exp. Bot. 72(11), 4038–4052. https://doi.org/10.1016/bs.aambs.2018.10.001

Pandey, A.K., Gautam, A., Dubey, R.S., 2019. Transport and detoxification of metalloids in plants in relation to plant-metalloid tolerance. Plant Gene, 17, 100171. https://doi.org/10.1016/j.plgene.2019.100171

Parrotta, L., Guerriero, G., Sergeant, K., Cai, G., Hausman, J.F., 2015. Target or barrier? The cell wall of early-and later-diverging plants vs cadmium toxicity: differences in the response mechanisms. Front. Plant Sci. 6, 123937. https://doi.org/10.3389/fpls.2015.00133

Pasricha, S., Mathur, V., Garg, A., Lenka, S., Verma, K., Agarwal, S., 2021. Molecular mechanisms underlying heavy metal uptake, translocation and tolerance in hyperaccumulators-an analysis: Heavy metal tolerance in hyperaccumulators. Environ. Chall. 4, 100197. https://doi.org/10.1016/j.envc.2021.100197

Pietrini, F., Iori, V., Cheremisina, A., Shevyakova, N.I., Radyukina, N., Kuznetsov, V.V., Zacchini, M., 2015. Evaluation of nickel tolerance in *Amaranthus paniculatus* L. plants by measuring photosynthesis, oxidative status, antioxidative response and metal-binding molecule content. Environ. Sci. Pollut. Res. 22(1), 482–494. https://doi.org/10.1007/s11356-014-3349-y

Raij, B.V., Andrade, J.C., Cantarella, H., Quaggio, J.A., 2001. Análise química para avaliação da fertilidade de solos tropicais. Instituto Agronômico de Campinas, Campinas.

Rizwan, M., Imtiaz, M., Dai, Z., Mehmood, S., Adeel, M., Liu, J., Tu, S., 2017. Nickel stressed responses of rice in Ni subcellular distribution, antioxidant production, and osmolyte accumulation. Environ. Sci. Pollut. Res. 24, 20587–20598. https://doi.org/10.1007/s11356-017-9665-2

Sagardoy, R., Morales, F., López-Millán, A., Abadía, A., Abadía, J., 2009. Effects of zinc toxicity on sugar beet (*Beta vulgaris* L.) plants grown in hydroponics. Plant Biol. 11(3), 339–350. https://doi.org/10.1111/j.1438-8677.2008.00153.x

Sandnes, A., Eldhuset, T.D., Wollebæk, G., 2005. Organic acids in root exudates and soil solution of Norway spruce and silver birch. Soil Biol. Biochem. 37(2), 259–269. https://doi.org/10.1016/j.soilbio.2004.07.036

Silvestro, D., Zizka, G., Schulte, K., 2014. Disentangling the effects of key innovations on the diversification of *Bromelioideae* (Bromeliaceae). Evolution 68, 163–175. https://doi.org/10.1111/evo.12236

Singh, A., Kumar, A., Yadav, S., Singh, I.K., 2019. Reactive oxygen species-mediated signaling during abiotic stress. Plant Gene 18, 100173. https://doi.org/10.1016/j.plgene.2019.100173

Singh, S., Yadav, V., Arif, N., Singh, V.P., Dubey, N.K., Ramawat, N., Prasad, R., Sahi, S., Tripathi, D.K., Chauhan, D.K., 2020. Heavy metal stress and plant life: uptake mechanisms,

toxicity, and alleviation. In: Tripathi, D.K., Singh, V.P., Chauhan, D.K., Sharma, S., Prasad, S.M., Dubey, N.K., Ramawat, N. (Eds.), Plant life under changing environment. Academic Press, Cambridge, pp. 271-287. https://doi.org/10.1016/B978-0-12-818204-8.00001-1

Soares, C.R.F.S., Siqueira, J.O., Carvalho, J.G.D., Moreira, F., Souza, M., Grazziotti, P.H., 2000. Growth and mineral nutrition of *Eucalyptus maculata* and *Eucalypts urophylla* in nutrient solution with increasing concentration of copper. Rev. Bras. Fisiol. Veg. 12, 213–225. https://doi.org/10.1590/S0103-31312000000300005

Talukder, P., 2021. Role of metallothionein and phytochelatin in combating abiotic stress imparted by copper-induced toxicity in brinjal (*Solanum melongena*). In: Ramkrishna, D., Sengupta, S., Dey Bandyopadhyay, S., Ghosh, A. (eds) Advances in Bioprocess Engineering and Technology. Lecture Notes in Bioengineering. Springer, Singapore, pp. 349-358. https://doi.org/10.1007/978-981-15-7409-2_35

Vardhan, K.H., Kumar, P.S., Panda, R.C., 2019. A review on heavy metal pollution, toxicity and remedial measures: Current trends and future perspectives. J. Mol. Liq. 290, 111197. https://doi.org/10.1016/j.molliq.2019.111197

Vasconcellos, T. J. D., Moreira, N. D. S., Santos, R. S. D., Anjos, M. J. D., Callado, C. H., 2021. Chemical elements analysis of the soil at an urbanization gradient in the Atlantic Forest. Revista Árvore, 45, e4504. https://doi.org/10.1590/1806-908820210000004

Vassilev, A., Perez-Sanz, A., Cuypers, A., Vangronsveld, J., 2007. Tolerance of two hydroponically grown *Salix* genotypes to excess zinc. J. Plant Nutrit. 30(9), 1471–1482. https://doi.org/10.1080/01904160701555671

Velazquez-Gonzalez, R.S., Garcia-Garcia, AL., Ventura-Zapata, E., Barceinas-Sanchez, J.D.O., Sosa-Savedra, J.C., 2022. A review on hydroponics and the technologies associated for medium-and small-scale operations. Agriculture 12(5), 646. https://doi.org/10.3390/agriculture12050646

Vives-Peris, V., De Ollas, C., Gómez-Cadenas, A., Pérez-Clemente, R.M., 2020. Root exudates: from plant to rhizosphere and beyond. Plant Cell Rep. 39(1), 3–17. https://doi.org/10.1007/s00299-019-02447-5

Wang, Y., Wang, S., Nan, Z., Ma, J., Zang, F., Chen, Y., Li, Y., Zhang, Q., 2015. Effects of Ni stress on the uptake and translocation of Ni and other mineral nutrition elements in mature wheat grown in sierozem from northwest of China. Environ. Sci. Pollut. Res. 22, 19756–19763. https://doi.org/10.1007/s11356-015-5153-8

Weisskopf, L., Le Bayon, R.C., Kohler, F., Page, V., Jossi, M., Gobat, J.M., Martinoia, E., Aragno, M., 2008. Spatio-temporal dynamics of bacterial communities associated with two plant species differing in organic acid secretion: a one-year microcosm study on lupin and

wheat. Soil Biol. Biochem. 40(7), 1772–1780. https://doi.org/10.1016/j.soilbio.2008.02.018

Whipps J.M., 1990. Carbon economy. In: The Rhizosphere (ed.J.M. Lynch), pp. 59–97. John Wiley & Sons Ltd, Essex.

Xie, L., Hao, P., Cheng, Y., Ahmed, I. M., Cao, F., 2018. Effect of combined application of lead, cadmium, chromium and copper on grain, leaf and stem heavy metal contents at different growth stages in rice. Ecotoxicology and Environmental Safety, 162, 71-76. https://doi.org/10.1016/j.ecoenv.2018.06.072

Yadav, S.K., 2010. Heavy metals toxicity in plants: an overview on the role of glutathione and phytochelatins in heavy metal stress tolerance of plants. S. Afr. J. Bot. 76, 167–179. https://doi.org/10.1016/j.sajb.2009.10.007

Young, J.L.M., Siqueira, M.C., Kanashiro, S., Silva, E.D., Tavares, A.R., 2022. Nutrients uptake by silver vase bromeliad roots. Ornam. Hort. 28, 340–346. https://doi.org/10.1590/2447-536X.v28i3.2460

Zang, F., Wang, S., Chen, Y., Nan, Z., & Zhao, C., 2020. Accumulation and translocation of copper in Cu-polluted sierozem in northwest China. Arch. Agron. Soil Sci. 67(10), 1301-1312. https://doi.org/10.1080/03650340.2020.1789968

Zaouali, W., Mahmoudi, H., Salah, I.B., Mejri, F., Casabianca, H., Hosni, K., Ouerghi, Z., 2020. Copper-induced changes in growth, photosynthesis, antioxidative system activities and lipid metabolism of cilantro (*Coriandrum sativum* L.). Biologia, 75, 367–380. https://doi.org/10.2478/s11756-020-00419-9

Zhang, Y., Fernie, A.R., 2023. The role of TCA cycle enzymes in plants. Adv. Biol. 7(8), 2200238. https://doi.org/10.1002/adbi.202200238

Zhang, Z.C., Chen, B.X., Qiu, B.S., 2010. Phytochelatin synthesis plays a similar role in shoots of the cadmium hyperaccumulator *Sedum alfredii* as in non-resistant plants. Plant Cell Environ. 33(8), 1248–1255. https://doi.org/10.1111/j.1365-3040.2010.02144.x

Zhu, X. F., Zheng, C., Hu, Y.T., Jiang, T.A.O., Liu, Y.U., Dong, N.Y., Yang, J.L., Zheng, S.J., 2011. Cadmium-induced oxalate secretion from root apex is associated with cadmium exclusion and resistance in *Lycopersicon esulentum*. Plant Cell Environ. 34(7), 1055–1064. https://doi.org/10.1111/j.1365-3040.2011.02304.x

Zwolak, A., Sarzyńska, M., Szpyrka, E., Stawarczyk, K., 2019. Sources of soil pollution by heavy metals and their accumulation in vegetables: A review. Water Air Soil Pollut. 230, 1–9. https://doi.org/10.1007/s11270-019-4221-y

Capítulo III

--

Manuscrito aceito para publicação na revista "*Journal of Forestry Research*", incluído com permissão de acordo com a política de direitos de autor da Springer Nature para teses e dissertações [*Reproduced with permission from Springer Nature*].

--

Biomass response of *Schinus terebinthifolia* to elevated ozone: evidence for a dose-dependent hormetic effect

Matheus Casarini Siqueira[a*], Barbara Baesso Moura[b,c], Yasutomo Hoshika[b,c], Elena Paoletti[b,c], Armando Reis Tavares[d], Marisa Domingos[a]

[a] *Environmental Research Institute, Av. Miguel Estefno, 3687, 04301-012, São Paulo Brazil.*

[b] *Institute of Research on Terrestrial Ecosystems (IRET), National Research Council, Via Madonna del Piano 10, 50019 Sesto Fiorentino, Italy*

[c] *National Biodiversity Future Center (NBFC), Palermo 90133, Italy*

[d] *Agronomic Institute, Av. Barão de Itapura, 1481, 13020-902, Jundiaí, Brazil*

[*] *Corresponding author: matheus.casarini1@gmail.com, +55 11 981846119, ORCID (0000-0001-7776-3805)*

Highlights

Ozone risk assessment for *Schinus terebinthifolia* was explored for the first time.

S. terebinthifolia stomatal ozone uptake model was parameterized.

Nonlinear stomatal flux-based models better predicted ozone risk to *S. terebinthifolia* biomass.

2.56 mmol O_3 m^{-2} POD_{16} and 3.37 mmol O_3 m^{-2} POD_{15} were the critical levels to prevent 4% of total and leaf biomass loss, respectively.

S. terebinthifolia is highly tolerant to ozone stress.

ABSTRACT

Schinus terebinthifolia (Raddi) is a tropical fast-growing broadleaf tree species from the Atlantic Forest in Brazil, a threatened biodiversity hotspot. The species has socioeconomic importance and is employed in forest restoration programs and urban greening. In urban environments, plants are exposed to several abiotic stressors, such as atmospheric pollution. Tropospheric ozone (O_3) is one of the main secondary pollutants that affect plant growth and survival. Therefore, determining the critical levels (CL) of phytotoxic O_3 is essential. Ozone risk assessment for *S. terebinthifolia* is unknown. Forty-five *S. terebinthifolia* seedlings were cultivated in pots and submitted to 5 ozone treatments (Ambient Air – AA; 1.5× AA; 2.0× AA; AA → 2.0× and 2.0× → AA) for three months in an O_3-free-air controlled exposure facility. Ozone risk assessment was conducted using environmental data, measurements of stomatal O_3 uptake and seedling biomass. To find the best model for predicting O_3-induced biomass loss, we tested the Accumulated Ozone exposure over a Threshold of 40 ppb (AOT40) and the Phytotoxic Ozone Dose above a threshold 'y' (POD_y) using linear and 116 nonlinear statistical models. POD_{16} and POD_{15} when applied with the four-parameter nonlinear logarithmic model "Bragg4" provided the best fit for assessing O_3 risk based on total and leaf biomass, respectively. The species exhibited a 4% biomass loss (CL) in total biomass at 2.56 mmol O_3 m^{-2} POD_{16} and in leaf biomass at 3.37 mmol O_3 m^{-2} POD_{15}. The results indicated that biomass accumulation was initially stimulated at low to moderate O_3 doses but reduced at higher doses. Overall, *S. terebinthifolia* demonstrated high tolerance to tropospheric O_3 stress.

Keywords: Tropical, tree, environment, ozone-stress, tolerance

INTRODUCTION

Due to anthropogenic activities, emissions of primary air pollutants (e.g., CO_2, CH_4, and NO_x) have reached concerning levels in recent decades (Lamb et al. 2021). This phenomenon has contributed to increasing levels of secondary air pollutants such as tropospheric ozone (O_3), which is formed in the presence of oxygen, primary pollutants (especially NO_x) and solar irradiation (Elshorbany et al. 2024). Tropospheric O_3 is a major air pollutant that impacts air quality, climate, human health and ecosystems (Mills et al. 2018). Its rising levels can negatively impact the growth, development, and productivity of plant species, including both crops and forests, representing a global environmental concern (Dewan and Lakhani 2022).

Multiple experimental approaches have been employed to investigate the detrimental effects of O_3 on plants, with biomass production serving as a particularly relevant indicator of O_3-induced risk (Moura et al. 2018; Kaylor et al. 2023; Manzini et al. 2025). Currently, experiments conducted using Free-Air Controlled Exposure (FACE) systems in open-air environments can provide reliable estimates of plant responses to O_3 under realistic environmental conditions (Paoletti et al. 2017; Hoshika et al. 2024).

The most commonly used exposure-based index for assessing O_3 risk to plant biomass production is the Accumulated Exposure Over Threshold of 40 ppb (AOT40), which is calculated based on tropospheric O_3 concentrations. However, since O_3 enters the leaf through the stomata, a flux-based index has proven to be more effective in predicting O_3-induced effects on vegetation (Hoshika et al. 2024). The Phytotoxic Ozone Dose (POD_y, where "y" represents the O_3 flux threshold) accounts for actual O_3 uptake by plants, considering both climate conditions and plant physiological characteristics. As such, it provides a more specific and realistic dose-response relationship for accurate estimation of O_3 critical levels (CLs) (Mills et al. 2011).

In general, linear models are used to predict the impacts of O_3 exposure on plant biomass loss. However, recent studies have shown that plants subjected to O_3 stress may exhibit hormetic responses (Agathokleous et al. 2019a; Li et al. 2021), which are more evident in tolerant species (Hoshika et al. 2024). Hormesis (or hormetic effect) is a dose–response effect characterized by a stimulatory or beneficial effect at low exposure levels to an environmental agent, followed by inhibitory or toxic effects at higher doses (Mattson 2008). In plants, the hormetic zone refers to a condition in which low levels of stress enhance growth, biomass production, and/or active defense mechanisms. In contrast, higher doses can lead to adverse physiological effects and growth inhibition (Calabrese and Blain 2009). Since linear models do not adequately capture hormetic responses, testing nonlinear models is essential for accurately predicting plant response to O_3, particularly for tolerant species, which are often

underrepresented in traditional dose-response studies based solely on linear modelling approaches (Agathokleous et al. 2019a).

Calculating O_3 flux and consequently POD_y requires species-specific parameterization to model stomatal O_3 uptake over time. This modeling is essential for determining CLs associated with biomass loss. According to the ICP Vegetation Manual, a CL based on a 4% biomass loss is recommended for tree species, particularly those growing in temperate climates (CLRTAP 2015). Although some parameterization of stomal conductance has been performed for subtropical tree species (e.g. Niu et al. 2016), studies involving tropical species remain scarce. To date, only a few tropical species have been parameterized, such as *Astronium graveolens* – Anacardiaceae (Cassimiro et al. 2016), *Eugenia uniflora* – Myrtaceae (Engela et al. 2021) and *Passiflora edulis* – Passifloraceae (Fernandes et al. 2019). However, for these species, CLs for biomass loss have not yet been calculated, despite increasing O_3 concentrations in many South America cities (Seguel et al. 2024). The climate in tropical regions favors a year-round O_3 formation (Moura et al., 2014), and this suggests that other tropical species from South America may also be at risk from elevated O_3 exposure, including *Schinus terebinthifolia* (Raddi - Anacardiaceae), commonly known as Brazilian pepper tree. The species is native to the tropical Atlantic Forest, a highly threatened and extremely important biodiversity hotspot (Marques and Grelle 2021), and holds significant regional socioeconomic value (Lorenzi 2016), with recommendation for ecological restoration programs and increasingly used in urban greening initiatives. Due to its rapid growth and high tolerance to soil pollutants, such as copper (Siqueira et al. 2021), iron (Silva et al 2024) and even diesel contamination (Bona et al. 2011), *S. terebinthifolia* hold attributes as an ideal plant model for stress tolerance studies.

Nature-based solutions (NBS) for mitigating the effects of climate change and air pollution in urban and peri-urban areas have become increasingly important (Hobbie and Grimm 2020). However, selecting suitable species for urban reforestation remains a complex task, particularly in cities where O_3 levels are rising (Nguyen et al. 2022). Urban reforestation planning must account for a wide range of plant traits, including morphological, physiological, and adaptive characteristics, highlighting species that provide high ecosystem services and exhibit tolerance to abiotic stressors (Miller et al. 2015). In this context, stomatal model parameterization and O_3 risk assessment for *S. terebinthifolia* are highly relevant for supporting public policy aimed at establishing limit concentrations of tropospheric O_3. Moreover, the response of this ecologically and economically important species to increasing O_3 levels is unknown, and thus, defining ozone thresholds and plant-stress sensibility can provide a scientific-based approach for tropical urban greening.

Therefore, we aimed to assess, for the first time, the parametrization of the stomatal

conductance model for the tropical tree species *S. terebinthifolia*. Specifically, we compared linear and several nonlinear dose-response functions to identify the most suitable for predicting the effects of increasing O_3 concentrations on the biomass of *S. terebinthifolia*, using AOT40 and POD_y indices as exposure metrics. Furthermore, we pursued to determine the CL of O_3 capable of causing significant biomass loss in this species. Since *S. terebinthifolia* is tolerant to soil pollutants, we hypothesize that the species could be also O_3-tolerant and present a hormetic biomass response to increasing ozone concentrations.

MATERIALS AND METHODS

Ozone face fumigation set-up and experimental design

The experiment was conducted at a free-air O_3 exposure facility in Sesto Fiorentino, Italy (43°48′59″N, 11°12′01″E, 55 m above sea level), which enables plant exposure under realistic environmental conditions. Briefly, O_3 was generated from pure oxygen using an O_3 generator (TGOC13X, Triogen Ltd., Glasgow, UK), then diluted with ambient air in a mixing tank and delivered through Teflon tubes suspended from a fixed grid above the plants (for details, see Paoletti et al. 2017). Environmental parameters include air temperature (Temp, °C), relative humidity (RH, %) and solar radiation (SR, W m^{-2}), that were hourly recorded by a Watchdog station (Mod. 2000; Spectrum Technology, Inc., Aurora, IL, USA) positioned 2.5 m above ground level.

Seeds of *S. terebinthifolia* were obtained from a commercial nursery (Arbocenter, Brazil). They were sown in seedling trays in November 2023 and grown inside a controlled environmental room (T: 25 °C, Photosynthetic Photon Flux Density [PPFD]: 500 μmol m^{-2} s^{-1}) until spring 2024. Subsequently, the plants were transferred to the experimental nursery and transplanted into 5 L pots containing 3.5 kg of natural soil. Ozone fumigation was carried out over three months during the summer of 2024 (day of year 161 to 259). Each pot received daily irrigation of 500 ± 50 mL day^{-1} via an automatic drip irrigation system, ensuring consistent soil water content throughout the experiment.

Plants were exposed for 90 days to three O_3 levels: Ambient Air (AA), 1.5 times the ambient of O_3 concentration (1.5×), and twice the ambient O_3 concentration (2.0×). To establish intermediate O_3 exposures and thus create five total treatments, plants from the AA and 2.0× groups were exchanged between plots midway through the experiment (45 days after the beginning, on August 1st). These plants were subjected to 45 days under AA followed by 45 days under 2.0× (AA → 2.0×), and vice versa (2.0× → AA). These pots were randomly reallocated within the new treatment. The experimental design consisted of 45 *S. terebinthifolia* plants distributed across 5 treatments, with 9 plants per treatment arranged in replicated square

plots (5 m × 5 m). A schematic representation of the experimental layout and the creation of intermediate O_3 treatments is provided in Figure IIIS1.

Biomass assessment

S. terebinthifolia biomass was assessed at the beginning (T_0) and at the end of the experiment (B_{final}). At harvest, plants were separated into leaves, stems, and roots, oven-dried at 70 °C for 5 days until reaching constant weight, then weighed (g) using an analytical scale (Sartorius, Goettingen, Germany). Total plant biomass was calculated as the sum of the dry weights of leaves, stems, and roots.

Differences in total and leaf dry biomass among O_3 treatments were analyzed through one-way ANOVA, followed by Tukey's multiple comparison test ($p \leq 0.05$).

A control reference biomass (B_{ref}) was calculated for risk assessment, following the approach proposed by Paoletti et al. (2017), assuming an average daily O_3 concentration of 20 ppb to represent the pre-industrial clean air condition (Tarasik et al. 2019). Relative biomass (B_{rel}) for both leaf and total biomass was then determined as the ratio: $B_{rel} = B_{final} / B_{ref}$.

Stomatal parametrization

Stomatal conductance to water vapor (*gsw*, mol H_2O m^{-2} s^{-1}), vapor pressure deficit (VPD, kPa) and leaf temperature (°C) of *S. terebinthifolia*, as well as the environmental light (PPFD, µmol m^{-2} s^{-1}) were measured using a portable porometer (LI-600, Li-Cor Inc. Lincoln, NE, USA). These measurements were used to parameterize the *gsw* model based on the multiplicative algorithm described by Jarvis (1976), suggested by Mills et al. (2003) and Hayes et al. (2012) following the ICP-vegetation mapping manual (CLRTAP, 2015):

$$gsw = g_{max} \times f_{light} \times \max\{f_{min}, (f_{\text{temp}} \times f_{\text{VPD}} \times f_{\text{phen}})$$

where g_{max} (mmol O_3 m^{-2} s^{-1}) and f_{min} (fraction) are the maximum and minimum stomatal conductance (95th and 5th percentiles of all *gsw* data, respectively), following the description of Bičárová et al. (2019) and Hoshika et al. (2020), while the other functions indicate the response of stomata to environmental factors as photon flux density at the leaf surface (f_{light}), air temperature (f_{temp}), vapor pressure deficit (f_{VPD}) and phenology (f_{phen}). The accuracy of model estimation was assessed by performing a linear regression between the measured and estimated *gsw* values (Figure IIIS2), as described by Hoshika et al. (2012).

Measurements were taken twice per week on two fully expanded leaves located at different positions on the main stem of each plant, resulting in a total of 2,048 measurements. The measurements were designed to capture a wide range of VPD, temperature, and photosynthetic photon flux density (PPFD) conditions to evaluate *gsw* responses under variable

environmental scenarios. The resulting parameterization was then used to calculate POD_y, based on the hourly stomatal O_3 flow (Hoshika et al. 2024).

Ozone indexes and critical levels (CLs) for risk assessment

The AOT40 index was calculated as the sum of the hourly O_3 concentrations exceeding 40 ppb during daylight hours (solar radiation ≥ 50 W m^{-2}), following the methodology established by the Convention on Long-range Transboundary Air Pollution (CLRTAP 2015).

POD_y was calculated by Eq. 1:

$$POD_y = \int \max(F_{st} - Y, 0) \times dt$$

where "y" is a species-specific threshold of the hourly stomatal O_3 flux, and F_{st} (nmol m^{-2} s^{-1}) is calculated as in Eq. 2:

$$F_{st} = [O_3] \times g_sO_3 \times r_c \div (r_b + r_c)$$

where $[O_3]$ is the hourly O_3 concentration (ppb); g_{sO3} (mol O_3 m^{-2} s^{-1}) is $g_{sw} \times 0.663$, considering the diffusivity ratio between O_3 and water vapor (CLRTAP 2015); r_c is the leaf surface resistance calculated as $r_c = 1/ g_{sO3} + 0.0164$ considering cuticular or external conductance (0.0164 mol m^{-2} s^{-1}, CLRTAP 2015) and r_b is the leaf boundary layer resistance calculated as $r_b = 1.3 \times 150 \times (L_d/\mu)^{0.5}$ where μ is the wind speed (m s^{-1}), L_d is the cross-wind leaf dimension (0.024 m, data obtained from Oliveira et al. 2019) and the factor 1.3 accounted for differences in diffusivity between heat and O_3 (CLRTAP 2015). Different POD_y detoxification thresholds were tested to identify the best POD_y index to predict O_3 effects on *S. terebinthifolia* total relative biomass.

Following the methodology by Hoshika et al. (2024), linear regression and 116 nonlinear statistical models were compared to identify the most suitable index for predicting biomass loss and leaf damage caused by O_3 toxicity. The analysis was conducted using the statistical software R, employing the packages "*drc*" (Ritz et al., 2015), "*modelr*" (Wickham, 2023), "*aomisc*" (Onofri, 2020), "*statforbiology*" (Onofri, 2024) and "*automation*" (Ruiz, 2023). Model selection was based on the following mathematical criteria: 1) lowest Akaike Information Criterion (AIC); 2) highest coefficient of determination (R^2); and 3) realistic biological responses (e.g. excluding models showing abrupt increases or decreases inconsistent with plant's visual condition during the experiment).

Finally, the best-fitting model predictor was used to calculate the critical levels of tropospheric O_3 (CL) required to induce 4% biomass loss, as recommended by CLRTAP (2015). Graphs were generated using Microsoft Excel, GraphPad Prism or with "*ggplot2*"

package (Wickham, 2016) in R.

RESULTS

Climate conditions and O_3 concentrations

During the experimental period, the mean daily solar radiation (SR) was 502.2 ± 249.9 W m^{-2}, the mean air relative humidity (RH) was 59.9 ± 19.4 %, and the mean daily air temperature (T) was 25.8 ± 5.9 ºC (Figure III1A). SR exhibited a gradual decline over the experiment, while air temperature initially increased, reaching a peak on day 226 before decreasing in the latter half of summer. Conversely, RH displayed an opposite trend to temperature.

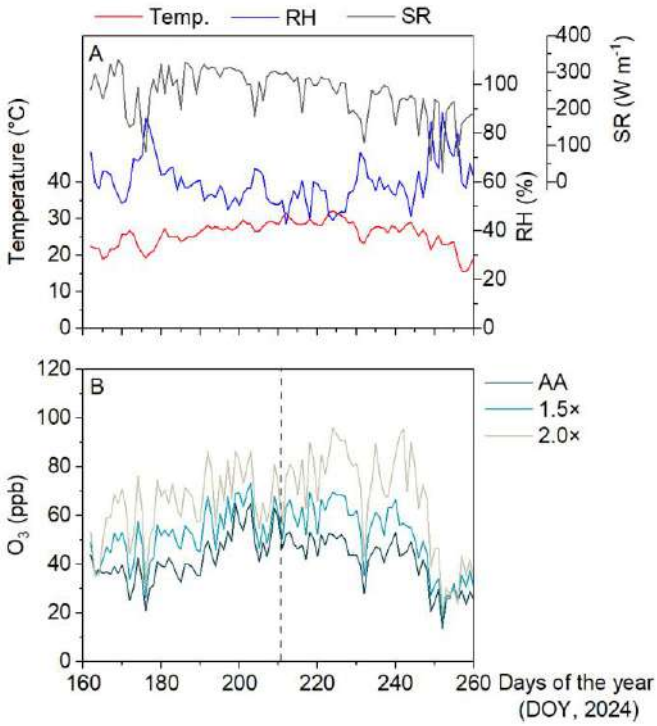

Fig. III 1. A. Daily means of solar radiation (SR), relative humidity (RH) and air temperature during the experiment. B. Daily means of tropospheric O_3 exposure in ambient (AA), 1.5 times ambient (1.5×), and 2.0 times ambient (2.0×). The dashed vertical line represents the midterm of the experiment and when part of the plants exposed to AA were switched to 2.0× (AA → 2.0×) and vice-versa (2.0× → AA).

The daily mean O_3 concentrations for the treatments AA, 1.5×, 2.0× are shown in Fig. III1B. In treatments AA and 1.5 × daily mean O_3 levels increased during the first half of the experimental period before declining toward the end. In contrast, the 2.0× treatment exhibited a slight increase beyond the midpoint before decreasing. The final O_3 mean hourly concentrations (ppb) over the experiment were 39.9, 46.3, 53.0, 64.0 and 69.3 for AA, 2.0×→AA, 1.5×, AA→2.0× and 2.0×, respectively.

Biomass

The final total dry biomass of *S. terebinthifolia* ($B_{final\text{-}T}$) increased in plants exposed to the 1.5× treatment, compared to all other treatments (Fig III2A). In contrast, the final leaf dry biomass ($B_{final\text{-}L}$) was significantly reduced in plants exposed to treatments 2.0×→AA and 2.0×, relative to those exposed to 1.5× treatment (Fig III2B).

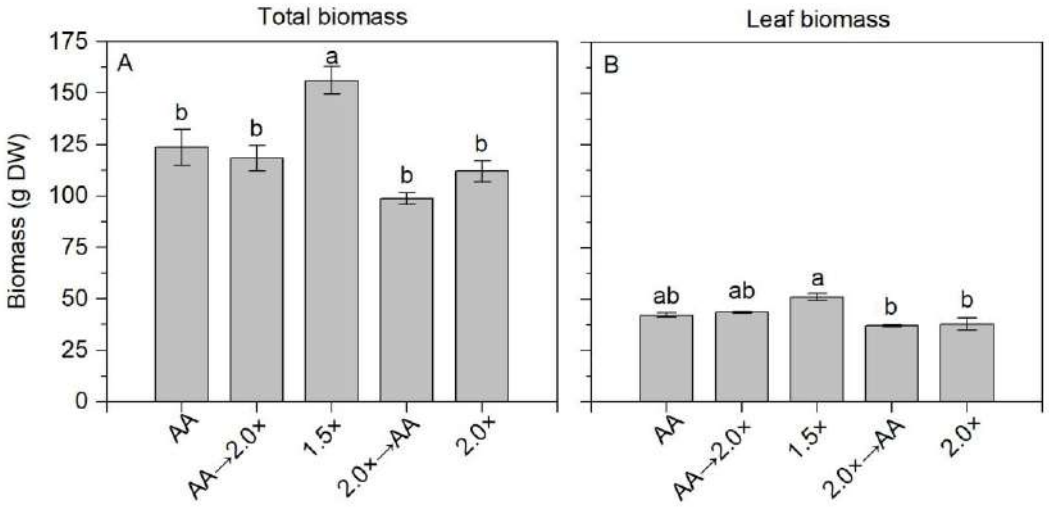

Fig. III 2. Total (A) and leaf (B) dry weight (DW) of *S. terebinthifolia* plants after 90 days of O_3 exposure in ambient air (AA), 1.5 times ambient air (1.5×), 2.0 times ambient air (2.0×), ambient to 2.0× after 45 days (AA→2.0×) and 2.0× to ambient after 45 days (2.0×→AA) conditions. Distinct letters indicate significant differences according to one-way ANOVA followed by Tukey's test ($p \leq 0.05$). Bars denote standard error (n = 9).

The calculated reference total biomass ($B_{ref\text{-}T}$) was 146.97 g (Fig III3A), while the reference leaf biomass ($B_{ref\text{-}L}$) was 50.44 g (Fig. III3B).

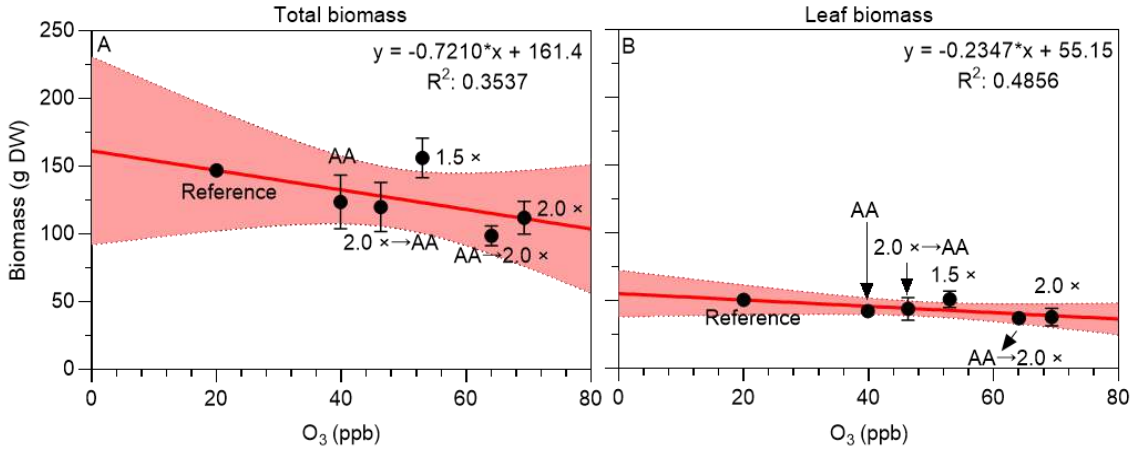

Fig. III 3. Linear regressions of total (A) and leaf (B) biomass of *S. terebinthifolia* plants exposed to distinct O_3 treatments and calculated reference biomass. Bars denote standard errors (n = 9). The red shaded areas represent the confidence intervals (95%). The regression equations and coefficient of determinations (R^2) are indicated in the upper right corner.

The calculated values of relative leaf biomass ($B_{rel\text{-}L}$) were 0.89, 0.92, 1.08, 0.78 and 0.80. and those of relative total biomass ($B_{rel\text{-}T}$) were 0.92, 0.89, 1.16, 0.73 and 0.83 for AA,

2.0×→AA, 1.5×, AA→2.0× and 2.0×, respectively. For both leaf and total biomass, *S. terebinthifolia* saplings showed the highest relative biomass in the 1.5× treatment, while all other treatments resulted in lower values compared to the reference biomass estimated for pre-industrial conditions.

Stomatal parameterization and O_3 indexes (AOT40 and POD_{0-22})

The parameterization of *S. terebinthifolia* seedlings (Table III1) allowed for the modeling of stomatal conductance (Fig. 4), resulting in a maximum stomatal conductance (g_{max}) of 0.525 mol H_2O m^{-2} s^{-1}. The model identified an optimal temperature of 31.3 °C, saturating light intensity (PPFD at g_{sw} reached 90% g_{max}) of 1054 µmol m^{-2} s^{-1}, and a maximum vapor pressure deficit (VPD) of 2.7 kPa. Peak phenological activity occurred around day of year 180.

Tab. III 1. Stomatal conductance parameterization of *S. terebinthifolia*, measured under natural conditions along the entire experimental period. g_{max} is maximum conductance; f_{min} is the minimum stomatal conductance (fraction); f_{temp}, f_{light}, f_{VPD} and f_{phen} are the variation in g_{max} with temperature (T, °C), photosynthetic photon flux density (PPFD, µmol m^2 s^{-1}), vapor pressure deficit (VPD, kPa) and phenology (day of the year), respectively. T_{max}, T_{opt} and T_{min}, are the maximum, optimal, and minimum air temperature for stomatal opening. The constant *a* determines the shape of the exponential relationship for f_{light} function. VPD_{max} and VPD_{min} are the vapor pressure deficit for attaining maximum and minimum stomatal aperture. Start and End are the days of start and end of the experiment. f_{phen_a} and f_{phen_b} are the number of days for f_{phen} to reach its maximum and minimum, respectively.

Parameter		Unit	*S. terebinthifolia*
g_{max}		mol H_2O m^{-2} s^{-1}	0.575
f_{min}		Fraction	0.059
f_{temp}	T_{max}	°C	40.7
	T_{opt}	°C	31.3
	T_{min}	°C	13.3
f_{light}	*A*	Constant	0.0054
f_{VPD}	VPD_{max}	kPa	2.7
	VPD_{min}	kPa	6.5
f_{phen}	Start	Day	161
	End	Day	259
	f_{phen_a}	Day	22
	f_{phen_b}	Day	76

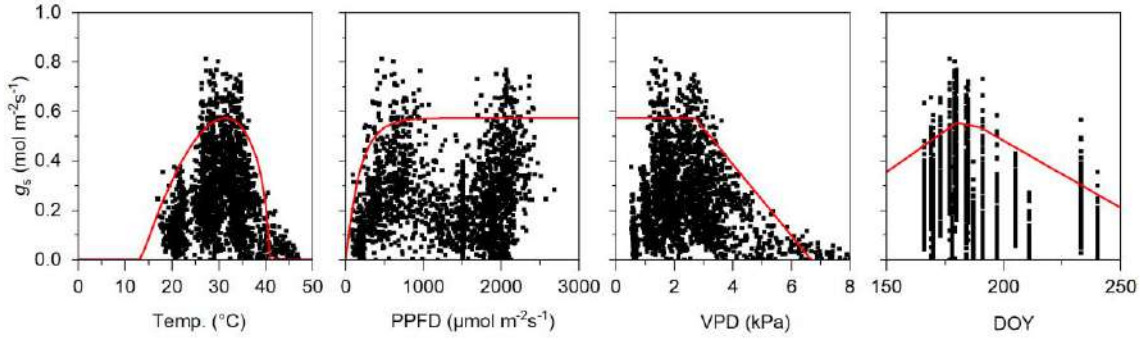

Fig. III 4. Modeling of stomatal conductance (*gsw* - mol H_2O m^{-2} s^{-1}) of *S. terebinthifolia* as a function of temperature (°C), radiation (PPFD - µmol m^{-2} s^{-1}), vapor pressure deficit (VPD -

kPa), and phenological activity (DOY - day of year). Black dots represent the measured stomatal conductance of *S. terebinthifolia*, and the solid red line represents the calculated parametrization model for each environmental parameter.

The AOT40 and POD_y values are shown in Table IIIS1. POD_{22} was established as the upper limit because POD_y values become zero beyond this point for at least one treatment and thus are negligible.

Flux-based dose-response functions and critical levels detection

Table IIIS1 and Table IIIS2 show the best 3 nonlinear and the linear regression models for AOT40 and POD_y (0 – 22) as a function of $B_{rel\text{-}L}$ and $B_{rel\text{-}T}$. The regression ranking is defined according to the results of AIC and R^2 calculations for each index individually.

For both total and leaf relative biomass, the linear regression was not the most suitable predictor of *S. terebinthifolia* biomass across the tested indices, as it consistently exhibited high AIC values and low R^2. Among the 117 models tested (116 nonlinear plus the linear model), the linear model ranked between 33rd (in POD_{13} for $B_{rel\text{-}T}$) and 82nd (in POD_0 for $B_{rel\text{-}T}$).

In contrast, several nonlinear models demonstrated superior performance, with higher goodness-of-fit and more favorable AIC values. Among all combinations of models and indices, the best predictor of total biomass was the four-parameter logistic model "Bragg.4" (AIC = -28.80, R^2 = 0.81) fitted to POD_{16} (Fig. III5A). For leaf biomass, the same nonlinear "Bragg.4" model was also the best fit (AIC = -37.61, R^2 = 0.82) but based on POD_{15} (Fig. III5B).

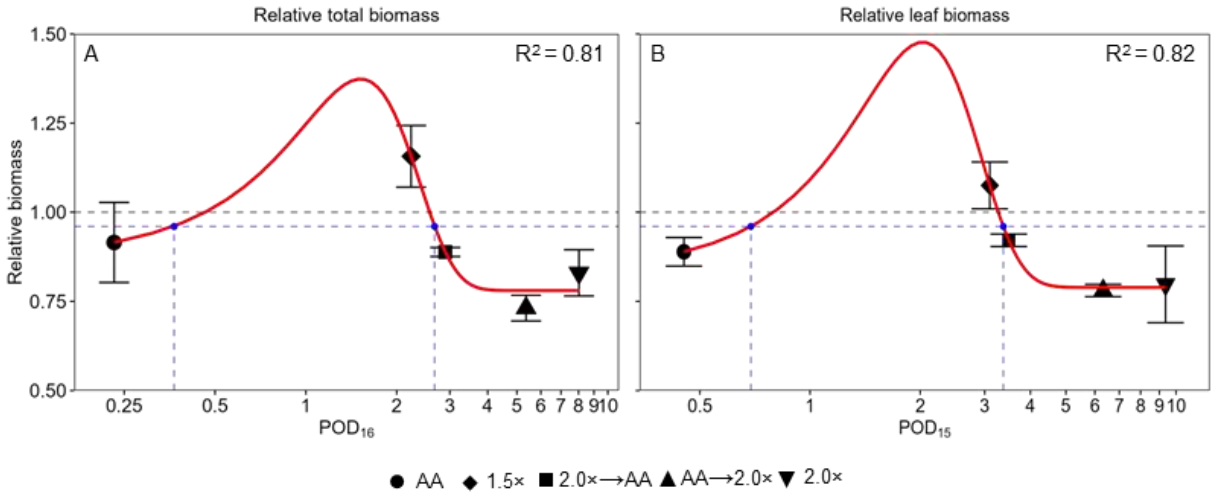

Fig. III 5. Nonlinear Bragg.4 model applied as a predictor of *S. terebinthifolia* relative total biomass as a function of POD_{16} (A), and relative leaf biomass as a function of POD_{15}. The black dashed line represents the hypothetical relative biomass in the pre-industrial era (B_{rel} = 1.00). The blue dots and blue dashed line represent the O_3 critical levels to achieve 0.96 of relative biomass (4% biomass loss from the pre-industrial era). The black symbols represent *S. terebinthifolia* relative biomass (± SD) under each O_3 treatment, and the solid red line represents the calculated nonlinear model.

Based on the best plausible model Bragg.4, the CLs to induce a 4% biomass loss were

determined at 2.66 mmol O_3 m^{-2} POD_{16} for total biomass, and 3.37 mmol O_3 m^{-2} POD_{15} for leaf biomass.

DISCUSSION

While *S. terebinthifolia* is a native tropical plant species, the experiment was conducted in Italy, a non-tropical climate region. However, the environmental variables measured throughout the experiment (in summer) showed moderate solar incidence (> 500 W m^{-2}), high relative humidity (> 50%) and mild temperatures (≈ 25 ºC), providing similar conditions of some Atlantic Forest regions in southern Brazil where *S. terebinthifolia* naturally occur (Olmedo et al, 2023). Also, *S. terebinthifolia* is noteworthy for its remarkable ability to adapt to various types of climate and conditions (Santos et al, 2024). While the environmental conditions proved to be adequate for *S. terebinthifolia* growth, we recognize that factors such as different photoperiods and soil characteristics may influence the biomass response, which constitutes a limitation of our study.

Regarding ozone, the mean hourly ozone concentration in natural ambient air (control) in Italy was approximately 40 ppb. In contrast, data from CETESB for the state of São Paulo (where the species is native and most of the remaining Dense Ombrophilous Atlantic Forest is located) in 2024 recorded a mean annual concentration of ≈ 82 ppb. This indicates that *S. terebinthifolia* is naturally exposed to even greater oxidative stress in its habitat than in our experimental setup. Consequently, the observed tolerance in our study likely reflects an existing adaptation of the species to high ozone concentrations, supporting its potential use in urban forestry in high-ozone regions like São Paulo. It is important to contextualize that these high regional levels, monitored by CETESB, also reflect the current reality of the Atlantic Forest biome, which is fragmented and heavily influenced by anthropogenic emissions from metropolitan areas nearby. Future dose-response studies within the remnants of the Atlantic Forest itself could further corroborate these findings.

The experimental conditions confirmed the effectiveness of the O_3-enrichment treatments in establishing distinct O_3 concentration levels, while maintaining a realistic environment for *S. terebinthifolia* growth under free-air conditions. As expected, the highest daily mean O_3 concentrations were recorded in the 2.0× treatment and the lowest in ambient air (AA). Mid-experiment plant transfers between AA and 2.0× effectively created intermediate levels of O_3 uptake, demonstrating that this simple approach can effectively broaden the range of exposure scenarios without requiring additional O_3 generation systems. Moreover, this method provides a practical solution for exploring seasonal variations in plant responses to O_3 exposure.

The observed reductions in total and leaf biomass of *S. terebinthifolia* under elevated

O_3 reflect O_3-induced physiological disruptions, such as impaired photosynthetic efficiency (Xu et al. 2023), stomatal alterations (Hoshika et al. 2015), shifts in nitrogen and carbon allocation (Shang et al. 2019), and oxidative damage to cellular structures (Baier et al. 2005). However, an increase in total biomass was observed under the 1.5× treatment compared to AA (control treatment), followed by reduction, suggesting a hormetic response to mid-low O_3 exposure. In this case, negative effects on total plant biomass were evident only under high O_3 concentrations, indicating a high capacity of *S. terebinthifolia* to tolerate O_3-induced oxidative stress. Hoshika et al. (2024) proposed that moderate/tolerant species may exhibit broad response ranges and nonlinear patterns of biomass production under increasing O_3 exposure, which is consistent with the pattern observed in our study. Furthermore, it is possible to verify that after a dose of 5 mmol O^3 m^{-2}, an almost flattened ozone-biomass response was exhibited. This indicates that the effect of O_3 in *S. terebinthifolia* biomass becomes negligible, reaching a saturation point and hormetic zone end (Erofeeva 2021), possibly due to stomatal O_3 uptake limit.

The POD_y index outperformed AOT40 in predicting both leaf and total biomass loss in *S. terebinthifolia*. Recent studies have demonstrated that POD_y provides greater accuracy than AOT40 in assessing O_3 effects on crop yield (Pleijel et al. 2022), biomass loss (Manzini et al. 2025) and for establishing CLs. But, up to our knowledge, no study has ever tested several non-linear regressions to assess biomass response to PODy or AOT40, highlighting the novelty of our study. As a species-specific, flux-based index that accounts for plant physiology and stomatal behavior, POD_y yields more realistic estimates of O_3 impacts (Mills et al. 2011). In our study, the superior predictive performance of POD_y was confirmed, and we recommend its use for O_3 risk assessment and CLs calculation for this species. Importantly, the most effective POD_y thresholds for assessing *S. terebinthifolia* were those with higher "y" values, especially above 15 nmol O_3 m^{-2} s^{-1}. High "y" thresholds typically indicate substantial detoxification capacity by plant species and may reflect an inherent tolerance to O_3 (Marzuoli et al. 2024). This suggests that *S. terebinthifolia* possess an effective defense system capable of mitigating oxidative stress form elevated O_3 uptake. Ongoing analyses of antioxidant activity and stress-related metabolic compounds may further clarify the physiological mechanisms underlying this apparent O_3 tolerance.

Regardless of the index used (AOT40 or POD_y), nonlinear models consistently outperformed linear regression in predicting the effects of O_3 on *S. terebinthifolia* leaf and total biomass, as indicated by higher R^2 values and lower AIC scores. Therefore, our discussion is focused on the non-linear models approach. The application of nonlinear models to assess O_3-induced impacts on plant biomass has been previously supported in literature, with several

studies highlighting their superior accuracy and greater biological realism compared to linear models (Agathokleous et al. 2019b; Conte et al. 2021). This finding aligns with the accumulated scientific evidence indicating that plant responses to environmental stressors, including O_3, often follow nonlinear patterns (Hoshika et al. 2024). Nonlinear models are better suited to capture the complex dose-response dynamics that characterize plant physiological processes under variable environmental conditions.

However, the use of nonlinear models for O_3 risk assessment should be approached with caution. In our study, the four-parameter logistic model "Bragg.4" based on POD_{16} was selected as the most suitable model for predicting both leaf and total biomass loss of *S. terebinthifolia* under O_3 exposure. Mathematically, other models, specifically the "Five-parameter Cedergreen-Ritz-Streibig a" or "UCRS.5a" model on POD_{16} and the "Four-parameter Cedergreen-Ritz-Streibig a" or "UCRS.4a" model on POD_{19}, demonstrated even better performance in terms of lower AIC values and higher R^2. Despite their statistical superiority, these models were excluded due to their lack of biological plausibility. In particular, they produced abrupt shifts in biomass response across the O_3 gradient (Fig. IIIS3 A) or failed to reflect a biological meaningful pattern in plant biomass production (Fig. IIIS3 B). As highlighted by Tredennick et al. (2021), caution is warranted when applying nonlinear models, as they can be prone to overfitting and may yield biological implausible interpretations. Our findings reinforce the importance of critically evaluating both the mathematical and biological validity of predictive models. When assessing O_3 risk, it is essential to prioritize models that not only perform well statistically but also reflect realistic biological responses to environmental stress.

Although we propose the use of nonlinear models to predict biomass responses to O_3 exposure, linear regression was used to define the reference biomass in our study. The definition of reference biomass under ambient exposure conditions, such as those found in free-air O_3 enrichment (FACE) experiments, remains a subject of debate within the scientific community (Hoshika et al. 2024). Establishing a "zero dose" reference can potentially lead to overestimation of relative biomass, making the use of a constant reference value a more practical and widely accepted alternative (Paoletti et al. 2017). To address possible uncertainties associated with this estimated reference, we adopted the "modified Paoletti's approach" proposed by Hoshika et al. (2024), which incorporates the mean, upper, and lower bounds of the 95% confidence interval. Based on the "best fit" estimation (i.e., the intercept of the linear regression), *S. terebinthifolia* exhibited a broad range of biomass responses. This supports the hypothesis by Hoshika et al. (2024) that O_3-tolerant species tend to display a wider response range, likely due to hormetic effects at low O_3 doses. Also, we performed the linear and non-

linear regressions without including the calculated reference value, relying on the actual experimental data only. It was chosen to avoid biasing the modeling by starting from an arbitrary point (i.e b_{ref} = 1.0), as done in previous ozone dose-response studies with experimental data (Manzini et al. 2025; Hoshika et al., 2018).

The CL for *S. terebinthifolia* leaf and total biomass loss were determined based on POD_{16} and POD_{15}, respectively. In contrast, the CLRTAP (2015) convention recommends a threshold of 1 mmol m^{-2} s^{-1} (i.e., POD_1) for forest tree species. If POD_1 were applied to *S. terebinthifolia*, the estimated CL would be 39.13 mmol m^{-2} for leaf biomass and 38.98 mmol m^{-2} for total biomass (data not shown). However, a POD_1-based threshold assumes the species can only detoxify up to 1 nmol m^{-2} s^{-1} of absorbed O_3, with any additional uptake potentially causing physiological impairment. Our findings suggest otherwise. The species moderate tolerance to O_3 and even stimulatory biomass effect observed at intermediate exposure levels (1.5×) indicate that *S. terebinthifolia* likely employs mechanisms beyond O_3 avoidance to maintain physiological functions and growth. Stomatal conductance data further support this, with high maximum stomatal conductance (g_{max}) of 0.525 mol H_2O m^{-2} s^{-1}, significantly exceeding values reported for other species, including *Cupressus sempervirens* (0.108 mol O_3 m^{-2} s^{-1}; Manzini et al. 2025), Mediterranean evergreen tree *Quercus ilex* (0.250 mol H_2O m^{-2} s^{-1}), Mediterranean deciduous tree *Q. pubescens* (0.340 mol H_2O m^{-2} s^{-1}), deciduous broadleaf species such as *Q. robur* (0.300 mol H_2O m^{-2} s^{-1}; Hoshika et al. 2018), *Alnus glutinosa* (0.300 mol H_2O m^{-2} s^{-1}), *Sorbus aucuparia* (0.240 mol H_2O m^{-2} s^{-1}), and herbaceous species like *Vaccinium myrtillus* (0.140 mol H_2O m^{-2} s^{-1}; Hoshika et al. 2020). The high stomatal conductance of *S. terebinthifolia* is evident even when compared with other tropical species of the Atlantic Forest, such as the moderately ozone-sensitive tree species *Astronium graviolens* (0.152 mol H_2O m^{-2} s^{-1}; Cassimiro et al. 2016), the ozone-sensitive *Eugenia uniflora* (0.082 mol O_3 m^{-2} s^{-1}; Engela et al. 2021) and the O_3-tolerant tropical liana species *Passiflora edulis* (0.160 mol O_3 m^{-2} s^{-1}; Fernandes et al. 2019). This highlights that even among species from the same biome and climate, the high stomatal conductivity of *S. terebinthifolia* is notorious.

Given this consistently high stomatal activity and POD_y (i.e. high O_3 flux threshold), it is unlikely that *S. terebinthifolia* mitigates O_3 stress through stomatal closure (i.e., avoidance mechanism). Instead, the species probably relies on active detoxication mechanisms, since *S. terebinthifolia* naturally synthesizes high levels of antioxidants compounds in leaves (Uliana et al., 2016; Oliveira et al., 2024), including ascorbic acid, glutathione and superoxide dismutase enzyme, key molecules known to mitigate O_3-induced oxidative stress (Siqueira et al. 2021). Therefore, it's plausible that *S. terebinthifolia* should rely on biochemical detoxification as a primary adaptive strategy to elevated O_3 stress, while maintaining sufficient stomatal opening

for carbon uptake. Further studies focusing on antioxidant mechanism and physiological parameters could confirm this hypothesis.

CONCLUSIONS

This study presents the first parametrization of the stomatal O_3 uptake model and O_3 risk assessment for *Schinus terebinthifolia*. Our findings support our hypothesis and suggest that *S. terebinthifolia* is highly tolerant to tropospheric O_3 stress. We recommend the use of the flux-based POD_y index as the most appropriate approach for assessing O_3 risk in this species, as it incorporates species-specific physiological responses. Critical levels were estimated at 2.66 mmol O_3 m^{-2} (POD_{16}) for total biomass and 3.37 mmol O_3 m^{-2} (POD_{15}) for leaf biomass, beyond which a 4% reduction in relative biomass is expected. Nonlinear models proved to be more suitable than traditional linear regression for capturing complex dose-response relationships, offering better fit and biological realism. Modest biomass production enhance was observed under low to moderate O_3 exposure (1.5×), followed by biomass reduction at higher doses, suggesting evidence consistent with hormesis effects. The species high stomatal conductance with high tolerance suggests that *S. terebinthifolia* tolerates O_3 not trough ozone uptake avoidance, but most likely relying on detoxification mechanisms. Future analyses of antioxidant activity and related metabolic compounds can further clarify the underlying *S. terebinthifolia* tolerance mechanisms. Given its demonstrated resilience and adaptive traits, *S. terebinthifolia* shows potential for use in urban greening and reforestation programs, particularly in regions affected by elevated tropospheric O_3 levels.

Acknowledgements

We thank Leonardo Lazzara, Jacopo Manzini, Andrea Viviano, Elena Marra and Cesare Garosi for field support, and National Research Council of Italy (CNR) - Institute of Research on Terrestrial Ecosystems (IRET) for infrastructure and ozone FACE facility. This work was financially supported by Fundação de Amparo à Pesquisa do Estado de São Paulo (FAPESP – Process 2023/16524-0). The research was funded by EU - Next Generation EU Mission 4 “Education and Research” - Component 2: “From research to business” - Investment 3.1: “Fund for the realization of an integrated system of research and innovation infrastructures” - Project IR0000032 – ITINERIS - Italian Integrated Environmental Research Infrastructures System - CUP B53C22002150006.

Data statement

All generated data is included in the article (and its supplementary information files). No additional external datasets were used.

Conflict of Interest

The authors declare that they have no conflict of interest.

REFERENCES

Agathokleous E, Araminiene V, Belz RG, Calatayud V, De Marco A, Domingos M, Feng Z, Hoshika Y, Kitao M, Koike T, Paoletti E, Saitanis CJ, Sicard P, Calabrese EJ (2019a) A quantitative assessment of hormetic responses of plants to ozone. Environ Res 176:108527. https://doi.org/10.1016/j.envres.2019.108527

Agathokleous E, Belz RG, Calatayud V, De Marco A, Hoshika Y, Kitao M, Saitanis CJ, Sicard P, Paoletti E, Calabrese EJ (2019b) Predicting the effect of ozone on vegetation via linear non-threshold (LNT), threshold and hormetic dose-response models. Sci Total Environ 649:61-74. https://doi.org/10.1016/j.scitotenv.2018.08.264

Baier M, Kandlbinder A, Golldack D, Dietz KJ (2005) Oxidative stress and ozone: perception, signalling and response. Plant, Cell & Environ 28(8):1012-1020. https://doi.org/10.1111/j.1365-3040.2005.01326.x

Bičárová S, Sitková Z, Pavlendová H, Fleischer Jr P, Fleischer Sr P, Bytnerowicz A (2019) The role of environmental factors in ozone uptake of *Pinus mugo* Turra. Atmos Pollut Res 10(1):283-293. https://doi.org/10.1016/j.apr.2018.08.003

Bona C, Silva MYBD, Rezende IMD, Santos GDO, Souza LAD, Inckot RC (2011) Effect of diesel contaminated soil on root and leaf of Sebastiania commersoniana (Euphorbiaceae) and Schinus terebinthifolius (Anacardiaceae). Acta Botanica Brasilica, 25, 277-285. https://doi.org/10.1590/S0102-33062011000200003

Calabrese EJ, Blain RB (2009) Hormesis and plant biology. Environ Poll 157(1):42-48. https://doi.org/10.1016/j.envpol.2008.07.028

Cassimiro JC, Moura BB, Alonso R, Meirelles ST, Moraes, RM (2016) Ozone stomatal flux and O_3 concentration-based metrics for *Astronium graveolens* Jacq., a Brazilian native forest tree species. Environ Pollut 213:1007-1015. https://doi.org/10.1016/j.envpol.2016.01.005

CETESB (2024) Qualidade do ar no estado de São Paulo. CETESB, São Paulo. 140 p. (Série Relatórios). Available at: https://cetesb.sp.gov.br/ar/wp-content/uploads/sites/28/2025/06/Relatorio-de-Metodologia-para-Avaliacao-da-Qualidade-do-Ar.pdf

CLRTAP (2015). Mapping critical levels for vegetation. chapter III of manual on methodologies and criteria for modelling and mapping critical loads and levels and air pollution effects. risks and trends. UNECE convention on long-range transboundary air pollution; accessed on 11 Jul 2025 on Web at: www.icpmapping.org

Conte A, Otu-Larbi F, Alivernini A, Hoshika Y, Paoletti E, Ashworth K, Fares S. (2021) Exploring new strategies for ozone-risk assessment: A dynamic-threshold case study. Environ Pollut 287:117620. https://doi.org/10.1016/j.envpol.2021.117620

Dewan S, Lakhani A (2022) Tropospheric ozone and its natural precursors impacted by climatic changes in emission and dynamics. Front Environ Sci 10:1007942. https://doi.org/10.3389/fenvs.2022.1007942

Elshorbany Y, Ziemke JR, Strode S, Petetin H, Miyazaki K, De Smedt I, Pickering K, Seguel RJ, Worden H, Emmerichs T, Taraborrelli D, Cazorla M, Fadnavis S, Buchholz RR, Gaubert B, Rojas NY, Nogueira T, Salameh T, Huang M (2024) Tropospheric ozone precursors: global and regional distributions, trends, and variability. Atmosp Chem Physics 24(21):12225-12257. https://doi.org/10.5194/acp-24-12225-2024

Engela MRGS, Furlan CM, Esposito MP, Fernandes FF, Carrari E, Domingos M, Paoletti E, Hoshika Y (2021) Metabolic and physiological alterations indicate that the tropical broadleaf tree *Eugenia uniflora* L. is sensitive to ozone. Sci Total Environ 769:145080 2021.

https://doi.org/10.1016/j.scitotenv.2021.145080

Fernandes FF, Esposito MP, Engela MRGS, Cardoso-Gustavson P, Furlan CM, Hoshika Y, Carrari E, Magni G, Domingos M, Paoletti E (2019) The passion fruit liana (*Passiflora edulis* Sims, Passifloraceae) is tolerant to ozone. Sci Total Environ 656:1091-1101. https://doi.org/10.1016/j.scitotenv.2018.11.425

H. Wickham. (2016). ggplot2: Elegant Graphics for Data Analysis. Springer-Verlag New York, <https://ggplot2.tidyverse.org>.

Hayes F, Wagg S, Mills G, Wilkinson S, Davies W (2012) Ozone effects in a drier climate: implications for stomatal fluxes of reduced stomatal sensitivity to soil drying in a typical grassland species. Glob Change Biol 18(3):948-959. https://doi.org/10.1111/j.1365-2486.2011.02613.x

Hobbie SE, Grimm NB (2020) Nature-based approaches to managing climate change impacts in cities. Philosop Transact Royal Soc B, 375(1794):20190124. https://doi.org/10.1098/rstb.2019.0124

Hoshika Y, Agathokleous E, Moura BB, Paoletti E (2024) Ozone risk assessment at Free-Air Controlled Exposure (FACE) experiments: A critical revisit. Environ Res 255:119215. https://doi.org/10.1016/j.envres.2024.119215

Hoshika Y, Carrari E, Mariotti B, Martini S, De Marco A, Sicard P, Paoletti E. (2020) Flux-based ozone risk assessment for a plant injury index (PII) in three European cool-temperate deciduous tree species. Forests 11(1):82. https://doi.org/10.3390/f11010082

Hoshika Y, Moura B, Paoletti E (2018) Ozone risk assessment in three oak species as affected by soil water availability. Environ Sci Pollut Res 25:8125-8136. https://doi.org/10.1016/j.atmosenv.2012.02.083

Hoshika Y, Watanabe M, Inada N, Koike T. (2012). Modeling of stomatal conductance for estimating ozone uptake of *Fagus crenata* under experimentally enhanced free-air ozone exposure. Water, Air, & Soil Pollution, 223(7):3893-3901. https://doi.org/10.1007/s11270-012-1158-9

Hoshika Y, Watanabe M, Kitao M, Häberle KH, Grams TE, Koike T, Matyssek R. (2015) Ozone induces stomatal narrowing in European and Siebold's beeches: a comparison between two experiments of free-air ozone exposure. Environ Pollut 196:527-533. https://doi.org/10.1016/j.envpol.2014.07.034

Jarvis PG (1976) Interpretation of variations in leaf water potential and stomatal conductance found in canopies in field. Philos Trans R Soc Lond B 273:593–610. https://doi.org/10.1098/rstb.1976.0035

Kaylor SD, Taylor SJS, Herrick JD (2023) Estimates of biomass reductions of ozone sensitive herbaceous plants in California. Sci Total Environ 878:163134. https://doi.org/10.1016/j.scitotenv.2023.163134

Lamb WF, Wiedmann T, Pongratz J, Andrew R, Crippa M, Olivier JGJ, Wiedenhofer D, Mattioli G, Al Khourdajie A, House J, Pachauri S, Figueroa M, Saheb Y, Slade R, Hubacek K, Sun L, Kahn Ribeiro S, Khennas S, de la Rue du Can S, Chapungu L, Davis SJ, Bashmakov I, Dai H, Dhakal S, Tan X, Geng Y, Gu B, Minx J (2021) A review of trends and drivers of greenhouse gas emissions by sector from 1990 to 2018. Environ Res Letters 16(7):073005. https://doi.org/10.1088/1748-9326/abee4e

Li Z, Yang J, Shang B, Agathokleous E, Rubert-Nason KF, Xu Y, Feng Z (2021) Nonlinear responses of foliar phenylpropanoids to increasing O_3 exposure: Ecological implications in a *Populus* model system. Sci Total Environ 767:144358. https://doi.org/10.1016/j.scitotenv.2020.144358

Lorenzi H (2016) Árvores brasileiras: manual de identificação e cultivo de plantas arbóreas nativas do Brasil. 7 ed. Plantarum, Nova Odessa.

Manzini J, Hoshika Y, Danti R, Moura BB, Paoletti E, Della Rocca G (2025) Ozone risk assessment of common cypress (*Cupressus sempervirens* L.) clones and effects of *Seiridium cardinale* infection. J Environ Sci 151:441-453. https://doi.org/10.1016/j.jes.2024.03.026

Marques MC, Grelle CE (2021) The Atlantic Forest. History, Biodiversity, Threats and Opportunities of the Mega-diverse Forest. Springer International Publishing. https://doi.org/10.1007/978-3-030-55322-7

Marzuoli R, Faoro F, Picchi V, Gerosa GA (2024) Phytotoxic Ozone Dose–Response Relationships for Durum Wheat (*Triticum durum*, Desf.). Plants 13(5):573. https://doi.org/10.3390/plants13050573

Mattson MP (2008) Hormesis defined. Ageing Res Rev 7(1):1-7. https://doi.org/10.1016/j.arr.2007.08.007

Miller RW, Hauer RJ, Werner LP (2015) Urban forestry: planning and managing urban greenspaces. Waveland press.

Mills G, Buker P, Hayes F, Emberson L, Werner W, Gimeno B, Pihl Karlsson G (2003) Developing ozone flux-effect models for white clover from the ICP Vegetation ambient air monitoring experiment. Swed Water Air Pollut Res Lab Publ IVL B:128-139.

Mills G, Pleijel H, Braun S, Büker P, Bermejo V, Calvo E, Danielsson H, Emberson L, González Fernández I, Grünhage L, Harmens H, Hayes F, Karlsson PE, Simpson D (2011) New stomatal flux-based critical levels for ozone effects on vegetation. Atmosp Environ 45(28):5064-5068. https://doi.org/10.1016/j.atmosenv.2011.06.009

Mills G, Pleijel, H, Malley, CS, Sinha, B, Cooper, OR, Schultz, MG, Neufeld, HS, Simpson, D, Sharps, K, Feng, Z, Gerosa, G, Harmens, H, Kobayashi, K, Saxena, P, Paoletti, E, Sinha V, Xu X (2018) Tropospheric Ozone Assessment Report: Present-day tropospheric ozone distribution and trends relevant to vegetation. Elem Sci Anth 6:47. https://doi.org/10.1525/elementa.302

Moura BB, Alves ES, de Souza SR, Domingos M, Vollenweider P (2014) Ozone phytotoxic potential with regard to fragments of the Atlantic Semi-deciduous Forest downwind of Sao Paulo, Brazil. Environ Pollut 192:65-73. https://doi.org/10.1016/j.envpol.2014.05.014
Moura BB, Hoshika Y, Ribeiro RV, Paoletti E (2018) Exposure-and flux-based assessment of ozone risk to sugarcane plants. Atmosp Environ 176 :252-260. https://doi.org/10.1016/j.atmosenv.2017.12.039

Nguyen DH, Lin C, Vu CT, Cheruiyot NK, Nguyen MK, Le TH, Lukkhasorn W, Vo TDH, Bui XT (2022) Tropospheric ozone and NOx: A review of worldwide variation and meteorological influences. Environ Tech Innov 28:102809. https://doi.org/10.1016/j.eti.2022.102809

Niu J, Zhao P, Sun Z, Zhu L, Ni G, Zeng X, Zhang Z, Zhao X, Zhao P, Gao J, Hu Y, Zeng X, Ouyang L (2016) Stomatal uptake of O_3 in a *Schima superba* plantation in subtropical China derived from sap flow measurements. Sci Total Environ 545:465-475. https://doi.org/10.1016/j.scitotenv.2015.12.122

Oliveira KC, Franciscato LM, Mendes SS, Barizon FM, Gonçalves DD, Barbosa LN, Faria MGI, Valle JS, Casalvara RFA, Gonçalves JE, Gazim ZC, Ruiz SP (2024) Essential Oil from the Leaves, Fruits and Twigs of *Schinus terebinthifolius*: Chemical Composition, Antioxidant and Antibacterial Potential. Molecules 29(2):469. https://doi.org/10.3390/molecules29020469

Oliveira VS, Covre AM, Gouvea DS, Canal L, Santos KTHS, Santos JSH, Santos GP,

Pinheiro APB, Schmilt O, Posse RP, Czepak MP, Arantes SD, Alexandre RS, Amaral JAT, Vitória EL, Schmilt ER (2019) Determination of the leaflet area of *Schinus terebinthifolius* Raddi in function of linear dimensions. J Agric Sci 11(14):198-198. https://doi.org/10.5539/jas.v11n14p198

Olmedo GM, Raguse-Quadros M, Conrado GT, Oliveira JM (2023) Climatic signals on phenological patterns among tree species in a subtropical forest community. Neotropical Biology and Conservation 18(3):191-208. https://doi.org/10.3897/neotropical.18.e103506

Onofri A (2024). _statforbiology: Tools for Data Analyses in Biology_. R package version 0.9.9, <https://CRAN.R-project.org/package=statforbiology>.

Onofri A. (2020) The broken bridge between biologists and statisticians: a blog and R package, Statforbiology, IT, <https://www.statforbiology.com>.

Paoletti E, Materassi A, Fasano G, Hoshika Y, Carriero G, Silaghi D, Badea O (2017) A new-generation 3D ozone FACE (free air controlled exposure). Sci Total Environ 575:1407-1414. https://doi.org/10.1016/j.scitotenv.2016.09.217

Pleijel H, Danielsson H, Broberg MC (2022) Benefits of the Phytotoxic Ozone Dose (POD) index in dose-response functions for wheat yield loss. Atmosp Environ 268:118797. https://dor.org/10.1016/j.atmosenv.2021.118797

Ritz, C., Baty, F., Streibig, J. C., & Gerhard, D. (2015). Dose-response analysis using R. *PloS one*, *10*(12), e0146021.

Ruiz, E. (2023). automation: Automation of statistical testing & non-linear modelling in R. R package version 0.1.0, (https://github.com/leliotruiz/automation>.

Santos RS, Alencar JBR, Gallo R (2024) Modeling the current and projected distribution of Brazilian peppertree *Schinus terebinthifolia* Raddi (Anacardiaceae) in the Americas. Braz J Biol 84:e279769. https://doi.org/10.1590/1519-6984.279769

Seguel RJ, Castillo L, Opazo C, Rojas NY, Nogueira T, Cazorla M, Gavidia-Calderón M, Gallardo L, Garreaud R, Carrasco-Escaff T, Elshorbany Y (2024) Changes in South American surface ozone trends: exploring the influences of precursors and extreme events. Atmos Chem Phys 24:8225–8242. https://doi.org/10.5194/acp-24-8225-2024

Shang B, Yuan X, Li P, Xu Y, Feng Z (2019) Effects of elevated ozone and water deficit on poplar saplings: Changes in carbon and nitrogen stocks and their allocation to different organs. Forest Ecol Manag 441:89-98. https://doi.org/10.1016/j.foreco.2019.03.042

Silva PN, Reis CHG, Duarte VP, Castro EM, Pádua MP, Pereira FJ (2024) Toxicity of iron mining tailings and potential for revegetation using Schinus terebinthifolia Raddi based on the emergence, growth, and anatomy of the species. Mining 4(3):719-732. https://doi.org/10.3390/mining4030040

Siqueira MC, Kanashiro S, Domingos M, Rinaldi MCS, Tavares AR (2021) Physiological and biochemical changes in tree seedlings growing in urban forest soil contaminated with copper in São Paulo, Brazil. Plant Soil 464:149-163. https://doi.org/10.1007/s11104-021-04948-3

Tarasick D, Galbally IE, Cooper OR, Schultz MG, Ancellet G, Leblanc T, Wallington TJ, Ziemke J, Liu X, Steinbacher M, Staehelin J, Vigouroux C, Hannigan JW, García O, Foret G, Zanis P, Weatherhead E, Petropavlovskikh I, Worden H, Osman M, Liu J, Chang K-L, Gaudel A, Lin M, Granados-Muñoz M, Thompson AM, Oltmans SJ, Cuesta J, Dufour G, Thouret V, Hassler B, Trickl T, Neu JL (2019). Tropospheric Ozone Assessment Report: Tropospheric ozone from 1877 to 2016, observed levels, trends and uncertainties. Elem Sci Anth 7:39. https://doi.org/10.1525/elementa.376

Tredennick AT, Hooker G, Ellner SP, Adler PB (2021) A practical guide to selecting models for exploration, inference, and prediction in ecology. Ecol 102(6):e03336. https://doi.org/10.1002/ecy.3336

Uliana MP, Fronza M, da Silva AG, Vargas TS, de Andrade TU, Scherer R (2016) Composition and biological activity of Brazilian rose pepper (*Schinus terebinthifolius* Raddi) leaves. Ind Crops Prod 83:235-240. https://doi.org/10.1016/j.indcrop.2015.11.077

Wickham H (2023). _modelr: Modelling Functions that Work with the Pipe_. R package version 0.1.11, <https://CRAN.R-project.org/package=modelr>.

Xu J, Zhao H, Wang S, Zheng Y, Mai B, Zhang X (2023) Assessment of photosynthesis and yield loss of winter wheat under ground-level ozone exposure. Environ Techn Innov 29:103013. https://doi.org/10.1016/j.eti.2023.103013

Capítulo IV

--

Revista pré-definida para submissão: Plant Stress

--

Root retention and metabolic adjustment: strategies of *Schinus terebinthifolia* to tolerate heavy metals and ozone

Matheus Casarini Siqueira[a*], Barbara Baesso Moura[b,c], Yasutomo Hoshika[b,c], Elena Paoletti[b,c], Cecilia Brunetti[b,c], Armando Reis Tavares[d], Marisa Domingos[a]

[a] *Environmental Research Institute, Av. Miguel Estefno, 3687, 04301-012, São Paulo Brazil.*

[b] *Institute of Research on Terrestrial Ecosystems (IRET), National Research Council, Via Madonna del Piano 10, 50019 Sesto Fiorentino, Italy*

[c] *National Biodiversity Future Center (NBFC), Palermo 90133, Italy*

[d] *Agronomic Institute, Av. Barão de Itapura, 1481, 13020-902, Jundiaí, Brazil*

[*] *Corresponding author: matheus.casarini1@gmail.com, +55 11 981846119, ORCID (0000-0001-7776-3805)*

ABSTRACT

Combined contamination by heavy metals (Cu, Zn, Ni) and tropospheric ozone (O_3) is frequent in urban and degraded areas, imposing abiotic stresses that negatively affect plant growth and survival. Tolerant species employ mechanisms such as root organic acid exudation, phytochelatin synthesis, antioxidant system activation, and free amino acid regulation to mitigate these damages. *Schinus terebinthifolia*, a species with known tolerance to some heavy metals and promising characteristics for urban afforestation, has been hypothesized to also be tolerant to O_3. This study analyzed the physiological (biomass, leaf damage, gas exchange, pigments), biochemical (root organic acids, phytochelatins, non-enzymatic antioxidants, free amino acids), and visual responses of this species to three O_3 concentrations (ambient air - AA, 1.5× AA, and 2.0× AA) and two metal treatments (control fertilization and fertilization enriched with Cu, Zn, and Ni). The results demonstrated that the species maintains its photosynthesis and antioxidant defenses despite visible leaf damage under high O_3, exhibits a hormetic response in biomass, and performs coordinated metabolic adjustments in the analyzed compounds. Critically, the species presents a high capacity for metal accumulation and retention in the roots, a mechanism that was not compromised by the additional O_3 stress. It is concluded that *S. terebinthifolia* has high tolerance to individual and/or combined stresses, demonstrating great potential for use in ecological restoration programs and urban afforestation in areas subject to this double environmental contamination.

Key-words: Tolerance, atmospheric pollution, soil contamination, biochemical compounds

INTRODUCTION

Due to increased human activities, environmental contamination by abiotic agents such as heavy metals (HMs) and secondary air pollutants like ozone (O_3) has become a growing global concern. HMs adsorbed on particulate material are primary pollutants that mainly affect soils, and the main sources are vehicle emissions, mining, and agricultural fertilizers (Timothy and Williams, 2019), while O_3 is a secondary pollutant formed from the reaction of oxygen in the presence of primary pollutants (NOx) and volatile organic compounds emitted by natural or anthropogenic sources (Donzelli and Suarez-Varela, 2024). Both are potent inducers of oxidative stress and cell damage, compromising plant development and survival (Demidchik, 2015).

To tolerate potential toxic effects of stress caused by HM or O_3 exposure, plants have evolved several physiological adaptations and biochemical defenses (Sarma et al., 2018). The exudation of root organic acids (ROAs), which can limit the absorption of toxic elements (Osmolovskaya et al., 2018), and the synthesis of phytochelatins (PCs) that act as binding molecules to heavy metals, trapping them in the vacuole and limiting their translocation within the plant (Inouhe, 2005) are key strategies to prevent HM toxicity. To mitigate oxidative stress from HMs or tropospheric O_3, plants rely on antioxidant defense molecules, such as ascorbate peroxidase, catalase, superoxide dismutase enzymes, and non-enzymatic molecules such as ascorbic acid (AA) and glutathione (GSH) (Hasanuzzaman and Fujita, 2022). In addition to specialized antioxidant compounds, metabolites from primary metabolism, such as free amino acids, also play crucial roles in stress responses (Kawade et al., 2023). Consequently, profiling of free amino acids can provide other key insights into the adaptive mechanisms underlying plant tolerance to combined stresses like tropospheric ozone and heavy metals.

Given the growing need for species that are resilient to climate change and tolerant to multiple urban pollutants, the identification of plants capable of tolerating combined stresses is increasingly critical for urban forestry and environmental restoration (Kisgarva et al., 2023). *Schinus terebinthifolia*, a tropical species native to the threatened Atlantic Forest, is valued for its ornamental use and medicinal properties, and exhibits desirable traits for urban landscaping (Carvalho et al., 2013), and is recommended to environmental restoration and ecological recompositing (Oliveira et al., 2025). Previous studies have shown that *S. terebinthifolia* is tolerant to heavy metals like iron (Silva et al., 2024), copper (Siqueira et al., 2021) and the combination of Cu, Zn, Ni under hydroponic conditions (Siqueira et al., 2026a). Also, a recent study showed that *S. terebinthifolia* is highly tolerant to O_3 individually, presenting hormetic responses under stress (Siqueira et al., 2026b). However, since the tolerance mechanisms to combining O_3 and HM stress remain unknown, our results are highly relevant for ecological

and urban aspects, as anthropized/contaminated environments targeted for restoration typically present a persistent combination of multiple stressors (Calfapietra et al., 2015). We therefore hypothesized that, given its tolerance to certain heavy metals and its robust antioxidant system, *S. terebinthifolia* may also exhibit tolerance to O_3 and mitigate ozone-induced oxidative stress. Conversely, we also raise the hypothesis that O_3 exposure could impair *S. terebinthifolia* heavy metal tolerance, leading to adverse physiological and developmental effects. Therefore, this study aims to analyze the visual (symptomatic damage), physiological (gas exchange, photosynthetic pigments, and biomass), and biochemical (non-enzymatic antioxidants, phytochelatins, root organic acids, and free amino acids) responses of *S. terebinthifolia* to increasing concentrations of tropospheric ozone and heavy metal exposure, in order to elucidate its physiological adaptations and defense strategies against multiple abiotic stressors.

MATERIAL AND METHODS

Experimental setup

The seedlings of *Schinus terebinthifolia* (Fig. IV1A) were obtained from the germination of seeds sent to CNR-IRET from Brazil in November 2023. The experiment was carried out from June to September 2024 in the Free Air Controlled Exposure (FACE) ozone fumigation system (Fig. IV1B and IV1C).

Fig. IV 1. *Schinus terebinthifolia* seedlings at the beginning of the experiment (A). Free air controlled exposure (FACE) ozone fumigation system (B-C).

Plants were grown for 3 months (July – September) under 3 atmospheric O_3 concentrations: Ambient air (AA - 39.9 ppb on average), 1.5× ambient air (1.5× – 53.0 ppb), and 2.0× ambient air (2.0× - 69.3 ppb) (Fig. IV2). In addition to the O_3 treatment, plants were grown under two fertilization treatments: 25% strength of balanced Hoagland and Arnon solution (Control), and 25% strength of balanced Hoagland and Arnon solution enriched with heavy metals (HM) (copper - Cu, zinc - Zn, and nickel - Ni, 1250 µM of each). O_3 treatment consisted of 3 blocks and 3 plants per block for each nutrient treatment (n = 9). These plants were fertilized with the Control treatment.

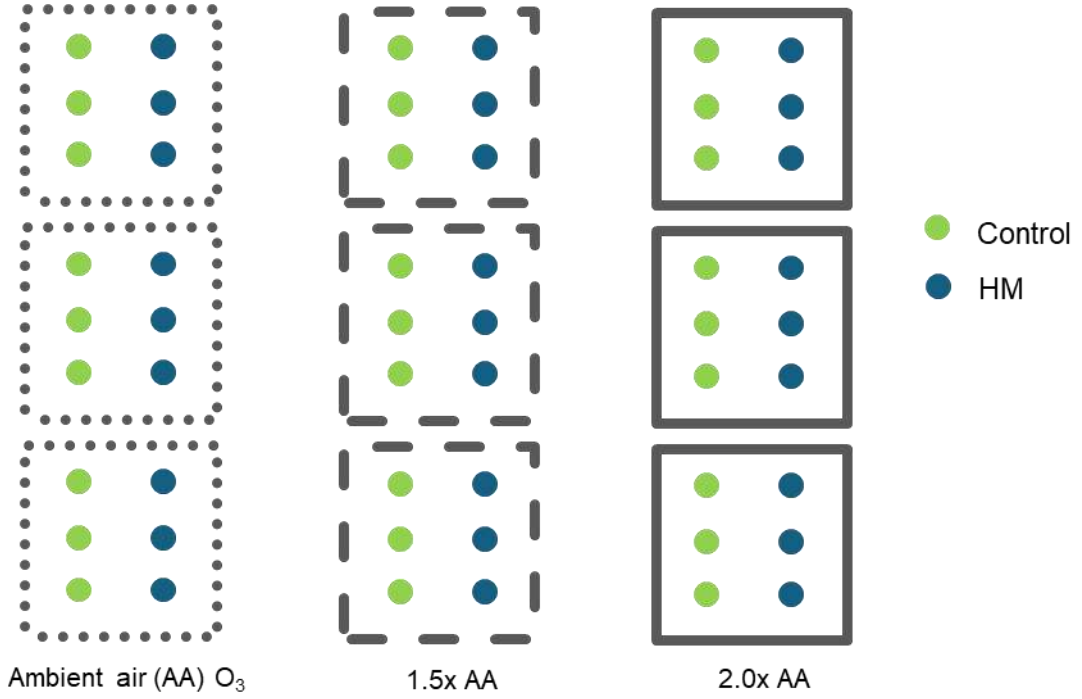

Fig. IV 2. Experimental design used for the study of *S. terebinthifolia* under 3 atmospheric ozone conditions (AA, 1.5× and 2.0×) and 2 nutrient treatments (Control and HM).

Leaf gas measurements and sampling

At the beginning of the experiment, monthly, and at the end of the experiment, the potential alterations in the photosynthetic process of *S. terebinthifolia* were investigated by measuring leaf gas exchange parameters [Net carbon assimilation (*A*) and stomatal conductance (*gsw*)) by an infra-red gas analyzer (IRGA - LI6800 – Li-Cor)]. Photos of leaves were taken to assess visible O_3 leaf damage.

At the end of the experiment, the plants were removed from the soil, and the roots were washed. Then roots were placed in 1L of deionized water for 2 hours to exudates sampling (Fig. IV3A and IV3B).

Fig. IV 3. *S. terebinthifolia* roots after washing (A) for root exudates collection in deionized water (B).

Fresh leaves in the upper (Top), middle (Mid) and lower (Bot) regions of the main stem of *S. terebinthifolia*, as well the fresh root tips were sampled and immediately crushed in liquid nitrogen for biochemical analyses. Since heavy metals have low mobility within tissues and their effects are observed mostly in young leaves (Page and Feller, 2015), while O_3 mainly affects older leaves (Pisuttu et al., 2024), we aim to identify the effects of these stressors at different leaf ages and main stem position.

Finally, the remaining parts of the plants were sectioned into leaves, stem and roots, and dried in an oven until constant weight. The samples were weighed and crushed in a mill to further quantification of heavy metals concentrations in tissues.

Biochemical measurements

Photosynthetic pigments

Total chlorophyll ($a + b$) and carotenoid concentrations (µg g^{-1} leaf fresh weight) were determined in frozen leaf samples immersed in 96% ethanol kept in the dark for 24 hours. The extract was spectrophotometrically analyzed at λ = 471 nm, 649 nm, 664 nm and 750 nm, and then chlorophyll *a* (*Chl a*), chlorophyll *b* (*Chl b*) and total carotenoids were determined by the formulas derived from Minocha et al. (2009):

$$Chl\ a = (13.36 \times A664) - (5.19 \times A649)$$

$$Chl\ b = (27.43 \times A649) - (8.12 \times A664)$$

$$Carotenoids = [(1000 \times A470) - (2.13 \times Chl\ a) - (97.64 \times Chl\ b)] \div 209$$

Antioxidants

Ascorbic acid (AA) concentration in reduced (AA_r) and total (AA_t) forms (mg g^{-1} leaf fresh weight) was determined in frozen leaf samples, after extraction with metaphosphoric acid (HPO_3), followed by centrifugation at 11,393.4 × g (10,000 rpm) for 15 minutes at 2 ºC. The supernatant was collected, filtered in hydrophilic nylon syringe filters (0.22 µm), and AA

concentrations were determined in RP-HPLC on a C-18 column, flow rate set to 1 ml min^{-1}, 25 ºC and detection under diode array detector (DAD) at λ = 245 nm, using isocratic elution of water acidified at pH 2.3 with H_3PO_4 (López et al., 2005).

Glutathione (GSH) concentration in reduced (GSHr) and total (GSHt) forms (mg g^{-1} leaf fresh weight) was determined in frozen leaf samples, after extraction with sulfosalicylic acid, followed by centrifugation at 11,393.4 × g (10,000 rpm) for 15 minutes at 2 ºC. The supernatant was collected and GSH concentrations were determined in spectrophotometer at λ = 412 nm (Anderson, 1985).

Phytochelatins

Phytochelatin (PC2 to PC6) concentrations (µg g^{-1} leaf or root fresh weight) were determined in frozen leaf and root samples, after extraction with 60% perchloric acid, vortexing for 1 minute, followed by centrifugation at 11,393.4 × g (10,000 rpm) for 15 minutes at 2 ºC. The supernatant was collected, filtered in hydrophilic nylon syringe filters (0.22 µm) and PC detection were determined in RP-HPLC (reverse phase high performance liquid chromatographic) on a C-18 column, flow rate set to 1 ml min^{-1}, 25 ºC and detection under DAD at λ = 214, using (A) 99.9% deionized water + 0.1% trifluoroacetic acid (v/v) and (B) acetonitrile for 25 minutes under linear elution gradient (1% decrease in A and 1% increase in B per minute) (Hunaiti et al., 2003).

Root organic acids

Root organic acids were detected in the sampled root exudated solution, after immersing the roots in 1L of distilled water for 2 hours. An aliquot of the solution (45 mL) was collected and filtered through qualitative cellulose membranes (grade 42) with 0.22 µm porosity. Then, it was freeze-dried and resuspended in 2 ml of distilled water acidified at pH 4.0 with H_3PO_4. Identification and quantification of ROAs were carried out in a RP-HPLC system, using a C-18 column and an isocratic elution of (A - 93%) 25 mM KH_2PO_4 in water and (B - 7%) methanol, with flow rate set to 1 ml min^{-1}, 25 ºC and detection under DAD at λ = 210 nm. Commercial organic acids (Acetic, Adipic, Ascorbic, Benzoic, Butyric, Citric, Formic, Fumaric, Isobutyric, Isocitric, Lactic, Maleic, Malic, Malonic, Oxalic, Phytic, Propionic, Quinic, Shikimic, Succinic and Tartaric - organic acids kit, Supelco, Merck Sigma-Aldrich) were used as a standard reference, and the identification of organic acids in the samples (µg ml^{-1}) was performed by first adding the standard to a blank sample (deionized water) and comparing the retention times of the sample with the standard reference, and second by adding the standard to a random sample and observing the increase in the corresponding organic acid peak (Cawthray, 2003). Calibration curve was performed in detected organic acids.

Free amino acids

Amino acids concentration (nmol g^{-1} of fresh tissue) was determined in frozen leaf and roots samples, by the adapted methanol-chloroform-water extraction (Lisec et al., 2006) and AccQ-Tag Ultra derivatization protocol and kit (Waters, 2007). 350 µl of pre-cooled (-20 °C) methanol was added to 50 mg of samples, vortexing for 10 seconds followed by heat extraction for 10 min at 70°C. After cooling to room temperature, the samples were centrifugated at 11,000 rpm for 10 minutes. The supernatant was collected, transferred to new vials, and then added 375 µL of pre-cooled (-20 °C) chloroform, vortexed for 10 seconds, and added 750 µL of ultrapure water. After centrifuging for 15 minutes at 2,200 rpm at room temperature to phase separation, 150 µL of the aqueous phase (upper part) was collected, transferred to new vials, and dried in a SpeedVac at 25 °C. In a vial, 5 µL of the sample reconstituted in water, 35 µL borate buffer, and 10 µL of 6-aminoquinolyl-N-hydroxysuccinimidyl carbamate (AQC - derivatizing) were added, vortexed for 10 seconds, and placed in a heater at 55°C for 10 minutes. The separation was performed under the ACQUITY UPLC system (Waters, Milford, MA, USA) with AccQ-Tag Ultra Column C18 (2.1x100 mm 1.7 µm) at 60°C with the following eluents: A- AccQ-Tag Ultra Eluent A (10% in water), B- AccQ-Tag Ultra Eluent B (100%), at a flow rate of 0.7 mL min^{-1}. The gradient was 0−0.54 min (99.9% A), 5.74 min (90.0% A), 7.74 min (78.8% A), 8.04−8.64 min (40.4% A), 8.73−10 min (99.9% A), with a 5 minute post-run procedure for column conditioning. Amino acids were detected by UV absorbance at 260 nm. To determine the concentration of each amino acid, a 8 point calibration curve with mix (Waters) and single standards (Merck Sigma-Aldrich) of the following 17 amino acids were used: Alanine (ALA), Arginine (ARG), Asparagine (ASP), Cysteine (CYS), Glycine (GLY), Glutamic acid (GLU), Histidine (HIS), Isoleucine (ILE), Leucine (LEU), Lysine (LYS), Methionine (MET), Phenylalanine (PHE), Proline (PRO), Serine (SER), Tyrosine (TYR), Threonine (THR) and Valine (VAL). The identification and calculation were performed at the Empower software (Waters, Milford, MA, USA).

To amino acid profile characterization of *S. terebinthifolia*, we selected the leaves and roots of plants in the absence of imposed stressors (MH and O_3), that is, in the Ambient Air (AA) and Control treatment, while the treatments with stressors were analyzed to verify the influence of those stressors on the amino acid profile.

Statistical analysis

Data was analyzed through GraphPad Prism v 9.0 and R software's. Data residuals were subjected to Shapiro-Wilk normality (parametric distribution) and Brown-Forsythe homoscedasticity (equality of variances) tests, and independence of observations to verify two-

way ANOVA assumptions. If these assumptions were met, differences between treatments were analyzed through Two-Way ANOVA (factors: HM × O_3), followed by Šídák's multiple comparison test ($p \leq 0.05$). Non-normal or heteroscedastic data were transformed (log or sqrt). If transformed data presented parametric but heteroscedastic distribution, Welch-correction ANOVA was applied. If even transformed data presented non-parametric residuals, data were analyzed through Scheirer-Ray-Hare test, followed by Dunn's post-hoc multiple comparison test ($p \leq 0.05$). Parametrical data was represented by mean bar (± standard deviation) graphs, while non-parametrical data was represented by median box plot (1.5 × interquartile range as whiskers) graphs.

Free amino acids were first exploratorily analyzed through Principal Component Analysis (PCA) with correlation matrix (standardized data) to identify possible treatment effect in overall amino acids profile. Further a two-way ANOVA (factors: HM × O_3) was performed to better assess treatment effects on individual amino acids concentration.

RESULTS

Visual aspects

There were visual differences in the growth of *S. terebinthifolia* seedlings subjected to O_3 treatments (Fig. IV4). Plants in the 1.5× treatment showed increased growth compared to the AA plants, while plants in the 2.0× treatment showed growth reduction. There were no visible differences between the Control and HM treatments, for all O_3 treatments.

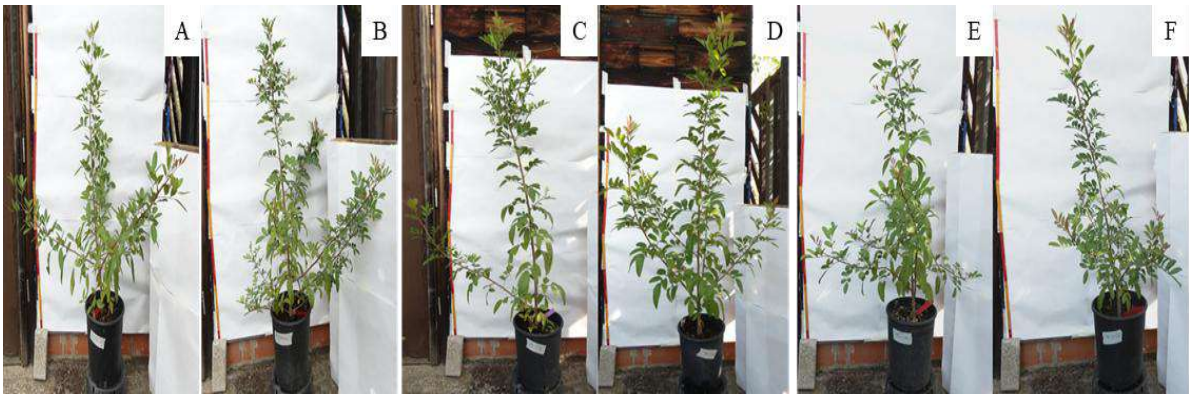

Fig. IV 4. *S. terebinthifolia* seedlings at the end of the experiment. A: Control AA; B: HM AA; C: Control 1.5×; D: HM 1.5×; E: Control 2.0×; F: HM 2.0×.

Visible leaf damage

Visible leaf damage caused by increased tropospheric O_3 exposure was observed in *S. terebinthifolia* (Fig. IV5). Plants in the AA treatment showed no O_3 damage, plants grown in the 1.5× treatment showed mild damage characterized by duller leaf coloration and development of small, localized stipples., while those plants in the 2.0× treatment showed severe visible damage, evidenced by extensive widespread O_3 damage (red spots) covering most of leaf blades. There were no visual differences between Control and HM treatments for all O_3 treatments.

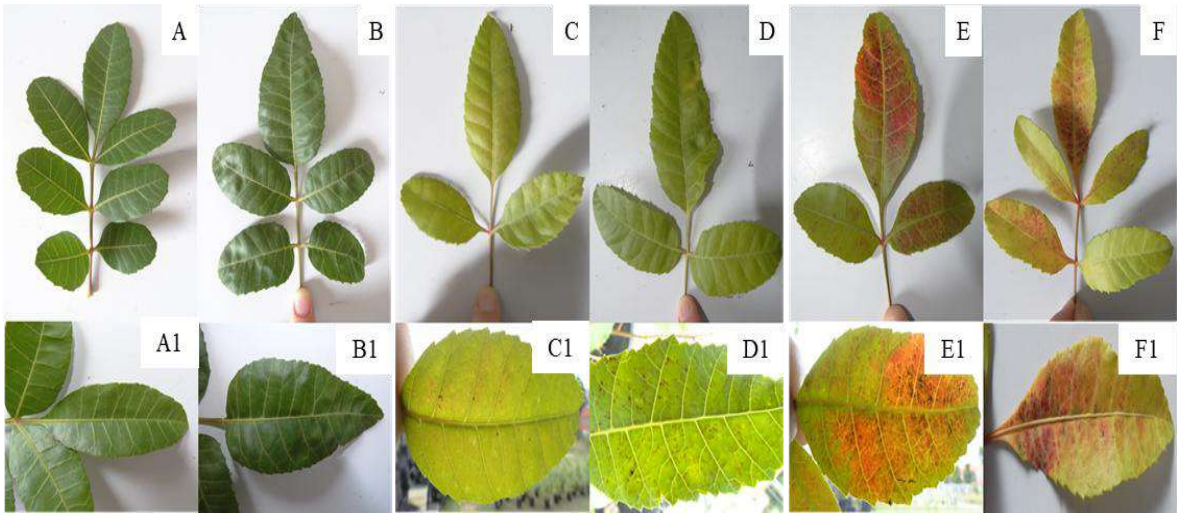

Fig. IV 5. Visible ozone leaf damage in *S. terebinthifolia*. A: Control AA; B: HM AA; C: Control 1.5×; D: HM 1.5×; E: Control 2.0×; F: HM 2.0×.

Biomass production

S. terebinthifolia total biomass production was affected by atmospheric O_3 concentration (Fig. IV6), but not by heavy metal content. Plants in the 1.5× treatment showed increased biomass compared to the AA plants, while plants in the 2.0× treatment showed reduced biomass production. There were no differences between the Control and HM treatments, for all O_3 treatments.

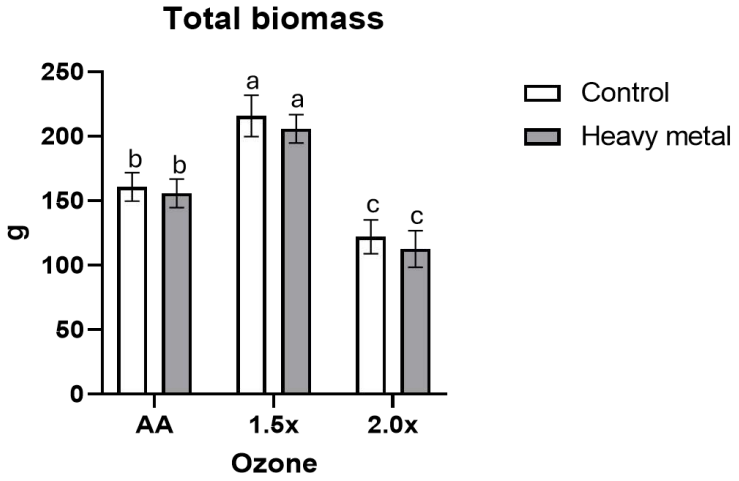

Fig. IV 6. *S. terebinthifolia* seedlings total biomass (g) under different ozone levels (AA, 1.5×, 2.0×) and nutrient solutions (Control and HM). Different lowercase letters indicate a significant difference between ozone treatments, according to two-way ANOVA followed by post-hoc Šídák's test ($p \leq 0.05$).

Heavy metal accumulation

Root accumulation of Cu, Zn, and Ni in *S. terebinthifolia* was primarily driven by heavy metal exposure, showing significantly higher levels under HM than the control, and occurring consistently across all O_3 treatments (Fig. IV7). In leaves, only Ni levels increased while Cu and Zn remained unchanged. In stems, Cu and Zn increased under heavy metals only at 2.0× O_3, whereas Ni increased at all O_3 treatments. In roots, Cu and Zn concentrations increased at 2.0× O_3 compared to 1.5× O_3. Ozone treatments did not affect Ni in any organ.

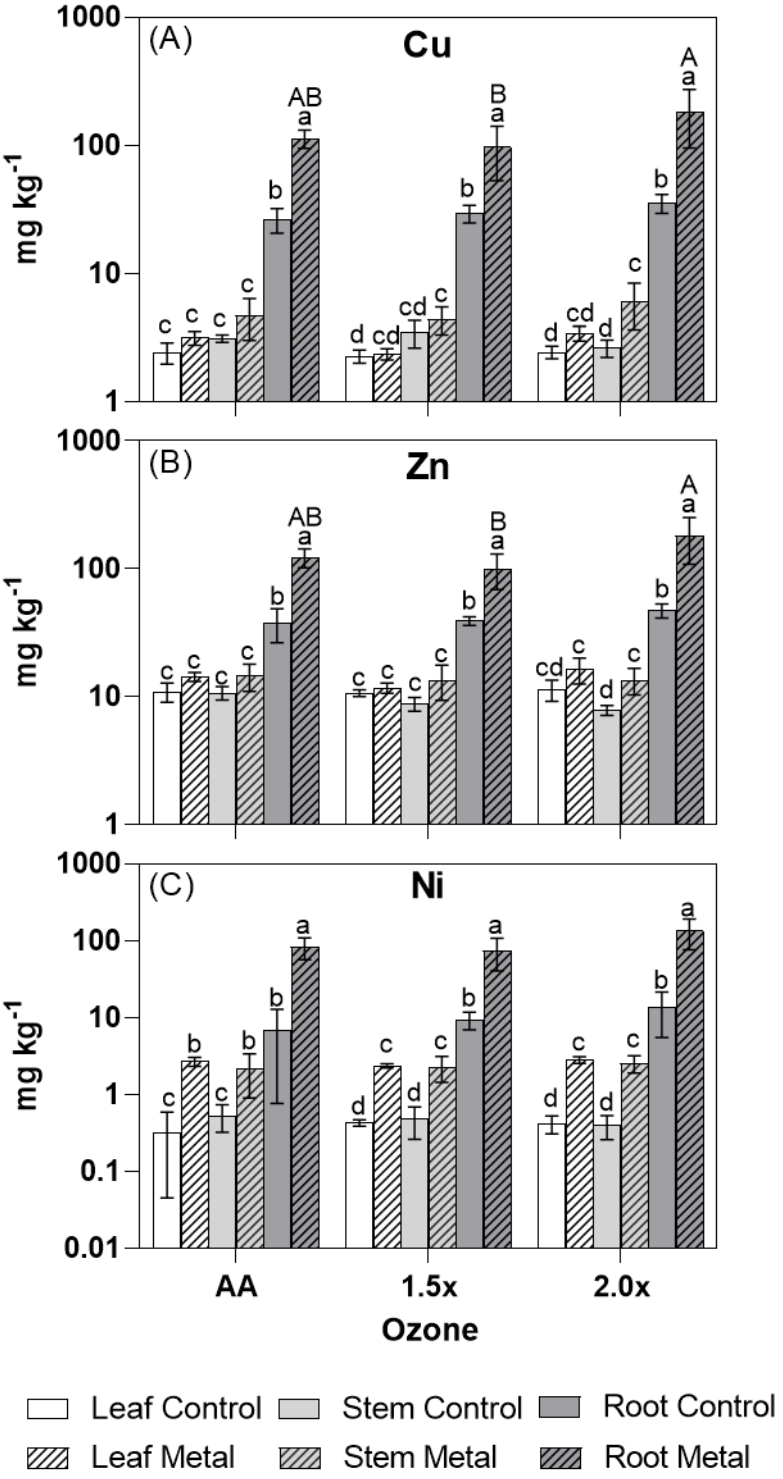

Fig. IV 7. Mean concentrations of copper (Cu - A), zinc (Zn - B) and nickel (Ni - C) (mg kg^{-1} dry mass), in leaves, stem and roots of *S. terebinthifolia* cultivated under Control or with excess of Cu, Zn and Ni (Metal). Distinct lowercase letters indicate significant differences between organs in the same ozone treatment, while uppercase letters indicate differences between ozone treatment in the same organ and metal treatment, according to two-way ANOVA followed by post-hoc Šídák's test ($p \leq 0.05$).

Gas exchange

When measured in the same leaves throughout the experiment, net carbon assimilation progressively decreased over the 90 days period of experiment, with no difference between O_3

or HM treatments (Fig IV8).

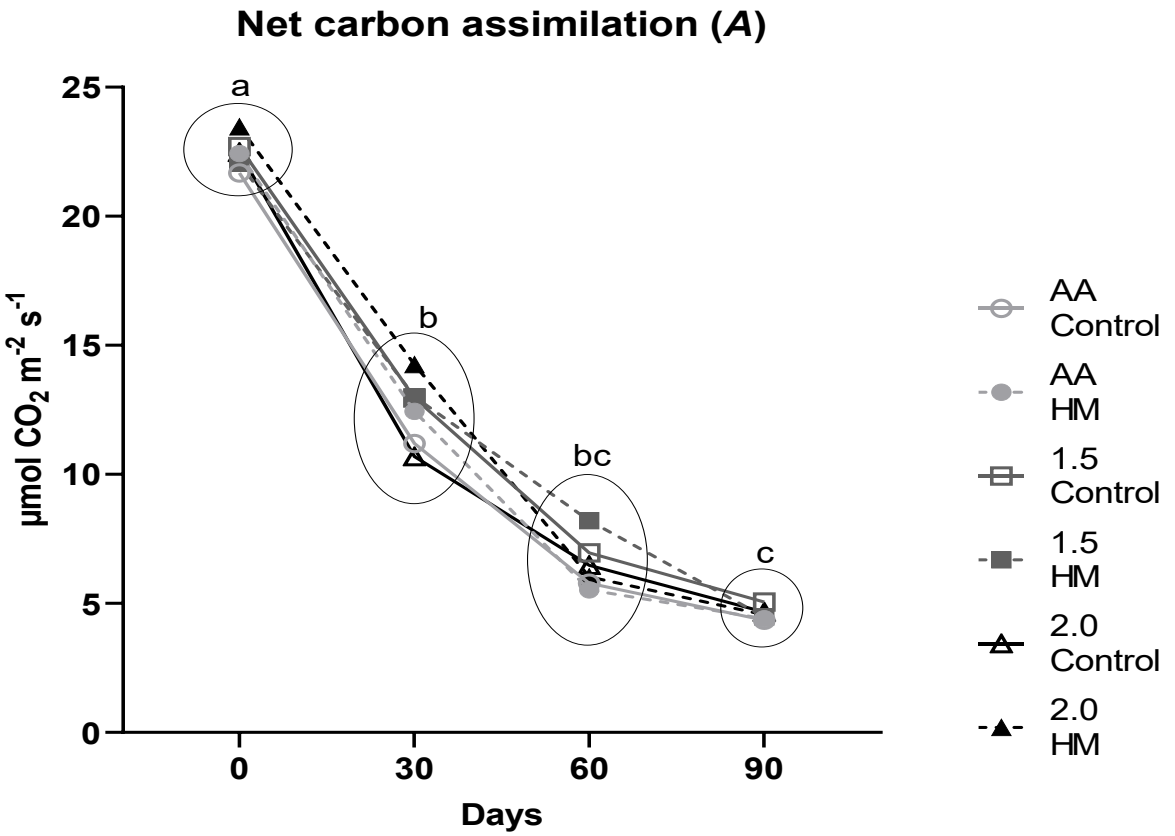

Fig. IV 8. Net carbon assimilation (*A*) of *S. terebinthifolia* leaves analyzed over 90 days under different ozone levels (AA, 1.5×, 2.0×) and nutrient solutions (Control and HM). Lowercase letters compare between times within the same treatment (The circle around the data represents the combination of the statistical result).

When measured at the end of experiment (90 days), there was a difference in net carbon assimilation (*A*) and stomatal conductance (*gsw*) for plants exposed to distinct O_3 concentrations under the same HM conditions, depending on the leaf age/position (top - young, middle - mature or bottom - old). There was a reduction in *A* in leaves from the central region of the stem (mature leaves - Middle), in plants under 2.0× O_3 treatment compared to 1.5× or AA treatments (Fig. IV9). There were no differences in *A* between the Control and HM treatments, for all O_3 treatments. There was an increase in *gsw* in leaves from the lower region of the stem (old leaves - Bottom) under 2.0× O_3 treatment compared to AA treatment. However, this difference was found only in seedlings under Control fertilization.

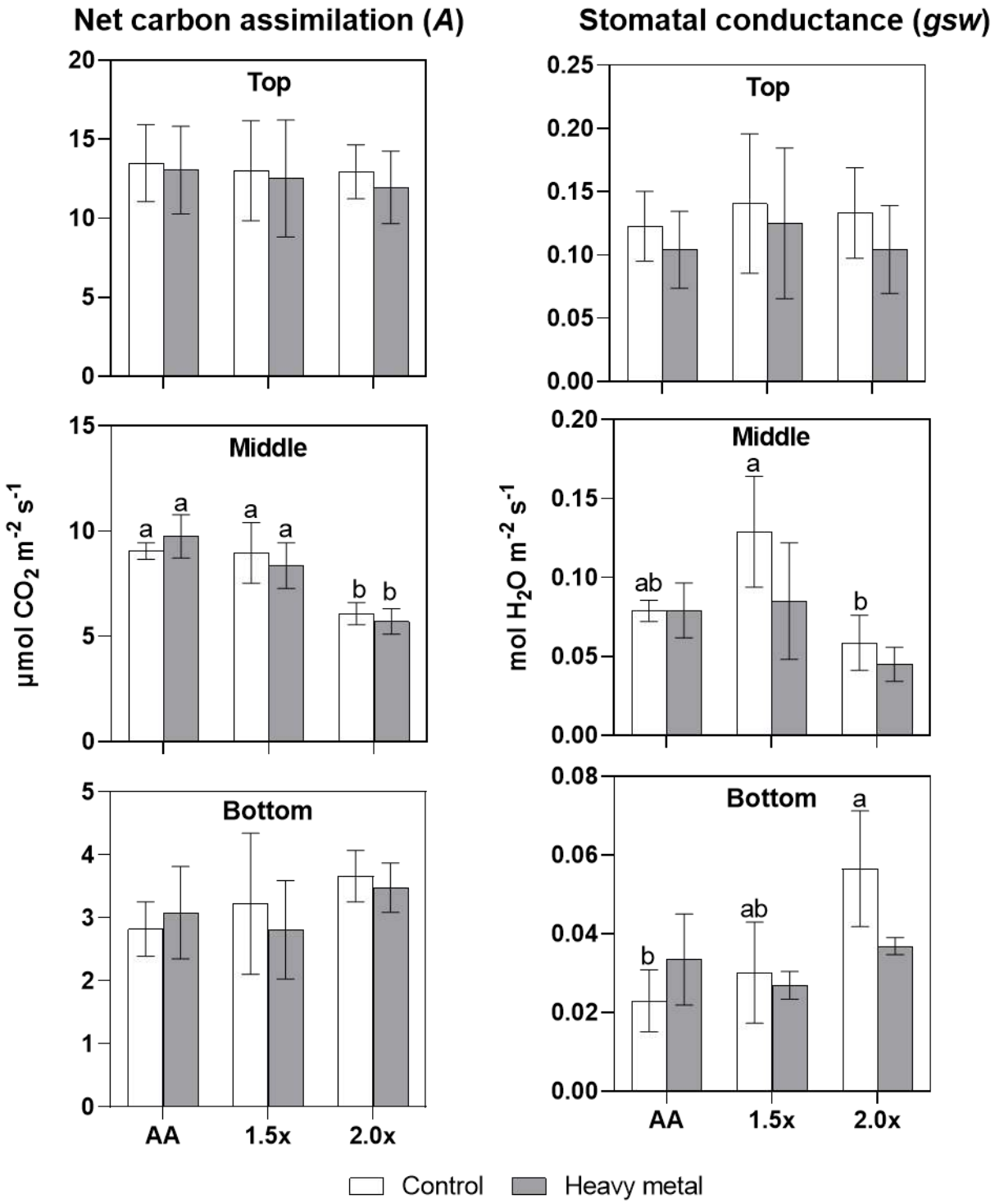

Fig. IV 9. Net carbon assimilation (*A*) and stomatal conductance (*gsw*) in leaves from the top, middle and bottom regions of *S. terebinthifolia* main stem, different ozone levels (AA, 1.5×, 2.0×) and nutrient solutions (Control and HM). Lowercase letters indicate significant differences among ozone treatments within the same HM treatment. Different letters mean significant differences according to two-way ANOVA followed by post-hoc Šídák's test ($p \leq 0.05$).

Antioxidants

No significant change was observed in the concentrations of ascorbic acid and glutathione in *S. terebinthifolia* leaves under excess metals or tropospheric O_3 (Fig. IV10).

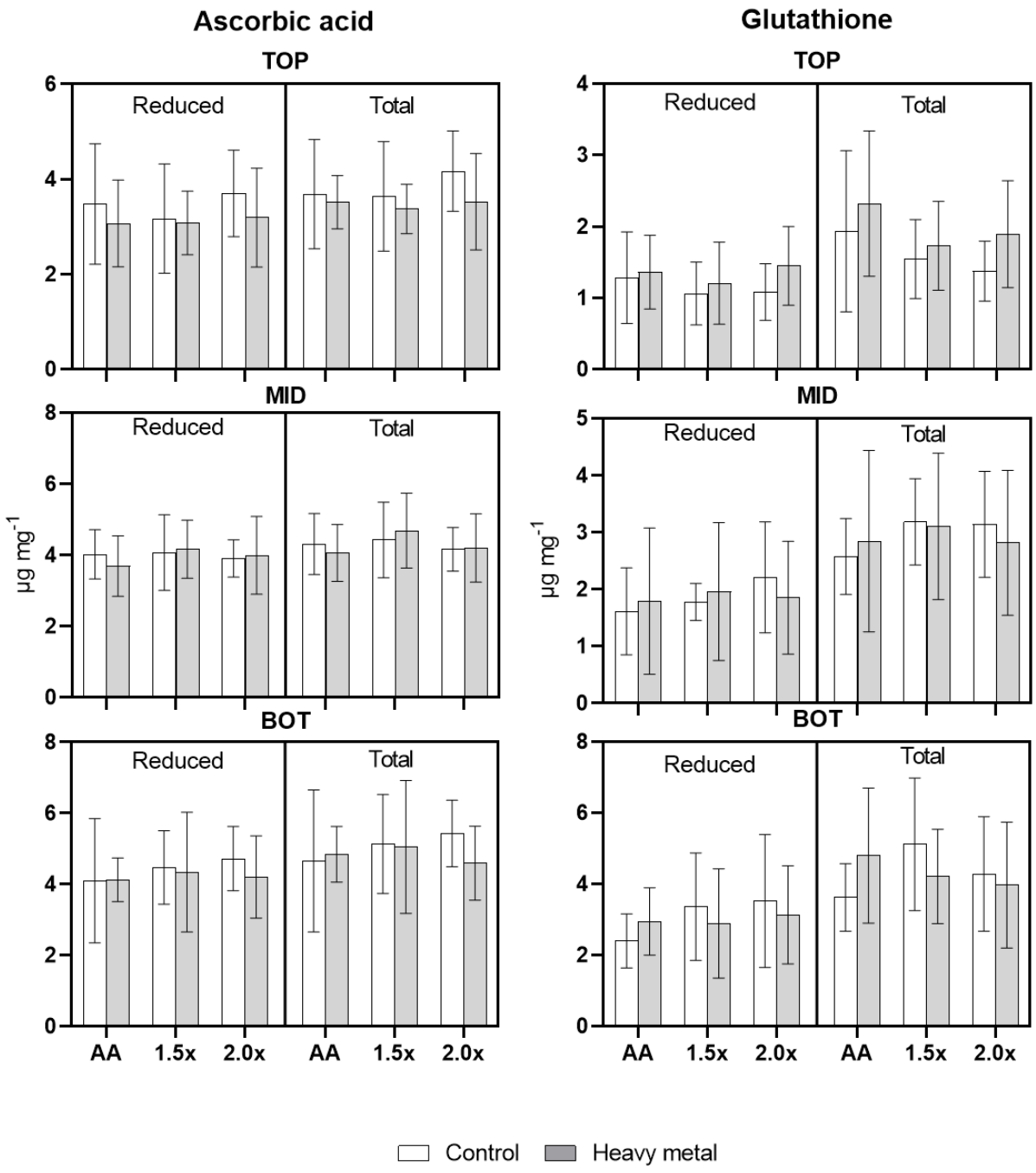

Fig. IV 10. Ascorbic acid and Glutathione in reduced or total forms, in leaves from the top, middle and bottom regions of *S. terebinthifolia* main stem, submitted to different ozone levels (AA, 1.5×, 2.0×) and nutrient solutions (Control and HM).

Photosynthetic pigments

The concentration of total chlorophylls and carotenoids decreased in the top leaves of *S. terebinthifolia* under HM exposed to 1.5× O_3 compared to AA (Fig. IV11). The effect of ozone on pigments became detectable only in plants exposed to HM, although the HM factor alone did not produce statistical differences. No differences were observed between the control and heavy metal treatments at any O_3 level. Pigment concentrations in mid-region leaves remained

unchanged. In bottom leaves, chlorophylls decreased under 1.5× O_3 compared to AA, in both the control and heavy metal conditions. For carotenoids, a reduction occurred at 1.5× O_3 only under HM. Carotenoid concentrations decreased under 1.5× compared to AA in HM exposure. Under 2.0× O_3, the carotenoid concentration of HM exposure plants was higher compared to control fertilization.

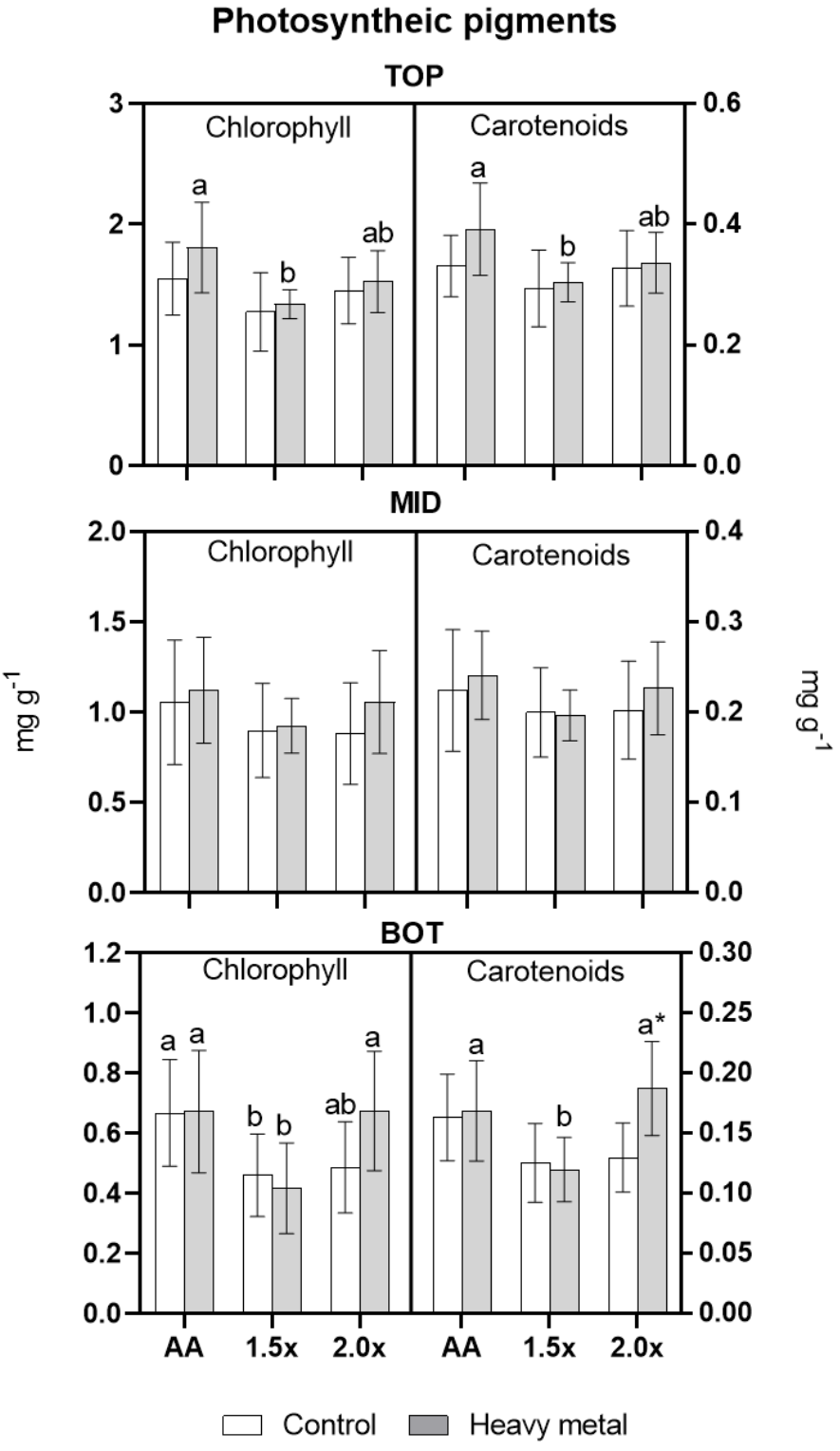

Fig. IV 11. Total chlorophyll and carotenoid content in leaves from the top, middle and bottom regions

of *S. terebinthifolia* main stem, submitted to different ozone levels (AA, 1.5×, 2.0×) and nutrient solutions (Control and HM). Lowercase letters compare ozone treatments, while * indicates significant difference between nutrient solution treatments in the same ozone level, according to two-way ANOVA followed by post-hoc Šídák's test ($p \leq 0.05$). left y-axis: chlorophyll, right y-axis: carotenoids.

Phytochelatins

The concentration of phytochelatins (PC2–PC6) did not change in the top and middle leaves of *S. terebinthifolia* under excess heavy metals or tropospheric O_3 (Fig IV12). In roots, PC6 increased in seedlings with control fertilization at 1.5× O_3 compared to 2.0× O_3, but PC6 concentration decreased in roots of plants under HM compared to control under 1.5× O_3.

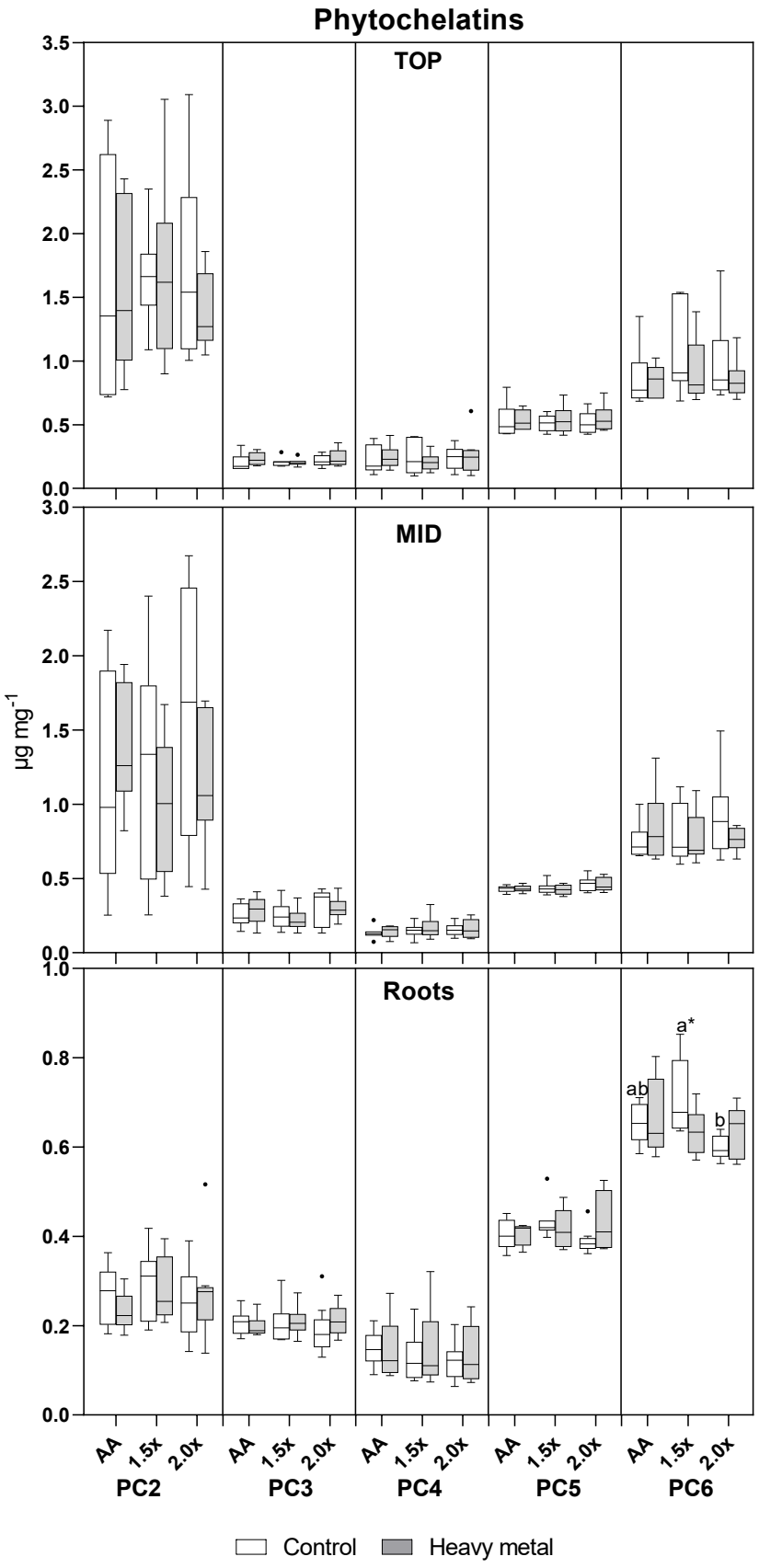

Fig. IV 12. Phytochelatins (PC2 – PC6) concentration (µg mg^{-1}) in the leaves of the upper and middle regions, and in the roots of *S. terebinthifolia* submitted to different ozone levels (AA, 1.5×, 2.0×) and nutrient solutions (Control and HM). Lowercase letters compare ozone treatments, while * indicates significant difference between nutrient solution treatments in the same ozone level, according to Scheirer-Ray-Hare followed by post-hoc Dunn's test ($p \leq 0.05$).

Root organic acids

The root exudates of *S. terebinthifolia* contained oxalic and maleic acids, which were detected under all metal and O_3 treatments (Fig. IV13). Maleic acid increased in seedlings exposed to metals under 2.0× O_3 compared to the 1.5× O_3 treatment. Oxalic acid levels remained unchanged under all treatments.

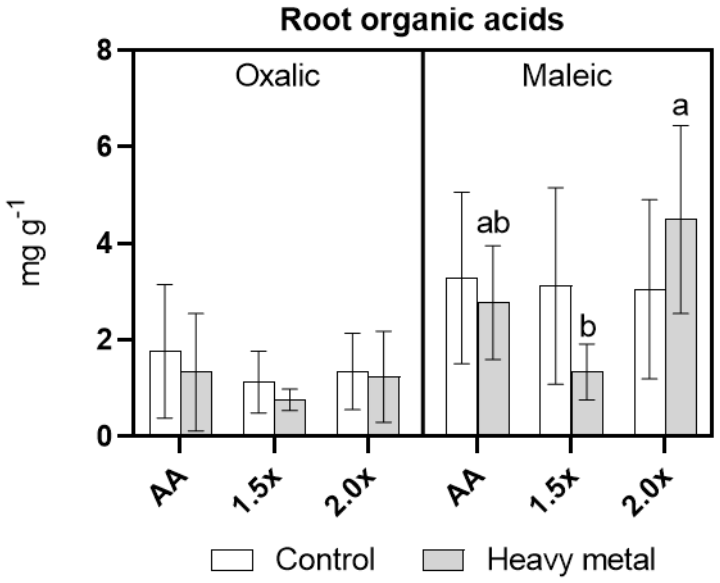

Fig. IV 13. Root organic acids (ROA – mg g^{-1} root dry weight) of *S. terebinthifolia*, submitted to different ozone levels (AA, 1.5×, 2.0×) and nutrient solutions (Control and HM). Lowercase letters indicate significant difference between ozone treatments, according to two-way ANOVA followed by post-hoc Šídák's test ($p \leq 0.05$).

Amino acids

All 17 evaluated amino acids were detected in the leaves (all positions) and roots of *S. terebinthifolia* (Fig. IV14). The amino acid profile revealed isoleucine (ILE) as the most abundant and histidine (HIS) as the least abundant in all plant tissues. While the distribution patterns among leaves from different positions (Top, Mid, Bot) were relatively similar, the amino acid profile in root differed from leaves, showing a greater predominance of arginine (ARG) and asparagine (ASP).

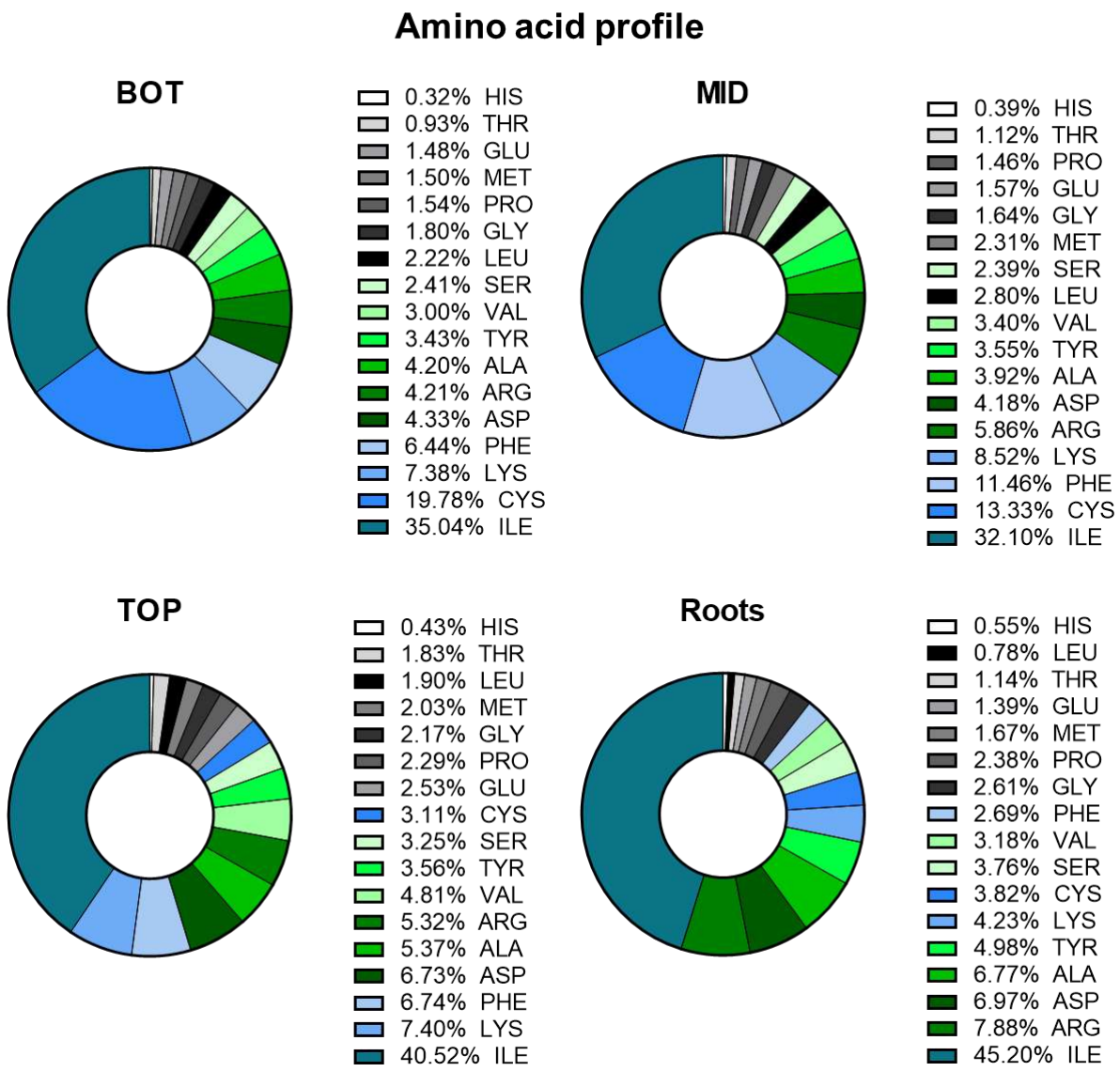

Fig. IV 14. Amino acids profile in leaves from upper (top), middle (mid) and lower (bot) regions of the stem, and roots of *S. terebinthifolia* cultivated under ambient air (AA) and Control nutrient solutions.

Principal Component Analysis (PCA) with correlation matrix explained 42.96% (leaf bot), 47.73% (leaf mid), 51.46% (leaf top) and 67.06% (roots) of the total variability in *S. terebinthifolia* amino acids content in tissues (FigIV15). PCA did not reveal clear separation of groups according to O_3 or heavy metal treatments, suggesting the treatments did not affect the overall amino acid profile of *S. terebinthifolia*, but the amino acids may vary independently. Therefore, two-way ANOVA was performed individually for each amino acid to assess treatment effects.

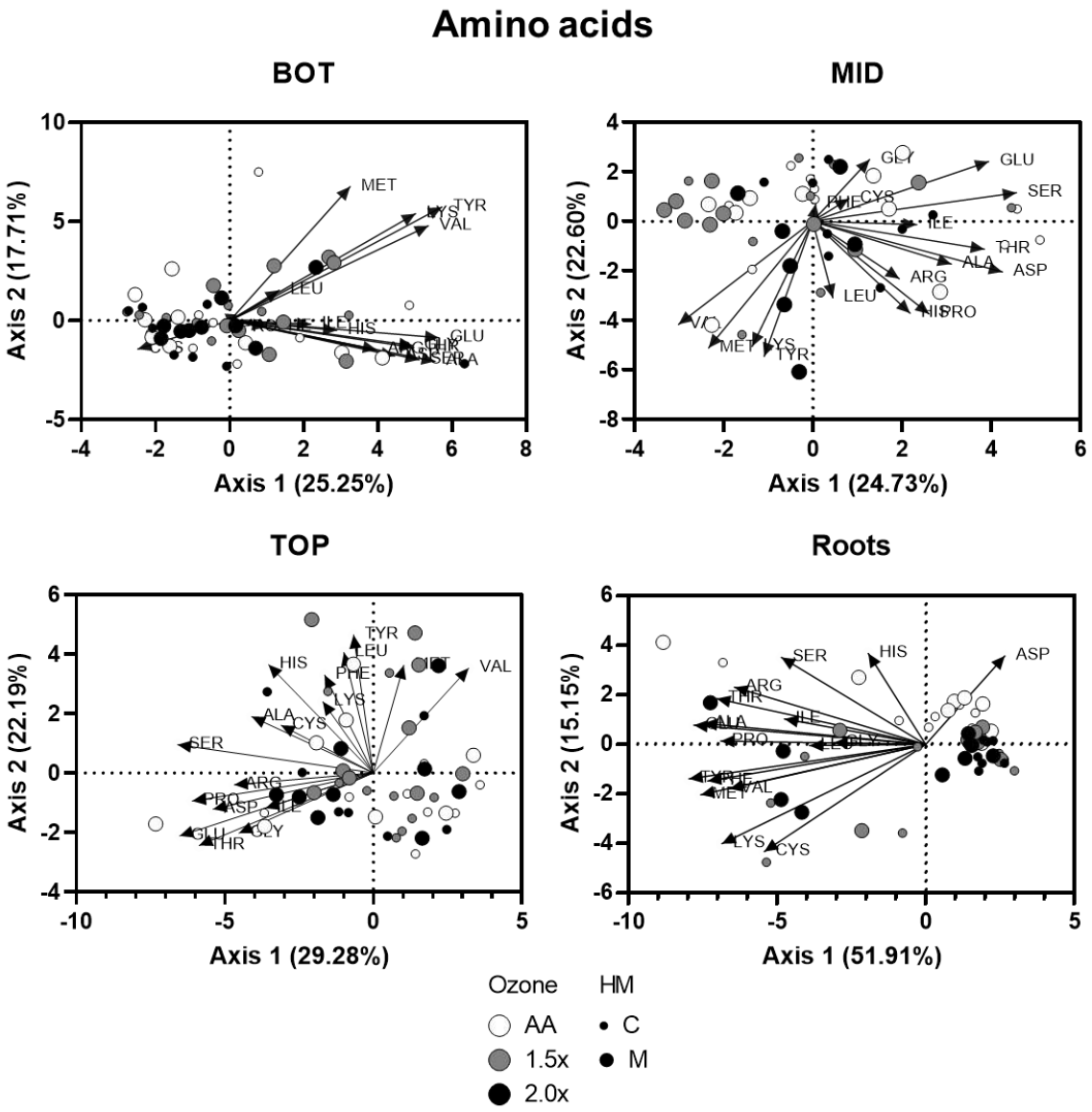

Fig. IV 15. Principal Component Analysis with correlation matrix in the leaves of the upper (top) and middle (mid) and lower (bot) regions of main stem, and in the roots of *S. terebinthifolia* submitted to different ozone levels (AA, 1.5×, 2.0×) and nutrient solutions (C and M).

The two-way ANOVA revealed differences between treatments for 5 individual amino acids (HIS, LYS, THR, GLU and PHE) in leaves (Fig. IV16). In the upper (top) leaves, HIS and LYS increased in plants grown under HM and 1.5× O_3 compared to the control fertilization in the same O_3 treatment. LYS also increased in treatment 1.5× O_3 compared to AA O_3 under HM treatment. In the middle (mid) leaves, THR decreased under 1.5× in both HM and Control fertilization, compared to AA O_3, while PHE in plants under HM increased at 1.5× O_3 to 2.0×. In bottom (bot) leaves, only GLU was affected by the treatments, increasing at 1.5× compared to AA under HM fertilization.

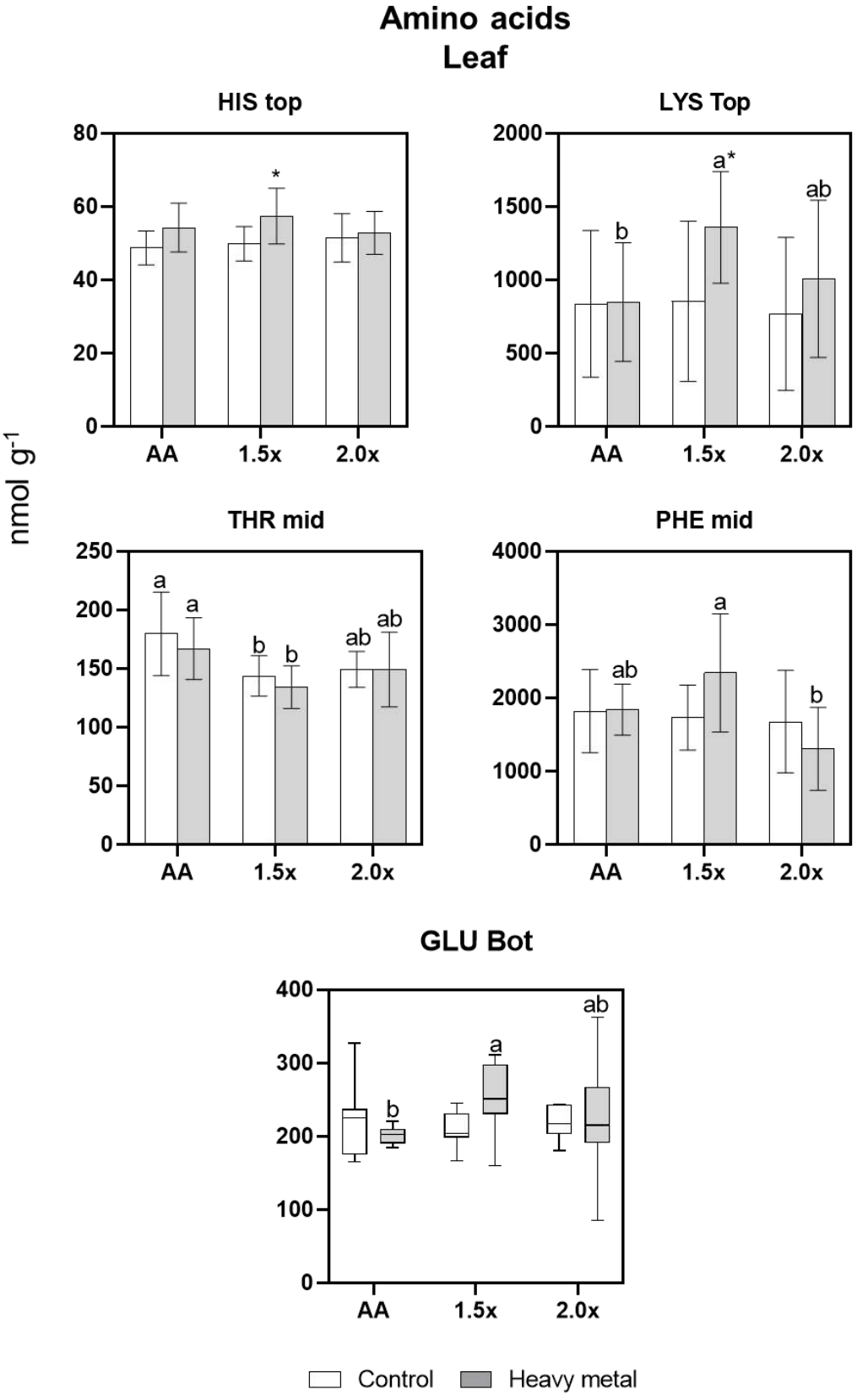

Fig. IV 16. Amino acids in the leaves of the upper (top) and middle (mid) and lower (bot) regions of main stem of *S. terebinthifolia* submitted to different ozone levels (AA, 1.5×, 2.0×) and nutrient solutions (Control and HM). Lowercase letters compare ozone treatments, while * indicates significant difference between nutrient solution treatments in the same ozone level, according to two-way ANOVA followed by post-hoc Šídák's test (bar graphs) or Scheirer-Ray-Hare followed by post-hoc Dunn's test (box-plot graphs) ($p \leq 0.05$).

In roots, 6 individual amino acids (ASP, THR, ALA, TYY, VAL and PHE) were affected by O_3 or HM treatments (Fig. IV17). THR, ALA, TYY, VAL and PHE increased in plants grown under HM compared to control fertilization at 2.0× O_3, while ASP increased under HM compared to control fertilization at 1.5× O_3. THR and VAL increased at 2.0× O_3 under HM, while ASP decreased. Also, ASP decreased at 1.5× O_3 under control, compared to AA and 2.0×.

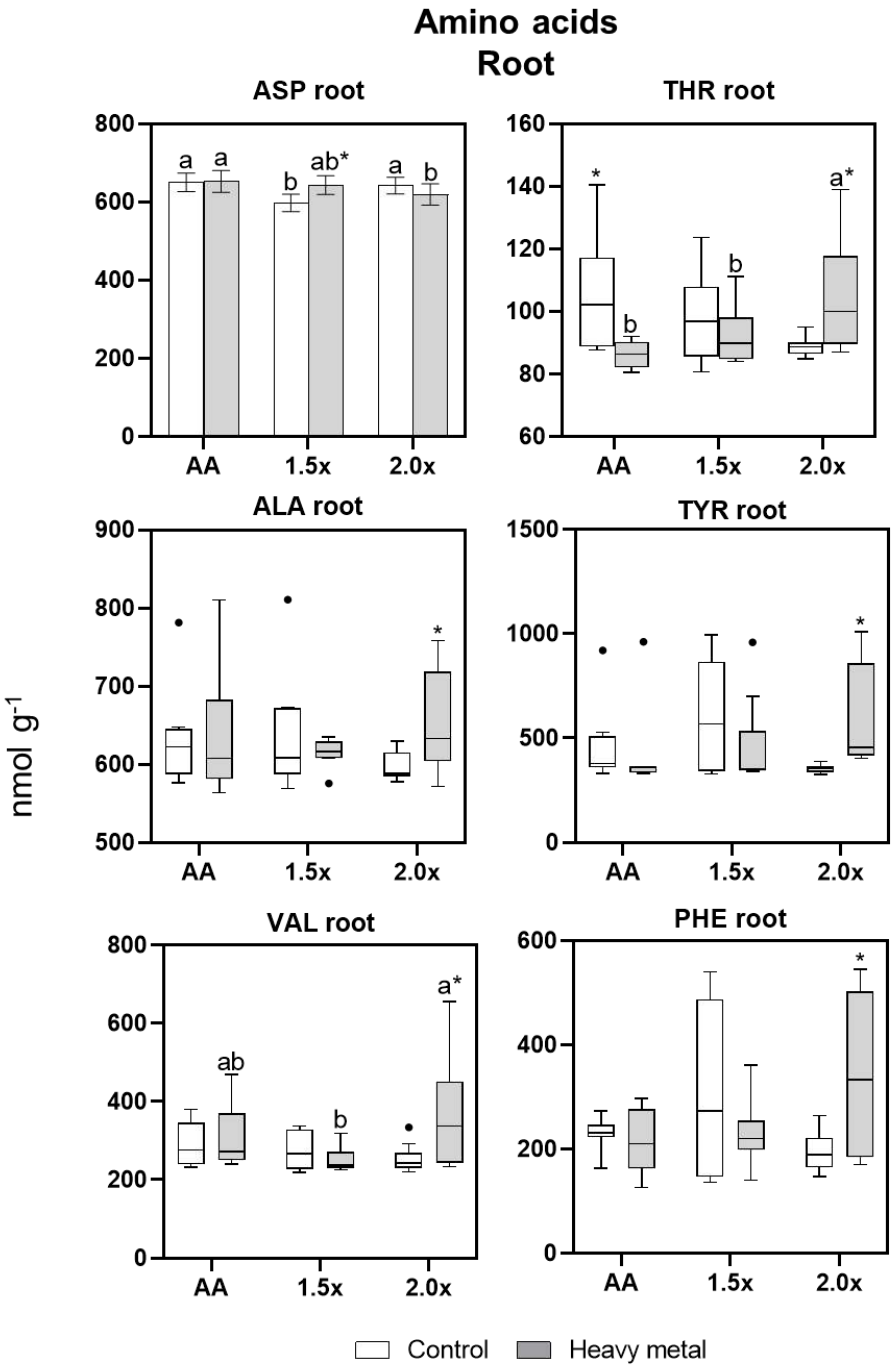

Fig. IV 17. Amino acids in roots of *S. terebinthifolia* submitted to different ozone levels (AA, 1.5×, 2.0×) and nutrient solutions (Control and HM). Lowercase letters compare ozone treatments, while * indicates significant difference between nutrient solution treatments in the same ozone level, according to two-way ANOVA followed by post-hoc Šídák's test (bar graphs) or Scheirer-Ray-Hare followed by post-hoc Dunn's test (box-plot graphs) ($p \leq 0.05$).

DISCUSSION

The addition of heavy metals to the substrate was effective, as evidenced by the increased tissue concentrations of these elements. In general, the elements were preferentially accumulated in the roots, a pattern consistent with previous studies on *S. terebinthifolia* under metal excess, such as iron (Dobbss et al., 2018), copper (Zabotto et al., 2020; Siqueira et al., 2021), Zn and Ni (Siqueira et al., 2026a). Nickel (Ni) was the only element whose leaf concentration increased after heavy metal application. Among the 3 elements added, Ni is required in the lowest concentration and, in general, plants show only trace concentrations under normal nutrient conditions (Barker and Pilbeam, 2015), and this pattern is confirmed in *S. terebinthifolia*. Therefore, *S. terebinthifolia* may have more specific retention mechanisms for abundant elements like Cu and Zn, while lacking equally efficient mechanisms to restrict Ni translocation.

Our results confirm the high capacity of *S. terebinthifolia* to accumulate and retain heavy metals preferentially in its root system. Furthermore, our results provide evidence that O_3 stress does not affect this allocation pattern, since HMs were mainly restricted in roots even with increasing atmospheric O_3 concentrations. The reduction in Cu and Zn levels in plants subjected to 1.5× O_3 compared to 2.0× O_3 occurred in conjunction with biomass increase in the 1.5× treatment. This result is most plausibly explained by the well-known dilution effect (Jarrell and Beverly, 1981), whereby a given amount of absorbed metal is diluted within a larger biomass; conversely, in the 2.0× treatment, lower biomass resulted in higher metal concentrations. Future studies could confirm whether the observed patterns are solely an indirect consequence of biomass alterations, or if there is a direct interference of O_3 stress in the absorption capacity of metals by plants (e.g. reduction in metal receptors in roots).

The maintenance of non-enzymatic antioxidants levels in leaves under HM may also result from the high capacity of *S. terebinthifolia* to retain metals in the roots, protecting the leaves from possible oxidative damage, thereby reducing the need to invest in antioxidant synthesis. (Bhaduri and Fulekar, 2012). We initially hypothesized that the additional O_3 stress might interfere with the protective mechanisms of *S. terebinthifolia* against HMs, by disrupting tolerance mechanisms through synergistic stress effects (Dietz, 2021). However, *S. terebinthifolia* maintained its non-enzymatic antioxidant synthesis capabilities under all O_3 levels, demonstrating that O_3 stress does not affect the natural tolerance capacity of *S. terebinthifolia* to HM stress. This is highly relevant when advocating for the use of *S. terebinthifolia* in urban afforestation and ecological restoration, where these two groups of stressors are often associated (Račić et al., 2025). Our finding of a species capable of tolerating combined heavy metal stress even under elevated O_3 levels represents a significant contribution

for urban greening species planning. Although *S. terebinthifolia* seedlings showed visible damage after O_3 treatment, they did not exhibit any alteration in their non-enzymatic antioxidant compounds. This suggests that the existing concentrations were likely already sufficient to combat the oxidative stress caused by O_3, evidenced by the maintenance of the photosynthetic capacity of the young leaves, showing that *S. terebinthifolia* exhibits tolerance and the ability to maintain growth under both HM and O_3 stress. However, our study was limited to the non-enzymatic antioxidant's ascorbic acid and glutathione, while other non-enzymatic antioxidants such as phenolic compounds, alkaloids, and terpenes, and enzymatic antioxidants such as catalase and superoxide dismutase, may also play a role in combating abiotic stress (Irato and Santovito, 2021). Future studies investigating other antioxidant and metabolic compounds may provide broader insights.

In general, *S. terebinthifolia* grown under 1.5× O_3 showed a reduction in chlorophyll and carotenoid content and in maleic acid exudation compared to other O_3 treatments. Contrary to a linear dose-response, a biphasic or "V"-shaped pattern was observed, where levels decreased at moderate O_3 but recovered at the 2.0× concentration. Conversely, an inverted pattern was noted for root PC6 and certain leaf amino acids, which increased at 1.5× O_3 and subsequently decreased at 2.0×. These non-linear, biphasic responses suggest the occurrence of hormetic effects, previously evidenced in plants under increasing O_3 concentrations (Agathokleous et. al., 2019). In fact, a recent study demonstrated that *S. terebinthifolia* exhibits a hormetic response when exposed to increasing concentrations of ozone (Siqueira et al., 2026b). This type of response may indicate 1) activation of preparatory compensatory mechanisms, where moderate levels of stress (in our case, 1.5× O_3) prepare the plant's defense system and metabolism against a possible subsequent more severe stress (Siemieniuk et al., 2025), or 2) emphasize the hormetic plasticity of *S. terebinthifolia* in physiological regulation, being able to redirect the energy from the synthesis of compounds to maintain growth (Erofeeva, 2024). Even when exhibiting visible leaf damage when subjected to increasing O_3 concentrations, *S. terebinthifolia* seedlings maintained their antioxidant system, oxalic acid exudation, and increased stomatal opening (*gsw*), confirming the evidence that *S. terebinthifolia* is a HM and O_3 tolerant species with considerable adaptive mechanisms.

Although few differences for phytochelatin concentrations between treatments were found, a distinct pattern was observed in the priority of synthesis of each phytochelatin, according to the organ analyzed (leaves or roots). The synthesis of phytochelatins in *S. terebinthifolia* exhibited tissue-specific prioritization: PC2 were prominent in leaves, while PC6 was prioritized in roots. This pattern aligns with the distinct functional demands of each organ. In leaves, the preference for the shorter-chain, more chemically stable PC2 may facilitate faster

translocation and ensure more durable responses due to lower degradation rates (Checkmeneva et al., 2011). Conversely, in roots, the prioritization of PC6 (phytochelatin with the greatest chelation capacity) may be related to the fact that roots are the primary site of heavy metal entry and thus metal immobilization are more required, instead of PCs mobility (Checkmeneva et al., 2011). A previous study with *S. terebinthifolia* had already provided evidence that this species prioritizes short-chain PCs in the leaves, while the roots accumulate more long-chain PCs (Siqueira et al., 2026a). The prioritization of longer PCs in root likely contributes to the evident root metal accumulation observed in *S. terebinthifolia*. Interestingly, the ozone treatment caused an increase in PC6 phytochelatins in roots under 1.5× O_3 and control, but not in plants exposed to metals. This may have occurred due to the hormetic effect provided by O_3, which stimulated the growth and overall metabolism of the plant in the absence of combined heavy metal stress (Erofeeva, 2024). These results highlight the complex interactive dynamics of stressors in plant biochemical responses.

The amino acid profile revealed that HIS is synthesized in lower concentrations, while LEU is prioritized. Leucine is an amino acid involved in stress responses, synthesis of volatile compounds and biochemical defenses, and especially involved in tolerance to heavy metals such as Cu (Sun et al., 2022). Therefore, the high levels of LEU in leaves and roots of *S. terebinthifolia* may contribute to the species' high tolerance capacity. HIS, which was found in low free concentrations, is an amino acid also related to tolerance to heavy metals, especially Ni, and often found in high concentrations in Ni hyperaccumulators (Krämer et al., 1996). *S. terebinthifolia* showed lower absorption and retention of Ni in the roots, compared to Cu and Zn, possibly due to the low synthesis of HIS. In the roots, in addition to the predominance of LEU, there was significant synthesis of ASP (Zn) and ARG. ASP is an amino acid that can act as a ligand for Cd, Pb, and Zn (Sharma and Dietz, 2006), while ARG is more related to general metabolic responses, such as the mobilization of nitrogen reserves, but also acts in adjusting developmental and defense mechanisms against stress (Winter et al., 2015). This demonstrates that although *S. terebinthifolia* is tolerant to heavy metals as a whole, the amino acid profile of this species confers greater tolerance and specific accumulation of Cu and Zn with rapid metabolic responses, but less tolerance and specific restriction to Ni.

Ozone and heavy metal treatments influenced amino acid concentration of *S. terebinthifolia*, but this alteration occurred in specific amino acids, without affecting the overall profile. The roots showed greater variation in amino acid concentration (6) in response to the treatments, compared to the leaves (5). This may be related to the fact that the roots accumulated more HM, and therefore, metabolic adjustments were required in this organ. In fact, changes in amino acid levels may indicate adaptive responses to stress, conferring greater capacity and

binding to metals (Kocaman 2023) and metabolic regulation for activation of enzymatic antioxidant defenses and increased expression of genes encoding defense molecules induced by tropospheric O_3 (Fu et al., 2025). Furthermore, it was verified that the alteration occurs in different amino acids in leaves from different positions, indicating that the metabolic adjustments seem to be related to leaf age, which may be caused by the leaf maturation/senescence process (Kanojia et al., 2021). Similar to the other compounds analyzed (pigments, organic acids, and phytochelatins), the amino acids showed hormetic responses to O_3, signaling adaptation followed by optimization. In response to heavy metals, the trend was an increase in the concentration of specific amino acids (especially at 2.0×), indicating that *S. terebinthifolia* exhibits an adaptive response, synthesizing amino acids that may aid in defense responses through direct binding with metals (Kocaman 2023), or through optimization of metabolic regulation to combat heavy metal stress (Ghori et al., 2019).

Overall, *S. terebinthifolia* exhibits desirable traits for restoration of areas impacted by both heavy metals and ozone pollution. However, caution is warranted in its recommendation, as certain species are known to emit high concentrations and a wide diversity of volatile organic compounds (VOCs), which can act as precursors to tropospheric ozone formation (Lerdau et al., 1997). Moreover, elevated atmospheric O3 concentrations have been shown to stimulate VOC synthesis and emission (Yang et al., 2025). A limitation our present study is that possible VOCs emitted by *S. terebinthifolia* were not measured. Consequently, despite its tolerance to O_3, the species may potentially exacerbate ozone pollution if it proves to be a high emitter of VOCs. Future investigations should focus on characterizing the quantity/composition of VOCs released by *S. terebinthifolia* and elucidating the interactions between VOC emissions and atmospheric ozone dynamics. Such data would support a more robust assessment of the species' suitability for restoration programs in areas with elevated tropospheric O_3 concentrations. Future species selection frameworks would benefit from integrating plant physiological tolerance with assessments of VOC emissions and their net effects on urban air quality.

CONCLUSIONS

Schinus terebinthifolia exhibits visible leaf damage when exposed to high ozone concentrations; however, it maintains photosynthetic rate and active antioxidant defenses. The species showed a hormetic effect of ozone on biomass, with a 1.5× stimulus followed by a 2.0× reduction. The hormetic response was conferred through metabolic adjustments evidenced by root organic acids, photosynthetic pigments, phytochelatins, and free amino acids. The species exhibits accumulation and retention of heavy metals in the roots. The addition of ozone stress did not affect the tolerance capacity of *S. terebinthifolia* to heavy metals. *S. terebinthifolia*

exhibits high tolerance to excess of Cu, Zn and Ni and to elevated ozone concentration, both individually or in combination, demonstrating its potential for use in areas affected by soil metal contamination and atmospheric ozone pollution, although the dynamics of interaction between VOCs and O_3 should be further explored for better suitability recommendation of *S. terebinthifolia* in O_3 affected areas.

Acknowledgements

We thank Leonardo Lazzara, Jacopo Manzini, Andrea Viviano, Elena Marra and Cesare Garosi for field support, and National Research Council of Italy (CNR) - Institute of Research on Terrestrial Ecosystems (IRET) for infrastructure and ozone FACE facility. This work was financially supported by Fundação de Amparo à Pesquisa do Estado de São Paulo (FAPESP – Process 2021/09686-9; 2017/50341-0, 2023/16524-0 and 2025/15561-5). The research was also funded by EU - Next Generation EU Mission 4 “Education and Research” - Component 2: “From research to business” - Investment 3.1: “Fund for the realization of an integrated system of research and innovation infrastructures” - Project IR0000032 – ITINERIS - Italian Integrated Environmental Research Infrastructures System - CUP B53C22002150006.

Data statement

All generated data is included in the article (and its supplementary information files). No additional external datasets were used.

Conflict of Interest

The authors declare that they have no conflict of interest.

REFERENCES

Agathokleous, E., Araminiene, V., Belz, R. G., Calatayud, V., De Marco, A., Domingos, M., ... & Calabrese, E. J. (2019). A quantitative assessment of hormetic responses of plants to ozone. *Environmental Research*, *176*, 108527.

Anderson, M.E., 1985. Determination of glutathione and glutathione disulfide in biological samples. Method. Enzymol. 113, 548–554.

Antenozio, M. L., Caissutti, C., Caporusso, F. M., Marzi, D., & Brunetti, P. (2024). Urban air pollution and plant tolerance: Omics responses to ozone, nitrogen oxides, and particulate matter. *Plants*, *13*(15), 2027.

Barker, A. V., & Pilbeam, D. J. (Eds.). (2015). *Handbook of plant nutrition*. CRC press.

Bhaduri, A. M., & Fulekar, M. H. (2012). Antioxidant enzyme responses of plants to heavy metal stress. *Reviews in Environmental Science and Bio/Technology*, *11*(1), 55-69.

Calfapietra, C., Peñuelas, J., & Niinemets, Ü. (2015). Urban plant physiology: adaptation-mitigation strategies under permanent stress. *Trends in plant science*, *20*(2), 72-75.

Carvalho, M. G., Melo, A. G. N., Aragão, C. F. S., Raffin, F. N., & Moura, T. F. A. L. (2013). Schinus

terebinthifolius Raddi: chemical composition, biological properties and toxicity. *Revista Brasileira de Plantas Medicinais*, *15*, 158-169.

Cawthray, G.R., 2003. An improved reversed-phase liquid chromatographic method for the analysis of low-molecular mass organic acids in plant root exudates. J. Chromatogr. 1011(1-2), 233–240

Chekmeneva, E., Gusmão, R., Díaz-Cruz, J. M., Ariño, C., & Esteban, M. (2011). From cysteine to longer chain thiols: thermodynamic analysis of cadmium binding by phytochelatins and their fragments. *Metallomics*, *3*(8), 838-846.

Demidchik, V. (2015). Mechanisms of oxidative stress in plants: from classical chemistry to cell biology. *Environmental and experimental botany*, *109*, 212-228.

Dobbss, L. B., Dos Santos, T. C., Pittarello, M., de Souza, S. B., Ramos, A. C., & Busato, J. G. (2018). Alleviation of iron toxicity in Schinus terebinthifolius Raddi (Anacardiaceae) by humic substances. *Environmental Science and Pollution Research*, *25*(10), 9416-9425.

Donzelli, G., & Suarez-Varela, M. M. (2024). Tropospheric Ozone: A critical review of the literature on emissions, exposure, and health effects. *Atmosphere*, *15*(7), 779.

Erofeeva, E. A. (2024). Plant hormesis: the energy aspect of low and high-dose stresses. *Plant Stress*, *14*, 100628.

Fu, X., Li, C., Zhao, M., Xu, Y., Guo, L., Yan, Y., ... & Gu, X. (2025). Ozone stress alters amino acid and flavonoid metabolism of Ziziphi Spinosae Folium. *Journal of Hazardous Materials*, 138647.

Ghori, N. H., Ghori, T., Hayat, M. Q., Imadi, S. R., Gul, A., Altay, V., & Ozturk, M. (2019). Heavy metal stress and responses in plants. *International journal of environmental science and technology*, *16*(3), 1807-1828.

Hasanuzzaman, M., & Fujita, M. (2022). Plant oxidative stress: biology, physiology and mitigation. *Plants*, *11*(9), 1185.

Hunaiti, A.A., Abukhalaf, I.K., Silvestrov, N., Bayorh, M., 2003. Rapid HPLC procedure for the quantitation of phytochelatins in plant tissue extracts. J. Liq. Chromatogr. 26(20), 3463–3473.

Inouhe, M. (2005). Phytochelatins. *Brazilian Journal of plant physiology*, *17*, 65-78.

Jarrell, W. M., & Beverly, R. B. (1981). The dilution effect in plant nutrition studies. Advances in agronomy, 34, 197-224.

Kanojia, A., Shrestha, D. K., & Dijkwel, P. P. (2021). Primary metabolic processes as drivers of leaf ageing. *Cellular and Molecular Life Sciences*, *78*(19-20), 6351-6364.

Kawade, K., Tabeta, H., Ferjani, A., & Hirai, M. Y. (2023). The roles of functional amino acids in plant growth and development. *Plant and Cell Physiology*, *64*(12), 1482-1493.

Kisvarga, S., Horotán, K., Wani, M. A., & Orlóci, L. (2023). Plant responses to global climate change and urbanization: Implications for sustainable urban landscapes. *Horticulturae*, *9*(9), 1051.

Kocaman, A. (2023). Combined interactions of amino acids and organic acids in heavy metal binding in plants. *Plant signaling & behavior*, *18*(1), 2064072.

Kocaman, A. (2023). Combined interactions of amino acids and organic acids in heavy metal binding in plants. *Plant signaling & behavior*, *18*(1), 2064072.

Krämer, U., Cotter-Howells, J. D., Charnock, J. M., Baker, A. J., & Smith, J. A. C. (1996). Free histidine as a metal chelator in plants that accumulate nickel. *Nature*, *379*(6566), 635-638.

López, A., Montaño, A., Garcia, P., Garrido, A., 2005. Note: Quantification of ascorbic acid and dehydroascorbic acid in fresh olives and in commercial presentations of table olives. Food Sci. Techn. Intern. 11(3), 199–204.

Minocha, R., Martinez, G., Lyons, B., Long, S., 2009. Development of a standardized methodology for quantifying total chlorophyll and carotenoids from foliage of hardwood and conifer tree species. Can. J. For. Res. 39(4), 849–861.

Oliveira, M. C., Borges, L. D. M., Ogata, R. S., & Ribeiro, J. F. (2025). Schinus terebinthifolia Raddi (Anacardiaceae) as facilitator in ecological recomposition. *Ciência Florestal*, *35*, e84796.

Osmolovskaya, N., Dung, V. V., & Kuchaeva, L. (2018). The role of organic acids in heavy metal tolerance in plants. *Biological Communications*, *63*(1), 9-16.

Page, V., & Feller, U. (2015). Heavy metals in crop plants: transport and redistribution processes on the whole plant level. *Agronomy*, *5*(3), 447-463.

Pisuttu, C., Risoli, S., Cotrozzi, L., Nali, C., Pellegrini, E., Hoshika, Y., ... & Paoletti, E. (2024). Untangling the role of leaf age specific osmoprotectant and antioxidant responses of two poplar clones under increasing ozone concentrations. *Plant Physiology and Biochemistry*, *208*, 108450

Račić, N., Ružičić, S., Pehnec, G., Jakovljević, I., Sever Štrukil, Z., Rinkovec, J., ... & Lovrić, M. (2025). Linking Atmospheric and Soil Contamination: A Comparative Study of PAHs and Metals in PM10 and Surface Soil near Urban Monitoring Stations. *Toxics*, *13*(10), 866.

Sarma, R. K., Gowtham, I., Bharadwaj, R. K. B., Hema, J., & Sathishkumar, R. (2018). Recent advances in metal induced stress tolerance in plants: possibilities and challenges. In: Hasanuzzaman M., Nahar K., Fujita M. (eds). Plants Under Metal and Metalloid Stress. Springer, Singapore.

Sharma, S. S., & Dietz, K. J. (2006). The significance of amino acids and amino acid-derived molecules in plant responses and adaptation to heavy metal stress. *Journal of experimental botany*, *57*(4), 711-726.

Siemieniuk, A., Rudnicka, M., Jemioła, G., & Małkowski, E. (2025). Hormesis as a Particular Type of Plant Stress Response. *Plants*, *14*(24), 3815.

Silva, P. N., Reis, C. H. G., Duarte, V. P., Castro, E. M., Pádua, M. P., & Pereira, F. J. (2024). Toxicity of iron mining tailings and potential for revegetation using Schinus terebinthifolia Raddi based on the emergence, growth, and anatomy of the species. *Mining*, *4*(3), 719-732.

Siqueira, M. C., Casimiro, J. V., Nascimento, A., Rinaldi, M. C. S., Tavares, A. R. & Domingos, M. (2026a). Heavy metal tolerance in Atlantic Forest species: Antioxidants, phytochelatins, or root exudates?. *Science of the Total Environment, 1024,* 181368.

Siqueira, M. C., Kanashiro, S., Domingos, M., Rinaldi, M. C. S., & Tavares, A. R. (2021). Physiological and biochemical changes in tree seedlings growing in urban forest soil contaminated with copper in São Paulo, Brazil. *Plant and Soil*, *464*(1), 149-163.

Siqueira, M. C., Moura, B. B., Hoshika, Y., Paoletti, E., Tavares, A. R., Domingos, M. (2026b). Biomass response of *Schinus terebinthifolia* to elevated ozone: evidence for a dose-dependent hormetic effect. *Journal of Forestry Research.* [Accepted article, In Press].

Sun, M., Li, S., Gong, Q., Xiao, Y., & Peng, F. (2022). Leucine contributes to copper stress tolerance in peach (Prunus persica) seedlings by enhancing photosynthesis and the antioxidant defense system. *Antioxidants*, *11*(12), 2455.

Timothy, N. A., & Williams, E. T. (2019). Environmental pollution by heavy metal: an overview. *International Journal of Environmental Chemistry*, *3*(2), 72-82.

Waters. (2007). UPLC amino acid analysis solution: system guide.

Winter, G., Todd, C. D., Trovato, M., Forlani, G., & Funck, D. (2015). Physiological implications of arginine metabolism in plants. *Frontiers in plant science*, *6*, 534.

Zabotto, A. R., França, W. S., Domingos, M., Rinaldi, M. C. S., Kanashiro, S., Ferreira, M. L., & Tavares, A. R. (2020). Copper accumulation and distribution in two arboreal species of the atlantic forest. *Floresta e Ambiente*, *27*(1), e20190027.

Lerdau, M., Guenther, A., & Monson, R. (1997). Plant production and emission of volatile organic compounds. Bioscience, 47(6), 373-383.

Yang, Y., Sun, F., Hu, C., Gao, J., Wang, W., Chen, Q., & Ye, J. (2025). Emissions of biogenic volatile organic compounds from plants: impacts of air pollutants and environmental variables. Current Pollution Reports, 11(1), 10.

Irato, P., & Santovito, G. (2021). Enzymatic and non-enzymatic molecules with antioxidant function. Antioxidants, 10(4), 579.

.

Considerações finais

A partir dos experimentos do capítulo I, foi possível estabelecer um protocolo de cultivo em sistema hidropônico eficiente para cultivo de espécies arbóreas. O sistema hidropônico de circulação contínua, estilo “dutch bucket”, se mostrou eficaz para o cultivo da espécie arbórea da Mata Atlântica *S. terebinthifolia*, sendo a perlita o substrato ideal para estudos visando análises radiculares. A concentração de 50 μM da combinação de Cu, Zn e Ni foi estabelecida como limite para estudos do efeito de metais pesados, devido à ativação de respostas ao estresse, sem comprometer a taxa de sobrevivência. *S. terebinthifolia* se mostrou tolerante aos metais pesados adicionados e com atributos para ser utilizada como espécie modelo em estudos visando compreender respostas de plantas aos metais pesados.

Os experimentos do capítulo II revelaram que 5 espécies da Mata Atlântica de diferentes hábitos de vida apresentam estratégias distintas de tolerância à exposição aos metais pesados. A taxa de crescimento da planta (crescimento lento x crescimento rápido) não se mostrou um preditor eficiente para classificação de espécies tolerantes à metais pesados, enquanto o hábito de vida e a avaliação das estratégias bioquímicas de cada espécie foram eficientes na detecção de espécies tolerantes. As 5 espécies estudadas puderam ser classificadas de acordo com a sua tolerância aos metais pesados Cu, Zn e Ni: *Schinus terebinthifolia* e *Aechmea fasciata* são tolerantes, *Cariniana legalis* é moderadamente tolerante, enquanto *Seemannia sylvatica* e *Passiflora edulis* são sensíveis.

O experimento do capítulo III originou a parametrização estomática de *Schinus terebinthifolia* pela primeira vez, demonstrando sua alta abertura estomática. O estudo revelou que *S. terebinthifolia* é tolerante ao ozônio, e apresenta resposta hormética da biomassa, tendo seu crescimento estimulado em baixas-médias concentrações de ozônio troposférico, seguido de efeito negativo em concentrações altas. A descoberta da tolerância de *S. terebinthifolia* ao ozônio troposférico amplia sua recomendação de uso em ambientes afetados pela poluição atmosférica deste estressor abiótico.

O experimento do capítulo IV revelou que *S. terebinthifolia* é tolerante à combinação da exposição de metais pesados e ozônio troposférico. A espécie mantém a capacidade de restrição radicular dos metais pesados e manutenção dos níveis de antioxidantes, aliadas a adaptações fisiológicas e regulação de aminoácidos como estratégias para tolerar a combinação de estressores. A adição do estresse pelo ozônio troposférico não afeta as capacidades de tolerância de *S. terebinthifolia* aos metais pesados Cu, Zn e Ni. Isso evidencia que a espécie pode ser indicada na utilização em ambientes afetados pela presença de metais pesados no solo e concentrações elevadas de ozônio troposférico.

Em síntese, a tese estabelece protocolos otimizado para cultivo de espécies nativas em

hidroponia, e classifica *S. terebinthifolia* como uma espécie-modelo eficaz para estudos de estresse abiótico, evidenciando sua intrínseca tolerância aos metais pesados Cu, Zn e Ni. Adicionalmente, demonstra que a espécie possui resiliência ao ozônio troposférico, exibindo uma resposta hormética que potencializa seu crescimento sob concentrações moderadas. A espécie mantém capacidade de acumulação radicular de metais e seu aparato de defesa antioxidante mesmo sob a pressão combinada de metais pesados e ozônio troposférico. O combinado perfil fisiológico e bioquímico de *S. terebinthifolia* apresenta características desejáveis como uma candidata para a revegetação e restauração ecológica de áreas urbanas e degradadas que sofrem simultaneamente com a poluição do solo por metais pesados e a poluição atmosférica por ozônio. A investigação comparativa entre cinco espécies sob estresse por metais pesados revelou que a tolerância não é eficazamente predita pela taxa de crescimento, mas pelo hábito de vida e estratégias fisiológicas/bioquímicas específicas. Portanto, avaliação dos aspectos ecológicos, fisiológicos e bioquímicos se mostra uma ferramenta eficiente na busca por espécies tolerântes à estressores abióticos e auxilia na seleção de outras espécies com potencial de tolerância.

Referências gerais

Agathokleous, E., Feng, Z., Oksanen, E., Sicard, P., Wang, Q., Saitanis, C.J., Araminiene, V., Blande, J.D., Hayes, F., Calatayud, V., Domingos, M., Veresoglou, S.D., Peñuelas, J., Wardle, D.A., Marco, A., Li, Z., Harmens, H., Yuan, X., Vitalle, M. & Paoletti, E. 2020. Ozone affects plant, insect, and soil microbial communities: A threat to terrestrial ecosystems and biodiversity. *Science Advances* 6(33): eabc1176.

Ahmad, M.S.A. & Ashraf, M. 2012. Essential roles and hazardous effects of nickel in plants. *In*: Whitacre, D. (ed.). *Reviews of Environmental Contamination and Toxicology (Continuation of Residue Reviews)*, vol. 214. Springer, New York.

Amarante, C.V.T.D., Zanardi, O.Z., Miqueloto, A., Steffens, C.A., Erhart, J. & Almeida, J.A.D. 2009. Quantificação da área e do teor de clorofilas em folhas de plantas jovens de videira 'Cabernet Sauvignon' mediante métodos não destrutivos. *Revista Brasileira de Fruticultura* 31(3): 680-686.

Argyraki, A., Kelepertzis, E., Botsou, F., Paraskevopoulou, V., Katsikis, I. & Trigoni, M. 2018. Environmental availability of trace elements (Pb, Cd, Zn, Cu) in soil from urban, suburban, rural and mining areas of Attica, Hellas. *Journal of Geochemical Exploration* 187: 201-213.

Barker, A.V. & Pilbeam, D.J. 2015. *Handbook of plant nutrition*. 2 ed. CRC Press, Boca Raton.

Beladi, M., Kashani, A., Habibi, D., Paknejad, F. & Golshan, M. 2011. Uptake and effects of lead and copper on three plant species in contaminated soils: role of phytochelatin. *African Journal of Agricultural Research* 6(15): 3483-3492.

Benatti, M., Yookongkaew, N., Meetam, M., Guo, W.J., Punyasuk, N., AbuQamar, S. & Goldsbrough, P. 2014. Metallothionein deficiency impacts copper accumulation and redistribution in leaves and seeds of Arabidopsis. *New Phytologist* 202: 940–951.

Brandão, S.E. 2020. Tolerância de espécies arbóreas nativas de Mata Atlântica ao excesso de Ni e Zn no solo. Tese de Doutorado, Instituto de Botânica, São Paulo.

Campostrini, E. 2001. *Fluorescência da clorofila a: considerações teóricas e aplicações práticas*. UFNF, Rio de Janeiro.

Cao, Y.Y., Qi, C.D., Li, S., Wang, Z., Wang, X., Wang, J., Ren, S., Li, X., Zhang, N. & Guo, Y.D. 2019. Melatonin alleviates copper toxicity via improving copper sequestration and ROS scavenging in cucumber. *Plant and Cell Physiology* 60(3): 562-574.

Chaudhary, K., Agarwal, S. & Khan, S. 2018. Role of phytochelatins (PCs), metallothioneins (MTs), and heavy metal ATPase (HMA) genes in heavy metal tolerance. *In*: Prasad, R. (ed.). *Mycoremediation and Environmental Sustainability*. Springer, Verlag.

Chen, A., Komives, E.A. & Schroeder, J.I. 2006. An improved grafting technique for mature Arabidopsis plants demonstrates long-distance shoot-to-root transport of phytochelatins in Arabidopsis. *Plant Physiology* 141(1): 108-120.

Cobbett, C. & Goldsbrough, P. 2002. Phytochelatins and metallothioneins: roles in heavy metal detoxification and homeostasis. *Annual Review of Plant Biology* 53(1): 159-182.

Dai, L., Li, P., Shang, B., Liu, S., Yang, A., Wang, Y. & Feng, Z. 2017. Differential responses of peach (Prunus persica) seedlings to elevated ozone are related with leaf mass per area, antioxidant enzymes activity rather than stomatal conductance. *Environmental Pollution* 227: 380-388.

DalCorso, G., Fasani, E., Manara, A., Visioli, G. & Furini, A. 2019. Heavy metal pollutions: state of the art and innovation in phytoremediation. *International Journal of Molecular Sciences* 20(14): 3412.

Donzelli, G., & Suarez-Varela, M. M. 2024. Tropospheric Ozone: A critical review of the literature on emissions, exposure, and health effects. *Atmosphere*, 15(7): 779.

Dusenge, M.E., Duarte, A.G. & Way, D.A. 2019. Plant carbon metabolism and climate change: elevated CO2 and temperature impacts on photosynthesis, photorespiration and respiration. *New Phytologist* 221(1): 32-49.

Engela, M.R.G.S., Furlan, C.M., Esposito, M.P., Fernandes, F.F., Carrari, E., Domingos, M., Paoletti, E. & Hoshika, Y. 2021. Metabolic and physiological alterations indicate that the tropical broadleaf tree Eugenia uniflora L. is sensitive to ozone. *Science of the Total Environment* 769: 145080.

Erk, M., Ivanković, D., Raspor, B. & Pavičić, J. 2002. Evaluation of different purification procedures for the electrochemical quantification of mussel metallothioneins. *Talanta* 57(6): 1211-1218.

Esposito, M.P., Nakazato, R.K., Pedroso, A.N.V., Lima, M.E.L., Figueiredo, M.A., Diniz, A.P., Kozovits, A.R. & Domingos, M. 2018. Oxidant-antioxidant balance and tolerance against oxidative stress in pioneer and non-pioneer tree species from the remaining Atlantic Forest. *Science of the Total Environment* 625: 382-393.

Fernandes, F.F., Esposito, M.P., Engela, M.R.G.S., Cardoso-Gustavson, P., Furlan, C.M., Hoshika, Y., Carrari, E., Magni, G., Domingos, M. & Paoletti, E. 2019. The passion fruit liana (Passiflora edulis Sims, Passifloraceae) is tolerant to ozone. *Science of the Total Environment* 656: 1091-1101.

Girkin, N.T., Turner, B.L., Ostle, N. & Sjögersten, S. 2018. Composition and concentration of root exudate analogues regulate greenhouse gas fluxes from tropical peat. *Soil Biology and Biochemistry* 127: 280-285.

Hassinen, V.H., Tervahauta, A.I., Schat, H. & Kärenlampi, S.O. 2011. Plant metallothioneins–metal chelators with ROS scavenging activity? *Plant Biology* 13(2): 225-232.

Hatfield, J.L. & Prueger, J.H. 2015. Temperature extremes: Effect on plant growth and development. *Weather and Climate Extremes* 10: 4-10.
Hoagland, D.R. & Arnon, D.I. 1950. The water-culture method for growing plants without soil. *Circular*. California Agricultural Experiment Station, Berkeley.

IAG/USP. 2014. *Boletim Meteorológico do ano de 2013*. Estação Meteorológica do IAG/USP. Seção Técnica de Serviços Meteorológicos, São Paulo.

IPCC. 2014. *Climate Change 2014: Synthesis Report. Contribution of Working Groups I, II and III to the Fifth Assessment Report of the Intergovernmental Panel on Climate Change* [Core Writing Team, R.K. Pachauri and L.A. Meyer (eds.)]. IPCC, Geneva,

Switzerland.

Jia, Y., Tang, S., Wang, R., Ju, X., Ding, Y., Tu, S. & Smith, D.L. 2010. Effects of elevated CO2 on growth, photosynthesis, elemental composition, antioxidant level, and phytochelatin concentration in Lolium mutiforum and Lolium perenne under Cd stress. *Journal of Hazardous Materials* 180(1-3): 384-394.

Jones, D.L. 1998. Organic acids in the rhizosphere: a critical review. *Plant and Soil* 205: 25–44.

Joshi, R., Pareek, A. & Singla-Pareek, S.L. 2016. Plant metallothioneins: classification, distribution, function, and regulation. *In*: Ahmad, P. (ed.). *Plant Metal Interaction*. Elsevier, Amsterdan.

Ju, X.H., Tang, S., Jia, Y., Guo, J., Ding, Y., Song, Z. & Zhao, Y. 2011. Determination and characterization of cysteine, glutathione and phytochelatins (PC2–6) in Lolium perenne L. exposed to Cd stress under ambient and elevated carbon dioxide using HPLC with fluorescence detection. *Journal of Chromatography B* 879(20): 1717-1724.

Kabata-Pendias, A. 2011. *Trace elements in soils and plants*. 3 ed. CRC Press, Boca Raton.

Kobayashi, R., Kobayashi, N.I., Tanoi, K., Masumori, M. & Tange, T. 2019. Potassium supply reduces cesium uptake in Konara oak not by an alteration of uptake mechanism, but by the uptake competition between the ions. *Journal of Environmental Radioactivity* 208: 106032.

Krämer, U. 2010. Metal Hyperaccumulation in Plants. *Annual Review of Plant Biology* 61: 517–534.

Li, Q., Chen, H.H., Qi, Y.P., Ye, X., Yang, L.T., Huang, Z.R. & Chen, L.S. 2019. Excess copper effects on growth, uptake of water and nutrients, carbohydrates, and PSII photochemistry revealed by OJIP transients in Citrus seedlings. *Environmental Science and Pollution Research* 26(29): 30188-30205.

Mahmud, J., Bhuyan, M.B., Anee, T.I., Nahar, K., Fujita, M. & Hasanuzzaman, M. 2019. Reactive oxygen species metabolism and antioxidant defense in plants under metal/metalloid stress. *In*: Hasanuzzaman M., Hakeem K., Nahar K., Alharby H. (eds.). *Plant Abiotic Stress Tolerance*. Springer, Cham.

Malavolta, E., Vitti, G.C. & Oliveira, S.A. 1997. *Avaliação do estado nutricional das plantas*. 1 ed. POTAFOS, Piracicaba.

Marques, M.C.M., Trindade, W., Bohn, A. & Grelle, C.E. 2021. The Atlantic Forest: an introduction to the megadiverse forest of South America. *In*: Marques M.C.M., Grelle C.E.V. (eds.). *The Atlantic Forest*. Springer, Cham.

Marriboina, S. & Attipalli, R.R. 2020. Optimization of hydroponic growth system and Na+-fluorescence measurements for tree species Pongamia pinnata (L.) pierre. *MethodsX* 7: 100809.

Martins, J.P.R., Vasconcelos, L.L., Braga, P.D.C.S., Rossini, F.P., Conde, L.T., Rodrigues, L.C.A., Falqueto, A.R. & Gontijo, A.B.P.L. 2020. Morphophysiological responses, bioaccumulation and tolerance of Alternanthera tenella Colla (Amaranthaceae) to excess copper under in vitro conditions. *Plant Cell, Tissue and Organ Culture* 143(2): 303-

318.

Matyssek, R., Kozovits, A.R., Schnitzler, J., Pretzsch, H., Dieler, J. & Wieser, G. 2014. Forest trees under air pollution as a factor of climate change. *In*: Tausz, M. & Grulke, N. (eds.). *Trees in a changing environment: Ecophysiology, adaptation and future survival*. Springer, Netherlands.

Mimmo, T., Del Buono, D., Terzano, R., Tomasi, N., Vigani, G., Crecchio, C., Pinton, R., Zocchi, G. & Cesco, S. 2014. Rhizospheric organic compounds in the soil–microorganism–plant system: their role in iron availability. *European Journal of Soil Science* 65(5): 629-642.

Minocha, R., Martinez, G., Lyons, B. & Long, S. 2009. Development of a standardized methodology for quantifying total chlorophyll and carotenoids from foliage of hardwood and conifer tree species. *Canadian Journal of Forest Research* 39(4): 849-861.

Minocha, R., Thangavel, P., Dhankher, O.P. & Long, S. 2008. Separation and quantification of monothiols and phytochelatins from a wide variety of cell cultures and tissues of trees and other plants using high performance liquid chromatography. *Journal of Chromatography A* 1207(1-2): 72-83.

Nagajyoti, P.C., Lee, K.D. & Sreekanth, T.V.M. 2010. Heavy metals, occurrence and toxicity for plants: a review. *Environmental Chemistry Letter* 8: 199-216.

Nakazato, R.K., Lourenço, I.S., Esposito, M.P., Lima, M.E., Ferreira, M.L., Campos, R.O.A, Rinaldi, M.C.S. & Domingos, M. 2021. Trace metals at the tree-litter-soil-interface in Brazilian Atlantic Forest plots surrounded by sources of air pollution. *Environmental Pollution* 268: 115797.

Navarrete, A., González, A., Gómez, M., Contreras, R.A., Díaz, P., Lobos, G., Brown, M.T., Sáez, C.A. & Moenne, A. 2019. Copper excess detoxification is mediated by a coordinated and complementary induction of glutathione, phytochelatins and metallothioneins in the green seaweed Ulva compressa. *Plant Physiology and Biochemistry* 135: 423-431.

Ogawa, S., Yoshidomi, T., Shirabe, T. & Yoshimura, E. 2010. HPLC method for the determination of phytochelatin synthase activity specific for soft metal ion chelators. *Journal of Inorganic Biochemistry* 104(4): 442-445.

Ontoria, Y., Gonzalez-Guedes, E., Sanmarti, N., Bernardeau-Esteller, J., Ruiz, J.M., Romero, J. & Perez, M. 2019. Interactive effects of global warming and eutrophication on a fast-growing Mediterranean seagrass. *Marine Environmental Research* 145: 27-38.

Panagos, P., Ballabio, C., Lugato, E., Jones, A., Borrelli, P., Scarpa, S., Orgiazzi, A. & Montanarella, L. 2018. Potential sources of anthropogenic copper inputs to European Agricultural Soils. *Sustainability* 10(7): 2380.

Paoletti, E., Feng, Z., De Marco, A., Hoshika, Y., Harmens, H., Agathokleous, E., Domingos, M., Mills, G., Sicard, P., Zhang, L. & Carrari, E. 2020. Challenges, gaps and opportunities in investigating the interactions of ozone pollution and plant ecosystems. *Science of the Total Environment* 709: 136188.

Pattillo, D.A. 2017. An Overview of Aquaponic Systems: Hydroponic Components. *North Central Regional Aquaculture Center Technical Bulletins* 19: 1-10.

Pedrete, T.A., Hauser-Davis, R.A., Pereira, L.H., Torres, M.B. & Moreira, J.C.

2020. Glutathione and metallothionein as oxidative stress biomarkers in the medicinal plant Chrysobalanus icaco L. from different Brazilian regions. *Journal of Plant Biology and Crop Research* 3(1): 1-6.

Pietrini, F., Iori, V., Cheremisina, A., Shevyakova, N.I., Radyukina, N., Kuznetsov, V.V. & Zacchini, M. 2015. Evaluation of nickel tolerance in Amaranthus paniculatus L. plants by measuring photosynthesis, oxidative status, antioxidative response and metal-binding molecule content. *Environmental Science and Pollution Research* 22(1): 482-494.

Rabêlo, F.H.S., Fernie, A.R., Navazas, A., Borgo, L., Keunen, E., Silva, B.K.D.A., Cuypers, A. & Lavres, J. 2018. A glimpse into the effect of sulfur supply on metabolite profiling, glutathione and phytochelatins in Panicum maximum cv. Massai exposed to cadmium. *Environmental and Experimental Botany* 151: 76-88.

Saleem, M.H., Fahad, S., Khan, S.U., Ahmar, S., Khan, M.H.U., Rehman, M., Maqbool, Z. & Liu, L. 2020. Morpho-physiological traits, gaseous exchange attributes, and phytoremediation potential of jute (Corchorus capsularis L.) grown in different concentrations of copper-contaminated soil. *Ecotoxicology and Environmental Safety* 189: 109915.

Sarma, R.K., Gowtham, I., Bharadwaj, R.K.B., Hema, J. & Sathishkumar, R. 2018. Recent advances in metal induced stress tolerance in plants: possibilities and challenges. *In*: Hasanuzzaman M., Nahar K., Fujita M. (eds.). *Plants Under Metal and Metalloid Stress*. Springer, Singapore.

Shabbir, Z., Sardar, A., Shabbir, A., Abbas, G., Shamshad, S., Khalid, S., Natasha, Murtaza, G., Dumat, C. & Shahid, M. 2020. Copper uptake, essentiality, toxicity, detoxification and risk assessment in soil-plant environment. *Chemosphere*: 127436.

Shang, B., Feng, Z., Li, P., Yuan, X., Xu, Y. & Calatayud, V. 2017. Ozone exposure-and flux-based response relationships with photosynthesis, leaf morphology and biomass in two poplar clones. *Science of the Total Environment* 603: 185-195.

Siqueira, M.C., Kanashiro, S., Domingos, M., Rinaldi, M.C.S. & Tavares, A.R. 2021. Physiological and biochemical changes in tree seedlings growing in urban forest soil contaminated with copper in São Paulo, Brazil. *Plant and Soil* 464(1): 149-163.

Soares, C.R.F.S., Siqueira, J.O., Carvalho, J.G.D., Moreira, F., Souza, M. & Grazziotti, P.H. 2000. Crescimento e nutrição mineral de Eucalyptus maculata e Eucalyptus urophylla em solução nutritiva com concentração crescente de cobre. *Revista Brasileira de Fisiologia Vegetal* 12: 213-225.

Szymańska, R., Ślesak, I., Orzechowska, A. & Kruk, J. 2017. Physiological and biochemical responses to high light and temperature stress in plants. *Environmental and Experimental Botany* 139: 165-177.

Taiz, L., Zeiger, E., Møller, I.M. & Murphy, A. 2017. *Fisiologia e desenvolvimento vegetal*. 6 ed. Artmed Editora, Porto Alegre.

Tsonev, T. & Lidon, F.J.C. 2012. Zinc in plants-an overview. *Emirates Journal of Food & Agriculture* 24(4).

Valentinuzzi, F., Cesco, S., Tomasi, N. & Mimmo, T. 2015. Influence of different trap solutions on the determination of root exudates in Lupinus albus L. *Biology and Fertility of Soils* 51(6): 757-765.

Vassilev, A., Perez-Sanz, A., Cuypers, A. & Vangronsveld, J. 2007. Tolerance of two hydroponically grown Salix genotypes to excess zinc. *Journal of Plant Nutrition* 30(9): 1471-1482.

Viarengo, A., Ponzano, E., Dondero, F. & Fabbri, R. 1997. A simple spectrophotometric method for metallothionein evaluation in marine organisms: an application to Mediterranean and Antarctic molluscs. *Marine Environmental Research* 44(1): 69-84.

Wu, J. & Yu, S. 2019. Effect of root exudates of Eucalyptus urophylla and Acacia mearnsii on soil microbes under simulated warming climate conditions. *BMC Microbiology* 19(1): 1-12.

Xu, Y., Feng, Z., Shang, B., Dai, L., Uddling, J. & Tarvainen, L. 2019. Mesophyll conductance limitation of photosynthesis in poplar under elevated ozone. *Science of the Total Environment* 657: 136-145.

Yadav, S.K. 2010. Heavy metals toxicity in plants: an overview on the role of glutathione and phytochelatins in heavy metal stress tolerance of plants. *South African Journal of Botany* 76: 167–179.

Zhang, H., Xu, W., Guo, J., He, Z. & Ma, M. 2005. Coordinated responses of phytochelatins and metallothioneins to heavy metals in garlic seedlings. *Plant Science* 169(6): 1059-1065.

Zhang, L., Hoshika, Y., Carrari, E., Badea, O. & Paoletti, E. 2018. Ozone risk assessment is affected by nutrient availability: evidence from a simulation experiment under free air-controlled exposure (FACE). *Environmental Pollution* 238: 812-822.

Ormrod, D. P. (1977). Cadmium and nickel effects on growth and ozone sensitivity of pea. Water, Air, and Soil Pollution, 8(3), 263-270.

Castagna, A., Di Baccio, D., Ranieri, A. M., Sebastiani, L., & Tognetti, R. (2015). Effects of combined ozone and cadmium stresses on leaf traits in two poplar clones. *Environmental Science and Pollution Research*, *22*(3), 2064-2075.

Xu, S., He, X. Y., Du, Z., Chen, W., Li, B., Li, Y., ... & Schaub, M. (2020). Tropospheric ozone and cadmium do not have interactive effects on growth, photosynthesis and mineral nutrients of Catalpa ovata seedlings in the urban areas of Northeast China. *Science of the Total Environment*, *704*, 135307.

Calfapietra, C., Peñuelas, J., & Niinemets, Ü. (2015). Urban plant physiology: adaptation-mitigation strategies under permanent stress. *Trends in plant science*, *20*(2), 72-75.

Dawud, K. M., Usman, U. L., Devi, C. A., & Pandey, A. K. (2026). Synergistic Effects of Heavy Metal-Induced Stress and High Tropospheric Ozone Concentration on Plant Productivity. In Tropospheric Ozone and Food Security: Interactions of Ozone with Other Major Abiotic Stresses and its Impact on Food Security (pp. 245-280). Cham: Springer Nature Switzerland.

Anexo A

Capítulo II - Supplementary material

Tab. II S 1. 25% strength of Hoagland and Arnon (1950) balanced nutrient solution (Control), or enriched with excess Cu, Zn, and Ni (CuZnNi).

Nutrient Source	Control	CuZnNi
--	µM	
KNO_3	1500	1500
$Ca(NO_3)_2$ $4H_2O$	1000	1000
$NH_4H_2PO_4$	500	500
$MgSO_4$ $7H_2O$	250	250
KCl	50	50
H_3BO_3	25	25
$MnSO_4$ H_2O	0.6	0.6
H_2MoO_4 (85%)	0.5	0.5
Fe - EDTA	19	19
$CuSO_4$ $5H_2O$	**0.1**	**25**
$ZnSO_4$ $7H_2O$	**0.5**	**25**
$NiSO_4$ $6H_2O$	**0.0**	**25**
$(NH_4)_2SO_4$	*299*	*225*
NH_4NO_3	*0*	*74*

Tab. II S 2. Calibration curve parameters and limits of detection (LOD) for target biochemical compounds analyzed by spectrophotometer-UV (Glutathione) or HPLC-UV (all others). Curves were constructed using analytical grade standard reference. LOD was calculated as 3σ/slope, where σ represents the standard deviation of y-intercept noise from a blank sample.

Compound	Calibration curve equation	R^2	Limit of detection
--	--	--	µg ml^{-1}
Ascorbic acid	y = 0.1681x + 0.4913	0.9972	0.0574
Glutathione	y = 424.27x - 2.3942	0.9781	1.3636
PC2	y = 0.00006x + 0.0208	0.9921	9.4652
PC3	y = 0.00008 + 0.0147	0.9616	4.1123
PC4	y = 0.00006 + 0.0203	0.9828	1.8777
PC5	y = 0.0001 + 0.0163	0.9945	6.5332
PC6	y = 0.00008 + 0.0114	0.9716	1.8208
Phytic acid	y = 0.0344x + 0.2671	0.9966	27.1750
Oxalic acid	y = 0.00003x - 0.0049	0.9935	0.0031
Formic acid	y = 0.0015x - 0.0508	0.9975	0.2652
Lactic acid	y = 0.0014x + 0.0089	0.9969	0.7209
Maleic acid	y = 0.00008 + 0.0017	0.9939	0.1679
Citric acid	y = 0.0008x + 0.0172	0.9599	0.1850
Fumaric acid	y = 0.00001x + 0.0018	0.9951	0.0120
Quinic acid	y = 0.0016x - 0.0251	0.9882	0.1732
Shikimic acid	y = 0.0182x - 0.0226	0.9799	2.9244
Tartaric acid	y = 0.0005x - 0.0287	0.9921	0.2333
Isobutyric acid	y = 0.0417x - 0.0131	0.9914	32.5474
Succinic acid	y = 0.0016x - 0.0217	0.9934	0.8503
Malic acid	y = 0.0011x - 0.0008	0.9945	0.3577

Tab. II S 3 Synthesis of Two-way ANOVA applied on data of phytochelatins concentrations (PC 2-6) observed in leaves or roots (Organ; factor 1) of pioneer tree, non-pioneer tree, herbaceous, liana and epiphyte under Control or CuZnNi (Treatment; factor 2), and Two-Way ANOVA applied on data of heavy metal concentrations (Cu, Zn or Ni) observed in leaves, stem or roots (Organ; factor 1) of pioneer tree, non-pioneer tree, herbaceous, liana and epiphyte under Control or CuZnNi (Treatment; factor 2). P-values equal or under 0.05 (bold) means statistical significative difference between variables.

		Phytochelatins					Heavy metals		
Life-form	Variable	PC 2	PC 3	PC 4	PC 5	PC 6	Cu	Zn	Ni
Pioneer tree	Organ	**<0.01**	**<0.01**	**<0.01**	0.86	0.30	**<0.01**	**<0.01**	**<0.01**
	Treatment	**<0.01**	**<0.01**	**0.03**	0.41	0.09	**<0.01**	**<0.01**	**<0.01**
	Interaction	**<0.01**	**0.04**	**<0.01**	0.45	0.29	**<0.01**	**<0.01**	**<0.01**
Non-Pioneer tree	Organ	**<0.01**	0.07	**<0.01**	**<0.01**	**<0.01**	**<0.01**	**<0.01**	**<0.01**
	Treatment	0.07	**<0.01**	0.11	**<0.01**	**<0.01**	**<0.01**	0.06	**<0.01**
	Interaction	0.38	0.64	0.05	**<0.01**	**<0.01**	**<0.01**	0.43	**<0.01**
Herbaceous	Organ	**0.02**	**0.01**	**<0.01**	0.23	**<0.01**	**<0.01**	**<0.01**	**<0.01**
	Treatment	**0.08**	**0.01**	**<0.01**	0.13	0.14	**<0.01**	**<0.01**	**<0.01**
	Interaction	**0.03**	0.06	**<0.01**	0.65	0.16	**<0.01**	**<0.01**	**<0.01**
Liana	Organ	**<0.01**	**0.02**	**<0.01**	--	**0.03**	**<0.01**	**<0.01**	**<0.01**
	Treatment	0.43	0.15	0.17	--	0.09	**<0.01**	**<0.01**	**<0.01**
	Interaction	0.56	0.07	0.41	--	**0.01**	**<0.01**	**<0.01**	**<0.01**
Epiphyte	Organ	**<0.01**	**<0.01**	0.71	**<0.01**	**<0.01**	**<0.01**	**<0.01**	**<0.01**
	Treatment	1.00	0.90	0.76	0.24	0.24	**<0.01**	**<0.01**	**<0.01**
	Interaction	0.33	0.59	0.99	0.69	0.21	**<0.01**	**<0.01**	**<0.01**

Tab. II S 4. Synthesis of Two-Way ANOVA applied on data of pH and Conductivity of nutrient solutions over time (Time; factor 1) under Control or CuZnNi (Treatment; factor 2). P-values equal or under 0.05 (bold) means statistical significative difference between variables.

		Nutrient solution	
Life-form	Variable	pH	Conductivity
Pioneer tree	Time	**<0.01**	0.87
	Treatment	**<0.01**	0.38
	Interaction	0.15	0.14
Non-Pioneer tree	Time	**<0.01**	**0.00**
	Treatment	0.27	**0.00**
	Interaction	**<0.01**	0.29
Herbaceous	Time	**<0.01**	0.71
	Treatment	**<0.01**	**0.00**
	Interaction	**<0.01**	**0.00**
Liana	Time	**<0.01**	**0.00**
	Treatment	**0.02**	0.21
	Interaction	0.11	**0.01**
Epiphyte	Time	**<0.01**	**0.00**
	Treatment	0.21	0.58
	Interaction	0.09	0.31

Tab. II S 5. Mean concentrations of copper (Cu), zinc (Zn) and nickel (Ni) (mg kg^{-1} dry mass) and dry biomass, with standard deviation (±) in leaves, stem and roots of pioneer tree, non-pioneer tree, herbaceous, liana and epiphyte species cultivated in nutrient solution (C - Control) or nutrient solution with excess of Cu, Zn and Ni (T - CuZnNi).

Life-form	Organ	Treatment	Cu	Zn	Ni	Dry biomass
			--- mg kg^{-1} ---	--- mg kg^{-1} ---	--- mg kg^{-1} ---	g
Pioneer tree	Leaf	Control	14.55 ± 1.56	28.64 ± 4.27	4.70 ± 0.87	2.21 ± 1.01
		CuZnNi	8.90 ± 2.64	31.00 ± 3.98	10.51 ± 1.95	1.59 ± 1.00
	Stem	Control	17.95 ± 5.03	44.15 ± 5.34	5.04 ± 3.07	2.72 ± 0.91
		CuZnNi	18.81 ± 5.07	58.78 ± 8.16	9.62 ± 1.22	2.69 ± 1.48
	Roots	Control	263.56 ± 88.88	75.99 ± 13.27	12.38 ± 2.30	0.90 ± 0.33
		CuZnNi	583.64 ± 45.97	218.49 ± 47.78	121.64 ± 29.35	0.88 ± 0.49
Non-Pioneer tree	Leaf	Control	4.79 ± 0.88	22.96 ± 2.54	1.30 ± 0.86	3.18 ± 0.99
		CuZnNi	3.22 ± 0.59	23.25 ± 2.34	3.40 ± 0.99	1.18 ± 0.34
	Stem	Control	6.42 ± 1.70	27.92 ± 5.61	1.06 ± 0.45	2.27 ± 0.60
		CuZnNi	17.67 ± 7.81	33.87 ± 9.38	6.99 ± 2.18	1.28 ± 0.49
	Roots	Control	17.30 ± 3.15	70.95 ± 19.71	2.46 ± 0.62	1.15 ± 0.32
		CuZnNi	199.11 ± 54.44	79.34 ± 15.88	31.40 ± 6.50	0.73 ± 0.32
Herbaceous	Leaf	Control	5.49 ± 1.17	22.54 ± 4.77	0.33 ± 0.28	2.60 ± 1.15
		CuZnNi	192.18 ± 171.01	121.73 ± 75.76	54.07 ± 32.88	0.43 ± 0.26
	Stem	Control	13.31 ± 7.15	85.71 ± 19.67	1.33 ± 1.57	0.75 ± 0.38
		CuZnNi	590.92 ± 156.39	445.68 ± 158.24	162.84 ± 49.96	0.35 ± 0.20
	Roots	Control	21.23 ± 7.04	201.96 ± 67.74	3.11 ± 1.00	0.59 ± 0.32
		CuZnNi	1083.40 ± 179.71	279.60 ± 84.34	123.47 ± 69.71	0.25 ± 0.16
Liana	Leaf	Control	4.33 ± 3.72	56.51 ± 9.66	1.28 ± 0.76	1.48 ± 0.57
		CuZnNi	12.12 ± 3.57	49.93 ± 12.92	24.04 ± 7.37	0.15 ± 0.06
	Stem	Control	5.06 ± 0.88	58.26 ± 8.33	2.00 ± 0.49	0.99 ± 0.24
		CuZnNi	138.56 ± 47.83	300.83 ± 52.24	102.43 ± 63.04	0.34 ± 0.08
	Roots	Control	6.49 ± 1.14	95.08 ± 23.60	4.99 ± 1.62	0.98 ± 0.15
		CuZnNi	1001.53 ± 210.79	629.97 ± 106.74	241.86 ± 49.86	0.13 ± 0.03
Epiphyte	Leaf	Control	6.82 ± 3.09	52.44 ± 10.43	3.99 ± 2.74	7.68 ± 2.58
		CuZnNi	15.94 ± 5.94	67.39 ± 17.44	7.87 ± 3.73	6.41 ± 2.74
	Stem	Control	9.43 ± 2.28	69.24 ± 13.42	2.61 ± 1.80	0.55 ± 0.20
		CuZnNi	10.38 ± 2.71	70.17 ± 13.13	5.64 ± 1.92	0.55 ± 0.20
	Roots	Control	9.85 ± 1.13	28.21 ± 3.97	2.22 ± 0.61	1.25 ± 0.48
		CuZnNi	263.50 ± 48.98	63.91 ± 12.27	29.44 ± 6.16	0.98 ± 0.37

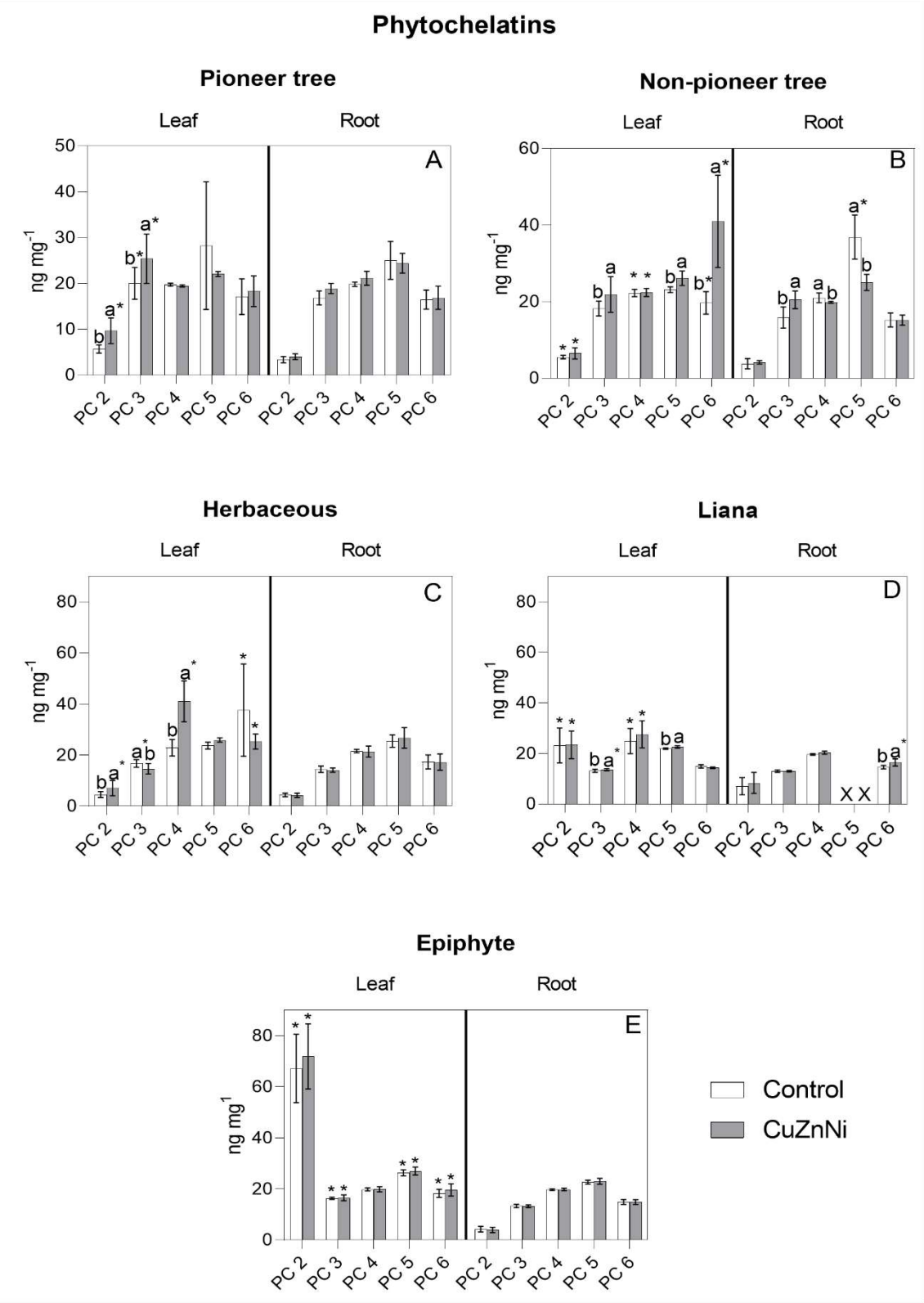

Fig. II S 1. Mean phytochelatins concentrations (PC2 to PC6; ng mg^{-1} fresh mass) in leaves or roots of pioneer tree (A), non-pioneer tree (B), herbaceous (C), liana (D) and epiphyte (E) cultivated in balanced nutrient solution (Control) or balanced nutrient solution with excess Cu, Zn and Ni (CuZnNi). Different letters indicate significant difference between treatments within same organ, while * indicates a significant difference between organs within same treatment, according to two-way ANOVA followed by the Šídák test ($p \leq 0.05$). "x" indicates undetected phytochelatin.

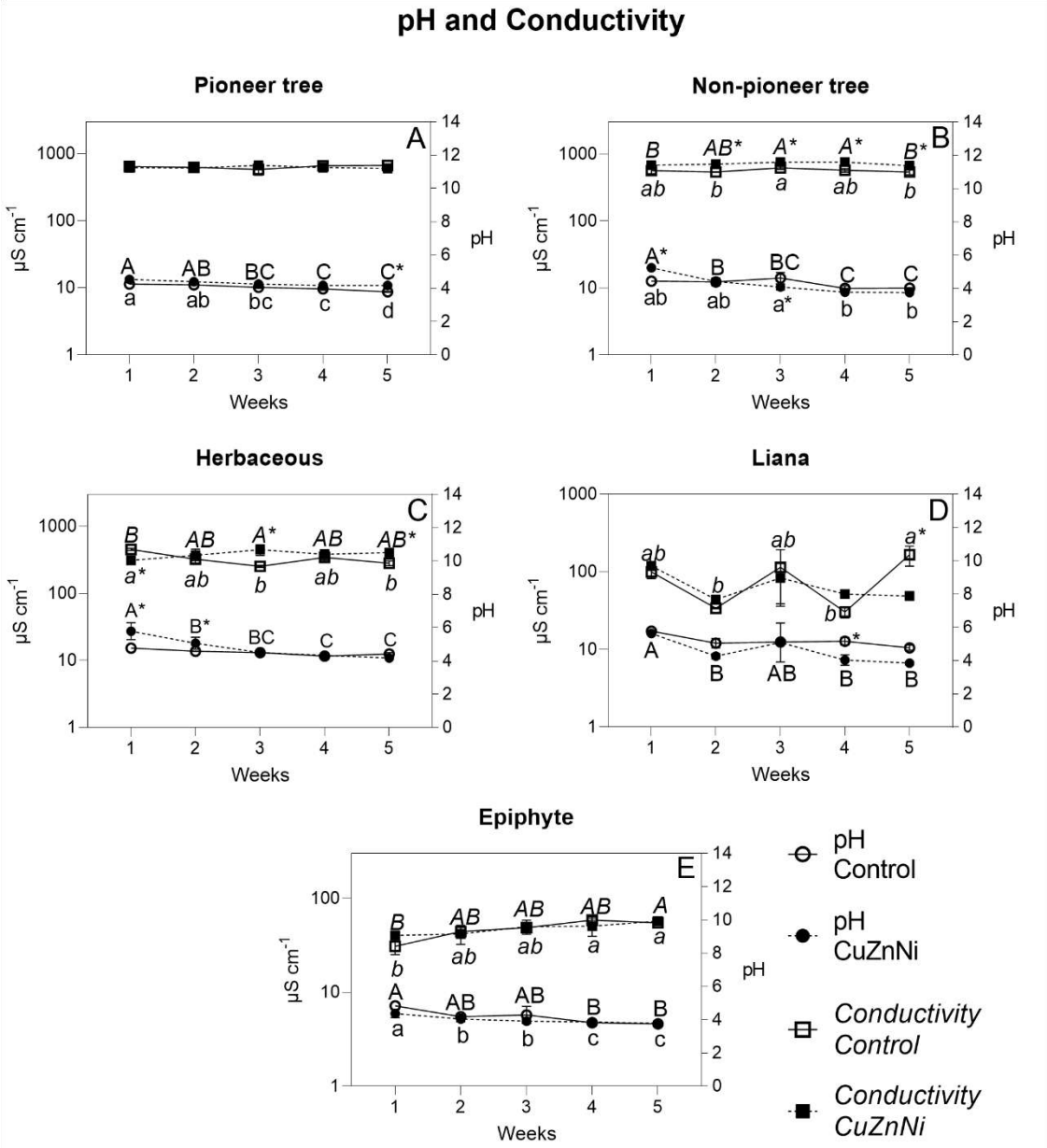

Fig. II S 2. Mean pH and conductivity values (µS cm^{-1}) of hydroponic solutions during 5 weeks of cultivation of pioneer tree (A), non-pioneer tree (B), herbaceous (C), liana (D) and epiphyte (E) grown in balanced nutrient solution (Control) or balanced nutrient solution with excess of Cu, Zn and Ni (CuZnNi). Different letters indicate a significant difference between weeks in the same treatment (lowercase letters compare in Control treatment; while uppercase letters compare in CuZnNi treatment), and * indicates a significant difference between treatments within the same week, according to two-way ANOVA followed by Šídák test ($p \leq 0.05$).

Anexo B

Capítulo III - Supplementary material

Tab. III S 1. AOT40 and POD_y values (0 – 22) of S. terebinthifolia cultivated in ambient (AA), 1.5 times ambient (1.5×), 2.0 times ambient (2.0×), ambient to 2.0× after 45 days (AA → 2.0×) and 2.0× to ambient after 45 days (2.0× → AA) conditions.

Index	AA	2.0× → AA	1.5×	AA → 2.0×	2.0×
--	---------- ppm ----------				
AOT40	16.39	22.13	27.89	40.12	45.86
--	---------- mmol m^{-2} ----------				
POD_0	33.59	38.73	42.05	48.35	53.49
POD_1	28.70	33.83	37.08	43.36	48.48
POD_2	24.43	29.53	32.68	38.94	44.03
POD_3	20.63	25.66	28.66	34.87	39.90
POD_4	17.27	22.24	25.01	31.08	36.04
POD_5	14.30	19.18	21.7	27.56	32.44
POD_6	11.67	16.46	18.73	24.31	29.11
POD_7	9.38	14.08	16.06	21.35	26.04
POD_8	7.42	12.01	13.65	18.62	23.21
POD_9	5.71	10.21	11.51	16.11	20.60
POD_{10}	4.27	8.65	9.62	13.88	18.25
POD_{11}	3.08	7.30	7.96	11.92	16.14
POD_{12}	2.08	6.10	6.50	10.17	14.19
POD_{13}	1.33	5.08	5.22	8.66	12.41
POD_{14}	0.80	4.21	4.09	7.41	10.82
POD_{15}	0.45	3.49	3.10	6.32	9.36
POD_{16}	0.23	2.90	2.23	5.36	8.03
POD_{17}	0.10	2.40	1.52	4.52	6.82
POD_{18}	0.04	1.98	1.01	3.77	5.71
POD_{19}	0.02	1.63	0.63	3.09	4.70
POD_{20}	0.01	1.33	0.36	2.48	3.79
POD_{21}	0.01	1.05	0.19	1.95	2.99
POD_{22}	0.01	0.80	0.09	1.50	2.30
POD_{23}	0.00	0.59	0.03	1.10	1.69

Tab. III S 2. Akaike indication criteria (AIC), coefficient of determination (R^2) and ranking of linear and the tree best non-linear models as function of AOT40 or $POD_{0\text{-}22}$ to predict relative leaf biomass in *S. terebinthifolia*. The line in bold font denotes the best predictor model.

Index	Model	AIC	R^2	Rank
AOT40	Four-parameter Lorentz	-33.0357	0.754927	1
	Brain-Cousens	-32.7727	0.781724	2
	Gaussian	-31.9286	0.76909	3
	Linear	-20.2583	0.250015	73
POD_0	Four-parameter Lorentz	-31.3483	0.725747	1
	Four-parameter Bragg	-31.0952	0.72108	2
	Brain-Cousens	-31.0286	0.754811	3
	Linear	-19.4145	0.206615	82
POD_1	Four-parameter Lorentz	-31.3607	0.725974	1
	Four-parameter Bragg	-31.0898	0.720978	2
	Brain-Cousens	-30.8385	0.751683	3
	Linear	-19.431	0.207491	69
POD_2	Two-phase	-31.7879	0.821472	1
	Four-parameter Lorentz	-31.3609	0.725977	2
	Four-parameter Bragg	-31.0895	0.720973	3
	Linear	-19.4738	0.209749	71
POD_3	Two-phase	-31.7852	0.82144	1
	Four-parameter Lorentz	-31.3123	0.725087	2
	Four-parameter Bragg	-31.0887	0.720958	3
	Linear	-19.5217	0.212264	75
POD_4	Two-phase	-31.788	0.821473	1
	Four-parameter Lorentz	-31.3136	0.725111	2
	Four-parameter Bragg	-31.0717	0.720643	3
	Linear	-19.5697	0.214784	75
POD_5	Two-phase	-31.5741	0.818909	1
	Four-parameter Lorentz	-31.2888	0.724657	2
	Four-parameter Bragg	-31.0889	0.720963	3
	Linear	-19.6094	0.216859	75
POD_6	Two-phase	-31.5735	0.818901	1
	Four-parameter Lorentz	-31.15	0.722098	2
	Four-parameter Bragg	-31.0772	0.720745	3
	Linear	-19.6139	0.217094	77
POD_7	Four-parameter Bragg	-31.084	0.720872	1
	Four-parameter Lorentz	-31.0392	0.720037	2
	Brain-Cousens	-29.3798	0.726321	3
	Linear	-19.6356	0.218226	71
POD_8	Two-phase	-31.7875	0.821467	1
	Four-parameter Bragg	-31.0787	0.720772	2
	Four-parameter Lorentz	-31.0653	0.720523	3
	Linear	-19.6693	0.21998	71
POD_9	Two-phase	-31.788	0.821473	1
	Four-parameter Lorentz	-30.8589	0.716651	2

	Gaussian	-29.1008	0.721183	3
	Linear	-19.6708	0.220056	71
POD_{10}	Two-phase	-31.7869	0.82146	1
	Four-parameter Lorentz	-30.7531	0.714645	2
	Gaussian	-29.1006	0.72118	3
	Linear	-19.7002	0.221585	67
POD_{11}	Log-normal gaussian	-29.1008	0.721184	1
	Gaussian	-29.1007	0.721183	2
	Brain-Cousens	-26.9261	0.677683	3
	Linear	-19.7591	0.224634	64
POD_{12}	Gaussian	-29.1009	0.721186	1
	Log-normal gaussian	-29.1008	0.721184	2
	Five-parameter Cedergreen-Ritz-Streibig "a"	-26.6202	0.721186	3
	Linear	-19.8235	0.227957	67
POD_{13}	Gaussian	-29.1009	0.721186	1
	Log-normal gaussian	-29.1009	0.721186	2
	Bragg4	-26.3886	0.618276	3
	Linear	-19.9911	0.236536	66
POD_{14}	Five-parameter Cedergreen-Ritz-Streibig "a"	-35.5999	0.721186	1
	Five-parameter Cedergreen-Ritz-Streibig "b"	-35.5929	0.721186	2
	Five-parameter Cedergreen-Ritz-Streibig "c"	-35.5569	0.721186	3
	Linear	-20.3361	0.253893	66
POD_{15}	**Four-parameter Bragg**	**-37.6057**	**0.81929**	**1**
	Four-parameter Cedergreen-Ritz-Streibig	-37.5946	0.721186	2
	Four-parameter Lorentz	-36.1437	0.80079	3
	Linear	-20.8447	0.278768	65
POD_{16}	Gaussian	-29.0496	0.72023	1
	Log-normal gaussian	-28.9626	0.718604	2
	Tree-parameter Lorentz	-28.3846	0.618173	3
	Linear	-16.0641	0.008056	65
POD_{17}	Four-parameter Bragg	-37.6012	0.819236	1
	Four-parameter Lorentz	-37.048	0.812445	2
	Gaussian	-35.6059	0.819292	3
	Linear	-22.3429	0.347326	62
POD_{18}	Four-parameter Bragg	-37.6006	0.819229	1
	Four-parameter Lorentz	-37.0438	0.812393	2
	Gaussian	-35.6038	0.819268	3
	Linear	-23.0963	0.379297	51
POD_{19}	Four-parameter Bragg	-37.602	0.819246	1
	Four-parameter Lorentz	-37.0868	0.812929	2
	Gaussian	-35.6041	0.819271	3
	Linear	-23.8017	0.407809	58
POD_{20}	Four-parameter Bragg	-37.6044	0.819274	1
	Four-parameter Lorentz	-37.1944	0.814266	2
	Multistage	-35.605	0.819281	3
	Linear	-24.4826	0.434091	47

POD_{21}	Four-parameter Bragg	-37.6033	0.819261	1
	Four-parameter Cedergreen-Ritz-Streibig	-35.6676	0.794366	2
	Multistage	-35.6046	0.819277	3
	Linear	-25.0723	0.455909	43
POD_{22}	Four-parameter Bragg	-37.5387	0.818481	1
	Multistage	-35.5994	0.819214	2
	Log-normal gaussian	-35.5877	0.819073	3
	Linear	-25.511	0.47159	39

Tab. III S 3 Akaike indication criteria (AIC), coefficient of determination (R^2) and ranking of linear and the three best non-linear models as function of AOT40 or POD_{0-22} to predict relative total biomass in S. terebinthifolia. The line in bold font denotes the best predictor model.

Index	Function	AIC	R^2	Rank
AOT40	Two-phase	-26.0148	0.847715	1
	Four-parameter Lorentz	-22.7676	0.717906	2
	Four-parameter Bragg	-22.2609	0.708214	3
	Linear	-10.6206	0.172255	59
POD0	Two-phase	-26.0488	0.84806	1
	Four-parameter Bragg	-22.2261	0.707537	2
	Four-parameter Lorentz	-21.8869	0.700847	3
	Linear	-9.9853	0.136444	63
POD1	Four-parameter Bragg	-22.2277	0.707569	1
	Four-parameter Lorentz	-21.8361	0.699834	2
	Gaussian	-19.294	0.688787	3
	Linear	-9.99929	0.137249	62
POD2	Four-parameter Bragg	-22.2303	0.707619	1
	Four-parameter Lorentz	-21.8634	0.70038	2
	Gaussian	-20.2426	0.707858	3
	Linear	-10.034	0.139244	62
POD3	Two-phase	-22.724	0.810357	1
	Four-parameter Bragg	-22.2311	0.707635	2
	Four-parameter Lorentz	-21.9256	0.701619	3
	Linear	-10.0734	0.1415	63
POD4	Two-phase	-25.9216	0.846765	1
	Four-parameter Bragg	-22.232	0.707651	2
	Four-parameter Lorentz	-21.9164	0.701436	3
	Linear	-10.1146	0.143856	63
POD5	Four-parameter Bragg	-22.2298	0.707608	1
	Four-parameter Lorentz	-21.8912	0.700935	2
	Gaussian	-19.0171	0.682989	3
	Linear	-10.1503	0.14589	63
POD6	Two-phase	-25.8417	0.845947	1
	Four-parameter Bragg	-22.2352	0.707714	2
	Four-parameter Lorentz	-21.8161	0.699432	3
	Linear	-10.1591	0.146394	62
POD7	Two-phase	-25.8565	0.846098	1
	Four-parameter Bragg	-22.2244	0.707503	2
	Four-parameter Lorentz	-21.7846	0.698801	3
	Linear	-10.1832	0.14776	62
POD8	Two-phase	-25.6903	0.844384	1
	Four-parameter Bragg	-22.2294	0.7076	2
	Four-parameter Lorentz	-21.9417	0.701939	3
	Linear	-10.2193	0.149808	64
POD9	Four-parameter Bragg	-22.2278	0.707571	1

	Four-parameter Lorentz	-21.7813	0.701939	2
	Weibull	-18.9835	0.682277	3
	Linear	-10.2317	0.150514	61
POD10	Four-parameter Lorentz	-21.6605	0.696299	1
	Weibull	-18.9833	0.682272	2
	Gaussian	-18.669	0.675545	3
	Linear	-10.2685	0.152595	60
POD11	Weibull	-18.9794	0.682191	1
	Gaussian	-17.4342	0.647706	2
	Log-normal gaussian	-17.2839	0.644159	3
	Linear	-10.3293	0.15602	53
POD12	Weibull	-18.9534	0.681704	1
	Gaussian	-18.1576	0.664292	2
	Log-normal gaussian	-15.3812	0.596034	3
	Linear	-10.3941	0.159661	46
POD13	Weibull	-18.9674	0.681937	1
	Gaussian	-18.9638	0.681861	2
	Three-parameter log-logistic	-14.2754	0.432229	3
	Linear	-10.5424	0.167926	33
POD14	Gaussian	-26.8003	0.811319	1
	Log-normal gaussian	-26.8	0.811315	2
	Five-parameter Cedergreen-Ritz-Streibig "c"	-26.7963	0.811268	3
	Linear	-10.8353	0.184019	36
POD15	Four-parameter Bragg	-28.7828	0.811099	1
	Gaussian	-26.8004	0.81132	2
	Log-normal gaussian	-26.8004	0.81132	3
	Linear	-11.2698	0.207317	50
POD16	Five-parameter Cedergreen-Ritz-Streibig "a"	-29.6395	0.843857	1
	Four-parameter Bragg	**-28.7999**	**0.811314**	**2**
	Four-parameter Lorentz	-27.5625	0.795089	3
	Linear	-11.8697	0.23839	57
POD17	Four-parameter Bragg	-28.7992	0.811305	1
	Five-parameter Cedergreen-Ritz-Streibig "a"	-28.4514	0.83099	2
	Five-parameter Cedergreen-Ritz-Streibig "b"	-27.9366	0.825084	3
	Linear	-12.5772	0.273478	64
POD18	Four-parameter Bragg	-28.7985	0.811296	1
	Four-parameter Lorentz	-27.8584	0.799091	2
	Gaussian	-26.7989	0.811302	3
	Linear	-13.2483	0.305269	61
POD19	Four-parameter Cedergreen-Ritz-Streibig "a"	-29.0717	0.814703	1
	Four-parameter Bragg	-28.7983	0.811293	2
	Four-parameter Lorentz	-27.8337	0.79876	3
	Linear	-13.8931	0.3345	63
POD20	Four-parameter Bragg	-28.7998	0.811312	1
	Four-parameter Cedergreen-Ritz-Streibig "a"	-28.2266	0.803963	2

	Four-parameter Lorentz	-27.7045	0.797019	3
	Linear	-14.5268	0.362029	63
POD21	Four-parameter Bragg	-28.799	0.811303	1
	Four-parameter Cedergreen-Ritz-Streibig "b"	-27.4464	0.793496	2
	Multistage	-26.7993	0.811306	3
	Linear	-15.0767	0.384994	56
POD22	Four-parameter Bragg	-28.798	0.81129	1
	Multistage	-26.7992	0.811305	2
	Log-normal gaussian	-26.7896	0.811184	3
	Linear	-15.4857	0.401538	44

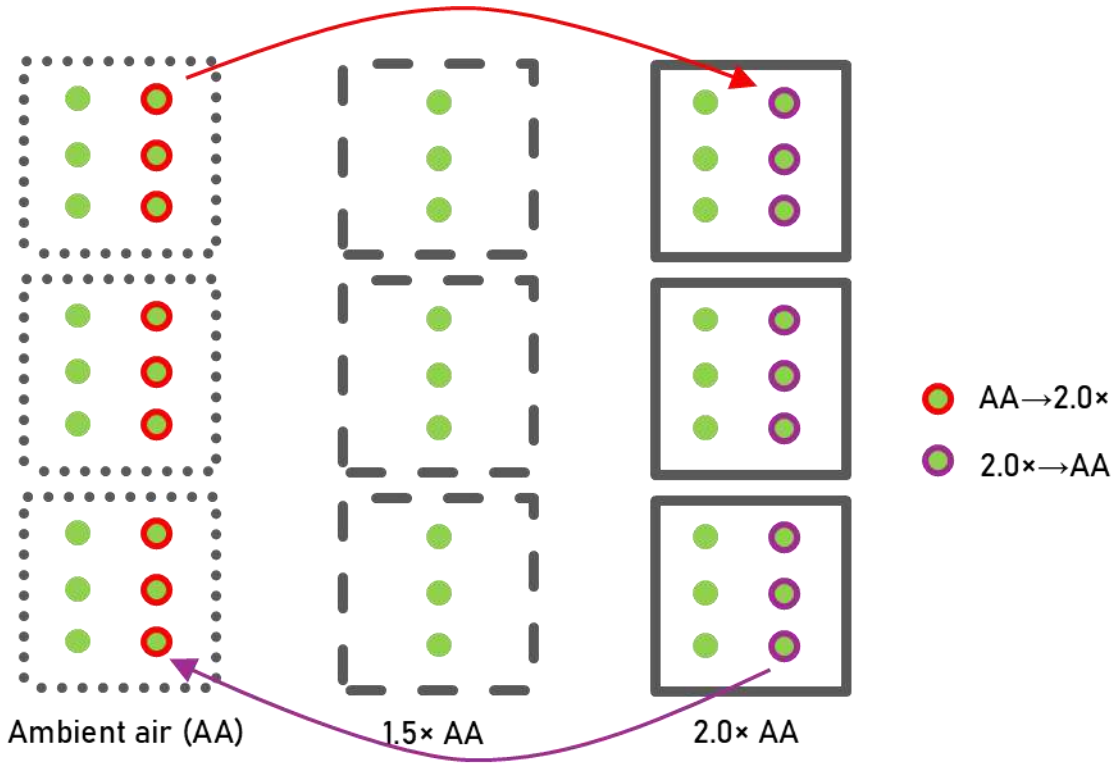

Fig. III S 1 Schematic representation of experimental design and ozone treatments.

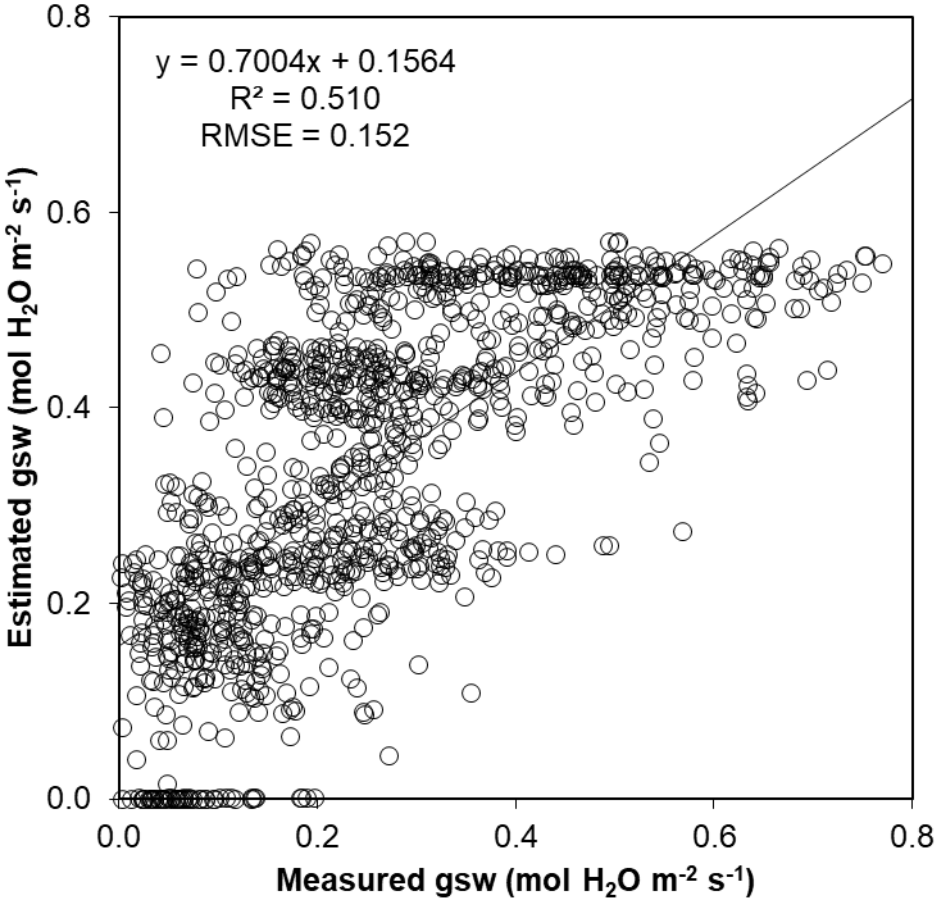

Fig. III S 2. Linear regression of measured and estimated stomatal conductance (*gsw*) in *Schinus terebinthifolia* leaves. RMSE = Root mean square error.

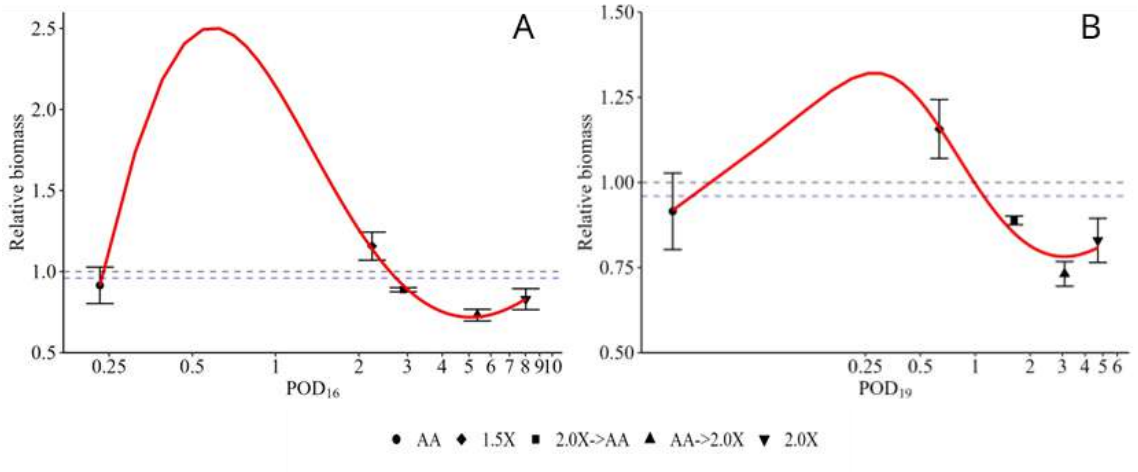

Fig. III S 3. Nonlinear UCRS.5a applied as a predictor of *S. terebinthifolia* relative total biomass of as a function of POD_{16} (A), and nonlinear UCRS.4a applied as a predictor of *S. terebinthifolia* relative total biomass of as a function of POD_{19}. Black dashed line represents the hypothetical relative biomass in pre-industrial era (B_{rel} = 1.00). The Blue dashed line represents the ozone critical levels to achieve 0.96 of relative biomass (4% biomass loss from pre-industrial era).